

SMART Mobility

Advanced Fueling Infrastructure Capstone Report

July 2020

(This Page Intentionally Left Blank)

Foreword

The U.S. Department of Energy's Systems and Modeling for Accelerated Research in Transportation (SMART) Mobility Consortium is a multiyear, multi-laboratory collaborative, managed by the Energy Efficient Mobility Systems Program of the Office of Energy Efficiency and Renewable Energy, Vehicle Technologies Office, dedicated to further understanding the energy implications and opportunities of advanced mobility technologies and services. The first three-year research phase of SMART Mobility occurred from 2017 through 2019 and included five research pillars: Connected and Automated Vehicles, Mobility Decision Science, Multi-Modal Freight, Urban Science, and Advanced Fueling Infrastructure. A sixth research thrust integrated aspects of all five pillars to develop a SMART Mobility Modeling Workflow to evaluate new transportation technologies and services at scale.

This report summarizes the work of the Advanced Fueling Infrastructure Pillar. This Pillar investigated the charging infrastructure needs of electric ride-hailing and car-sharing vehicles, automated shuttle buses, and freight-delivery truck fleets. For information about the other Pillars and about the SMART Mobility Modeling Workflow, please refer to the relevant Pillar's Capstone Report.

Acknowledgments

This material is based upon work supported by the U.S. Department of Energy, Office of Energy Efficiency and Renewable Energy (EERE), specifically the Vehicle Technologies Office (VTO) under the Systems and Modeling for Accelerated Research in Transportation (SMART) Mobility Laboratory Consortium, an initiative of the Energy Efficient Mobility Systems (EEMS) Program.

This report was prepared as an account of work sponsored by an agency of the United States Government. Neither the United States Government nor any agency thereof, nor any of its employees, makes any warranty, express or implied, or assumes any legal liability or responsibility for the accuracy, completeness, or usefulness of any information, apparatus, product, or process disclosed, or represents that its use would not infringe privately owned rights. Reference herein to any specific commercial product, process, or service by trade name, trademark, manufacturer, or otherwise does not necessarily constitute or imply its endorsement, recommendation, or favoring by the United States Government or any agency thereof. The views and opinions of authors expressed herein do not necessarily state or reflect those of the United States Government or any agency thereof.

The following DOE Office of Energy Efficiency and Renewable Energy (EERE) managers played important roles in establishing the project concept, advancing implementation, and providing ongoing guidance: David Anderson, Erin Boyd, Heather Croteau, and Prasad Gupte.

The Advanced Fueling Infrastructure Pillar acknowledges the contributions of:

John Smart¹, Zicheng Bi³, Alicia Birky², Brennan Borlaug², Erin Burrell², Eleftheria Kontou², Dong-Yeon Lee², Timothy Lipman⁵, Andrew Meintz², Eric Miller², Ahmed Mohamed², Matthew Moniot², Amy Moore⁴, Yutaka Motoaki¹, Zachary Needell⁵, Omer Onar⁴, Clement Rames², Nicholas Reinicke², Mohammad Roni¹, Shawn Salisbury¹, Colin Sheppard⁵, Danho Ange Lionel Toba¹, Victor Walker¹, Dustin Weigl², Eric Wood², Fei Xie⁴, Zonggen Yi¹, Teng Zeng⁵, Hongcai Zhang⁵, Yan Zhou³, Zhi Zhou³

¹ Idaho National Laboratory

² National Renewable Energy Laboratory

³ Argonne National Laboratory

⁴ Oak Ridge National Laboratory

⁵ Lawrence Berkeley National Laboratory

This work was authored for the U.S. Department of Energy (DOE), by Lawrence Berkeley National Laboratory under Contract No. DE-AC02-05CH11231, Argonne National Laboratory under Contract No. DE-AC02-06CH11357, Idaho National Laboratory under Contract No. DE-AC07-05ID14517, National Renewable Energy Laboratory under Contract No. DE-AC36-08GO28308, and Oak Ridge National Laboratory under Contract No. DE-AC05-00OR22725. Funding provided by U.S. Department of Energy, Office of Energy Efficiency and Renewable Energy, Vehicle Technologies Office.

List of Acronyms

AADT	average annual daily traffic
AC	alternating current
AEO	Annual Energy Outlook
AES	automated electric shuttles
AEV	automated electric vehicle
AFDC	Alternative Fuels Data Center
AFI	Advanced Fueling Infrastructure
BEV	battery electric vehicle
CAV	connected and automated vehicle
CMIP	charging management and infrastructure planning
C-rate	Charging rate
CYC	Columbus Yellow Cabs
DC	direct current
DCFC	direct current fast charging
DFHV	Department of For-Hire Vehicles
DOE	Department of Energy
DWPT	Dynamic wireless power transfer
E-CAV	electrified connected and automated vehicles
EIA	Energy Information Administration
EMT	electromagnetic transient
EV	electric vehicle
FCS	fast-charging stations
FEA	finite-element analysis
GA	Genetic algorithm
GPS	global position system
GRT	group rapid transit
HD	heavy-duty
HDV	heavy-duty vehicle
HEV	hybrid electric vehicle
ICEV	internal-combustion-engine vehicle
LD	light-duty
LDV	light-duty vehicle
LTL	less-than-truckload
MDS	Mobility Decision Science

MMF	Multi-Modal Freight
NHTS	national household travel survey
PEV	plug-in electric vehicle
PMT	passenger-miles traveled
RDC	regional distribution center
SAES	shared automated electric shuttle
SAEV	shared automated electric vehicles
SMART	Systems and Modeling for Accelerated Research in Transportation
SOC	state of charge
TCO	total cost of ownership
TL	truckload
TNC	transportation network company
U.S.	United States
US	Urban Science
VMT	vehicle-miles traveled
WPT	wireless power transfer

Executive Summary

Electrification of Diverse Transportation Modes Prompts New Questions About Charging Infrastructure

The simultaneous trends of electrification, sharing, and automation inspire visions of a future in which personal mobility and delivery of goods are cheap, accessible, and efficient.

Since the introduction of modern electric vehicles (EVs) in 2010, sales have been on a steady upward trajectory, with cumulative sales of 1.3 million electric vehicles in the United States through September 2019.¹ Public and private forecasts suggest that EV market share will continue to grow in the long term. The U.S. Energy Information Administration's 2019 Annual Energy Outlook projects that annual sales of EVs in the United States will exceed 1 million vehicles per year by 2030.²

During this same time period, the concept of ride-hailing has risen in popularity. Transportation network companies (TNCs) such as Uber and Lyft have popularized the practice of private vehicle owners providing ride-hailing services using their own cars. The number of rides offered by TNCs has increased dramatically; the ride-hailing company Uber took 5 years to deliver its first billion rides, but delivered its second billion in the first half of 2016 alone.³ By December 2018, Uber had delivered 10 billion trips worldwide.⁴

In parallel with the rise of shared mobility, the technology (tech) and automotive industries have made significant investments to develop fully automated, self-driving vehicles. Many established and startup companies are actively developing and demonstrating self-driving vehicle technology. Waymo was the first company to launch an automated ride-hailing fleet for paying customers in 2018.⁵ Automakers, shared-mobility service companies, tech companies, and market analysts are all predicting that automated ride-hailing vehicles will bring about disruptive market changes.

Transportation electrification and automation in the United States is growing beyond light-duty passenger cars. An increasing variety of truck manufacturers, transit agencies, shipping companies, and other organizations are conducting pilot deployments of medium- and heavy-duty electric and automated trucks and buses to transport people and goods.

The electrification of increasingly diverse transportation modes and vehicle types raises many questions about how charging infrastructure could evolve to meet the needs of human-driven and automated EVs providing ride-hailing, car-sharing, automated transit, and freight-delivery services. What is the right kind of charging infrastructure for each mode? How much is needed? Where should it be located? Benefits of transportation electrification can only be realized if adequate, cost-effective charging infrastructure is in place to support it.

U.S. Department of Energy's Systems and Modeling for Accelerated Research in Transportation (SMART) Mobility Advanced Fueling Infrastructure Pillar

The U.S. Department of Energy (DOE) developed a research agenda to examine the charging infrastructure needs of human-driven and automated EVs providing ride-hailing, car-sharing, and freight-delivery services and automated shuttles. This effort was coordinated through the Advanced Fueling Infrastructure (AFI) Pillar, one of five research pillars in the U.S. DOE's SMART Mobility Consortium, a multi-year, multi-laboratory collaborative dedicated to further understanding the energy implications and opportunities of advanced mobility technologies and services.

Between 2016 and 2019, researchers in the AFI Pillar used sophisticated modeling, simulation, and data analysis tools to investigate tradeoffs in different charging infrastructure network designs for human-driven and fully automated ride-hailing EVs, electric car-sharing fleets, automated shuttle buses for fixed-route transit, and freight-delivery truck fleets. (An example of a present-day EV operating within a TNC fleet in Sacramento, California is shown in Figure ES-1.) The AFI Pillar also researched the impact of two potentially game-changing technologies: intelligent management for automated electric vehicle (AEV) fleets and dynamic wireless power transfer. Finally, the AFI Pillar assessed the potential of charging infrastructure installed to support ride hailing to influence mobility and energy-consumption trends on a national scale.

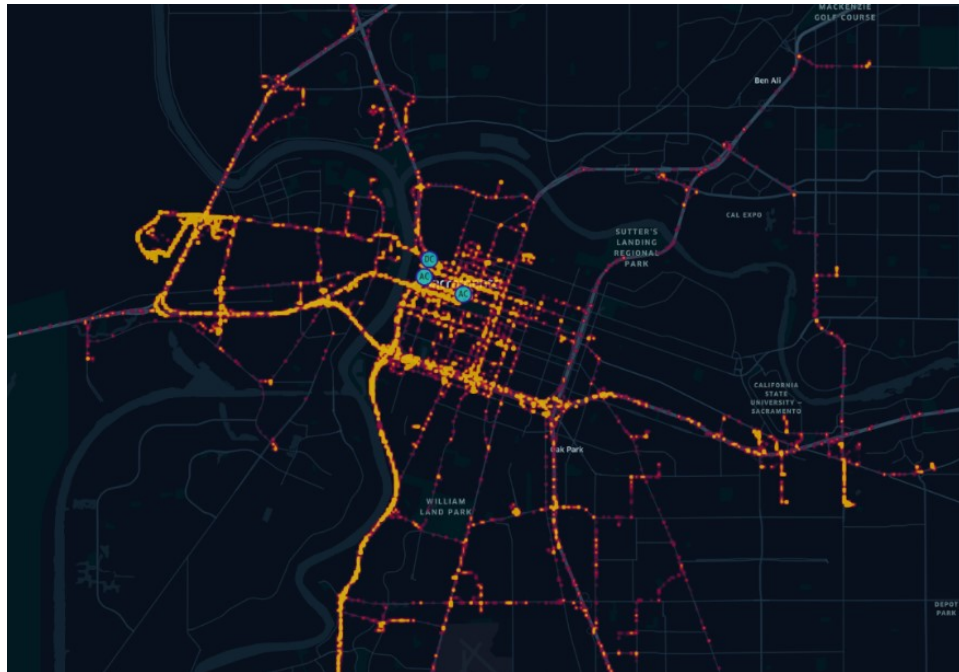


Figure ES-1. Map visualizing the driving and public charging locations (alternating current [AC] Level 2 and direct current [DC] fast chargers indicated by the blue circles) used by a single ride-hailing EV driver in Sacramento, California

The AFI Pillar organized its activities around five primary research questions:

- What are the characteristics of potential transportation market segments employing human-driven and automated EVs that future charging infrastructure will need to serve?
- What are the cost/benefit tradeoffs inherent with different approaches to designing charging infrastructure to serve light-duty human-driven and automated electric ride-hailing vehicles?
- What are the tradeoffs inherent with different approaches to designing charging infrastructure for Class 7/8 electric trucks for freight transport?
- What is the potential for automated-vehicle charging to create new charging paradigms that improve automated electric ride-hailing vehicles and transit?
- What is the benefit to the nation of charging infrastructure deployed to serve ride-hailing EVs?

Key Findings

A recurring theme in the AFI Pillar’s research is that tradeoffs abound. There is no “right” amount of charging infrastructure because charging needs vary dramatically across and within increasingly diverse segments of the EV market. Circumstances, interests, and behaviors of individual EV drivers vary dramatically, rendering a single, ideal charging infrastructure design impossible. For operators of human-driven and automated EV fleets, decisions related to charging are closely coupled with many other investment and operations decisions, including the number and type of vehicles they place in their fleet and how vehicles are dispatched. The conclusions of AFI Pillar research summarize many of the tradeoffs that must be managed and the cost/benefit relationships that emerge in different approaches to charging infrastructure network design for future electric mobility.

Understanding New Market Segments for Transportation Electrification

Light-Duty Vehicle Market Segmentation

The AFI Pillar performed behavioral segmentation to study the potential future charging infrastructure needs of various EV market segments. One of these market segments for which data are available today is human-

driven ride hailing. For the study of human-driven ride-hailing fleets, real-world TNC and taxi activity data from RideAustin and Columbus Yellow Cabs (CYC) were analyzed, alongside a national TNC driver survey from Populus, to shed light on incentives and barriers for electrification. The following are key insights from the data-analysis efforts:

- EVs are not cost competitive for many TNC drivers without financial incentives or less expensive vehicles.

The majority of TNC drivers in the RideAustin and Populus data were found to drive part time, with relatively low annual vehicle-miles traveled (VMT). A minority of TNC drivers operate full time (~10%), with high annual VMT; the average annual VMT for this group was about 30,000 miles. CYC taxicab drivers, considered full-time drivers, averaged 40,000 miles per year.

A total cost of ownership (TCO) study for TNC drivers quantified the cost competitiveness of EVs for TNC drivers with primarily financial motivations. This study showed that battery electric vehicles (BEVs) with 250 miles of range (referred to as BEV250s) have the lowest TCO for vehicles driven at least 42,000 miles per year, compared to equivalent internal-combustion-engine vehicles (ICEVs), hybrid electric vehicles (HEVs), and BEV150s, assuming current vehicle prices, access to home charging at \$0.13 per kWh, gasoline cost of \$3.00 per gallon, and opportunity cost of public charging of \$15 per hour. HEVs are the lowest-cost option when vehicles are driven between 12,000 and 42,000 miles annually. The annual VMT threshold above which BEV250s become the lowest-cost option decreases as the cost of vehicle purchase goes down or BEV purchase incentives are introduced.

- Home charging obviates most of the need for public direct-current fast charging (DCFC), but there are mixed reports on TNC driver access to home charging.

Most full-time TNC driving days in the RideAustin and CYC data could be accomplished with a BEV250 and overnight charging, as data the AFI Pillar collected from a small number of EV TNC drivers showed. For more than three months, these drivers conducted approximately 65% of their charging events at home, 8% at DCFC stations, and the remaining 27% using public Level 2 charging units. All but one driver had access to charging at home. The driver that could not charge at home was responsible for most of the public Level 2 charging and conducted most of that overnight.

Two other data sources suggest that home charging access will be less prevalent in a larger sample of drivers. Approximately 40% of TNC driver respondents to the Populus survey reported living in an apartment (see Figure ES-2), where installing and accessing charging stations may be problematic. Maven reported that more than 95% of Maven Gig TNC drivers did not have access to home charging.⁶

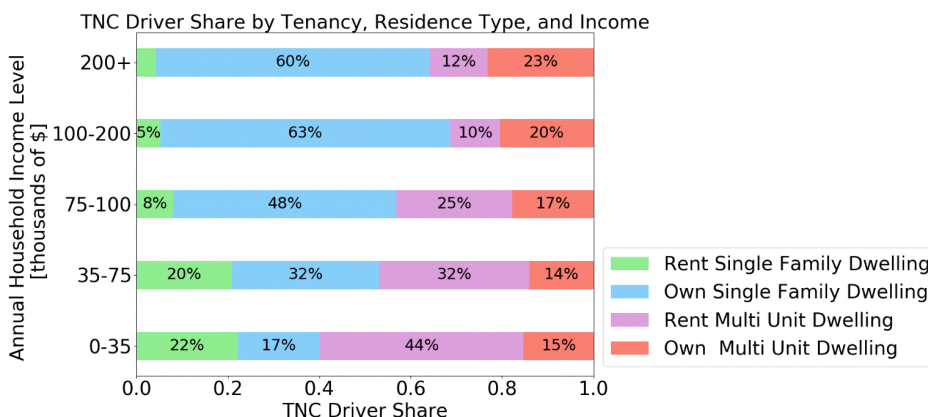


Figure ES-2. Populus survey results for TNC driver share by residence type, tenure, and income

- TNC drivers have different motivations, and not all are financially motivated.

TNC driver respondents to the Populus survey reported many motivations for why they drive for a TNC, such as being between jobs or preferring flexible hours. Interestingly, nearly a quarter of drivers report nonfinancial reasons as their primary motivation (e.g. to keep busy, to meet new people).

These findings highlight stark differences in charging needs between segments. For some TNC drivers, accessible, fast, public charging infrastructure at minimal cost is a top priority. Others have considerably more flexibility in their charging choices.

Freight-Trucking Industry Segmentation

The AFI Pillar also studied the freight industry to determine the charging needs of electric trucks used for shipping goods. This is an important area of study because widespread truck electrification has the potential to significantly reduce petroleum consumption and cost; trucks moving freight account for 25% of all fuel consumed by U.S. transportation, and fuel accounts for 20% of operation costs for freight companies.^{7, 8} However, the freight industry is complex, and numerous business models would require varying degrees of charging infrastructure or changes to operations in order to adopt electric trucks, because the range of these trucks will be limited compared to conventional diesel trucks. The Pillar analyzed predominant industry segments and examined the nature of trucking operations, owner-operator interests, and regulations that govern operations in each segment. Results of this analysis led to the following findings.

- Class 7 and 8 heavy-duty trucks account for 86% of all miles driven by medium- and heavy-duty trucks transporting freight in the U.S., so electrification of these heavy trucks has much higher potential for energy consumption reductions.
- Class 7 and 8 trucks in for-hire/truckload and for-hire/less-than-truckload motor-carrier segments often do not consistently drive the same routes or stop at the same locations, making charging infrastructure siting difficult. Private carriers transport their own company's cargo and operate exclusively between their own terminals, so installing charging infrastructure at their own facilities may be more practical.
- Electric-truck operations must also be conducted within the confines of regulation, including the maximum allowable time drivers can continuously operate their trucks. The relatively long times that charging requires, even with high-power chargers, may be highly problematic for trucking companies that strive to maximize miles driven within regulated shift lengths.
- The variety and complexity of operations in the freight-trucking industry make it challenging to discern the fleets and applications in which electric trucks are beneficial, what kind of charging infrastructure is needed for electrification to be feasible, and who bears the costs and receives the benefits of charging infrastructure investment. Charging infrastructure costs must be weighed against the cost of operational changes, such as routing and dispatching changes. New tools are needed to help trucking companies holistically manage complex decisions surrounding electrification and charging infrastructure.

Charging Network Design Tradeoffs

The AFI Pillar used multiple modeling tools and analytical methods to design charging networks and simulate their use by EVs in specific case studies. This provided a means to examine the cost/benefit tradeoffs inherent with different approaches to charging infrastructure to serve human-driven and automated electric vehicles. These studies varied multiple charging infrastructure parameters, such as the number, location, and power level of charging stations, to determine the effect on EV use and cost. The AFI Pillar studied charging network design tradeoffs for three cases: ride-hailing vehicles, car-sharing fleets, and heavy-duty trucking for freight delivery. The following are the key findings from this research.

Charging Network Design to Support Electric Ride-hailing Vehicles

- Overcoming barriers to home or depot charging for TNC and taxi drivers is a powerful enabler for ride-hailing electrification.

EVI-Pro simulation results based on real-world TNC and taxi data in Columbus, Ohio, and Austin, Texas, confirmed that the feasibility of fleet electrification is strongly correlated to charging infrastructure access. Simulations were conducted with full-time ride-hailing drivers operating BEV250s with the capacity to

charge at up to 50 kW, following historical driving patterns of full-time drivers in vehicles powered by internal combustion engines.

Successful charging solutions were identified for 96% of vehicle-days (where a vehicle-day is a 24-hr period of travel for a single vehicle) when drivers had access to overnight residential or depot charging. However, only 40% of vehicle-days could be successfully completed without consistent access to overnight charging, even with plentiful DCFC opportunities. Results indicate that overnight charging access significantly increases the feasibility of electrification for full-time TNC and taxi fleets. Drivers without home charging access, whose simulated charging activity is shown in the map on the right in Figure ES-3, will need to use public DCFC frequently. If they cannot charge at power levels above 50 kW, their daily driving distance will be limited relative to how they have historically driven conventional gas-powered vehicles because some of the time that might be spent driving will be displaced by time spent charging.



Figure ES-3. Heatmaps of simulated DCFC demand in Columbus, Ohio from electric taxi fleet with access to overnight charging (at left) and without (at right).

- Placing DCFC stations at locations where ride-hailing EV demand will be highest is more economical in the long run for the charging network provider than locations where installation is the cheapest. Not only are the overall economics of charging station ownership improved with high utilization, but the effect of uncertainty in installation cost for different locations is also greatly diminished.

The AFI Pillar partnered with AEP Ohio, an electric utility serving Columbus, Ohio, to estimate the cost to install 50-kW DCFC stations at 12 locations in Columbus. The Pillar also simulated the use of those stations by personal-use and ride-hailing EV drivers and calculated operating costs. The study showed that the cost and use of public DCFC stations vary tremendously by location.

Utilization of 12 DCFC stations by simulated EVs varied from 2 to 48 charging sessions per day. The largest, most expensive charging station was estimated to have total monthly capital and operating expenses of up to \$6,400 per month while the smallest charging station that was the cheapest to install would cost as little as \$1,100 per month (excluding real estate costs).

The effect of variation in fixed, upfront capital and installation costs diminishes as fixed costs are amortized across a greater number of charging sessions. The largest, most expensive charging station was also the most active, resulting in a normalized cost of \$4.45 per session; small, inexpensive, poorly utilized stations would see costs of up to \$42 per session.

Therefore, in the cases where DCFC networks require payment per use, charging station providers can more effectively balance cost and revenue by prioritizing placement of chargers at sites that are expected

to experience higher utilization, rather than sites where installation cost will be lowest. Such sites are likely to include urban cores, transit hubs, and airports. Note that the cost of real estate was not included in this study and can add substantially to the overall cost of a charging station; however, site-specific real estate cost is more easily estimated than installation cost.

- To expand the capacity for human-driven and AEV ride-hailing fleets to serve more passengers, increasing the size of the DCFC network serving the vehicles, increasing charging power, or increasing vehicle EV range are each similarly cost-effective, but there is a point of diminished returns at which additional chargers do not yield additional fleet productivity, in terms of passenger-miles traveled (PMT).

A case study of charging infrastructure to support AEV and human-driven ride hailing in the San Francisco Bay Area in California examined how varying vehicle range, fleet size, charge power, and number and locations of charging stations affects ride-hailing fleet utility, in terms of cost per PMT. To facilitate this study, multiple charging networks of varying size and concentration were developed for the simulation, as shown in Figure ES-4.

Compared to a reference case of 50-kW chargers, 100-mile range BEVs, and sparse charging infrastructure coverage, investments to increase charger power, vehicle range, and infrastructure density are all roughly equally cost-effective means of increasing the amount of travel demand served by an electric ride-hailing fleet, with increases in charging power offering slightly more benefit. In a hybrid ride-hailing fleet with both AEVs and human drivers, charging infrastructure can make a substantial difference in the ability of the overall fleet to serve customer demand, especially for low-range BEVs. With a fleet of 100-mile BEVs, adding approximately 4,200 50-kW DCFC plugs to a sparse charging network (at a cost of approximately \$0.01/passenger-mile – a 14% increase from the base cost of \$0.06/passenger-mile) can increase the number of passenger-miles served by 90%. Alternatively, increasing the power of the chargers in the sparse charging network from 50-kW to 100-kW (for the same number of charging stations and plugs) can increase total passenger-miles served by 108%, at an additional cost of \$0.005/passenger-mile – a 7% increase.

The amount of available charging infrastructure and charging-power capacity influence the ability of an AEV fleet to serve passengers. An electric ride-hailing fleet of inexpensive, low-range EVs (BEV100s) with access to widespread, 50-kW charging infrastructure (1 plug per 7 vehicles) can serve 150 passenger miles per vehicle in a day. Expanding the charging network to 1 plug per 3 vehicles reduces queuing time and allows the fleet to serve 180 passenger miles per vehicle per day. However, adding more charging infrastructure beyond this point cannot cost-effectively increase passenger miles served by the fleet because charging time, not queuing time, becomes the bottleneck. EV range or charging power must be increased to alleviate this constraint. The same size fleet of BEV200s with access to widespread, 100-kW charging infrastructure (1 plug per 7 vehicles) can cost-effectively serve 230 passenger miles per vehicle per day. Increasing the range of the vehicles in the fleet to BEV300s captures 250 passenger miles per vehicle per day. Adding more plugs does not increase passenger miles served.

The cost to the fleet per passenger mile served is the same for each of these cases. Therefore, fleet management should define a target for passenger miles they wish to serve and then choose the least expensive charging infrastructure and vehicle designs that meets that target.

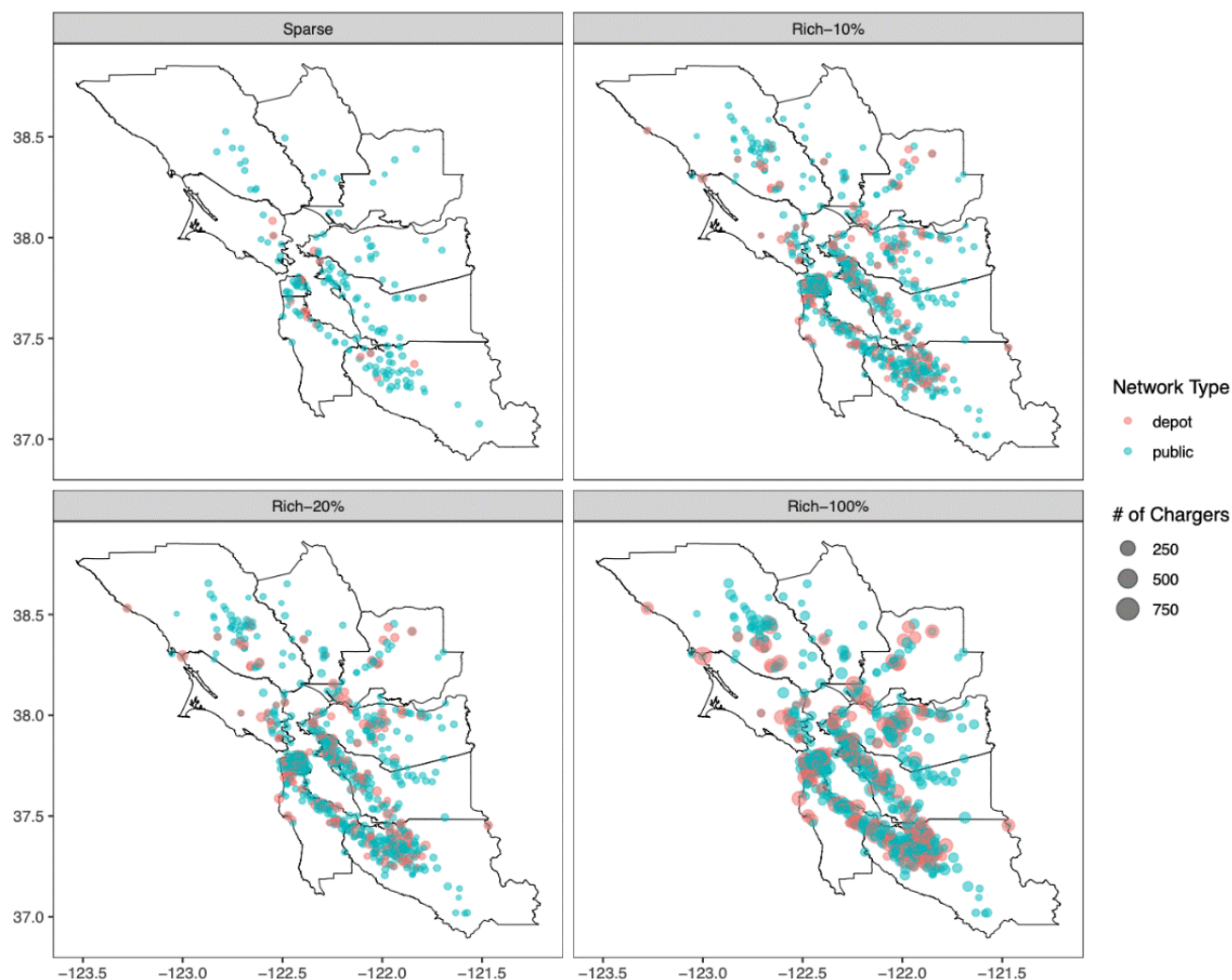


Figure ES-4. Spatial distribution of simulated charging stations in the San Francisco Bay Area by network type. Note: “depot” means charging stations that are dedicated to the AEV fleet, “Sparse,” “Rich-10%,” “Rich-20%,” and “Rich-100%” are DCFC networks of differing sizes used in simulation scenarios.

Charging Network Design to Support Electric Vehicles in Free-floating Car-sharing Fleets

For free-floating car-sharing vehicles and, potentially, for other commercial EVs operating in a small geographic area, increasing charging power above 50 kW will have a much greater effect on minimizing charging-trip downtime than would adding additional charging stations. This is because charging time is usually the dominant factor in the total downtime of a charging trip. In the scenario studied, increasing the number of charging stations from six to 26 only reduced total downtime due to charging by 4%, whereas doubling the charging power of the six charging stations could reduce downtime due to charging by 36%.

A simulation of a free-floating car-sharing fleet of electric vehicles in Seattle, Washington (see Figure ES-5), showed that optimizing the number and location of charging stations can significantly reduce the time and miles required for vehicles to reach charging stations between periods of customer use. However, adding many charging stations reduces the total downtime required for charging by just a small fraction. The time spent charging at 50-kW DCFC stations is a much larger component of the total time vehicles are out of service for

charging than the time spent traveling to a station. In this case, it is more effective to invest in technology that decreases charging time, rather than increasing the number of DCFC stations.

It is important to note that this finding applies when fleet managers are concerned about maximizing vehicles' time in service and minimizing the number of trips taken for charging. It may not be necessary to minimize downtime for charging if vehicles can be pulled out of service for charging during periods of low demand. This latter approach shifts the focus from faster charging to more sophisticated fleet management.

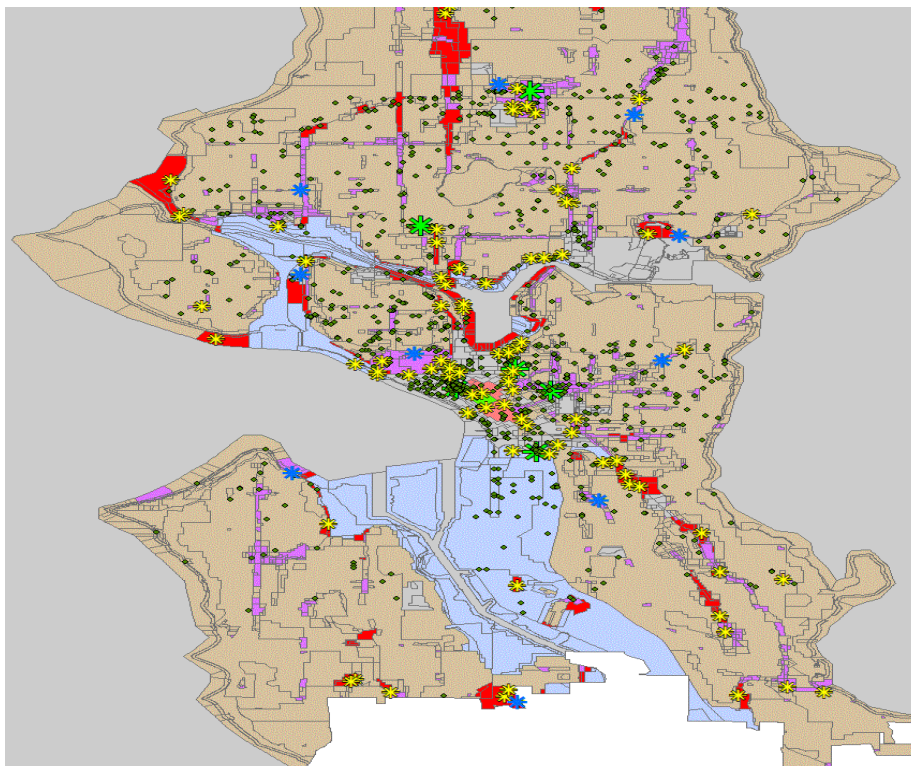


Figure ES-5. Optimal locations of ten new charging stations (blue stars) to serve a free-floating electric car-sharing fleet, based on historical trip information.

Charging Network Design to Support Electric Trucks for Freight Delivery

Electrification of Class 7 and 8 heavy-duty trucks used to transport freight may require substantially higher charging power than 350 kW and/or changes to fleet operations, even in hub-and-spoke regional operations with primary trip lengths of less than 200 miles.

In a case study of a private, regional-haul, hub-and-spoke motor carrier based in Dallas, Texas, truck-fleet operation was modeled with high-power fast chargers at the central distribution center and at the loading docks of all destinations. Real-world data describing the operation of this fleet indicated that drivers often chain trips together, resulting in an overall distance traveled before returning home that often exceeded 500 miles. Modeling found that even when employing trucks with 500 miles of EV range and 350-kW chargers during loading, unloading, and other typical dwell times, some trucks did not have sufficient range to complete their routes. This suggests that freight-trucking fleets of this type will need to adjust their operations to accommodate electrification. Fleets may need to lengthen dwell times to allow for sufficient charging, take time to charge at public charging stations, and/or limit electric trucks to specific routes. These complexities add real costs to fleet operations that must be balanced with the cost of increasing EV range and charging power to realize the financial benefits of electrification. All of these factors may limit the utility of electric trucks relative to their conventional counterparts, which could reduce resale value and put pressure on the business case for heavy-truck electrification.

Exploring New Paradigms Created by Automated-Vehicle Charging

Charging Decision Making for Automated Ride-hailing Fleets

AEVs in commercial ride-hailing fleets must have the intelligence and awareness needed to decide when and where to charge. These decisions need to be made as part of an overall fleet-management approach that dispatches vehicles to pick up passengers and repositions idle vehicles to better serve future passengers. The AFI Pillar developed heuristic and system-optimization approaches for repositioning and charging decisions and simulated the operation of a fleet of ride-hailing AEVs in New York City to compare the performance of the two approaches. The following are key findings from this research:

- Increasing the sophistication of AEV ride-hailing vehicle management allows AEV fleets to downsize and balance the cost of operations with the benefits of serving more passengers.

A simulation of an AEV ride-hailing fleet in New York City, New York, experimented with different approaches for managing AEVs while they are idle between fares. The purpose of this research was to determine the potential for system-wide performance gains by introducing intelligent fleet-management strategies, including autonomous charging decision making. Results show that mathematical optimization allows the fleet to reduce zero-occupancy VMT, serve more ride-hailing requests, and better manage the utilization rate of charging infrastructure relative to fleet management using simple heuristics.

- Repositioning idle vehicles properly can effectively increase the number of passenger ride requests satisfied, but it increases fleet operating costs because overall zero-occupancy vehicle miles (i.e., deadheading) increase. Optimization-based fleet management can balance these two competing priorities at the fleet level (see Figure ES-6). Additionally, fleet managers should carefully select key performance indicators so that fleet-management strategies are appropriately focused and avoid perverse incentives.
- A well-designed strategy for managing idle vehicles can improve AEV fleet operational efficiency by systematically directing AEVs to upcoming ride-hailing requests and reducing time spent driving to and dwelling at charging stations. Compared to a simple heuristic approach, an optimization-based approach can help satisfy considerably more travel requests and reduce zero-occupancy VMT.

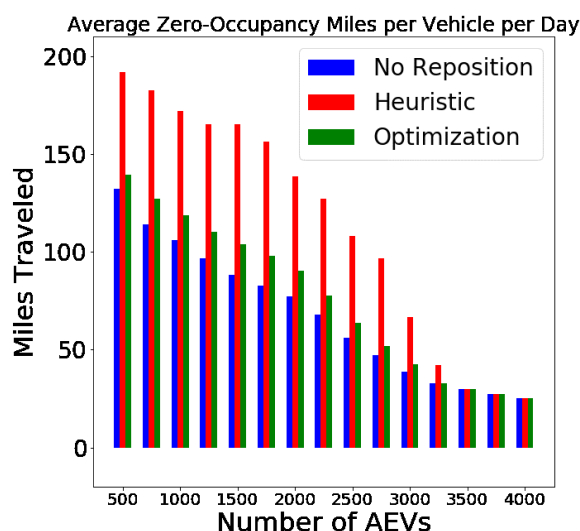


Figure ES-6. The overall average deadhead miles per vehicle per day for different fleet sizes.

Dynamic Wireless Charging for Automated Electric Transit

Dynamic wireless power transfer (DWPT) for automated electric transit has significant potential to improve operational efficiency of transit operations because DWPT can automate the charging process of AEVs and enable them to charge while driving. Currently, a major focus for automating transit vehicles is with automated electric shuttles capable of transporting 8–12 passengers. Although this application is currently a small niche

case, these vehicles have the potential to significantly decrease operational cost, increase safety, and allow transit agencies to adopt more flexible route designs. This could prompt these vehicles to become more mainstream as transit agencies look for ways to become more efficient and increase the level of service they provide to riders.

A simulation of two automated electric shuttle-bus networks showed that a 5-m long, 100-kW wireless charging system located at bus stops located about every mile along a fixed route could allow electric 8–12-passenger shuttle buses to operate continually at low speeds (i.e., up to 15 mph). Increasing the wireless charging system length to 175 m could allow automated electric shuttles to operate continuously at speeds of up to 50 mph.

This means driverless shuttle buses can operate with near-zero downtime, which enables fewer buses to provide increased quality of service, potentially at lower cost, compared to equivalent human-driven shuttle buses without DWPT. Implementing such a system could potentially reduce the size and cost of vehicle batteries by more than 50%. Preliminary cost analysis suggests that a DWPT system can be cost competitive with high-power conductive charging in automated, electric transit applications.

Beyond transit, analysis of DWPT to support highway driving found that a DWPT system capable of providing up to 250 kW of charging power, installed in 8%–10% of the primary roadways in the United States, is sufficient to enable continuous, charge-sustaining operation for light-duty vehicles averaging 65 mph. As with the transit application, DWPT technology allows EVs to have smaller batteries and use narrower state-of-charge windows, which reduce cost and increase battery life.

Preliminary analysis of DWPT with grid-integration requirements found that DWPT systems will need voltage and reactive power control or will need to be integrated with energy storage and/or renewable energy systems to dampen transients in power flow from the grid and prevent grid-stability problems.

National Impact of Charging Infrastructure for Electric Ride-Hailing Vehicles

The AFI Pillar quantified national energy impacts of ride-hailing EVs as a function of different levels of charging infrastructure support and ride-hailing demand. Consumer adoption modeling determined that increasing charging infrastructure availability for ride-hailing EVs induces EV adoption among personal-use vehicle owners. Also, increased ride-hailing demand creates faster vehicle turnover because full-time ride-hailing vehicles, on average, travel more miles per year than vehicles used solely for personal use. With increased charging availability and demand for ride hailing, the average fuel efficiency of the United States light-duty vehicle fleet would improve more quickly as EVs and other more efficient vehicles are introduced into the fleet sooner. Increased VMT by ride-hailing vehicles due to deadheading offsets some of the benefit of reduced energy consumption resulting from electrification and increased ride hailing.

Scenario analysis shows that high ride-hailing demand and electrified ride-hailing vehicles with charging infrastructure support could reduce national energy consumption of light-duty vehicles (LDVs) by up to 38% in 2030 over 2017 levels. Of this reduction, 25% is from increased electrification due to non-infrastructure factors, 2%–3% is due to increased infrastructure support, and 10–11% is due to ride hailing and faster fleet turnover. Petroleum consumption is reduced by up to 51% from 2017 to 2030, of which 33% is from increased electrification due to non-infrastructure factors, 4%–6% is due to increased infrastructure support, and 12%–14% is due to faster fleet turnover.

The results show that because of deadheading trips, petroleum-consumption reductions relative to the base case begin when BEV market penetration (i.e., sales) is higher than 40% and ride-hailing demand is higher than 35% in urban areas in 2030 with optimized charging infrastructure support (green area in Figure ES-7[a]). The electricity consumption, however, has an opposite trend (Figure ES-7 [b]).

(a) Gasoline:

		Ride-hailing battery electric vehicle stock % 2030:																									
		12%	16%	19%	22%	26%	29%	32%	35%	38%	42%	45%	47%	Ride-hailing battery electric vehicle sales % 2030:													
		18%	25%	30%	35%	40%	45%	50%	55%	60%	65%	70%	74%														
Ride-hailing demand	0.29%	10.24	10.24	10.24	10.24	10.24	10.24	10.23	10.23	10.23	10.23	10.23	10.23	10.24	10.24	10.24	10.24	10.24	10.23	10.23	10.23	10.23	10.23	10.23	10.23		
	5%	10.47	10.43	10.41	10.39	10.37	10.34	10.32	10.30	10.27	10.25	10.23	10.21	10.47	10.43	10.41	10.39	10.37	10.34	10.32	10.30	10.27	10.25	10.23	10.21		
	10%	10.66	10.60	10.55	10.51	10.46	10.42	10.38	10.33	10.29	10.24	10.20	10.16	10.66	10.60	10.55	10.51	10.46	10.42	10.38	10.33	10.29	10.24	10.20	10.16		
	15%	10.81	10.72	10.66	10.60	10.53	10.47	10.40	10.34	10.27	10.21	10.15	10.09	10.81	10.72	10.66	10.60	10.53	10.47	10.40	10.34	10.27	10.21	10.15	10.09		
	20%	10.93	10.82	10.74	10.65	10.57	10.49	10.40	10.32	10.23	10.14	10.04	9.97	10.93	10.82	10.74	10.65	10.57	10.49	10.40	10.32	10.23	10.14	10.04	9.97		
	25%	11.02	10.88	10.78	10.68	10.58	10.48	10.37	10.26	10.14	10.03	9.92	9.84	11.02	10.88	10.78	10.68	10.58	10.48	10.37	10.26	10.14	10.03	9.92	9.84		
	30%	11.07	10.92	10.80	10.69	10.58	10.43	10.30	10.18	10.05	9.92	9.80	9.70	11.07	10.92	10.80	10.69	10.58	10.43	10.30	10.18	10.05	9.92	9.80	9.70		
	35%	11.10	10.93	10.80	10.68	10.51	10.37	10.22	10.08	9.94	9.80	9.66	9.55	11.10	10.93	10.80	10.68	10.51	10.37	10.22	10.08	9.94	9.80	9.66	9.55		
	40%	11.11	10.92	10.77	10.61	10.45	10.29	10.13	9.98	9.82	9.67	9.52	9.40	11.11	10.92	10.77	10.61	10.45	10.29	10.13	9.98	9.82	9.67	9.52	9.40		
	45%	11.10	10.89	10.71	10.54	10.37	10.20	10.03	9.86	9.70	9.53	9.37	9.24	11.10	10.89	10.71	10.54	10.37	10.20	10.03	9.86	9.70	9.53	9.37	9.24		
	50%	11.07	10.83	10.64	10.46	10.28	10.10	9.92	9.74	9.56	9.39	9.21	9.07	11.07	10.83	10.64	10.46	10.28	10.10	9.92	9.74	9.56	9.39	9.21	9.07		
	55%	11.02	10.76	10.56	10.37	10.18	9.99	9.80	9.61	9.42	9.23	9.05	8.90	11.02	10.76	10.56	10.37	10.18	9.99	9.80	9.61	9.42	9.23	9.05	8.90		
60%	10.95	10.67	10.47	10.27	10.06	9.86	9.67	9.47	9.27	9.07	8.88	8.72	10.95	10.67	10.47	10.27	10.06	9.86	9.67	9.47	9.27	9.07	8.88	8.72			
65%	10.87	10.58	10.36	10.15	9.94	9.73	9.53	9.32	9.11	8.91	8.70	8.54	10.87	10.58	10.36	10.15	9.94	9.73	9.53	9.32	9.11	8.91	8.70	8.54			
70%	10.78	10.47	10.25	10.03	9.81	9.59	9.38	9.16	8.95	8.73	8.52	8.35	10.78	10.47	10.25	10.03	9.81	9.59	9.38	9.16	8.95	8.73	8.52	8.35			
75%	10.67	10.35	10.13	9.90	9.67	9.45	9.22	9.00	8.77	8.55	8.33	8.15	10.67	10.35	10.13	9.90	9.67	9.45	9.22	9.00	8.77	8.55	8.33	8.15			
80%	10.55	10.23	9.99	9.76	9.52	9.29	9.06	8.83	8.60	8.36	8.13	7.95	10.55	10.23	9.99	9.76	9.52	9.29	9.06	8.83	8.60	8.36	8.13	7.95			
85%	10.42	10.09	9.85	9.61	9.37	9.13	8.89	8.65	8.41	8.17	7.93	7.74	10.42	10.09	9.85	9.61	9.37	9.13	8.89	8.65	8.41	8.17	7.93	7.74			
90%	10.29	9.95	9.70	9.45	9.21	8.96	8.71	8.47	8.22	7.97	7.73	7.53	10.29	9.95	9.70	9.45	9.21	8.96	8.71	8.47	8.22	7.97	7.73	7.53			
95%	10.15	9.80	9.55	9.29	9.04	8.78	8.53	8.28	8.02	7.77	7.52	7.32	10.15	9.80	9.55	9.29	9.04	8.78	8.53	8.28	8.02	7.77	7.52	7.32			
100%	9.99	9.64	9.38	9.12	8.86	8.60	8.34	8.08	7.82	7.56	7.30	7.10	9.99	9.64	9.38	9.12	8.86	8.60	8.34	8.08	7.82	7.56	7.30	7.10			

(b) Electricity:

		Ride-hailing battery electric vehicle stock % 2030:																									
		12%	16%	19%	22%	26%	29%	32%	35%	38%	42%	45%	47%	Ride-hailing battery electric vehicle sales % 2030:													
		18%	25%	30%	35%	40%	45%	50%	55%	60%	65%	70%	74%														
Ride-hailing demand	0.29%	0.86	0.86	0.86	0.86	0.86	0.86	0.86	0.86	0.86	0.86	0.86	0.86	0.86	0.86	0.86	0.86	0.86	0.86	0.86	0.86	0.86	0.86	0.87			
	5%	0.87	0.88	0.90	0.91	0.92	0.93	0.94	0.95	0.97	0.98	0.99	1.00	0.87	0.88	0.90	0.91	0.92	0.93	0.94	0.95	0.97	0.98	0.99	1.00		
	10%	0.88	0.91	0.93	0.95	0.97	1.00	1.02	1.04	1.06	1.09	1.11	1.13	0.88	0.91	0.93	0.95	0.97	1.00	1.02	1.04	1.06	1.09	1.11	1.13		
	15%	0.88	0.92	0.96	0.99	1.02	1.05	1.08	1.12	1.15	1.18	1.21	1.24	0.88	0.92	0.96	0.99	1.02	1.05	1.08	1.12	1.15	1.18	1.21	1.24		
	20%	0.88	0.94	0.98	1.02	1.06	1.10	1.14	1.19	1.23	1.28	1.33	1.36	0.88	0.94	0.98	1.02	1.06	1.10	1.14	1.19	1.23	1.28	1.33	1.36		
	25%	0.88	0.95	1.00	1.05	1.10	1.15	1.20	1.26	1.32	1.37	1.43	1.47	0.88	0.95	1.00	1.05	1.10	1.15	1.20	1.26	1.32	1.37	1.43	1.47		
	30%	0.87	0.95	1.01	1.07	1.13	1.20	1.26	1.32	1.39	1.45	1.52	1.57	0.87	0.95	1.01	1.07	1.13	1.20	1.26	1.32	1.39	1.45	1.52	1.57		
	35%	0.87	0.95	1.02	1.09	1.16	1.24	1.31	1.38	1.45	1.52	1.59	1.65	0.87	0.95	1.02	1.09	1.16	1.24	1.31	1.38	1.45	1.52	1.59	1.65		
	40%	0.86	0.96	1.03	1.11	1.19	1.27	1.35	1.43	1.51	1.58	1.66	1.72	0.86	0.96	1.03	1.11	1.19	1.27	1.35	1.43	1.51	1.58	1.66	1.72		
	45%	0.85	0.95	1.04	1.13	1.21	1.30	1.38	1.47	1.55	1.63	1.72	1.78	0.85	0.95	1.04	1.13	1.21	1.30	1.38	1.47	1.55	1.63	1.72	1.78		
	50%	0.83	0.95	1.05	1.14	1.23	1.32	1.41	1.50	1.59	1.68	1.77	1.84	0.83	0.95	1.05	1.14	1.23	1.32	1.41	1.50	1.59	1.68	1.77	1.84		
	55%	0.82	0.95	1.05	1.15	1.24	1.34	1.44	1.53	1.62	1.72	1.81	1.89	0.82	0.95	1.05	1.15	1.24	1.34	1.44	1.53	1.62	1.72	1.81	1.89		
60%	0.80	0.95	1.05	1.15	1.25	1.35	1.45	1.55	1.65	1.75	1.85	1.93	0.80	0.95	1.05	1.15	1.25	1.35	1.45	1.55	1.65	1.75	1.85	1.93			
65%	0.79	0.94	1.04	1.15	1.26	1.36	1.47	1.57	1.68	1.78	1.88	1.96	0.79	0.94	1.04	1.15	1.26	1.36	1.47	1.57	1.68	1.78	1.88	1.96			
70%	0.77	0.93	1.04	1.15	1.26	1.37	1.48	1.59	1.69	1.80	1.91	2.00	0.77	0.93	1.04	1.15	1.26	1.37	1.48	1.59	1.69	1.80	1.91	2.00			
75%	0.75	0.91	1.03	1.14	1.26	1.37	1.48	1.60	1.71	1.82	1.93	2.02	0.75	0.91	1.03	1.14	1.26	1.37	1.48	1.60	1.71	1.82	1.93	2.02			
80%	0.74	0.90	1.02	1.14	1.25	1.37	1.49	1.60	1.72	1.84	1.95	2.05	0.74	0.90	1.02	1.14	1.25	1.37	1.49	1.60	1.72	1.84	1.95	2.05			
85%	0.71	0.88	1.00	1.12	1.25	1.37	1.49	1.61	1.73	1.85	1.97	2.06	0.71	0.88	1.00	1.12	1.25	1.37	1.49	1.61	1.73	1.85	1.97	2.06			
90%	0.69	0.86	0.99	1.11	1.24	1.36	1.49	1.61	1.73	1.86	1.98	2.08	0.69	0.86	0.99	1.11	1.24	1.36	1.49	1.61	1.73	1.86	1.98	2.08			
95%	0.67	0.84	0.97	1.10	1.23	1.35	1.48	1.61	1.74	1.86	1.99	2.09	0.67	0.84	0.97	1.10	1.23	1.35	1.48	1.61	1.74	1.86	1.99	2.09			
100%	0.64	0.82	0.95	1.08	1.21	1.34	1.47	1.60	1.74	1.87	2.00	2.10	0.64	0.82	0.95	1.08	1.21	1.34	1.47	1.60	1.74	1.87	2.00	2.10			

Figure ES-7. Energy consumption (quads) in 2030 for the case with charging infrastructure growth: (a) gasoline consumption (quads) and (b) electricity consumption (quads).

Conclusion and Recommendations for Future Work

The AFI Pillar conducted multiple case studies to investigate how charging infrastructure design influences economics for the charging network provider, the ability of electric mobility providers (ride-hailing EV drivers, car-sharing fleets, and AEV fleets) to serve customers, and the ability of motor carriers to efficiently deliver freight. Because many factors important to these relationships will always be case-specific for different cities, fleets, and drivers, it is difficult to draw generalizable principles from this research. Nevertheless, some trends are evident in the Pillar’s findings.

- **Design charging networks around demand.** Strategic siting of public charging stations in locations where ride-hailing drivers need to use them benefits charging providers even if those locations require expensive installations. Therefore, charging infrastructure planners may consider partnering with TNCs, automakers, or other organizations who understand ride-hailing vehicle driving behavior.
- **Look beyond simply adding more charging stations.** Planners should be aware that there is a limit to the gains afforded to an electric vehicle fleet by increasing the number of available charging stations and plugs. This is true even if the network becomes widespread and charging stations are optimally sited. Simulation of a ride-hailing fleet in the San Francisco Bay Area demonstrated that when employing low-range EVs (i.e., BEV100s) and 50-kW DCFC stations, adding more charging infrastructure cannot cost-effectively increase the capacity of the fleet in terms of passenger miles per vehicle per day. This is because charging time becomes the bottleneck limiting vehicle time in service. The value of increasing charging power beyond 50 kW to reduce downtime for charging was evident for all use cases studied. A similar effect is achieved by adopting EVs with longer electric driving range to reduce charging frequency. Case studies suggest that longer EV range should be combined with increased access to charging infrastructure and/or higher-power charging to provide EVs with comparable utility to their ICEV counterparts.
- **Recognize there is still value in slow charging.** Case studies suggest that exploiting times when vehicles are naturally parked for long periods of time is an alternative to faster charging. This is already conventional wisdom for personal-use EV drivers, and it is clear from the case study comparing TNC and taxi drivers with and without access to overnight charging. However, it is less obvious when commercial fleets that respond to time-varying customer demand can afford to charge vehicles slowly. Electric car-sharing, ride-hailing, and truck fleet managers that understand when downtime has minimal impact on their ability to serve customers can exploit this knowledge to charge slowly during those times using less expensive, low-power charging infrastructure.

- **Optimize AEV fleets through coordinated control.** Intelligent fleet management, using optimization routines to manage repositioning and charging of the fleet, can increase productivity and revenue potential by increasing the number of ride requests satisfied. At the same time, this approach to fleet management can decrease wasted driving (empty miles), energy consumption, and cost. It can also enable fleet downsizing and help AEVs make more effective use of available charging infrastructure.
- **Leverage DWPT to keep automated transit vehicles on the road.** DWPT technology has the potential to allow driverless shuttle buses to operate with near-zero downtime, which greatly reduces operating cost compared to equivalent human-driven shuttle buses without DWPT. Implementing such a system also has the potential to reduce the size and cost of vehicle batteries by more than 50%. This technology can be extended to highway vehicles.

Finally, the effort required to design and deploy charging infrastructure to support electrification of transportation modes beyond light-duty, personal-use vehicles has the potential for large returns to the nation. Electrification of ride-hailing for personal mobility and heavy-duty trucking for freight movement has the potential to significantly reduce U.S. transportation energy consumption.

Additional research is needed to further explore the complex cost/benefit tradeoffs inherent with planning charging infrastructure for EVs in different market segments. In partnership with industry, future research should build on the tools developed and findings produced by this research to plan and optimize economically viable, grid-integrated charging infrastructure to serve personal-use, ride-hailing, transit, and freight vehicles within and between diverse urban areas.

Table of Contents

1.	Introduction.....	26
1.1	Electrification of Diverse Transportation Modes Prompts New Questions About Charging Infrastructure.....	26
1.2	Lessons from Early Electric Shared-Mobility Deployments	27
1.3	U.S. Department of Energy’s Systems and Modeling for Accelerated Research in Transportation (SMART) Mobility Advanced Fueling Infrastructure Pillar.....	28
1.4	Overview of Previous Work and Gaps in Literature.....	28
1.5	Research Questions Addressed.....	29
2.	Research Approach and Results	31
2.1	Understanding New Market Segments for Transportation Electrification	31
2.1.1	Light-duty Vehicle Market Segmentation	31
2.1.2	Freight-Trucking Industry Segmentation.....	45
2.2	Charging Network Design Tradeoffs.....	56
2.2.1	Charging Network Design to Support Electric Ride-hailing Vehicles	56
2.2.2	Charging Network Design to Support Electric Vehicles in Free-Floating Car-Sharing Fleets	80
2.2.3	Charging Network Design to Support Electric Trucks for Freight Delivery	86
2.3	Exploring New Paradigms Created by Automated-Vehicle Charging	94
2.3.1	Charging Decision Making for Automated Ride-Hailing Fleets.....	95
2.3.2	Dynamic Wireless Charging for Automated Electric Transit	109
2.4	National Impact of Charging Infrastructure for Electric Ride-hailing Vehicles.....	128
2.4.1	Key Findings	128
2.4.2	Introduction.....	128
2.4.3	Research Approach.....	128
2.4.4	Quantifying Energy Consumption of National Light-duty Passenger Vehicle Fleet.....	134
3.	Conclusion	141
3.1	Summary of Findings and Their Implications	141
3.1.1	What are the characteristics of potential future transportation market segments employing human-driven and automated EVs that charging infrastructure will need to serve?	141
3.1.2	What are the cost/benefit tradeoffs inherent with different approaches to designing charging infrastructure to serve light-duty human-driven and automated electric passenger vehicles?	142
3.1.3	What is needed to understand tradeoffs inherent with different approaches to designing charging infrastructure for Class 7/8 electric trucks for freight transport?.....	142
3.1.4	What is the potential for automated vehicle charging to create new charging paradigms that improve the automated, electric ride-hailing and transit?.....	143

3.1.5	What is the benefit to the nation of charging infrastructure deployed to serve ride-hailing EVs?	143
3.2	Recommendations for Future Work	143
4.	References	145
	Appendix A: Total Cost of Ownership of Ride-Hailing Vehicles	156
	Appendix B: Charging Network Design to Support Electric Vehicles in Free-floating Car-sharing Fleets	159
	Appendix C: Dynamic Wireless Power Transfer System Modeling	170
	Appendix D: National Energy Impact of Charging Infrastructure for Ride-Hailing EVs.....	178
	Appendix E: Calculating Monthly Electricity Bill	181

List of Figures

Figure ES-1. Map visualizing the driving and public charging locations (alternating current [AC] Level 2 and direct current [DC] fast chargers indicated by the blue circles) used by a single ride-hailing EV driver in Sacramento, California.....	6
Figure ES-2. Populus survey results for TNC driver share by residence type, tenure, and income.....	7
Figure ES-3. Heatmaps of simulated DCFC demand in Columbus, Ohio from electric taxi fleet with access to overnight charging (at left) and without (at right).....	9
Figure ES-4. Spatial distribution of simulated charging stations in the San Francisco Bay Area by network type. Note: “depot” means charging stations that are dedicated to the AEV fleet, “Sparse,” “Rich-10%,” “Rich-20%,” and “Rich-100%” are DCFC networks of differing sizes used in simulation scenarios.....	11
Figure ES-5. Optimal locations of ten new charging stations (blue stars) to serve a free-floating electric car-sharing fleet, based on historical trip information.....	12
Figure ES-6. The overall average deadhead miles per vehicle per day for different fleet sizes.....	13
Figure ES-7. Energy consumption (quads) in 2030 for the case with charging infrastructure growth: (a) gasoline consumption (quads) and (b) electricity consumption (quads).....	15
Figure 1-1. The "charging pyramid" guides planners to concentrate charging infrastructure installations at residences and workplaces.....	29
Figure 2-1. Characterization of the light-duty EV market.....	33
Figure 2-2. Map visualizing RideAustin passenger drop-off locations in Austin, Texas. More frequent drop-off locations are depicted with a brighter color.....	34
Figure 2-3. Map visualizing the density of CYC trips in Columbus, Ohio. More frequently traveled road sections are shown in a brighter color.....	35
Figure 2-4. Map visualizing driving and public charging locations (AC Level 2 and DC fast chargers indicated by the blue circles) used by a single ride-hailing EV driver in Sacramento, California.....	36
Figure 2-5. Populus survey results for TNC driver share by driving frequency and income.....	37
Figure 2-6. Populus survey results for TNC driver share by residence type, tenure, and income.....	38
Figure 2-7. Populus survey results for TNC driver share by motivation and income.....	38
Figure 2-8. Daily VMT (dVMT) distributions from full-time RideAustin drivers (Blue = all driving days, orange = maximum distance driving day per vehicle).....	39
Figure 2-9. Daily VMT comparison between CYC and full-time RideAustin drivers.....	40
Figure 2-10. Observed initial/final state of charge distributions for residential and public charge events from EVs operating within TNC fleets.....	41
Figure 2-11. Total cost of ownership for different vehicle types for varying miles driven per year.....	44
Figure 2-12. Vehicle ownership cost parametric sensitivity analysis, based on the driving and simulated charging behavior of the median RideAustin TNC driver.....	45
Figure 2-13. Miles traveled per vehicle.....	47
Figure 2-14. Fuel economy.....	47

Figure 2-15. Distribution of trucks and annual miles within weight class by primary trip distance. 51

Figure 2-16. Average annual miles traveled per vehicle by primary trip distance and vehicle weight class. 52

Figure 2-17. An example of truckload carrier operation. 53

Figure 2-18. An example of less-than-truckload carrier operation. 53

Figure 2-19. Distribution of trucks and miles by truck weight class for truckload and less-than-truckload service. Source: U.S. Department of Commerce, Bureau of the Census, 2002 Vehicle Inventory and Use Survey. 54

Figure 2-20. Distribution of miles by primary-trip distance for truckload and less-than-truckload service. Source: U.S. Department of Commerce, Bureau of the Census, 2002 Vehicle Inventory and Use Survey..... 54

Figure 2-21. EVI-Pro example from Austin, Texas of simulating unconstrained demand using a dense lattice of chargers (left) and clustering resulting demand to form a public network (right). 57

Figure 2-22. FCSPlan and BEAM integration. 58

Figure 2-23. Hosting venues of Electrify America's DC fast chargers. 59

Figure 2-24. Hosting venues of EVGo's DC fast chargers. 59

Figure 2-25. Correlation between cost efficiency and number of charging sessions at the 12 simulated DCFC stations in Columbus. 63

Figure 2-26. Image of candidate location for DC fast charger 10. Satellite imagery credit: © 2017 Google, Map Data ©2017 Tele Atlas..... 65

Figure 2-27. Total cost of charging infrastructure per site, calculated on a per-session basis. Error bars represent the expected range of installation cost, which varies depending on the specific location chosen for the charging site..... 66

Figure 2-28. Heatmaps of simulated charging demand in Columbus, Ohio from electric taxi fleet for infrastructure Scenarios 1 (at left) and 2 (at right). 69

Figure 2-29. Spatial distribution of DC fast chargers in San Francisco Bay Area by network type. Depot chargers are exclusively available to AEV ride-hailing vehicles while public chargers are shared between human-operated ride-hailing and personal-use EV drivers. 72

Figure 2-30. Number of vehicles (left) in all simulation scenarios and number of fast chargers (right) in each infrastructure scenario 73

Figure 2-31. Number of charging sessions by infrastructure scenario (x-axis), vehicle range scenario (panel), and charger power (data point color) 74

Figure 2-32. Passenger miles served by ride-hailing EVs by infrastructure scenario (x-axis), EV range scenario (panel), and charger power scenario (trend color). 75

Figure 2-33. Distribution of the ride-hailing fleet into operating states over the 24-hour simulation period for scenario with 100-mile range EVs and sparse, 50-kW charging infrastructure..... 76

Figure 2-34. Distribution of the ride-hailing fleet into operating states over the 24-hour simulation period for scenario with 100-mile range EVs and rich, 50-kW charging infrastructure. 77

Figure 2-35. Cost per passenger-mile traveled for ride-hailing EVs (both human-driven and AEVs) for both DCFC networks (public and depot) and for cost of electricity necessary to fuel the fleet. 78

Figure 2-36. Average passenger-miles served per vehicle as a function of total amortized daily cost of operating a ride-hailing fleet (both human-driven and AEVs), showing the cost effectiveness of serving additional passenger travel demand through investments in increased vehicle battery capacity, charging power, and number of charging plugs, while holding the total number of ride-hailing vehicles constant. 79

Figure 2-37. Computational framework of the CMIP model. 81

Figure 2-38. The impact of adding a new charging station on total travel and charging times. Travel time includes the time a vehicle spends during traveling from trip origin to a DCFC. Charging time is the total time to charge the vehicle based on the charging rate model, initial battery SOC, and desired final SOC..... 83

Figure 2-39. The optimal locations of an additional ten new charging stations (blue stars) based on historical trip information. The new locations are dispersed across the region. 84

Figure 2-40. The impact of an increased number of trips on average downtime per charging trip from the base-case scenario. 85

Figure 2-41. Average downtime per charging trip as the number of 50-kW charging stations increases (base case) and as the number of 100-kW charging stations increases (case where charging power is doubled). 86

Figure 2-42. Distribution routes for 22 trucks originating from their home RDC near Dallas, Texas. Some destinations are shown as red squares (RDCs) and green stars (retail stores). 89

Figure 2-43. Circuits driven by a single truck over several days, each starting and ending at the home RDC (yellow star). 89

Figure 2-44. Range remaining at the end of each trip for six successive circuits. Charging was only allowed at RDCs, marked with stars. 91

Figure 2-45. Range remaining at each stop on a journey of six successive circuits if charging is available at each stop. 92

Figure 2-46. Distribution of range remaining at the end of trips for 300-mile range trucks charging at 150 or 350 kW at the end of every trip. 93

Figure 2-47. Distribution of range remaining at the end of trips for 500-mile range trucks charging at 150 or 350 kW at the end of every trip. 94

Figure 2-48. Uber and Lyft customer pickup location distribution in San Francisco on a weekday. Source: tncstoday.sfcta.org. 96

Figure 2-49. A diagram of centralized framework for AEV fleet dispatching and charging management. 97

Figure 2-50. A promising procedure for fleet dispatching and charging management. 98

Figure 2-51. A potential procedure for idle-vehicle management. 98

Figure 2-52. Information flow of heuristic approach. 98

Figure 2-53. Information flow of optimization-based approach. 99

Figure 2-54. Probability density of time distribution across a day for both pickup and drop-off actions..... 100

Figure 2-55. Spatial distribution of public charging stations (AC Level 2 and DCFC stations) in New York City..... 100

Figure 2-56. The overall average zero-occupancy miles traveled per vehicle per day for different fleet sizes. 102

Figure 2-57. Detailed zero-occupancy vehicle miles traveled, including: (a) average reposition miles traveled per vehicle per day, (b) average allocation miles traveled per vehicle per day, (c) average charging trip miles traveled per vehicle per day. 103

Figure 2-58. Average charging trip miles per vehicle per day, which is an enlarged version from Figure 3 58(c). 103

Figure 2-59. Average increased zero occupancy vehicle miles per vehicle allocation mile reduction..... 104

Figure 2-60. Zero-occupancy vehicle miles traveled for simulation case where all charging stations have 50-kW DCFC 105

Figure 2-61. Ratio of ride requests successfully served under different fleet sizes and different fleet management strategies: (a) mixed AC Level 2 and DCFC stations; (b) all 50-kW DCFC stations..... 106

Figure 2-62. Average charging downtime per vehicle per day: (a) mixed AC Level 2 and DCFC stations; (b) all 50-kW DCFC stations. 106

Figure 2-63. Overall average utilization rate for the entire charging station network with mixed AC Level 2 and DCFC when using optimization (left) and heuristic (right) approaches for fleet management. 107

Figure 2-64. Overall average utilization rate for the entire charging station network with all 50kW chargers when using optimization (left) and heuristic (right) approaches for fleet management..... 108

Figure 2-65. Block diagram of a typical track-based DWPT system. 110

Figure 2-66. An example of a DWPT system using paralleled short sectional 100-kW primary couplers and arrays of pickup couplers. 112

Figure 2-67. Illustration of groups of AEVs over a DWPT enabled roadway..... 113

Figure 2-68. WPTSim, a system planning and optimization platform. 114

Figure 2-69. Wireless charger power model including (a) power profiles in travel and lane direction and (b) a look-up table integrated with WPTSim for a 100-kW system..... 115

Figure 2-70. Pareto solutions from the optimization model for two different cases (LDV only [blue] and LDV and HDV [red])..... 116

Figure 2-71. Optimization output for the short-term and long-term cases at 55 and 70 mph. 117

Figure 2-72. The hypothetical diamond-shape automated mobility network in SUMO tool..... 118

Figure 2-73. Optimal driving performance of SAEV..... 119

Figure 2-74. Test network at Greenville, South Carolina..... 120

Figure 2-75. Current driving performance. 120

Figure 2-76. Greenville SUMO simulation network and fixed-route configuration. 121

Figure 2-77. Optimal driving performance. 121

Figure 2-78. NAVYA Arma SAEV route at University of Michigan, Ann Arbor, Michigan. 122

Figure 2-79. DC kWh/mile versus aux. load for ARMA 1..... 123

Figure 2-80. DC kWh/mile versus aux. load for ARMA2..... 123

Figure 2-81. Current driving performance of Arma 1 and Arma 2..... 124

Figure 2-82. SAEV’s performance, considering different charging technology designs for present- (left) and future-day (right) operations..... 127

Figure 2-83. Survival functions and vehicle-miles traveled for car and light trucks: (a) car survival rate, (b) light truck survival rate, (c) car vehicle-miles traveled, and (d) light truck vehicle-miles traveled. 130

Figure 2-84. Analytical framework of national energy impacts of ride-hailing and personal EVs..... 132

Figure 2-85. Number of chargers with respect to number of full-time ride-hailing battery EVs per square mile, based on simulation of RideAustin data in EVI-Pro. 133

Figure 2-86. Number of grid cells and percentages of total trips ending in Chicago population-density groups..... 133

Figure 2-87. Probabilistic approach to estimate required charging coverage, based on percentage of trips served by ride-hailing BEVs..... 134

Figure 2-88. National energy impact of electrified ride-hailing light-duty vehicles in 2030 (based on Austin simulation results). RH = ride-hailing, EV = electric vehicles, +Infrastructure = charging infrastructure growth in response to number of ride-hailing EVs. 136

Figure 2-89. National energy impact of electrified ride-hailing light-duty vehicles in 2030, based on Columbus simulation results. 137

Figure 2-90. National energy consumption reduction (shown as percentages) as a function of ride-hailing demand, BEV market penetration, and charging infrastructure..... 138

Figure 2-91. Energy consumption (quads) in 2030 for the case with charging infrastructure growth: (a) gasoline consumption, and (b) electricity consumption..... 139

Figure 2-92. National carbon emissions reduction, shown as percentages, original unit is million metric tons of carbon equivalent (MMTC) as a function of ride-hailing demand, BEV market penetration, and charging infrastructure..... 140

Figure 2-93. National carbon emissions at different electricity grid mixes. 140

Figure A- 1. Cost variation among BEV150 and BEV250 depending upon charging availability. ‘Home’ means the driver can charge at home, ‘Public L2’ means the driver does not have home charging, but can substitute with Level 2 charging, and ‘DCFC Only’ means the driver must rely only on DCFC..... 157

Figure A- 2. Cost comparison when BEV drivers have Austin Energy BEV-specific home electricity rate 158

Figure A- 3. Comparison of weekly costs for full-time driver with weekly lease rate offered by Maven for use of a Chevrolet Bolt..... 158

Figure B- 1. Utilization probabilities of three DC fast-charging stations in Seattle in 2014. Historical charging behavior data show different use patterns across charging stations

over time. The low utilization probabilities in these data are caused by the low penetration of EVs in 2014. 160

Figure B- 2. Average waiting time of three DC fast-charging stations in Seattle in 2012. Each DCFC includes two subfigures to illustrate the average waiting time during both weekdays and weekends, respectively. 161

Figure B- 3. Ending SOC of 2014 BMW i3 relative to charging time when charging using a 50-kW DCFC. The charging time of the y axis in this figure is calculated as the time cost when the SOC increases from zero to each ending SOC..... 162

Figure B- 4. The energy-cost distribution per mile relative to vehicle speed. The energy cost per mile of the 2014 BMW i3 is relative to the average vehicle speed (blue dots) and the fitted average energy-cost prediction function (orange line). 163

Figure B- 5. Assignment EVs to charging stations in a time-space network. Each node represents the charge state of an individual vehicle. 165

Figure B- 6. An example of the various types of trip assignments with one trip, three charging stations, and four periods. Assignment types defined by k33, k23, k13, k123, k22 , k11, k12 are shown as colored arrows. 167

Figure C- 1. Power consumption of LDV and HDV at constant speeds..... 170

Figure C- 2. Example 100 kW dynamic WPT secondary coil parameters for a roadway embedded ferrite track. 171

Figure C- 3. Airgap field distribution for the 100kW DWPT system deployment. 172

Figure C- 4. Variation of track-to-vehicle mutual inductance with respect to vehicle position..... 172

Figure C- 5. Battery cell cost (\$/kWh) at different C-rate and Δ SOC (NMC622-Graphite, 85-kWh, 900-DCV battery pack, \$80/kWh for 1C, 80% Δ SOC) 177

Figure C- 6. Battery cell cost coefficient at different charging power and battery capacity 177

List of Tables

Table 2-1. Distribution of RideAustin drivers segmented by activity level..... 39

Table 2-2. Ride-hailing vehicle driver segmentation results. 42

Table 2-3. Estimated annual VMT driven by medium and heavy-duty trucks to transport freight in the U.S. 46

Table 2-4. Factors by which to segment the freight-trucking industry. 48

Table 2-5. Distribution of fleets and trucks by fleet size..... 48

Table 2-6. Ten largest for-hire carriers in the United States in 2019..... 49

Table 2-7. Ten largest private motor carriers in the United States in 2019 50

Table 2-8. Infrastructure requirements that would be necessary to support electrification of the two vehicle groups (5,000 personal vehicles or 3,726 ride-hailing vehicles plus 1,108 personal vehicles). 61

Table 2-9. Simulated use profiles of 12 DCFC stations by personal-use and ride-hailing EVs during a single day in Columbus, Ohio..... 61

Table 2-10. DC fast charger installation cost attribute data collected. 64

Table 2-11. Regression model coefficient estimates for the cost to install a DCFC station. 65

Table 2-12. Selected EVI-Pro Results for Scenario 1 and 2 for analysis of 35,000 CYC vehicle-days simulated as being driven by BEV250s. 68

Table 2-13. Three parameters (vehicle range, charger power capacity, and charging network size) varied across the 24 simulated scenarios with other key assumptions used in this analysis. 71

Table 2-14. Number of charging stations in each modeling scenario. 82

Table 2-15. The number of charging stations and fleet downtime for traveling, charging and waiting in minutes. 82

Table 2-16. Approximate charge times (in hours) for different types of chargers based on a 2 kWh/mile usage. 88

Table 2-17. Summary table of truck sample. 90

Table 2-18. Number and percentage of all trips driven by the fleet that ended with range remaining without public charging during the trip. 93

Table 2-19. Optimal design solution. 118

Table 2-20. Performance parameters. 118

Table 2-21. Auxiliary load results for Arma1 and 2 considering different charger efficiency and vehicle status. Min was estimated assuming the vehicle was ON at parking. Max was estimated assuming the vehicle was OFF at parking. 123

Table 2-22. Parameters for present and future-day. 125

Table 2-23. Search variables for different optimizations 125

Table 2-24. Planning optimization results for different charging technologies, considering different operating scenarios (present- and future-day). 126

Table 2-25. Performance comparison among QDWPT, DCFC, and L2 charging technology. 127

Table 2-26. Daily trip stops by ride-hailing BEV penetration levels. 134

Table 2-27. Definition of low ride-hailing demand case and high ride-hailing demand case. 135

Table 2-28. Grid mix assumed for each scenario. 140

Table A- 1. Vehicle characteristics. 157

Table B- 1. Coefficients of the charging time estimation model. 162

Table B- 2. Definitions of sets and input parameters for the IP model. 166

Table C- 1. Vehicle parameters. 170

Table C- 2. Efficiency analysis of track-based DWPT system with respect to the track length. 172

Table C- 3. Optimization variables and parameters 175

Table E- 1. Input parameters needed to calculate electricity bills 181

1. Introduction

1.1 Electrification of Diverse Transportation Modes Prompts New Questions About Charging Infrastructure

Since the introduction of modern electric vehicles (EVs) in 2010, charging infrastructure installed in the United States has been steadily growing to meet the changing needs of a small but growing EV market.⁹ By Spring 2019, an estimated 4,446 private and 28,122 public charging stations were installed nationwide, according to the U.S. Department of Energy's (DOE's) Alternative Fuels Data Center (AFDC).¹⁰ In conjunction with the building of charging infrastructure, academic, government, and private non-residential organizations have conducted numerous studies and research projects to understand the charging needs of EV drivers and to develop new methods for efficiently planning charging infrastructure.^{11, 12, 13, 14} The vast majority of this work has been focused on developing charging infrastructure to serve privately owned, light-duty EVs operated for personal use.

During this same time period, shared-mobility services have risen in popularity. Enabled by information technology, ridesourcing companies now offer inexpensive, flexible, convenient personal transportation as an alternative to conventional taxi and delivery services. Transportation network companies (TNCs) such as Uber and Lyft have popularized the practice of private-vehicle owners providing ride-hailing services using their own cars. The number of rides offered by TNCs has increased dramatically; the ride-hailing company Uber took 5 years to deliver its first billion rides, but delivered its second billion in the first half of 2016 alone.¹⁵ By December 2018, Uber had delivered 10 billion trips worldwide.¹⁶ Car-sharing services have also grown in popularity in recent years. These commercial services operate their own vehicle fleets and offer various short-term vehicle rental options to members. Car-sharing companies had nearly 5 million members worldwide in 2014, up from 350,000 in 2006, and are projected to have more than 23 million members globally by 2024.¹⁷

In parallel with the rise of shared mobility, the technology (tech) and automotive industries have made significant investments to develop fully automated self-driving vehicles. A plethora of established and startup companies such as Waymo, Cruise, Zoox, Tesla Motors, Uber, Lyft, and Ford Motor Company are actively developing and demonstrating self-driving vehicle technology. Waymo was the first company to launch an automated ride-hailing fleet for paying customers; in 2018, its Waymo One service began operating commercially owned, autonomous vehicles to provide rides for a limited membership of consumers in the greater Phoenix, Arizona, metropolitan area.¹⁸ Other companies have announced that they will introduce automated ride-hailing services in other cities soon.¹⁹ Automakers, shared-mobility service companies, tech companies, and market analysts all predict that automated ride-hailing vehicles will bring about disruptive market changes.^{20, 21}

Shared and automated mobility are seemingly compelling cases for electrification. Because shared vehicles, such as TNC ride-hailing vehicles, traditional taxis, and car-sharing fleet vehicles, are typically driven much farther per year than personal-use vehicles, the high efficiency of EVs can significantly reduce fuel consumption over the life of a vehicle relative to an equivalent gas-powered vehicle. This equates to lower lifetime fuel cost and energy impact. These factors, plus the low cost of electricity relative to gasoline and potential for reduced maintenance on an EV, are often equated with low overall cost of ownership. According to one report, driving an EV can save full-time ride-hailing drivers more than \$2,500 per year compared to a similar vehicle powered by an internal combustion engine, assuming drivers can charge at home and gasoline cost of \$2.50 per gallon.²² This report will show that those estimates are overly optimistic for many ride-hailing drivers; nevertheless, the notion of electrification of high-mileage ride-hailing vehicles for financial benefit is receiving a lot of attention.

The same reasons lead to transportation electrification in the United States growing beyond light-duty passenger cars. An increasing variety of truck manufacturers, transit agencies, shipping companies, and other organizations are conducting pilot deployments of medium- and heavy-duty electric trucks and buses to transport people and goods. For example, UPS and FedEx are operating medium- and heavy-duty electric delivery vehicles in focused deployments.^{23, 24, 25} Mainstream truck manufacturers like Daimler Trucks North America and Volvo Trucks and startups Tesla and Nikola have announced plans to produce Class 8 electric

trucks for short-haul freight transport.^{26, 27, 28} Public transit agencies around the United States have added electric transit buses to their fleets.^{29, 30, 31}

Efforts are also underway to develop automated trucks and buses. To improve safety and reduce operating cost, numerous truck manufacturers, logistics companies, and startups apply vehicle automation technology to medium- and heavy-duty trucks for goods delivery.^{32, 33} At least one manufacturer, Tesla Motors, is exclusively developing *electric*, automated trucks.³⁴ As for the movement of people, startups like Local Motors and EZMile are piloting automated electric shuttles in cities and on campuses in multiple United States regions in an effort to develop the next generation of public transit.^{35, 36, 37, 38}

As the transportation market and vehicle technology change, charging infrastructure technology also advances. Extreme or ultra-fast charging is now on the market, with charging-power capacity up to 350 kW to charge long-range EVs in 30 minutes.³⁹ Dynamic wireless power transfer (DWPT), also called in-road wireless charging, could become the automotive equivalent to aviation's in-flight refueling, eliminating the need to stop at charging stations. Finally, EVs that can drive themselves can also make decisions about when and where to charge themselves, relieving drivers of this burden and eliminating range anxiety.

The electrification of increasingly diverse transportation modes and vehicle types raises many questions about how charging infrastructure should evolve to meet the needs of human-driven and automated EVs providing ride-hailing, car-sharing, automated transit, and freight-delivery services. What is the right kind of charging infrastructure for each mode? How much is needed? Where should it be located? After all, benefits of transportation electrification can only be realized if adequate, cost-effective charging infrastructure is in place to support it.

1.2 Lessons from Early Electric Shared-Mobility Deployments

The private sector has begun to plan and experiment with charging infrastructure that addresses emerging use cases for electrification. Early pilots of electric shared mobility have demonstrated that intentionally planned and well-designed charging infrastructure is critical for the success of a shared electric vehicle fleet.

In 2016, the Department of For-Hire Vehicles (DFHV) in Washington, D.C., launched an electric taxi program, issuing new cab licenses to drivers of first-generation Nissan LEAFs, a battery electric vehicle (BEV) with a 75-mile electric range (referred to as a BEV75). The DFHV provided a limited number of \$10,000 grants to help drivers cover the cost of a new car, but it did not involve itself in charging infrastructure planning or incentivization. Sparse charging opportunities within D.C. forced drivers to wait in line or travel outside D.C. to charge during shifts. This led to considerable downtime, lost revenue, and driver frustration.⁴⁰

Likewise, the New York City Taxi and Limousine Commission Electric Vehicle Pilot program that ran from 2013 to 2015 saw a reduction in service among EVs relative to conventional taxis because of sparse charging infrastructure. The four participants in the pilot drove BEV75s and had access to only two direct current (DC) fast chargers in Manhattan. These drivers averaged 15.5 trips per shift versus the industry-wide average of 20 trips per shift, because of the time they spent driving to and waiting at the two charging stations. The Taxi and Limousine Commission concluded that many more stations would be needed if more taxi fleets adopt EVs.⁴¹

In 2016, Car2go replaced all of its car-sharing EVs in San Diego with conventional vehicles, citing high expenses due to the lack of charging infrastructure and long charging time.⁴²

EVgo, one of the leading DC fast charging (DCFC) providers in the United States, entered into an agreement with shared-mobility company Maven, allowing Maven Gig ride-hailing drivers of Chevrolet Bolt EVs to charge for free in seven cities. EVgo found that demand for charging by ride-hailing EV drivers was so high that they were overwhelming the existing network. In 2018, EVgo announced a project with Maven to construct a charging network dedicated to Maven Gig drivers.⁴³

Looking forward, Electrify America has cited the importance of planning and deploying infrastructure to support shared and automated mobility as part of their \$300 million Cycle 2 National Zero Emission Vehicle Investment Plan. This plan focuses investment on DCFC in metro areas, in part to serve shared-mobility fleets.⁴⁴

Lessons learned and perspectives from industry clearly demonstrate that further research is warranted to better understand the charging infrastructure needs of emerging and future use cases for electrification.

1.3 U.S. Department of Energy’s Systems and Modeling for Accelerated Research in Transportation (SMART) Mobility Advanced Fueling Infrastructure Pillar

Because of this need, DOE developed a research agenda to examine the charging needs of human-driven and automated EVs providing ride-hailing, car-sharing, automated transit, and freight-delivery services. This endeavor became one of five research pillars in DOE’s SMART Mobility Consortium, a multi-year, multi-laboratory collaborative dedicated to further understanding the energy implications and opportunities of advanced mobility technologies and services. The SMART Mobility Consortium’s five research pillars are described as follows:

- Connected and Automated Vehicles (CAVs): Identifying the energy, technology, and usage implications of connectivity and automation and identifying efficient CAV solutions
- Mobility Decision Science (MDS): Understanding the human role in the mobility system including travel decision-making and technology adoption in the context of future mobility
- Multi-Modal Freight (MMF): Evaluating the evolution of freight movement and understanding the impacts of new modes for long-distance goods transport and last-mile package delivery
- Urban Science (US): Understanding the linkages between transportation networks and the built environment and identifying the potential to enhance access to economic opportunity
- Advanced Fueling Infrastructure (AFI): Understanding the costs, benefits, and requirements for fueling/charging infrastructure to support energy-efficient future mobility systems

The SMART Mobility Consortium creates tools and generates knowledge about how future mobility systems may evolve and identifies ways to improve their mobility energy productivity (MEP).^a The consortium also identifies R&D gaps that the Energy Efficient Mobility Systems Program may address through its advanced research portfolio and generates insights that will be shared with mobility stakeholders.

Between 2016 and 2019, researchers in the AFI Pillar used sophisticated modeling, simulation, and data analysis tools to investigate tradeoffs in different charging infrastructure network designs for human-driven and fully automated ride-hailing EVs, electric car-sharing fleets, automated shuttle buses for fixed-route transit, and freight-delivery truck fleets. The AFI Pillar also researched the impact of two potentially game-changing charging technologies—autonomous fleet management and DWPT—on automated and electrified fleet efficiency and productivity. Finally, the AFI Pillar assessed the potential of charging infrastructure installed to support shared mobility to influence mobility and energy-consumption trends on a national scale.

This report shares findings from this research to inform planners of charging infrastructure serving diverse transportation modes. The information in this report is intended to inform decisions about EVs and charging infrastructure deployment in shared and commercial fleets, thus lowering investment risk and increasing transportation efficiency and affordability. Although this report concludes that there is no “right” amount of charging infrastructure, the results of AFI Pillar research presented herein will highlight the value of different approaches to charging infrastructure network design to support future electric mobility.

1.4 Overview of Previous Work and Gaps in Literature

Much research to date has focused on understanding the charging behavior of EV drivers and describing the charging infrastructure required to satisfy their needs. Many behavioral observations discussed in literature and in the media have been translated into accepted principles that guide charging infrastructure planning decisions. For example, it is now considered conventional wisdom that most EV charging is done at home and work. This principle is often visualized with a triangle that represents the proportion of charging conducted at

^a MEP, a multimodal metric created by the SMART Mobility Laboratory Consortium, quantifies the effectiveness of mobility in a region, while taking energy and affordability aspects into consideration. For more information on MEP, see the Urban Science Pillar capstone report.

home, work, and other public locations, as shown in Figure 1-1. The charging pyramid, as it is sometimes called, is based on conjecture that was validated by studies of charging behavior.⁴⁵ Figure 1-1 shows the percent of charging events by location performed by MY11-13 Nissan LEAF drivers in the EV Project.

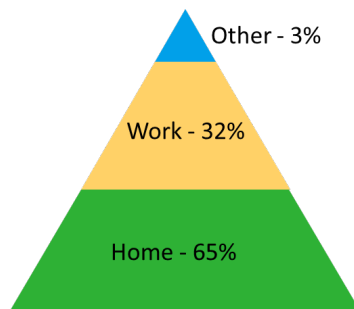


Figure 1-1. The "charging pyramid" guides planners to concentrate charging infrastructure installations at residences and workplaces. This figure shows the percent of charging events by location performed by MY11-13 Nissan Leaf drivers in the EV Project.⁴⁶

Other studies have identified that public DCFC may help address the needs of users with limited access to home charging, but do not eliminate the need for continued installation of better home, apartment, and workplace charging.^{47, 48}

However, it is important to recognize that these principles came from studies of privately owned, personal-use EVs, and they may not be transferrable to new mobility use cases, including electric taxi and TNC drivers who do not have access to charging at home, automated electric ride-hailing and electric car-sharing fleets, and medium- and heavy-duty EV cases.⁴⁹

Considerable additional research has focused on developing sophisticated methodologies to select charging station locations to serve various market segments and EV use cases. One study proposed a decision-support system built on a variant of the maximal covering location problem to optimize charging station locations for electric taxis.⁵⁰ Another study presented a data-driven, optimization-based approach to allocate chargers for BEV taxis throughout a city with the objective of minimizing the infrastructure investment.⁵¹ Two additional studies used a simulation approach for economic analysis considering possible configurations of numbers of electric taxis and numbers of charging stations, and the impacts on service quality compared to conventionally operated taxi fleets when facing increased demand.^{52, 53}

Additional research explored the management of a fleet of autonomous electric ride-hailing vehicles. Using simulation, the operation of shared, automated electric vehicles (SAEVs) has been examined under various vehicle range and charging infrastructure scenarios.^{54, 55, 56}

Unfortunately, the bulk of this research is idealized, and its outcomes are not used in practice. A major reason for this is that academic research tends to produce ideal, optimal charging infrastructure solutions for specific cases, without regard to real-world business constraints. Instead, research should provide practitioners generalizable knowledge that they can apply to understand the effects of cost/benefit tradeoffs that must be made under highly constrained conditions found in the real world.⁵⁷ The AFI Pillar made this the goal of its research.

1.5 Research Questions Addressed

Considering the gaps in knowledge and dearth of best practices for planning charging infrastructure for human-driven and automated EVs providing ride-hailing, car-sharing, automated transit, and freight-delivery services, the AFI Pillar focused its research on answering the following five questions:

1. What are the characteristics of potential future transportation market segments employing human-driven and automated EVs that charging infrastructure will need to serve?
2. What are the cost/benefit tradeoffs inherent in different approaches to the design of charging infrastructure to serve light-duty human-driven and automated electric ride-hailing vehicles?

3. What is needed to understand tradeoffs inherent with different approaches to designing charging infrastructure for Class 7/8 electric trucks for freight transport?
4. What is the potential for automated-vehicle charging to create new charging paradigms that improve automated electric ride-hailing vehicles and transit?
5. What is the benefit to the nation of charging infrastructure deployed to serve ride-hailing EVs?

The remaining sections of this report describe the research conducted to answer these questions. Section 2.1 addresses the first research question. Section 2.4 addresses Questions 2 and 3. Sections 2.3 and 2.3.2 address questions 4 and 5, respectively. Each of these sections describe the methodology, tools, and data used to conduct simulation and analysis necessary to address the research questions, followed by presentation and discussion of results. Conclusions are given in Section 3, including a summary of the answers to the five research questions above.

2. Research Approach and Results

This section presents the AFI Pillar’s research on the charging needs of new electric transportation modes. Section 2.1 shares results of market analysis and data-driven behavioral segmentation to describe potential users of future charging infrastructure. Section 2.2 presents a series of case studies set in different U.S. cities that explore tradeoffs in planning charging networks to serve different types of vehicles. Section 2.3 discusses new opportunities created by automated EVs that can drive and charge themselves—namely, intelligent management of automated electric ride-hailing fleets and dynamic wireless charging of automated electric transit vehicles. This section culminates in Section 2.3.2 with a discussion on the impacts of charging infrastructure for electric ride hailing at the national level.

2.1 Understanding New Market Segments for Transportation Electrification

To understand the charging infrastructure needed to support future mobility, scenarios for analysis and simulation must be developed that describe what the future market might look like. Although it is not possible to accurately predict the future, factors that motivate consumer behavior can be examined to develop reasonable potential future scenarios. The three SMART mobility workflow common scenarios discussed in the SMART Mobility Modeling Workflow Report were created in this way to provide a uniform set of scenarios for all researchers across the SMART Mobility Laboratory Consortium. To define these scenarios, the consortium established assumptions for a broad range of behavioral factors, such as traveler preference for personal-vehicle use versus other modes like ride hailing or transit, consumer adoption of different vehicle technologies like automation, and propensity of consumers to shop online. The consortium also defined system-level assumptions consistent with behavioral assumptions, such as freight demand and land use, to provide necessary inputs for simulation.

Because the AFI Pillar focused on EVs and charging infrastructure to a greater degree than other pillars, it needed to establish additional scenarios and assumptions. The AFI Pillar performed analysis to add detailed assumptions to the three common scenarios and to develop additional scenarios for modeling and simulation that are necessary to address the AFI research questions. To do this, the Pillar had to answer its first question: What are the characteristics of market segments and EV operators that charging infrastructure will serve in the future? This section of the report answers this question for light-duty vehicles and for heavy-duty trucks used to ship freight.

The AFI Pillar sought real-world data from present-day operations as a basis for answering this question and to inform modeling assumptions and simulation scenario development. Data collected describing the use of human-driven ride-hailing and heavy-duty freight vehicles are described in this section to help ground the case studies presented in Section 3.2 in presently observable trends.

2.1.1 Light-duty Vehicle Market Segmentation

Key findings

To understand the characteristics of the light-duty EV market that charging infrastructure will need to serve, the AFI Pillar performed behavioral segmentation analysis of the light-duty EV market, with a focus on human-driven ride hailing. This segment was chosen because the behaviors, motivations, and circumstances of drivers in this segment vary tremendously. To better understand these drivers, the Pillar obtained and analyzed data from Populus, RideAustin, and Columbus Yellow Cabs (CYC). This analysis provided the basis for scenarios and assumptions used in the AFI Pillar simulation of this segment (described in Section 3.2.1). Insights produced from this data collection and analysis effort include the following:

- The majority of ride-hailing drivers in RideAustin and Populus data were found to drive part time, with relatively low VMT. A minority of TNC drivers (~10%) operate full time, with high annual VMT (~30,000 miles, excluding VMT accumulation for personal travel). CYC taxicab drivers, considered full-time drivers, averaged 40,000 miles per year.
- On most days, full-time ride-hailing driving days in RideAustin and CYC data involved driving less than 250 miles. This suggests that if drivers adopt BEVs with 250 miles of range (referred to as BEV250s),

overnight or taxi depot charging could accommodate almost all of their energy needs. However, approximately 40% of Populus TNC drivers report living in multi-unit dwellings, where access to residential charging is often problematic.

- Drivers reported a plethora of motivations for why they drive for a TNC, such as being between jobs or preferring flexible hours. Nearly a quarter of TNC drivers may choose not to purchase EVs solely for financial reasons because they reported nonfinancial reasons as their primary motivation (e.g., keep busy, meet new people).
- In the case in which home charging is \$0.13 per kWh, gasoline costs \$3.00 per gallon, the opportunity cost of public charging is \$15 per hour, and vehicle costs are representative of current offerings, a BEV250 offers the lowest total cost of ownership for drivers that travel more than 42,000 miles a year, relative to comparable models of conventional internal combustion engine vehicles (ICEVs), hybrid electric vehicles (HEVs), and BEVs with 150 miles of range (BEV150s). HEVs offer the lowest overall cost when annual VMT ranges from 12,000 to 42,000 miles, and ICEVs are the cheapest below 12,000 miles per year. These findings, when compared to annual VMT statistics from RideAustin and CYC, suggest that many ride-hailing drivers who are financially motivated may not adopt BEVs.

Introduction

The light-duty EV market can be characterized by three factors: vehicle ownership, use, and degree of automation. Vehicles can be privately owned (or leased) by individuals or owned (or leased) by commercial enterprises. Vehicle use is classified in this research according to the extent to which a vehicle is driven to satisfy the owner's travel needs versus providing a mobility service to paying customers. The former is referred to as personal use. In this research, the latter comprises both ride hailing, conducted by conventional taxicab companies or TNCs, and car sharing provided by commercial enterprises (e.g., ZipCar, car2go, ReachNow). Of course, light-duty EVs may also be used in other applications, such as company motor pools, government fleets, or goods delivery, but the AFI Pillar did not consider those cases.

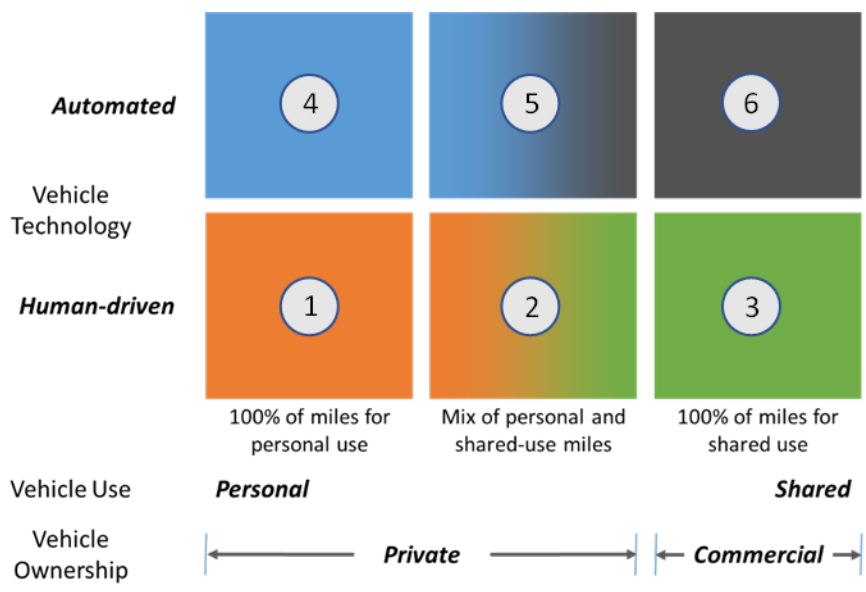
Several different combinations of vehicle ownership and use are prevalent today:

- Privately owned vehicles operated solely for personal use represent the segment that has traditionally dominated the United States light-duty passenger vehicle market. These are the cars, SUVs, and light trucks that households own or lease and use daily for commuting, errands, and other personal travel.
- TNC drivers and some taxi drivers own their vehicles and use them for both personal use and shared use; they provide ride-hailing services for others.
- Many commercially owned vehicles are operated solely for sequential shared use. These are fleet-owned taxis, limousines, and other livery vehicles that provide ride-hailing and limo services. Traditional rental cars and car-sharing (i.e., short-term rental) vehicles also fall into this category.

Drivers and fleets employ EVs in each of these categories today and greater EV adoption is generally anticipated in each category in the future.

The final factor, automation, is defined as the degree to which vehicles can drive themselves. For simplicity, the AFI Pillar differentiated the levels of automation based on whether a human driver is required to operate a vehicle.

The three factors that characterize the light-duty EV market are visualized in Figure 2-1, with distinct combinations of the three factors shown as one of six panels. These panels represent six distinct market segments.



- Six market segments:
- ① Privately owned, human-driven EVs operated solely for personal use
 - ② Privately owned, human-driven EVs operated for both personal and shared use
 - ③ Commercially owned, human-driven EVs operated solely for shared use
 - ④ Privately owned, automated EVs operated solely for personal use
 - ⑤ Privately owned, automated EVs operated for both personal and shared use
 - ⑥ Commercially owned, automated EVs operated solely for shared use

Figure 2-1. Characterization of the light-duty EV market

Most research to date into charging infrastructure needs has been focused on Segment 1 (privately owned, human-driven EVs operated solely for personal use). Because of the opportunities presented by the combination of ride hailing and electrification, the AFI Pillar chose to focus its efforts on Segment 2, hereafter described as human-driven ride hailing; Segment 3, with focus on free-floating car-sharing services; and Segment 6, consisting of fully automated, self-driving vehicles that are dedicated to providing ride-hailing services. Vehicles in Segment 6, colloquially referred to as “robotaxis,” will be referred to in this report as automated electric vehicles (AEVs) for ride-hailing.

With market segments defined, methods for characterizing EV owner-operator interests and vehicle use within each segment were chosen to more fully define modeling scenarios and assumptions. The remainder of this section describes the approach to and results of research to characterize the human-driven ride-hailing segment because this segment is the most heterogeneous. Analysis of factors influencing the use and operation of free-floating car-sharing services and AEV ride-hailing fleets is found in Sections 3.2.2 and 3.3.1, respectively.

Research Approach

Ride-hailing drivers who own or lease their own EVs have varying motivations, interests, and opportunities. In fact, the TNC business model was intentionally designed to provide flexible employment opportunities amenable to people in a variety of circumstances, from professional drivers to part-time “gig” workers. Therefore, the AFI Pillar used behavioral segmentation to characterize ride-hailing EV driving and charging.

Behavioral segmentation is a market research technique that groups consumers, product users, organizations, or other entities according to their behavior, rather than by demographic descriptions. Grouping individuals or

entities with similar behavior allows researchers to more easily infer how each group may select or use a product (such as an EV) or service (such as EV charging). Once groups are established, researchers can assess the size or significance of each group and select the group or groups of interest for further research.

Behavioral segmentation requires data. The AFI Pillar obtained data to characterize the human-driven ride-hailing segment by examining three aspects of behavior: (1) driving behavior, (2) charging behavior, and (3) the likelihood of EV adoption based on financial interests, in terms of TCO. The following three sections describe the data the Pillar collected or generated in each of these three areas.

Driving Behavior of Ride-hailing Drivers

To understand TNC driver behaviors and motivations, the AFI Pillar purchased data from a survey of TNC drivers from Populus, a company that conducts recurring travel surveys in major metropolitan areas. The Populus TNC Driver Survey contains responses from more than 1,000 drivers in 10 cities^b to questions related to TNC driver motivations for driving, frequency of driving, and housing/demographic data (relevant for residential EV charging potential). Most respondents drove conventional internal-combustion-engine vehicles, with a small minority of drivers using HEVs and plug-in electric vehicles (PHEVs).

The Populus TNC Driver Survey represents a subset of responses from a general population survey, filtered to only individuals reporting to have recently driven for a TNC. Given a lack of demographic data on the overall population of present-day TNC drivers, the AFI Pillar did not have the means to determine how representative the Populus sample is of the broader TNC driver community. For this reason, only summaries of raw-response data were calculated and presented in this report.

The AFI Pillar also acquired and analyzed two data sets collected by electronic data loggers in non-EV TNC fleets. One data set came from RideAustin, a ride-hailing firm based in Austin, Texas, which publicly released data describing approximately 1.5 million ride-hailing trips collected from June 2016 through April 2017 (a period of 10 months) in Austin.⁵⁸ A heatmap visualizing the density of RideAustin passenger drop-off locations in the greater Austin metropolitan area is shown in Figure 2-2. All colored dots on this map represent passenger drop-off locations, with more frequent drop-off locations depicted with a brighter color. For reference, the dark line bisecting the concentration of bright orange and yellow in the center of the image is the Colorado River that flow through the center of Austin. The map shows that most passengers' destinations were in the urban center, but RideAustin vehicles served passengers traveling to destinations across the entire metro area.

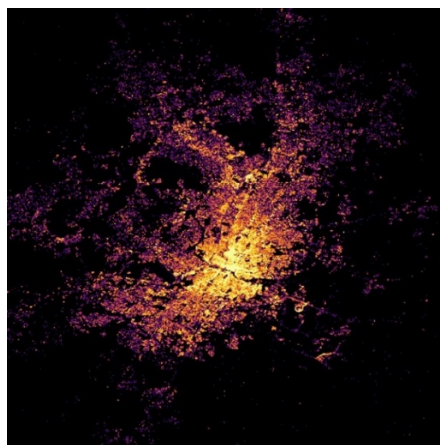


Figure 2-2. Map visualizing RideAustin passenger drop-off locations in Austin, Texas. More frequent drop-off locations are depicted with a brighter color. The concentration of bright orange and yellow in the center of the image indicates that most passenger destinations were in the urban center, but RideAustin vehicles served passengers traveling to destinations across the entire metro area.

^b The Populus survey was conducted in Washington, D.C.; San Francisco, CA; Los Angeles, CA; Austin, TX; Chicago, IL; Seattle, WA; Denver, CO; Atlanta, GA; New York City, NY; and Boston, MA

Because the ride-hailing market segment also includes conventional taxis, and traditional taxi companies continue to represent an important mobility option for travelers, the AFI Pillar also obtained data from a taxi fleet. Columbus Yellow Cabs (CYC) shared a private data set containing 13 months of real-world taxi data, including approximately 840,000 ride-hailing trips taken in Columbus, Ohio, from April 2017 through April 2018. CYC served rides requested through a ride-hailing app, as well as through conventional line-of-sight hailing and phone reservations.

The supplied data consisted of 70 million unique global positioning system (GPS) data points describing the location of each CYC taxicab as it drove. An additional field from the taxi's meter allowed researchers to distinguish a paid trip with passengers from vehicle travel with no passengers, sometimes referred to as driving empty or deadheading. The geographic extent of the GPS data from CYC is visualized in a map of the greater Columbus metropolitan area in Figure 2-3. In this map, lines of any color represent sections of road traveled by at least one CYC vehicle. More frequently traveled road sections are shown in a brighter color. As may be expected, CYC cabs drove most in the urban center and on interstates, with fewer trips traveling on arterial roadways outside of the city.



Figure 2-3. Map visualizing the density of CYC trips in Columbus, Ohio. More frequently traveled road sections are shown in a brighter color.

Data from CYC described the travel of 170 unique taxicabs, with 146 unique fleet vehicles active per month, on average, over the 13-month data-collection period. Average annual operation amounted to 280 days of use per year per vehicle and 154 miles per day driven. In total, 35,112 unique vehicle-days were present within the data set. A vehicle-day describes all driving and standing or parking events by a single vehicle over a 24-hour period. A vehicle-day was counted for each vehicle with one or more trips during the day.

Charging Behavior of Electric Ride-hailing Drivers

Because the Populus survey, RideAustin, and CYC data samples included very few EV drivers, additional data sources were needed to understand ride-hailing EV drivers' charging behavior and preferences. Past observation of behavior of privately owned, personal-use EV drivers showed that charging habits vary between drivers and is not easily predictable.⁵⁹ Therefore, characterizing ride-hailing EV drivers' charging behavior must be a data-driven process.

The AFI Pillar obtained and analyzed revealed preference data from electric taxi and TNC vehicles from two sources. The first source was a past project conducted by Nissan North America, Idaho National Laboratory, and the New York City Taxi and Limousine Commission that collected driving and charging data from five model-year 2012 Nissan LEAFs used as taxis in New York City between April 2013 and March 2015.⁶⁰ For the second source, the AFI Pillar led an effort in 2019 to collect vehicle data from EVs serving in TNC fleets. The Pillar worked with Geotab and Sawatch Labs to recruit drivers who consented to installing data loggers in their vehicles to develop a pipeline of vehicle telematics data. This data collection effort is ongoing at the time

of this writing and has logged more than 15,000 miles of driving and more than 200 charging events since the beginning of July 2019. Figure 2-4 visualizes about 3 months of driving by a single ride-hailing EV operating in the Sacramento, California, area. Roads traveled by the vehicle are highlighted with shades of red, orange, and yellow. Sections of road traveled more often are displayed with a brighter color. The majority of this driver's charging took place at home (not shown). A single DC fast charger and two alternating current (AC) Level 2 charging units used occasionally by the driver are shown as light blue circles.

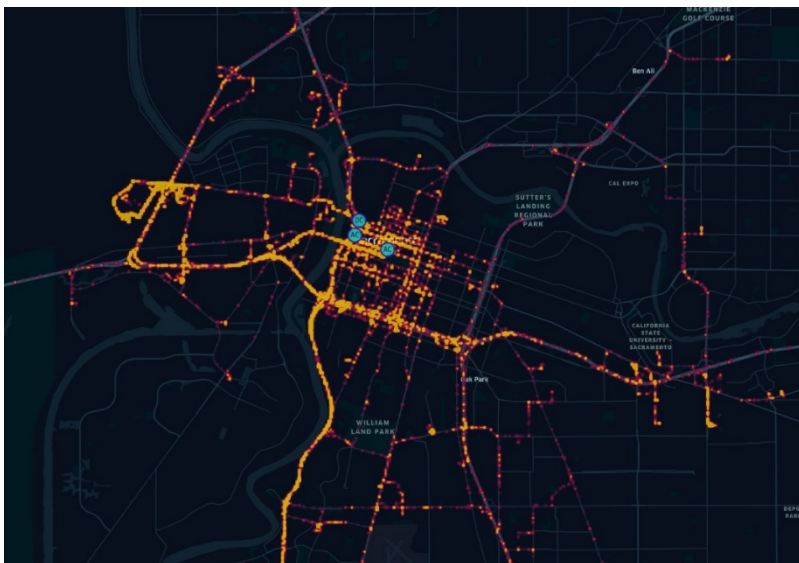


Figure 2-4. Map visualizing driving and public charging locations (AC Level 2 and DC fast chargers indicated by the blue circles) used by a single ride-hailing EV driver in Sacramento, California. Sections of road traveled more often are displayed with a brighter color.

Likelihood of Electric Vehicle Adoption Based on Total Cost of Ownership

In order to understand the motivations and interests of ride-hailing EV drivers, it is important to gain insights into who will adopt EVs in the first place. Studies and articles have claimed that EVs, and BEVs in particular, will be popularly adopted as ride-hailing vehicles because of their low operating costs costs.^{61, 62} Such reports commonly examine the question of EV adoption by ride-hailing drivers through a narrow lens, basing financial analysis on statistical averages and generalizations.

The market reality is much more complex. Myriad factors affect the degree to which ride-hailing drivers are financially motivated in their decisions and how much EVs will cost them to drive. Furthermore, these factors vary widely across drivers and locations. After all, individual ride-hailing drivers, like consumers in general, make vehicle-purchase decisions based on their own unique circumstances.

Therefore, more careful analysis was needed to shed light on the extent to which EVs will be appealing for ride-hailing drivers—a necessary basis for assumptions about EV adoption in AFI Pillar simulation. To accomplish this, the AFI Pillar first examined data from the Populus TNC Driver Survey to estimate the fraction of TNC drivers who are financially motivated and who could be assumed to find inexpensive vehicles appealing. Secondly, the Pillar conducted a thorough study of EV TCO for ride-hailing drivers to explore the relative costs of owning and operating BEVs as ride-hailing vehicles compared to other vehicle types.

For the TCO analysis, the Pillar analyzed real-world data from RideAustin to understand the operation of current ride-hailing vehicles. This process included running simulations using EVI-Pro to determine the charging needs of ride-hailing vehicles, assuming those vehicles were BEVs. (The SMART Mobility Model Appendix gives a detailed description of EVI-Pro; see Section 3.2.1 of this report for a description of the EVI-Pro simulation based on RideAustin data.) Results were used as inputs to TCO modeling, which captured the costs of owning and operating vehicles over their lifetime.

The TCO model used included traditional costs, like vehicle depreciation, maintenance, and fueling or charging. It also included the opportunity cost of time spent charging during a shift. This is an important consideration because, for a ride-hailing driver, time spent out of service for charging translates directly to lost ride-hailing revenue (or the perception thereof). Finally, several operating scenarios were considered to represent different ride-hailing driver behaviors, vehicle designs, and other factors that vary across the market.

Results of Data Analysis and Behavior Segmentation of Human-driven Ride-Hailing Drivers

Driving Behavior of Ride-hailing Drivers

The Populus TNC Driver Survey results were analyzed and grouped by household income. Responses to three questions related to driving frequency, residence type, and motivation for driving for a TNC provided useful insights into TNC driver behavior and mindsets. Figure 2-5 summarizes the responses to the first of these questions by showing the distribution of TNC drivers by frequency of driving for a TNC (i.e., how often they used their personal vehicle to provide rides to paying customers) and household income. A minority of drivers (~10%) report driving for a TNC on a daily basis (i.e., full time). Over half of drivers drove for a TNC for two days per week or less. No meaningful differences by income bin were observed.

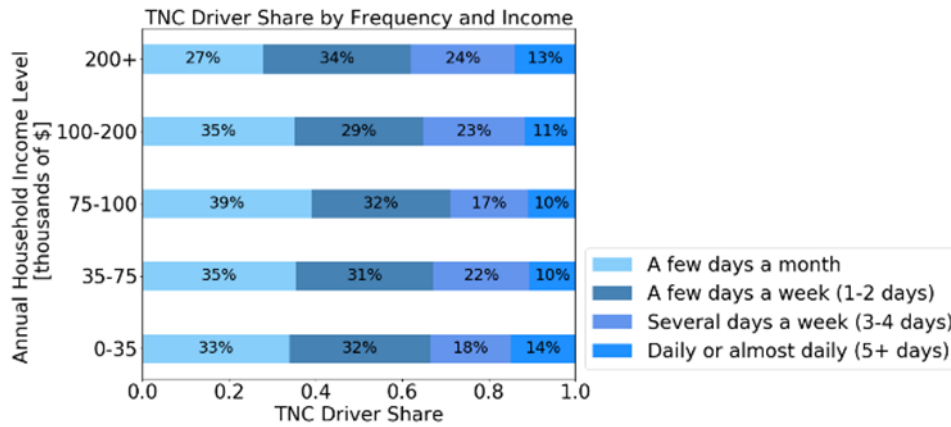


Figure 2-5. Populus survey results for TNC driver share by driving frequency and income.

Figure 2-6 shows the distribution of TNC drivers by residency type (single versus multi-family home and whether the driver rents or owns the home). Residence type was found to correlate strongly with household income, with the share of drivers renting their home or living in a multi-family unit increasing dramatically as household income decreases. Given the residential charging challenges typically associated with multi-family housing, these data suggest the potential for poor access to residential charging for many TNC drivers, especially those with low incomes.

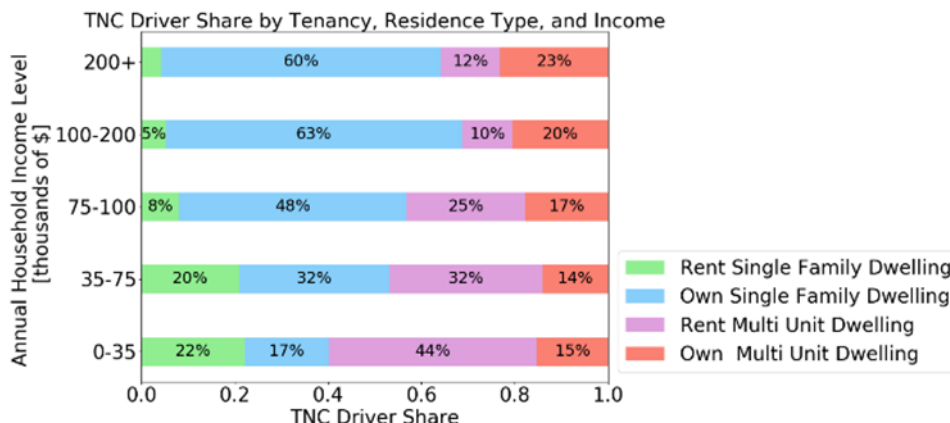


Figure 2-6. Populus survey results for TNC driver share by residence type, tenure, and income.

Figure 2-7 shows the distribution of TNC driver responses when asked to list the primary reason they are currently (or have recently) driven for a TNC. Drivers report a plethora of motivations, such as being between jobs or preferring flexible hours. Interestingly, nearly a quarter of drivers report nonfinancial reasons as their primary motivation (e.g., to keep busy or meet new people). This provides evidence that 25% of TNC drivers may not choose whether to purchase EVs solely for financial reasons. The share of drivers reporting discretionary motivations generally decreases with decreasing household income.

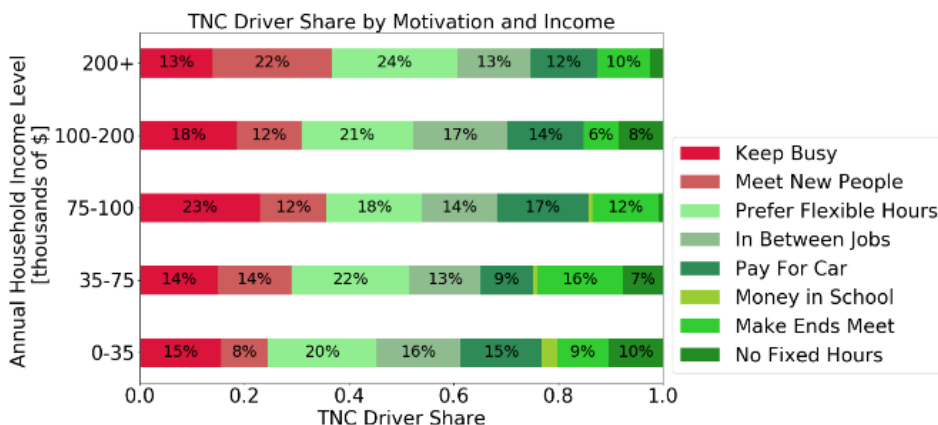


Figure 2-7. Populus survey results for TNC driver share by motivation and income.

Populus survey results also suggest that vehicles used within ride-hailing fleets are likely to be more fuel efficient than the average light-duty vehicles (LDVs) in the U.S. market, with TNC drivers reporting high shares of sedan body types and relatively recent model years, no doubt because of TNC requirements for the age and design of drivers’ vehicles. Additionally, approximately 50% of drivers appear to be buying new vehicles for TNC use.

The AFI Pillar also analyzed RideAustin data to add to its understanding of TNC driver behavior. Given that driving for a TNC service allows drivers to work flexible hours, RideAustin drivers were segmented based upon average hours of in-service activity per week, with full-time drivers defined as driving more than 35 hours per week. Analysis excluded drivers that drove less than two weeks of service during the data collection period. As shown in Table 2-1, a majority of drivers (89%) were classified as either part-time or half-time drivers, accumulating less than 35 hours per week. This is consistent with and equivalent to the percentage of drivers driving less than five days per week in the Populus survey results (see Figure 2-5). The remaining 11%

of drivers are considered full-time drivers. They serviced 29% of all rides in the dataset and accumulated annualized VMT of approximately 29,000 miles, on average.

Table 2-1. Distribution of RideAustin drivers segmented by activity level.

	Part-time Drivers (Less than 10 hours/week)	Half-time Drivers (10-35 hours/week)	Full-time Drivers (More than 35 hours/week)
Percent of drivers	49%	40%	11%
Percent of rides served	14%	57%	29%
Average annual VMT ^a	7,000	13,000	29,000

^a Annual VMT was calculated from driving distance during shifts and during commutes before and after shifts. It does not include commuting by part-time and half-time drivers to other employment, nor does it include personal travel. Average annual VMT for full-time drivers is considered a conservatively low, but reasonable estimate for this research.

For TNC drivers to be able to consider electrification, some combination of electric driving range and charging infrastructure must be available to accommodate daily driving needs. In order to quantify these needs, the RideAustin data were analyzed on a daily basis, with average and maximum daily VMT calculated for each driver. Figure 2-8 shows distributions of these metrics for all full-time drivers. Note that approximately 70% of vehicles never experience a driving day of more than 250 miles, and the mean daily driving distance is below 100 miles.

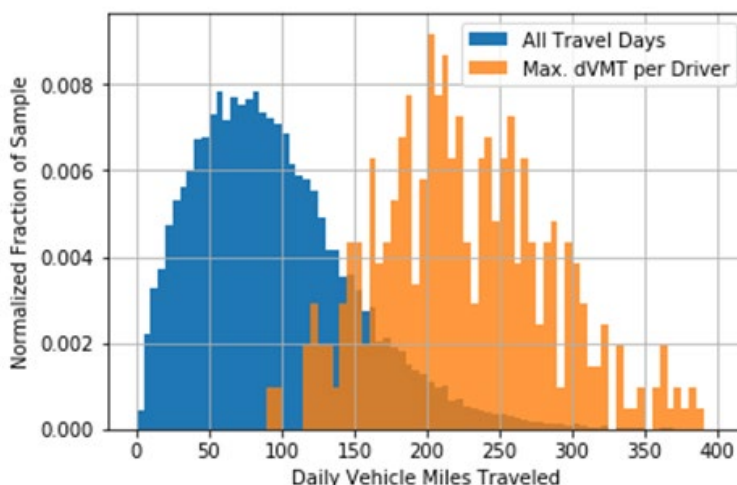


Figure 2-8. Daily VMT (dVMT) distributions from full-time RideAustin drivers (Blue = all driving days, orange = maximum distance driving day per vehicle).

Finally, comparative analysis between data from CYC and RideAustin was performed to understand the similarities and differences in vehicle utilization between conventional taxis and TNCs. Over the 13-month data collection period, CYC vehicles averaged 154 miles of driving per day on an average of 280 days per year. When evaluated annually, vehicles were utilized at an average annualized VMT of approximately 40,000 miles. Full-time RideAustin drivers also drove on approximately 280 days per year, but with a smaller average daily and annual VMT. Figure 2-9 shows cumulative distributions to illustrate the differences in miles traveled per day for all CYC vehicles versus RideAustin vehicles driven by full-time drivers. For example, 20% of CYC driving days (red line) had a daily VMT below 100 miles, whereas full-time RideAustin drivers drove less than 100 miles on 60% of their driving days (black dashed line).

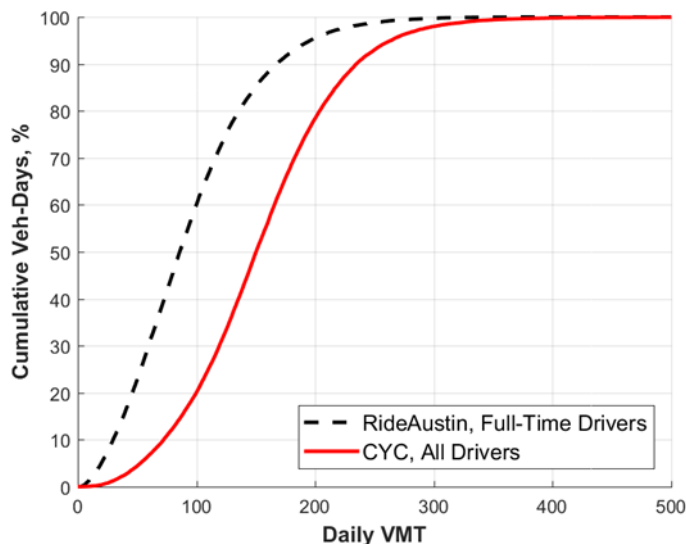


Figure 2-9. Daily VMT comparison between CYC and full-time RideAustin drivers.

Calculation of the distance driven between fares in both the RideAustin and CYC data sets, referred to as deadheading, found that deadheading represents a significant percentage of present-day ride-hailing operations, accounting for approximately 50% of vehicle miles traveled (VMT) in both fleets. Although this information was not needed for AFI Pillar simulation—the simulations determined deadheading themselves—it is an important point of reference. Deadheading contributes to congestion and increases transportation energy consumption and emissions.

Charging Behavior of Electric Ride-hailing Drivers

The AFI Pillar analyzed data collected in 2019 from personally owned EVs used to drive for TNCs. Analysis found that drivers of these vehicles conducted approximately 65% of charging events at home, 8% at DC fast chargers, and the remaining 27% at public Level 2 chargers. The data sample at the time of this writing consisted of seven TNC drivers, including four full-time drivers (full-time as defined in the driver segmentation approach presented in the following section). Interestingly, one of the full-time drivers did not have access to residential charging and has been primarily relying on publicly accessible L2 EVSE for charging his 2019 Chevrolet Bolt.

Although the sample size was small, some initial aggregate trends in charging behavior indicated differences in usage between home and public charging stations for EV TNC drivers. Figure 2-10 shows the initial and final battery state of charge (SOC) for all charging events in the data set, split between public (both AC Level 2 [L2] and DC chargers) and home chargers. The distribution of initial SOC for public charging events is relatively uniform, potentially implying an opportunistic approach to public charging. By contrast, drivers were much less likely to initiate home charging events below 30% SOC and were more likely to continue charging at home until a full charge has been reached.

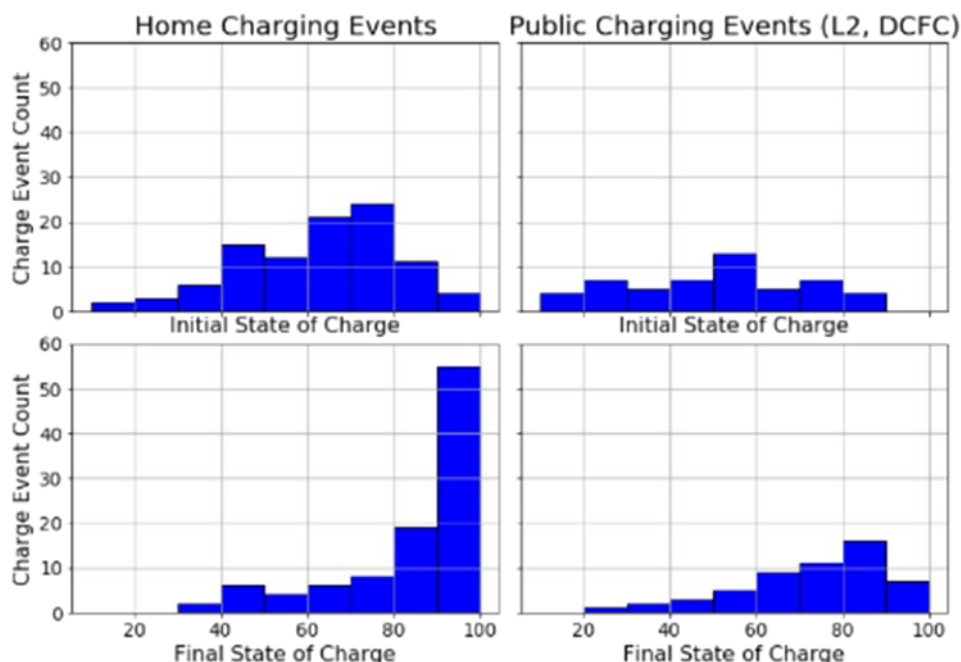


Figure 2-10. Observed initial/final state of charge distributions for residential and public charge events from EVs operating within TNC fleets.

Ride-hailing Driver Behavioral Segmentation Analysis

The AFI Pillar’s analysis of driving and charging data from ride-hailing vehicles, described above, provided valuable insights into the nature and behavior of ride-hailing drivers and their motivations. These insights became the basis for many assumptions used in simulation. Furthermore, these findings allowed the AFI Pillar to conduct in-depth behavioral segmentation for today’s ride-hailing drivers to better understand potential future ride-hailing EV drivers and choose which segments should be represented in simulation. To segment drivers, two primary factors were chosen: driving activity and access to home charging, described as follows.

Driving activity

Drivers were categorized by the time they spend driving for a TNC each week. Two categories were chosen: full time and part time, based on the definitions given in Table 2-1. Populus and RideAustin data indicated that full-time drivers represent about 10% of all TNC drivers. About 50% of all drivers spend less than 10 hours per week driving for a TNC (see Table 2-1).

Access to home charging

The extent to which EV drivers charge at home has a tremendous influence on demand for public charging infrastructure (as will be shown in Section 3.2.1). Home charging reduces the need for public charging. Drivers who charge at home and accumulate low to moderate daily mileage may get by with little or no public charging. Home charging also makes high-mileage driving more practical by allowing drivers to start each day (or shift) with a fully charged battery. For example, it allows TNC drivers who live outside areas of high demand for mobility services to commute into those areas without a pre-commute fast charge.

Drivers who live in single- or multi-unit dwellings with garages or carports with electrical connections are much more likely to charge at home, either using an AC Level 1 120-volt cord set or by installing a faster AC Level 2 charging unit. Home charging is problematic, if not impossible, for drivers living in multi-unit dwellings without dedicated parking spots, unless property owners install charging units (and even then, drivers may face charging fees, as well as competition for charging and accompanying uncertainty about charging access).

Three secondary factors were also considered: motivation, commitment, and access to away-from-home destination charging, described as follows.

Motivation

Driving activity is closely tied to a driver’s motivation or incentive to drive for a TNC. Some drivers are motivated to drive because it is their primary source of income. Others view it as a source of supplemental income. As mentioned previously, there is another group of drivers, not insignificant in size, that is not primarily motivated by earning money. They drive to meet new people, stay busy, or for other reasons.

Commitment

Drivers’ commitments to their jobs as a TNC drivers have some bearing on the likelihood they will adopt EVs or install home charging units. Drivers may consider themselves professional drivers, driving for a TNC for a long period of time. Alternatively, they may consider driving as a temporary job to bridge the gap between jobs in their preferred professions. Finally, driving for a TNC may be a side “gig,” in addition to other jobs or schooling.

Intuitively, drivers’ expectations for the length of their employment as TNC drivers would influence their vehicle purchases. For example, those considering themselves professional drivers for the long term are probably more likely to choose a vehicle with low cost of ownership, such as an EV. However, introduction of short-term EV leases by companies such as Maven decouples commitment from vehicle-acquisition decisions.⁶³ Nevertheless, commitment as a factor for segmentation may still be relevant because it influences the likelihood of home charging. Maven has reported that greater than 95% of their weekly lessees rely on public charging exclusively, perhaps because those who do not commit to driving an EV do not invest in home charging equipment.⁶⁴ Note that Maven offers unlimited free charging at select public charging stations.⁶⁵

Access to Away-from-Home Destination Charging

Part-time drivers with other jobs or who attend school may park their vehicles for long periods of time while at work or school. If they have access to charging at these locations, using these destination charging facilities can supplement or replace other charging and greatly diminish, if not eliminate, drivers’ need for other public charging.

The human-driven ride-hailing driver segment was subdivided into segments by categorizing groups of drivers according to these five factors. Table 2-2 lists the resulting segments and descriptive information. The following two questions were answered for each segment to examine behavioral differences: (1) What are the general charging needs for drivers in this segment if they were to drive an EV? (2) What conditions would an EV to be attractive to drivers in the segment?

Table 2-2. Ride-hailing vehicle driver segmentation results.

Segment Number	Segment Description	Anticipated driver charging needs	Assumed conditions required for BEV adoption
2.1	Full-time drivers motivated by earnings with access to home charging	<p>These drivers typically start their shift with a fully charged battery, but may need to charge throughout the shift to maintain sufficient battery charge to meet their higher demand for VMT.</p> <p>They need to take breaks during their shift, so fast charging stations collocated with other facilities would allow them to charge during natural downtime.</p>	<p>Because these drivers are financially motivated, total cost of BEV ownership should be lower than the equivalent conventional vehicle.</p> <p>High-mileage accumulation is advantageous because of BEV low per-mile cost, but actual and opportunity cost of charging must not outweigh those gains.</p> <p>Higher EV range (e.g., 250 miles) alleviates charging cost pressure and uncertainty.</p>

Segment Number	Segment Description	Anticipated driver charging needs	Assumed conditions required for BEV adoption
2.2	Full-time drivers motivated by earnings <i>without</i> access to home charging	<p>These drivers rely on public charging exclusively; they may need to charge immediately following their pre-shift commute, during breaks, and/or before or immediately after their after-shift commute.</p> <p>Because they may need to charge more frequently than they would otherwise take breaks, these drivers want to charge quickly (<20 min per charge) and cannot afford to wait in queues for charging.</p>	<p>Total cost of BEV ownership should be lower than the equivalent conventional vehicle.</p> <p>Actual and opportunity cost of charging is even more important for this segment, because they will need to charge in public more often than Segment 2.1.</p> <p>Charging power should be higher (e.g., 150 kW) for reduced downtime.</p>
2.3	Part-time drivers motivated by earnings with access to home and/or other destination charging	<p>These drivers spend less time on the clock, so they drive fewer miles; however, their personal-vehicle use is more variable than that of full-time drivers.</p> <p>Lower VMT and charging at home and other destinations means these drivers get by with occasional or no public fast charging.</p>	<p>These drivers are primarily concerned with having sufficient vehicle range to avoid needing fast charging.</p> <p>Because they use their vehicle for personal use, other non-rational reasons have greater influence on their decisions.</p>
2.4	Part-time drivers motivated by earnings <i>without</i> access to home or other destination charging	<p>These drivers have lower but more variable VMT, like Segment 2.3, but public charging must meet all their energy needs.</p> <p>Further, they have limited time for charging: they do not take breaks during their short shifts and their only charging opportunities are between shifts. They cannot afford to dwell at charging stations in queues or while charging.</p>	<p>BEVs will likely not be economical options for this segment until the proliferation of widespread, ultra-fast (e.g., 10 min) charging.</p>
2.5	Part-time drivers motivated by something other than earning money with home charging	<p>These drivers have the most charging flexibility because they have less (or no) time pressure.</p> <p>Because these drivers tend to be financially well off, they have access to home charging.</p>	<p>Because they are not financially motivated, they would choose BEVs for a variety of non-economic reasons.</p>

This analysis highlights stark differences in charging needs between segments. For some TNC drivers, accessible, fast, public charging infrastructure at minimal cost is a top priority. Others have considerable flexibility in their charging choices.

The three case studies presented in Section 3.2.1 used simulation to study tradeoffs in charging infrastructure design for different ride-hailing driver segments. The first case study, set in Columbus, Ohio, simulated full-time ride-hailing vehicles in Segment 2.1. The second case study, also set in Columbus, conducted simulations to compare the charging infrastructure needed to support a fleet of drivers in Segment 2.1 versus Segment 2.2. The third case study was set in the San Francisco Bay Area and simulated the operation of human-driven ride-hailing vehicles by part-time drivers in Segments 2.3 and 2.4. Simulation of drivers in Segment 2.5 was reserved for future work.

Likelihood of Electric Vehicle Adoption Based on Total Cost of Ownership

To shed light on the conditions under which BEVs are financially advantageous for ride-hailing drivers, the lifetime cost to own and operate a ride-hailing vehicle with different powertrain types was calculated. These calculations were based on the driving and simulated charging behavior of the full-time RideAustin driver with the median annual VMT of 29,000 miles.^c AFI researchers compared the residual cost (purchase cost, less resale value), operating and maintenance costs, and opportunity cost of fueling or charging for a comparable ICEV, HEV, BEV150, BEV250, and BEV400. The following fundamental assumptions were chosen for this analysis:

- Vehicle purchase prices were assumed to be \$20,000 for an ICEV, \$27,500 for a BEV100, \$30,000 for a BEV150, \$35,000 for a BEV250, and \$40,000 for a BEV400
- The driver has access to home charging and public DCFC: charging costs range from \$0.13/kWh for home charging to \$0.50/kWh for fast charging
- Value of charging time for a ride-hailing driver during a shift is \$15/hour
- Vehicle ownership period is 5 years
- Gasoline price is \$3.00 per gallon
- ICEV and HEV fuel economy are 33 and 46 miles per gallon, respectively; all BEVs consume 285 watt-hours per mile.

Figure 2-11 shows lifetime costs (i.e., TCO) across different vehicle types and varying levels of yearly VMT. Additional assumptions used in calculating these costs can be found in Appendix A.

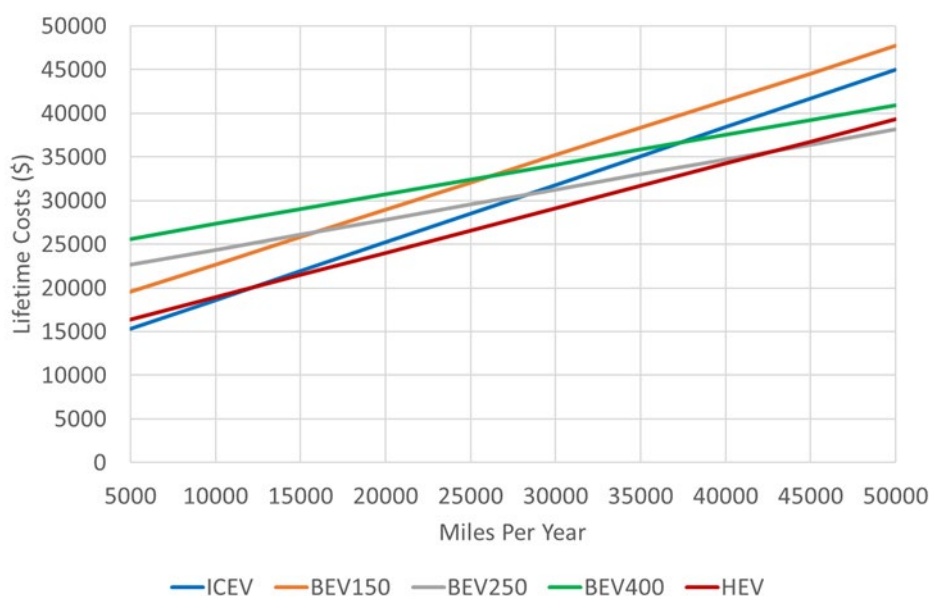


Figure 2-11. Total cost of ownership for different vehicle types for varying miles driven per year.

This figure shows that the HEV is the lowest-cost vehicle for a very large range of yearly VMT. It is only when yearly VMT is above 42,000 miles that a BEV—i.e., the BEV250—offers the lowest cost of ownership. Below 12,000 miles per year, the ICEV is the cheapest option. Compared directly to the ICEV, BEVs offer

^c Median annual VMT only considering full-time drivers. For more information on simulated TNC driver charging behavior based on RideAustin data, see the case study entitled “Home Charging Matters—Feasibility Analysis of Fleet Electrification in Columbus, Ohio and Austin, Texas” in Section 3.1.2.

lower cost when driving exceeds about 25,000 miles per year. Recall that the vast majority of TNC drivers only drive part time and accumulate far fewer miles annually than this (see Table 2-1).

To explore how TCO varies for factors other than VMT, a tornado plot was created to show how the costs of three different vehicle types can change due to variability in input assumptions. Figure 2-12 shows how TCO changes for the median full-time RideAustin driver as any single input factor is varied between low, baseline, and high-cost values.

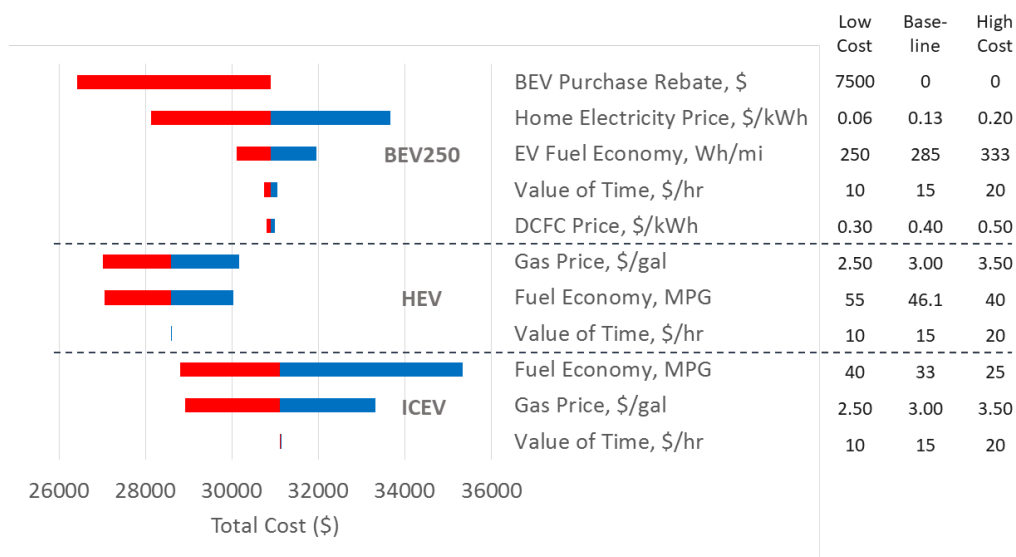


Figure 2-12. Vehicle ownership cost parametric sensitivity analysis, based on the driving and simulated charging behavior of the median RideAustin TNC driver.

The most influential cost factors are shown to be electricity price, gasoline price, vehicle fuel economy, and BEV purchase rebate amount. Any one of these factors can change whether an ICEV, HEV, or BEV is the lowest-cost vehicle for a particular scenario. For all the vehicles analyzed, the value of time variable has a limited effect because the median full-time RideAustin driver rarely exceeded 250 miles of driving in a single day, and all three vehicle types in this analysis have a range of 250 miles or more. Therefore, they rarely need to fuel or charge during a shift. With a shorter-range BEV like a BEV150, the need to charge more during shifts will increase the effect of that input.

In addition to the variability of the inputs in Figure 2-12, there are a number of considerations that should be made when determining vehicle suitability for ride-hailing drivers, including, drivers who do not have access to home charging, BEV-specific electricity rates, and short-term BEV leases for use in ride-hailing. More discussion on each of these topics can be found in Appendix A.

The results of this analysis indicate that care should be taken to avoid jumping to conclusions about the cost competitiveness of BEVs for ride-hailing drivers. There are scenarios in which BEVs will be financially advantageous, but clearly, that will not always be the case. Care should be taken to select a BEV mix that makes sense for the scenario being studied. Accordingly, the AFI Pillar’s large case study based in the San Francisco Bay Area described in Section 3.2.1 includes both conventional ICEVs and BEVs as human-driven ride-hailing vehicles, with the former group being much larger (see Figure 2-31. Number of vehicles (left) in all simulation scenarios and number of fast chargers (right) in each infrastructure scenario).

2.1.2 Freight-Trucking Industry Segmentation

Key Findings

The AFI Pillar analyzed the freight-trucking industry to understand the characteristics of the potential future electric freight-truck market segments that charging infrastructure will need to serve. The Pillar defined prevalent industry segments and described the nature of trucking operations, owner/operator interests, and

regulations that govern operations in each segment. Results of this analysis were used to define scenarios and assumptions needed to model charging infrastructure for electric freight delivery (described in Section 3.2.3). Insights gained from this analysis effort include the following:

- Class 7-8 trucks are responsible for 86% of all miles driven by medium-duty (Class 3–6) and heavy-duty (Class 7–8) trucks transporting freight in the U.S. annually. Annual miles traveled per heavy truck is considerably higher than miles traveled per lighter truck, with Class 7–8 trucks averaging 45,240 miles per year, more than three times that of Class 4–6 trucks, which average 13,650 miles annually.
- About 50% of mileage for Class 7–8 trucks is accrued by trucks with primary trip distance of less than 200 miles; however, this statistic should not be used as a benchmark for selecting EV range for electric trucks. It is distance that trucks drive between charging opportunities that matters, not individual trip distance.
- Private carriers transport their own company’s cargo and operate exclusively between their own terminals. For-hire carriers operate as either truckload (TL) carriers who drive Class 7/8 trucks between varying client facilities as needed and often provide long-haul transport, or as less-than-truckload (LTL) carriers who operate on set and variable routes between the carriers’ own hub terminals and varying client facilities.
- Motor carriers and their drivers have strong incentives to maximize miles driven and the amount of freight transported within regulated time and weight limits. Given expectations for range, battery weight, and charging time requirements of electric trucks, modeling tools are needed to manage tradeoffs necessary for successful electric truck adoption in the freight-trucking industry.

For its research into how to manage these tradeoffs, the AFI Pillar chose to focus on Class 7/8 tractor-trailers because of the high potential for reduction in energy consumption due to the large share of miles driven by these truck classes. The Pillar chose a use case that would be most amenable to electrification: a regional-haul, private motor carrier that follows a hub-and-spoke model, transporting freight on set routes between a central warehouse and distributed destinations owned by its parent company.

Introduction

Electrification of trucks for freight transport offers a significant opportunity to reduce energy use. Today, trucks are by far the dominant mode for domestic freight in the United States, moving 72% of tonnage in 2017 and 73% of the value.⁶⁶ Trucks consume about 44,000 million gallons of diesel, gasoline, and other fuels, which account for 25% of all fuel consumed by United States transportation.⁶⁷ The miles traveled and fuel used per vehicle is far larger for medium and heavy trucks compared to light-duty vehicles (Figure 2-13).

While the fuel economy of the light-duty vehicle population has significantly improved in the past 50 years, that of the Class 3–8 truck population has held steady at around 6 MPG (Figure 2-14), partially because vehicle turnover can be quite slow in this market. Fuel economy has not changed much, despite the fact that diesel fuel is often the second-highest expense for motor carriers after labor and can be as much as 20% of total operating costs.⁶⁸ Deployment of new, more efficient trucks would drive more rapid change in the aggregate fuel economy in this sector.

Given their higher usage and annual fuel consumption, improvements to the efficiency of commercial trucks would have a proportionally higher impact on national energy demand, compared to light-duty vehicles, while cost-effective technologies would provide economic benefits by decreasing the cost of shipping.

Analysis of VIUS 2002 and 2013 IHS Polk registration data found that heavy-duty Class 7 and 8 trucks drive 86% of all miles medium and heavy-duty trucks drive to transport freight in the U.S. annually (Table 2-3). Therefore, electrification of Class 7/8 trucks has great potential to reduce national energy demand.

Table 2-3. Estimated annual VMT driven by medium and heavy-duty trucks to transport freight in the U.S.

Truck Class	Class 3	Class 4	Class 5	Class 6	Class 7	Class 8
VMT (millions)	5,815	10,474	5,084	12,328	17,152	177,460

Percentage	3%	5%	2%	5%	8%	78%
------------	----	----	----	----	----	-----

Source: National Renewable Energy Laboratory

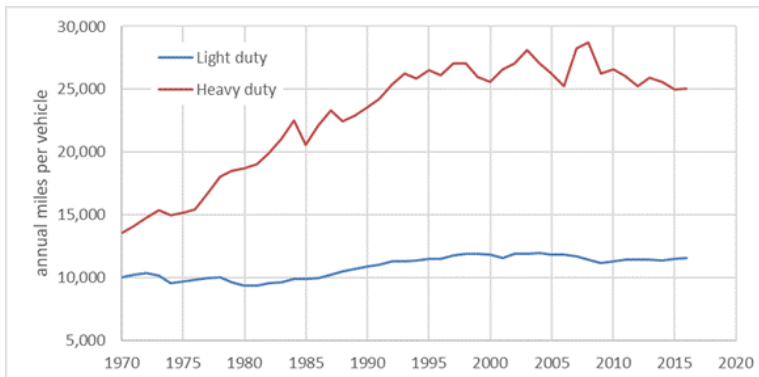


Figure 2-13. Miles traveled per vehicle.

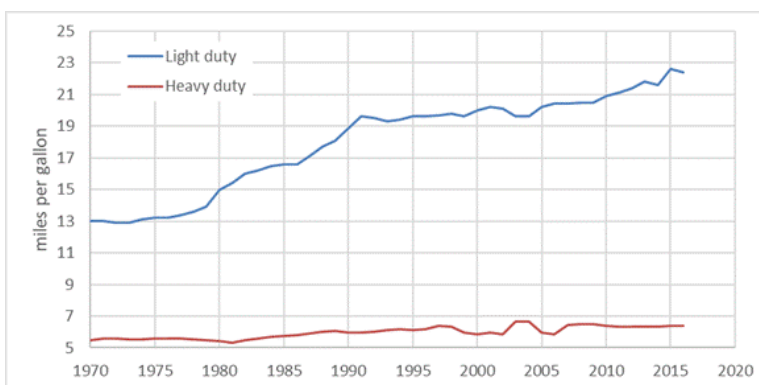


Figure 2-14. Fuel economy. Data source: Stacy C. Davis, Robert G. Boundy, Transportation Energy Databook Edition 37.1, 2019. Oak Ridge National Laboratory. tedb.ornl.gov/. Light-duty (e.g., passenger cars, light trucks, vans, and sport utility) vehicles and heavy-duty (i.e., single-unit trucks with a gross vehicle-weight rating exceeding 10,000 pounds and combination trucks) were defined differently prior to 2007 for heavy duty and 2008 for light duty and are not comparable to prior years.

For these and other reasons, truck manufacturers are bringing electric trucks to market, and these trucks will need charging infrastructure to support them. Therefore, the AFI Pillar analyzed the freight-trucking industry to understand the characteristics of potential future electric freight-truck market segments that charging infrastructure will need to serve. This understanding would serve as a foundation upon which to build scenarios and assumptions for modeling charging infrastructure to serve electric freight trucks (described in Section 3.2.3).

Research Approach

Pillar researchers reviewed data and reports about the industry to characterize the complex and highly segmented freight-trucking industry. Data were obtained from publicly available sources, such as the U.S. Department of Transportation’s Federal Motor Carrier Safety Administration, the U.S. Department of Commerce, and private databases.

The Pillar used these data to quantify the number and size of trucking companies, also known as motor carriers, in operation in the U.S. today. Pillar researchers also defined trucking industry segments based on operations of different types of motor carriers. Four factors were considered: cargo ownership, cargo type, shipment size, and typical operating range.⁶⁹ For each of these factors, motor carrier operations were placed within two or three categories, as shown in Table 2.4.

Table 2-4. Factors by which to segment the freight-trucking industry.

Cargo Ownership	Cargo Type	Operating Range	Shipment Size
For-hire Private	Freight Parcel Specialized	Local Regional Long-haul	Truckload Less-than-truckload

After using this framework to define the prevalent industry segments, the AFI Pillar characterized regulations that govern operations and owner/operator incentives within different industry segments. Results of this segmentation analysis and characterization of regulations and incentives are provided in the next two sections. A discussion on the implications of trucking operation on design of charging infrastructure for electric freight trucks is included throughout. Then, a final section identifies the industry segment that the AFI Pillar selected as a use case for charging infrastructure modeling (described in Section 3.2.3).

Results of Industry Segmentation Analysis

The United States motor carrier industry has a complex business and operational structure that includes many firms with diverse interests. Analysis of 2013 IHS Polk registration data shows that there were about 8.5 million medium- and heavy-duty vehicles. About 2.4 million of these are registered to individuals, with the remaining vehicles registered to around 940,000 unique businesses.^d The majority of fleets are small. Table 2-5 shows that 95% of motor carriers own five or fewer trucks while 99% own 25 or fewer. There are about 300 fleets that own more than 1,000 vehicles each and these fleets account for 20% of all registered trucks.

Table 2-5. Distribution of fleets and trucks by fleet size.

Number of vehicles	<5	5–25	26–100	101–250	251–1000	>1000
Percentage of fleets	95.3%	3.90%	0.62%	0.10%	0.04%	0.01%
Percentage of trucks	43.8%	14.4%	10.0%	5.2%	6.7%	19.9%

The size of its fleet may significantly impact whether an operator will choose to invest in capital-intensive electric charging infrastructure for the trucks or rely on public charging. Because many smaller operators contract with others to haul freight, the investment in private charging infrastructure serving multiple fleets may involve split incentives: those that would benefit most from electrification may not be the ones with the capital to install charging infrastructure while those that have adequate finances and facilities may not see a direct return on investment for purchased equipment.

Similarly, different segments of the motor carrier industry will have different opportunities and challenges when considering EV charging infrastructure. For the purposes of this study, motor carriers were categorized into industry segments based on their cargo ownership, cargo type, shipper load size, and typical operating range as shown in Table 2-4⁷⁰ Each of these factors, which dictate distinctly different aspects of operations, is described in more detail below, along with implications of each factor on the design of charging infrastructure for electric freight trucks.

Cargo Ownership

Motor carriers can be classified into two groups based on the ownership of cargo, as follows:

^d Includes vehicles with a gross vehicle weight rating (GVWR) over 10,000 lbs. Unique businesses were estimated from a unique combination of business name, vocation, and carrier type designation.

- For-hire carriers that transport passengers, regulated property, or household goods owned by others for compensation⁷¹
- Private motor carriers that transport their own cargo, usually as a part of a business that produces, uses, sells, and/or buys the cargo that is being hauled.⁷²

Table 2-6 and Table 2-7 show the ten largest for-hire and private motor carriers, respectively, in terms of the number of tractors and straight trucks owned.

Table 2-6. Ten largest for-hire carriers in the United States in 2019.

Carrier Name	Number of Tractors
FedEx Corp.	29,813
UPS, Inc.	19,732
Knight-Swift Transportation Holdings	19,156
TFI, International	15,992
J.B. Hunt Transport Services, Inc.	15,808
XPO Logistics	14,438
YRC Worldwide	14,100
Schneider	13,700
Landstar System	10,599
Old Dominion Freight Line, Inc.	9,254

Source: Transport Topics, [ttnews.com/top100/for-hire/2019](https://www.ttnews.com/top100/for-hire/2019)

Table 2-7. Ten largest private motor carriers in the United States in 2019

Carrier Name	Number of Tractors	Number of Straight Trucks
PepsiCo, Inc.	11,250	4,300
Sysco Corp.	8,544	1,053
US Foods	6,968	440
Walmart, Inc.	6,556	95
Reyes Holdings	5,802	938
Halliburton Co.	5,771	4,559
Nutrien	4,349	2,261
McLane Co.	3,809	105
Schlumberger, Limited	3,652	510
Performance Food Group	3,307	383

Source: Transport Topics, [ttnews.com/top100/private/2019](https://www.ttnews.com/top100/private/2019)

Cargo ownership can impact where private charging infrastructure should be installed. Typically, private motor carriers deliver freight exclusively to their own facilities, and those would be obvious locations for installing private chargers. On the other hand, for-hire carriers make deliveries to facilities owned by others, so accessing chargers may be more complicated.

Cargo Type

Another factor by which to segment the motor carrier industry is cargo type, or the major type of goods that a motor carrier is moving. There are three main cargo types, as follows:

- Freight consists of bulk items typically in large containers or portions of containers, or items that can be placed in a specific trailer for movement. The vast majority of all goods transported are freight.
- Parcel delivery is defined as the transportation of cargo owned by others as individual packages. These packages are normally smaller items weighing less than 150 pounds that can be combined with many other packages in a distribution network.
- Specialized cargo requires specific types of vehicles to move freight. This may include material such as cement or non-trailer supported vehicles. It can also provide movement as part of a shipping system, such as drayage and transloading. (These normally take place in localized environments such as ports, container yards, and rail yards.)

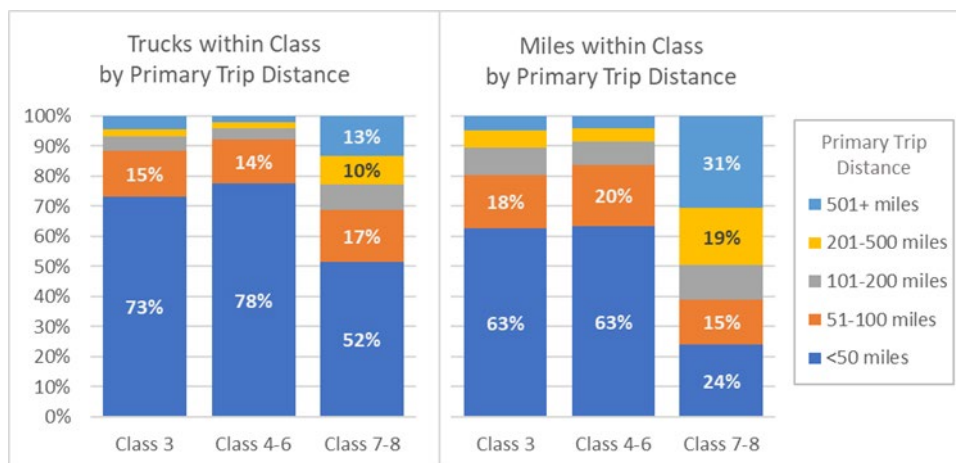
The cargo type can impact electrification and charging infrastructure because it influences the types of vehicles needed to support the business and the way these vehicles are operated. The movement of typical freight can normally be achieved with a Class 7 or 8 tractor pulling a trailer and can be accomplished with several types of operations. Parcel delivery, however, often requires a specialized approach to networked sorting and a variety of vehicle classes for pickup, intermediate distribution, and final delivery. Specialized cargo may require custom vehicles that operate in limited environments and may need a specialized charging infrastructure.

Operating Range

Motor carriers and vehicles also can be classified into segments based on their primary range of operation. The AFI Pillar chose three classifications for operating range: long-haul, regional, and local carriers. Generally, long-haul trucking moves goods more than 500 miles, whereas regional carriers move goods from 50 to 500 miles, and local carriers cover a radius of less than 50 miles.

Figure 2-15 shows the distribution of trucks and miles by primary trip distance for each truck weight class. Figure 2-16 shows the average annual miles traveled per vehicle. From these figures, the following important trends in motor carrier truck usage can be discerned:

- The majority of Class 3–6 trucks are used primarily in local service with trip length of 50 miles or less.
- About half of Class 7–8 trucks are used locally while 23% are used primarily for trips more than 200 miles.
- Within each interval of range of operation, the annual miles traveled per heavy truck is considerably higher than miles traveled per lighter truck, with Class 7–8 trucks averaging 45,240 miles per year, more than three times that of Class 4–6 trucks, which average 13,650 miles annually.



Source: U.S. Department of Commerce, Bureau of the Census, 2002 Vehicle Inventory and Use Survey

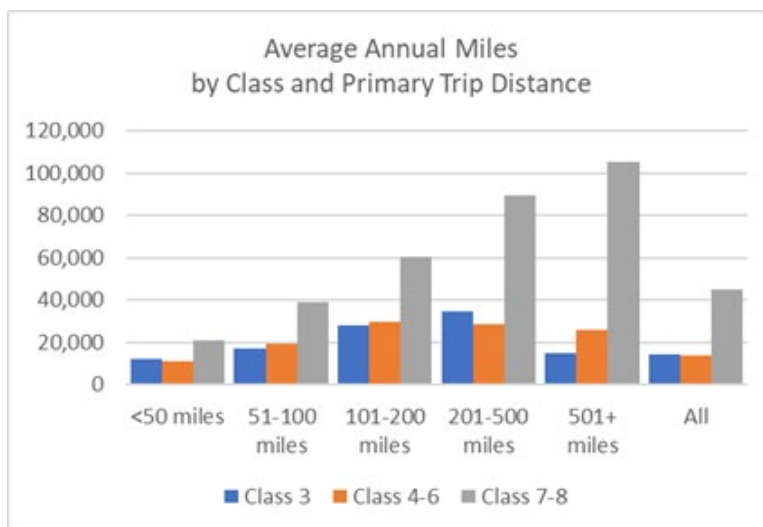
Vehicle class is defined as follows:

Class 3: gross vehicle-weight rating is 10,001 to 19,500 pounds.

Class 4-6: gross vehicle-weight rating is 19,501 to 26,000 pounds.

Class 7-8: gross vehicle-weight rating is 26,001 pounds or more.

Figure 2-15. Distribution of trucks and annual miles within weight class by primary trip distance.



Source: U.S. Department of Commerce, Bureau of the Census, 2002 Vehicle Inventory and Use Survey

Figure 2-16. Average annual miles traveled per vehicle by primary trip distance and vehicle weight class.

Operating range has a significant impact on the way that a charging infrastructure may be deployed. Operating range is typically defined from a central location, like a depot. Local and regional operations have a greater opportunity to use private charging infrastructure because electric trucks in these operations are more likely to return home (i.e., to the depot) prior to exceeding their EV range. Long-haul truck operations will be more heavily dependent on public charging infrastructure.

Shipment Size

For-hire carriers can be further segmented based on the type of service, according to the following two classifications:

- TL carriers contract an entire truck or trailer to move a load for a single shipper with one origin and destination, typically in long-haul service.
- LTL carriers collect smaller shipments from multiple cargo owners at local pickup points, consolidate them onto a truck, and distribute goods through a delivery network. These networks may consist of both regional distribution routes and long-haul segments.

The operating patterns of TL and LTL carriers are often different. In TL operations, the trucks often do not operate on fixed routes and schedules, but instead move between various client facilities as needed (see Figure 2-17). On the other hand, an LTL firm usually operates on set routes between its hub terminals and between these terminals and client origins and destinations (see Figure 2-18). Each LTL business may have a uniquely designed network operation for its specific purposes, and these operations can be complicated. Some LTL firms are dedicated to regional service, wherein drivers depart from each terminal, deliver and pick up loads, and return to the terminal. Other firms may also provide a nationwide long-haul service that involves long-distance transports that can be in excess of 1,000 miles.⁷³

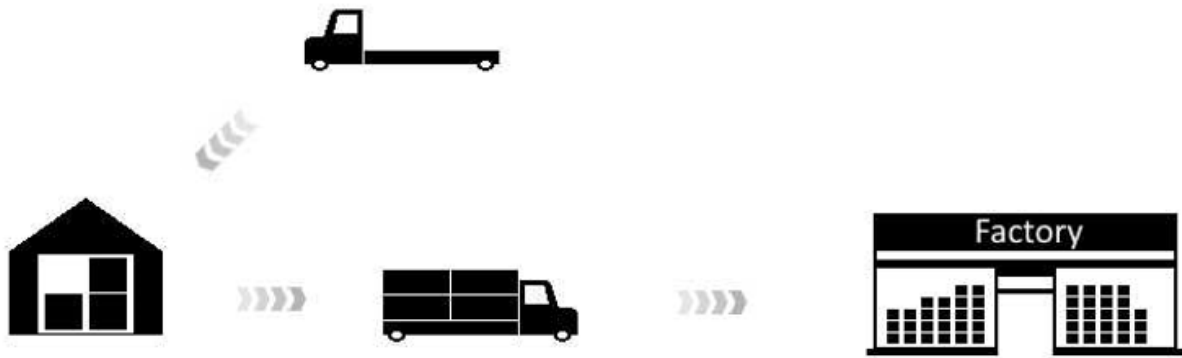


Figure 2-17. An example of truckload carrier operation.

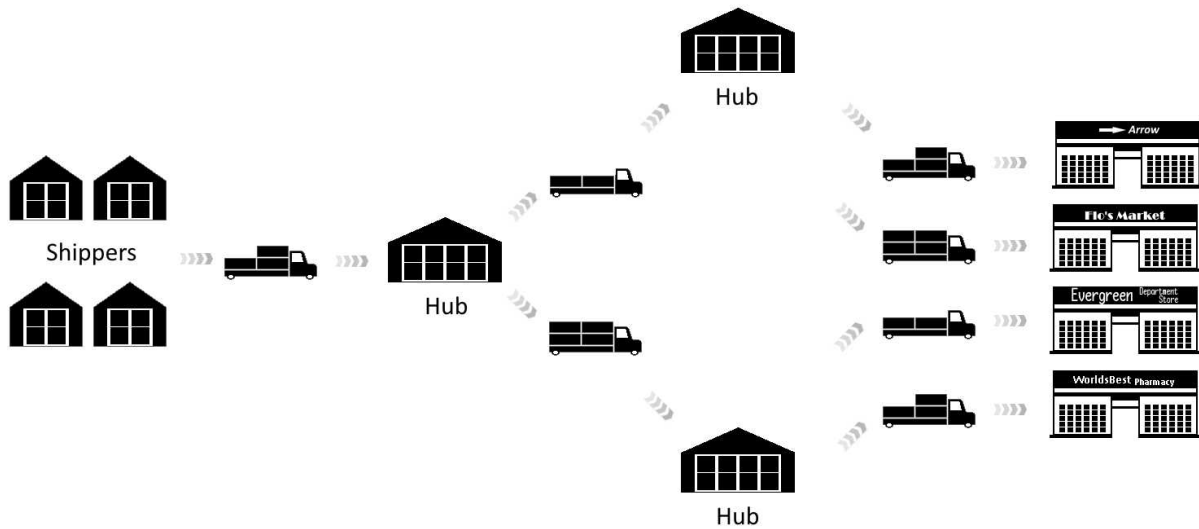


Figure 2-18. An example of less-than-truckload carrier operation.

Figure 2-19 shows the distribution of trucks used and miles traveled by truck weight class for TL and LTL carriers. Figure 2-20 shows that TL carriers' operations are characterized by longer hauls and heavier vehicles, with 63% of miles accounted for by trucks with primary trip distances of more than 200 miles, 96% of those miles traveled by Class 7–8 trucks. Meanwhile, LTL carriers use Class 4–6 vehicles as often as Class 7–8, though the smaller vehicles are used for shorter trips, such that more than two-thirds of the miles are accounted for by Class 7–8.



Figure 2-19. Distribution of trucks and miles by truck weight class for truckload and less-than-truckload service. Source: U.S. Department of Commerce, Bureau of the Census, 2002 Vehicle Inventory and Use Survey.

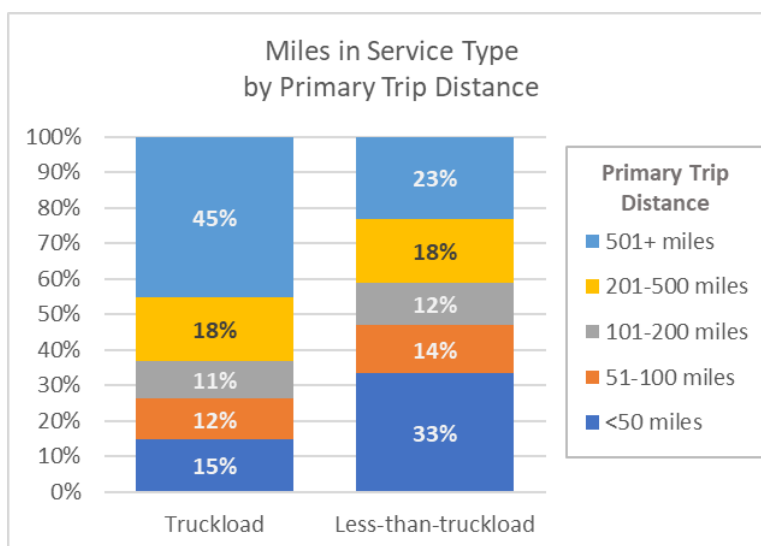


Figure 2-20. Distribution of miles by primary-trip distance for truckload and less-than-truckload service. Source: U.S. Department of Commerce, Bureau of the Census, 2002 Vehicle Inventory and Use Survey

The operating patterns associated with for-hire carrier shipment sizes will influence where a private charging infrastructure could be made available. An LTL hub-and-spoke model and designated routes may render private chargers installed at the carrier’s own facilities effective in meeting a large portion of the fleet’s energy needs. TL point-to-point operations may depend more on public infrastructure.

Review of Motor Carrier Industry Regulations and Incentives

Trucking Regulations

Motor carriers determine their operating model and type of trucks based on the factors described above. However, both the operations and the vehicles are constrained by regulations set by the Federal Motor Carrier Safety Administration of the U.S. Department of Transportation. These regulations significantly influence motor carrier operations. In order for electric trucks to be practical for motor carriers, the vehicles and charging infrastructure must be designed to enable operation that complies with regulations and aligns with motor carrier interests and incentives.

For example, truck driver pay structure affects the truckers' driving behavior, which in turn sets the requirements for the vehicle performance and operations. Drivers of heavy trucks and tractor-trailers are usually paid by how many miles they drive.⁷⁴ A survey conducted by the National Institute for Occupational Safety and Health reported that 65.9% of the respondents were paid by the mile.⁷⁵ This means that many drivers, especially those who operate long-haul transports, have an incentive to drive consecutive hours without stopping. However, drivers' hours of service are subject to the following regulations:⁷⁶

11-Hour Driving Limit: driver may drive a maximum of 11 hours after 10 consecutive hours off duty

- 14-Hour Limit: driver may not drive beyond the 14th consecutive hour after coming on duty, following 10 consecutive hours off duty
- Rest Breaks: driver must take a 30-minute break after 8 consecutive hours of driving
- 60/70-Hour Limit: driver may not drive after 60/70 hours on duty in 7/8 consecutive days.

Currently, driver time spent fueling trucks is considered time on duty. This is also true of time spent at loading docks. Increasing fueling time to charge an electric truck would restrict the miles driven within regulated time limits and thereby limit driver pay. It would also constrain a motor carrier's route choices and ability to meet their delivery demands.

With respect to the vehicle, federal weight standards are perhaps the most limiting factor influencing truck operations. Federal weight standards apply to commercial vehicles operating on the Interstate Highway System. These standards limit gross weight and per-axle weight and also specify axle spacing to reduce the risk of damage to highway bridges. Federal standards for commercial vehicle maximum weights on the interstate highway system are as follows:⁷⁷

Single-Axle Weight: The total weight on one or more axles whose centers are spaced not more than 40 inches apart. The federal single-axle weight limit on the interstate highway system is 20,000 pounds.

- Tandem-Axle Weight: The total weight on two or more consecutive axles whose centers are spaced more than 40 inches apart, but not more than 96 inches apart. The federal tandem-axle weight limit on the interstate highway system is 34,000 pounds.
- Gross Weight: The maximum weight of a vehicle or vehicle combination and any load thereon on the interstate highway system is 80,000 pounds.

States may set their own commercial vehicle weight standards and have different exceptions to federal truck weight limits.

Electric trucks may be heavier than their conventional diesel counterparts due to the weight of large battery packs necessary to provide trucks with long range. If this is the case, higher vehicle weight will limit payload capacity, given gross vehicle weight limits. This will directly impact motor carrier operations and earnings potential.

In conclusion, motor carriers and their drivers have strong incentives to maximize the miles driven and the amount of payload transported within regulated time and weight limits. Within current industry norms, motor carriers would ideally adopt vehicles that impose little or no weight restrictions and provide the means for charging them that have little or no time penalties relative to conventional diesel trucks. Given expectations for range, battery weight, and charging time limitations of electric trucks, motor carriers will likely need to make tradeoffs to successfully adopt EVs. New tools are needed to help them understand and manage these tradeoffs.

Selection of Use Case for Modeling Charging Infrastructure

The variety and complexity of operations in the freight-trucking industry make it challenging to discern where electric trucks are beneficial, what kind of charging infrastructure is needed for electrification to be feasible, and who will bear the costs of and receive benefits from charging infrastructure investment. Charging infrastructure costs must be weighed against the cost of operational changes, such as routing and dispatching changes. The AFI Pillar chose to model the operation and charging of electric trucks to quantify some of the

tradeoffs necessary for trucking electrification and charging infrastructure. For this exercise, the Pillar chose to focus on Class 7/8 tractor-trailers, because of the high potential for reductions in energy consumption, due to the large share of miles driven by these truck classes. Based on results of segmentation analysis and review of regulations and incentives, the Pillar chose to model a use case that would be most amenable to electrification: a regional-haul, private motor carrier that follows a hub-and-spoke model, transporting freight between a central warehouse and distributed destinations that its parent company owns. Section 3.2.3 describes this modeling work in detail.

2.2 Charging Network Design Tradeoffs

After characterizing EV market segments and the interests of EV operators, the AFI Pillar was prepared with scenarios and assumptions for modeling and simulation necessary to address its second and third research questions, restated as follows:

- What are the cost/benefit tradeoffs inherent with different approaches to designing charging infrastructure to serve light-duty human-driven and automated electric passenger vehicles?
- What is needed to understand tradeoffs inherent with different approaches to designing charging infrastructure for Class 7/8 electric trucks for freight transport?

To address charging infrastructure for light-duty vehicles, the AFI Pillar used multiple modeling and simulation tools and analytical methods to design and simulate the use of charging infrastructure by EVs in specific case studies. For the electrification of freight trucks, modeling and simulation tools are immature, so the AFI Pillar employed a simple model in a case study to investigate the scope of the challenge of heavy-duty truck electrification. In these case studies, parameters defining charging infrastructure, such as the number, location, and power level of charging stations, were varied to determine the effect on EV use and cost.

In summary, the AFI Pillar studied charging network design tradeoffs for three cases: ride-hailing vehicles, car-sharing fleets, and heavy-duty trucking for freight delivery.

2.2.1 Charging Network Design to Support Electric Ride-hailing Vehicles

Introduction

Building charging infrastructure is expensive, and any public or private entity motivated to install public charging stations enters the planning process with a finite budget. To achieve the greatest return on investment, it is important to estimate the charging station locations, number of plugs at each station, and charging power that an EV fleet may demand of the future network. This type of forecasting problem is one that lends itself well to a simulation-oriented approach informed by high-resolution spatial-temporal data.

The AFI Pillar conducted three simulation-based case studies, each building on the previous one, to investigate tradeoffs in designing charging infrastructure to serve ride-hailing EVs. The following is a summary of each case study:

Case Study 1 was done from the perspective of a charging network provider in Columbus, Ohio, that is planning charging infrastructure for human-driven ride-hailing vehicles. This study confirmed that choosing locations for DCFC stations in areas of high demand is economically advantageous for the charging provider.

Case Study 2 took the perspective of TNC and taxi drivers in Columbus, Ohio, and Austin, Texas, who have switched from ICEVs to BEV250s. Simulation showed that even with multi-plug, 50-kW DCFC stations installed at high-demand locations, on 60% of days, drivers without access to overnight charging could not complete the same amount of daily driving in a BEV250 as they had in an ICEV. They simply would not have enough time at charging stations on high-mileage driving days. If they could charge at home or a depot every night, they would almost always be able to perform the same driving in a BEV250 as they did in an ICEV because they start the day with fully charged batteries.

Case Study 3 explored tradeoffs further by varying not only charging station availability, but also charging power and EV range; this study simulated different configurations of human-driven and AEV ride-hailing vehicles and charging infrastructure in the San Francisco Bay Area in California. This study found that there is a limit to the passenger trips and miles traveled that ride-hailing fleets can serve, whether human-driven or

automated, if they employ low-range EVs (i.e., BEV100s) with access to a 50-kW DCFC network, even if that network is vastly more dense and widespread than today’s network. Ride-hailing drivers and companies that want capacity to serve high customer demand should employ EVs with increased EV range and capacity for higher-power charging, in addition to ensuring access to higher-power charging infrastructure.

Additional details supporting these findings, as well as other key findings, are provided in this section for each case study.

Research Approach

The AFI Pillar used two simulation tools, EVI-Pro and FCSPlan, to study public charging infrastructure for ride-hailing vehicles. These tools use a similar approach, simulating charging demand using an unconstrained network and then clustering the resulting demand for charging in time and space to design a public network. This approach is illustrated in Figure 2-21 for an EVI-Pro simulation in Austin, Texas. EVI-Pro relies on real-world travel data, such as the datasets from RideAustin and CYC, to simulate charging behavior for various fleet electrification scenarios. In this example, a dense lattice of charging stations is uniformly spaced across Austin with an unlimited number of charging plugs at each location to form an unconstrained network of public chargers. This network is simulated in EVI-Pro with EVs utilizing charging stations whenever and wherever needed to have sufficient range to complete daily driving. This identifies charging demand at all possible locations where EVs might charge, given the opportunity. Simulated demand from the unconstrained network is then spatially aggregated using a hierarchical clustering algorithm in EVI-Pro to generate a set of discrete charging locations, each with a limited number of plugs and charging capacity. The AFI Pillar used EVI-Pro to simulate charging infrastructure to serve human-driven ride-hailing vehicles in case studies in multiple cities.

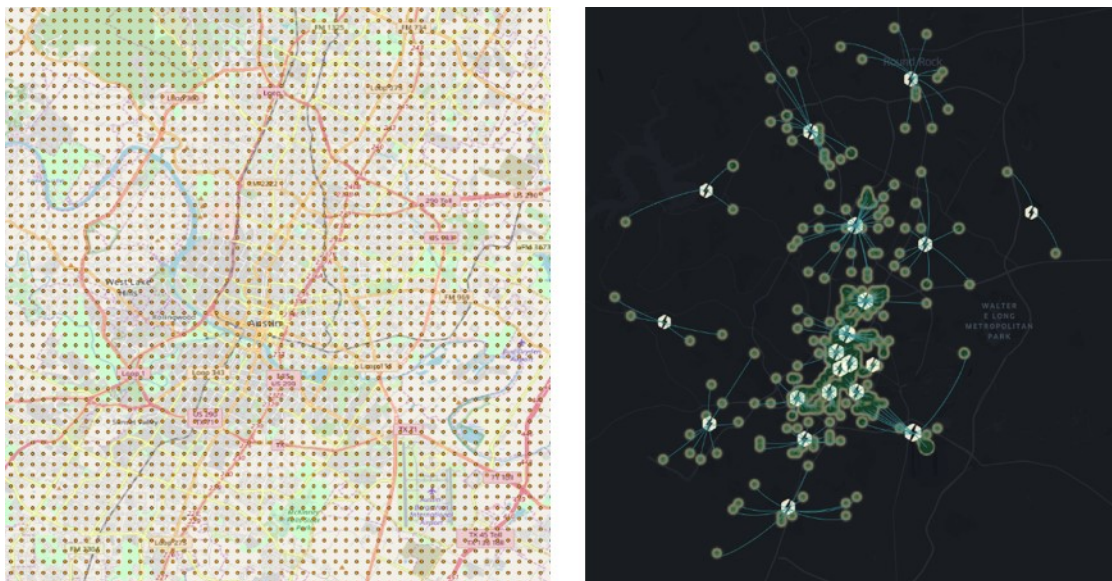


Figure 2-21. EVI-Pro example from Austin, Texas of simulating unconstrained demand using a dense lattice of chargers (left) and clustering resulting demand to form a public network (right).

Similar to the hierarchical clustering approach used in EVI-Pro, FCSPlan uses K-means clustering to site charging station locations and numbers of individual charge plugs for automated ride-hailing vehicles in simulated networks. The AFI Pillar used this tool to simulate charging networks for automated electric ride-hailing fleets in the San Francisco Bay Area in California. Concepts for charger system planning and design were combined with large-scale transportation system network modeling using BEAM. BEAM is an agent-based transportation system model designed for analyzing future transportation network scenarios. Further details of BEAM are provided in the SMART Mobility Model Appendix.

FCSPlan was integrated with BEAM to take advantage of BEAM’s simulation of the detailed operations of a ride-hailing fleet. Automated electric ride-hailing vehicles are assumed to charge at a set of charging depots

that can be accessed only by automated ride-hailing vehicles, while human-driven electric ride-hailing vehicles compete with non-ride-hailing vehicles on the general network. The optimal depot charging network is defined by FCSPlan, and the public charging network is defined by EVI-Pro, both with an iterative process. In the first iteration of this process, vehicles are simulated as having access to DCFC at all potential parking spots. Using initial outputs from BEAM, based on nodal demands in this scenario with unconstrained charging infrastructure, the FCSPlan model then chooses optimal locations for a limited amount of DCFC stations to support the operation of the automated electric ride-hailing vehicles. EVI-Pro uses the methodology described above to site charging infrastructure so as to meet charging demand from human-driven ride-hailing and personal-use vehicles. The constrained charging networks generated by FCSPlan and EVI-Pro are input into BEAM for subsequent runs with the same vehicle fleet, and system performance metrics are produced using this more detailed fleet simulation.

FCSPlan uses a two-stage computational-geometry-based heuristic approach. In the first stage, BEAM outputs are used to identify charging demands from an AEV fleet serving elastic demand. These demands are based on the simulated operation of the vehicles, including driving, parking, and charging events. Whenever a vehicle’s battery SOC drops below a defined threshold, the vehicle’s location at the end of its trip is identified as a location of charging demand. All locations of charging demand are recorded for use in the second stage, where a hybrid algorithm based on K-means clustering is used to site and size charging stations to meet the identified charging demand. K-means clustering is a widely used and understood method for solving this type of problem. The FCSPlan approach is summarized graphically in Figure 2-22.



Figure 2-22. FCSPlan and BEAM integration.

EVI-Pro and FCSPlan are designed to optimize charging networks to satisfy all charging demand. These tools provide useful insights about ideal charging infrastructure design, but they do not take into account practical constraints on charging station installation, such as real estate scarcity, unwillingness of local land owners to install charging stations, and adequacy of facilities at desired locations to support charging stations and their users.⁷⁸ Therefore, the AFI Pillar developed an alternative to the simulation-centered approaches of EVI-Pro and FCSPlan to envision future charging infrastructure that mimics today’s networks. This alternative trend-based approach uses existing data on real-world public charging networks. The AFDC provided data on DC fast charger locations which were manually classified based on location type.

Analysis of the two largest DCFC networks indicated that a majority of present-day DCFC are hosted in retail spaces.

Figure 2-23 shows that 96% of Electrify America’s DC fast chargers are hosted by retail businesses. The right chart shows that 65% of the retail businesses hosting DC fast chargers are big box stores such as Walmart. Figure 2-24 provides a similar assessment of EVgo’s network. About 87% of EVgo’s DC fast chargers are hosted by retail stores, showing a similar trend to Electrify America. DC fast charger installation in these large retail spaces is potentially convenient due to the large parking areas and availability of high electric power capacity.

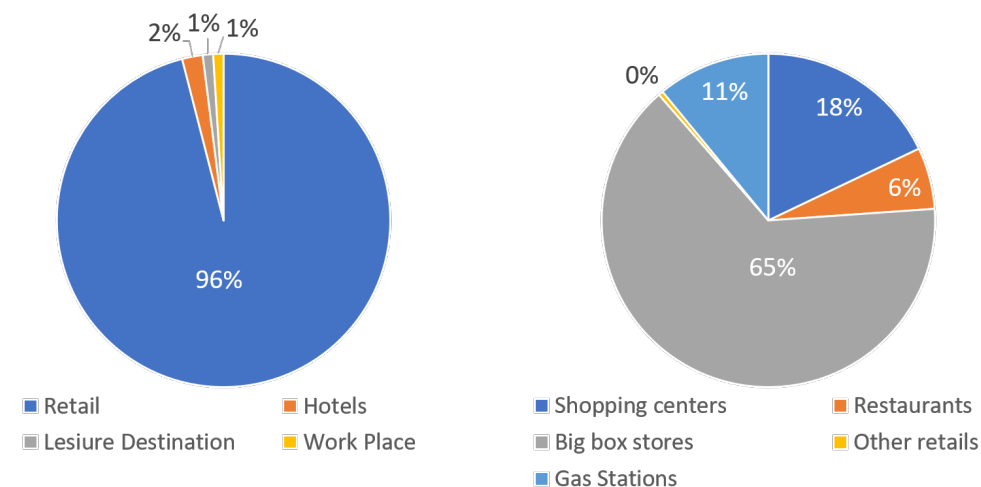


Figure 2-23. Hosting venues of Electrify America's DC fast chargers.

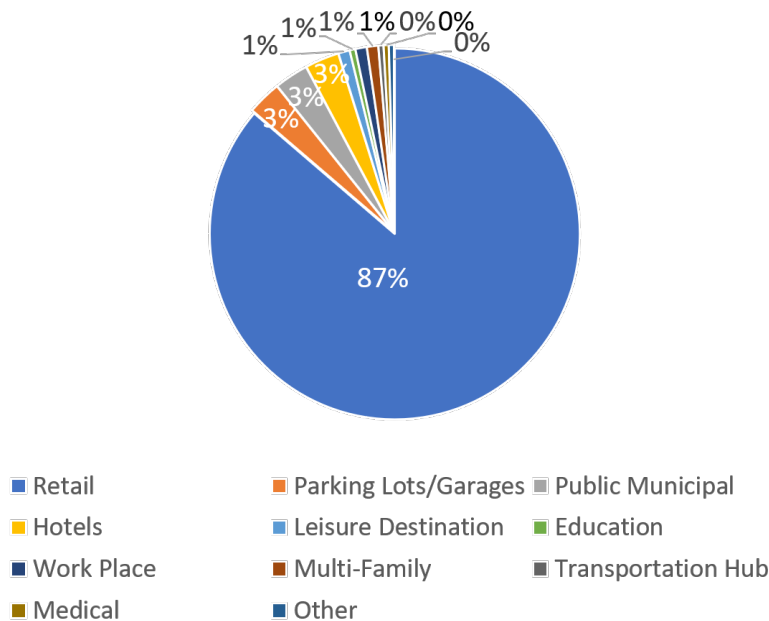


Figure 2-24. Hosting venues of EVGo's DC fast chargers.

The AFI Pillar used these trends to create a future hypothetical charging infrastructure network that mimics today’s network. To do so, the AFI Pillar increased the number of DCFC station locations in a metropolitan area by 50%, siting stations at locations representative of today’s location types. The number of charging plugs at each location was selected so that the distribution of the number of plugs at new stations matched the distribution of the number of plugs at today’s stations. This approach (called the “trend-based” approach)

created a sparse charging network, relative to the demand-based, rich charging networks generated by EVI-Pro and FCSPlan.

These approaches to the design of charging infrastructure networks were implemented in three case studies. EVI-Pro was used in the studies set in Columbus, Ohio, and Austin, Texas, described in the next two sections. FCSPlan, EVI-Pro, and the trend-based approach were used in a case study set in the San Francisco Bay Area, described in the third section below.

Case Study 1: Capture Maximum Demand or Minimize Cost? Designing a Direct-Current Fast Charger Network for Human-Driven Electric Ride-Hailing Vehicles in Columbus, Ohio

Key Findings

Cost modeling of simulated DCFC stations serving personal-use and ride-hailing EVs in Columbus, Ohio, found that the utilization of and cost to install and operate DCFC stations varies dramatically by location.

Utilization of 12 DCFC stations by simulated EVs varied from two to 48 charging sessions per day. The largest, most expensive charging station was estimated to have a total monthly cost of up to \$6,400 per month, while the smallest charging station that was cheapest to install would cost as little as \$1,100 per month (excluding real estate costs).

However, the effect of variation in fixed upfront capital and installation costs diminishes as fixed costs are amortized across a greater number of charging sessions. The largest, most expensive charging station was also the most active, resulting in a normalized cost of \$4.45 per session; small, inexpensive, but poorly utilized stations would see costs of up to \$42 per session.

Therefore, in the cases where DCFC networks require payment per use, charging station providers can more effectively balance cost and revenue by prioritizing placement of chargers at sites that are expected to experience higher utilization, rather than sites where installation cost will be lowest. Such sites are likely to include urban cores, transit hubs, and airports.

Introduction

AFI Pillar research found that DCFC is an important enabler for ride-hailing EVs. In order for DCFC networks to be economically viable, they must have both high utilization and low installation and operating costs; however, it is difficult for charging network providers to determine the degree to which they should prioritize expected utilization versus cost when siting charging stations. Furthermore, both utilization and cost are hard to predict. Both the operation and installation costs can vary dramatically. Past studies pointed out great uncertainty in identifying and quantifying significant cost factors of DC fast chargers.^{79, 80} At the same time, uncertainty persists in the operational characteristics of ride-hailing fleets and how they may evolve in the future.^{81, 82, 83, 84, 85} Therefore, the AFI Pillar saw the need for rigorous research on assessing economic feasibility of DC fast chargers for ride-hailing vehicles. Results shared in this section suggests that when choosing DC fast charger sites to serve ride-hailing EVs, charging providers should place priority on locations with the potential for high utilization rather than choosing locations with low installation cost.

Simulated Charging Demand

Understanding vehicle driving and parking patterns is key to determining EV charging infrastructure requirements. Therefore, analysis of ride-hailing vehicle use patterns was a necessary first step in estimating DC fast charger needs for ride-hailing EVs. Given the lack of available ride-hailing data sets when this case study was conducted (circa 2017), the AFI Pillar first developed a procedure for synthesizing hypothetical ride-hailing activity patterns from personally owned vehicle datasets and applied the procedure to an example dataset. A heuristic emulated ride-hailing vehicle data for ride-hailing systems, using personal trip data sets as inputs. The heuristic process objective was to enable matching of personal trips to hypothetical TNC vehicles by chained-together trips that could be conducted consecutively and by allocating trip chains to hypothetical TNC vehicles.

The AFI Pillar applied the methodology to 5,000 passenger travel-days from personal GPS trip data from Columbus, Ohio. Trips were assumed to be completed in individual vehicles without allowing for pooling. The ride-hailing emulation attempted to match trips by minimizing deadheading distance and wait time with

constraints of a maximum of 5 miles or 20 minutes between a given passenger drop-off location and the next passenger pickup location. Ride-hailing vehicles must satisfy the same travel demand (all trips are served by these vehicles). Trip chains were thus locally optimized, meeting the objective of minimum deadheading distance for each TNC vehicle, but not optimized globally at the system level.

EVI-Pro then estimated EV charging infrastructure requirements for two EV fleets operating in Columbus, Ohio. The first fleet of 5,000 EVs consisted entirely of personal-use vehicles driven by owners in the traditional context (as described in the raw data). The second fleet consisted of a mix of personal-use and TNC EVs with a similar total fleet size. The fleet size of the ride-hailing fleet was selected to maximize utilization of ride-hailing vehicles through the trip-chaining heuristic, resulting in a fleet of 3,726 ride-hailing vehicles and 1,108 personal vehicles. Trips that could not be successfully chained were assigned to personal vehicles. All drivers were assumed to have access to charging at home. EVI-Pro simulation output the number of charging units by type that would be needed to enable both fleets to satisfy passenger travel requirements. These results are shown in Table 2-8.

Table 2-8. Infrastructure requirements that would be necessary to support electrification of the two vehicle groups (5,000 personal vehicles or 3,726 ride-hailing vehicles plus 1,108 personal vehicles).

Charger type	Number of charging plugs needed to meet demand from 5,000 personal vehicles	Number of charging plugs need to meet demand from 3,726 ride-hailing and 1,108 personal vehicles	Ratio $\left(\frac{\text{ride-hailing}}{\text{personal}}\right)$
Home Single Family L1	3,732	3,555	0.95
Home Single Family L2	172	212	1.23
Home Multi-unit L2	702	702	1.00
Work L2	222	160	0.72
Public L2	211	387	1.83
Public DCFC	13	24	1.85

While residential charging requirements remain similar for personal-use and ride-hailing vehicles, the demand for non-residential charging is drastically different. Ride-hailing drivers’ shorter dwell times at work (i.e., other gigs) reduce the demand for workplace charging by 28% while more frequent dwell events in public locations combined with higher daily VMT increases the need for public L2 and DC fast charger by 83% and 85%, respectively.

EVI-Pro output the basic electricity consumption profiles, including peak demand, of the 12 public DCFC stations used by personal-use and ride-hailing EVs during a single day. This information is shown in Table 2-9. Recall that EVI-Pro recommends charging stations be placed at locations where EVs need to be charged in order for them to complete their daily driving (that, in the real world, drivers completed in ICEVs). It also recommends the number of charging plugs at each location to meet all demand without the need for queuing. It does not estimate demand that might be induced by the presence or size of a charging station.

Table 2-9. Simulated use profiles of 12 DCFC stations by personal-use and ride-hailing EVs during a single day in Columbus, Ohio.

Charging Station Number	Sessions	No. of plugs	Daily energy usage (kWh)	Maximum demand (kW)
1	6	2	117.81	82.06
2	17	4	297.11	61.5

Charging Station Number	Sessions	No. of plugs	Daily energy usage (kWh)	Maximum demand (kW)
3	2	2	85.24	61.5
4	2	2	91.51	61.5
5	6	2	94.17	66.85
6	6	2	155.66	61.5
7	48	7	638.35	78.91
8	2	1	17.58	28.93
9	3	1	30.75	28.75
10	2	1	26.63	20.5
11	7	2	52.91	33.55
12	3	1	23.36	20.5

Charging Infrastructure Cost

Operating, installation, and capital equipment costs were estimated for candidate DCFC locations output by EVI-Pro to show the relationships between location, cost, and use. The AFI Pillar partnered with AEP Ohio, an electric utility serving part of the Columbus area, to estimate the total cost of DCFC stations at 12 locations recommended by EVI-Pro that are in AEP Ohio’s service territory. This analysis found that not only can costs be high, but they also vary widely depending on how the DC fast charger is used and where it is located.

Operating Cost of Charging Infrastructure

Operating costs of the 12 DCFC stations were quantified based on utilization simulated by EVI-Pro. Because the cost of electricity is a large component of DCFC operating cost, the Pillar conducted a thorough analysis to accurately estimate electricity cost using actual AEP Ohio electricity rate plans. The analysis included three major assumptions: (1) a single charging network provider owns and operates all 12 DCFC stations, (2) the provider must buy all the station’s electricity from the local electric utility, and (3) the stations are metered separately from surrounding facilities, meaning that the providers pay for electricity exclusively consumed by the charging stations.

Like all electric utilities, AEP Ohio has multiple rate plans designed for different customers with varying voltage and power demand requirements. An electricity rate plan is composed of several charges, including a monthly service charge, energy charge, and demand charge. ^e

A customer may be eligible for more than one rate plan. Peak demand usually determines rate plan eligibility.

The energy consumption profiles in Table 2-8 were used to select the lowest-cost commercial rate plan offered by AEP Ohio (i.e., GS-2 Secondary Service ^f) for the hypothetical charging provider. The charging network provider’s monthly electric cost was calculated using these DCFC station use profiles, assuming daily charging

^e The plan may also include riders, which may be flat rates, may depend on energy or power consumption, or may be a percentage increase on the base bill. In addition, some utilities have rates that differ depending on the season and the time of day. See California Public Utilities Commission, 2017. What are TOU rates? www.cpuc.ca.gov/General.aspx?id=12194

^f This rate plan is available for general service to customers with maximum demands greater than 10kW, provided by Columbus Southern Power, a subsidiary of AEP Ohio. Source: Public Utilities Commission of Ohio, “AEP Ohio Standard Tariff”, AEP Ohio (2017).

behavior was consistent across a month. The calculations required to determine the charging provider's monthly electricity bill are included in Appendix E.

The total monthly electricity cost for the 12 simulated charging stations in the AEP Ohio service territory in Columbus ranges from around \$320 to almost \$1,400. The total operating costs for each DCFC station were assumed to be the monthly electricity cost plus \$100/month for warranty, maintenance, network service, and other fees. As a more generalizable metric, cost efficiency, in terms of dollars per kilowatt-hour, was calculated by dividing the monthly electricity bill by the total energy consumption. Figure 2-25 shows the cost efficiency calculated for each of the 12 simulated charging stations, based on one month of simulated charging. The electricity cost for the 12 stations ranged from \$0.12/kWh for the most highly utilized charging station (#7) to \$0.75/kWh for the least utilized station (#8).

As the trendline in Figure 2-25 shows, the cost per unit of energy consumption decreases as number of charging sessions increase at a charging station. This relationship exists because the monthly fixed and demand charges average out as they are amortized across a greater number of charging sessions. If the number of charging sessions continues to increase, cost efficiency will approach, but never meet, the energy-related charges (\$0.0684/kWh for the energy and rider charges, in this case). This is because busier charging stations see coincident charging of multiple vehicles, which raises peak power demand, incurring a greater demand charge, such that the total cost per unit energy increases. Such complexities in electricity rate structures make it difficult for charging network providers to estimate operating cost without sophisticated models and data analytics.

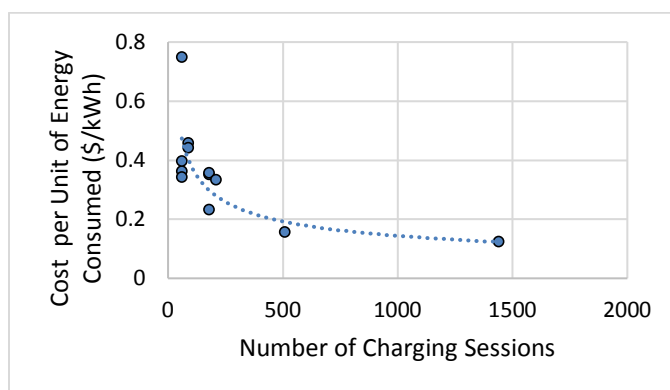


Figure 2-25. Correlation between cost efficiency and number of charging sessions at the 12 simulated DCFC stations in Columbus.

Installation Cost of Charging Infrastructure

The cost of charging station construction, including charging equipment installation, can be a significant burden in materializing a DCFC provider's business. Installation costs of DC fast chargers can vary depending on many different technical and environmental factors. Cost data for charging infrastructure is currently limited and can be found in few peer-reviewed journal articles.^{86, 87}

The AFI Pillar analyzed DC fast charger installation cost data from the EV Project. Results are summarized as follows:

- Average cost = \$23,700
- Median cost = \$22,600
- Minimum = \$8,500
- Maximum = \$50,820.

The total cost of the installations cited above includes only costs paid to the electrical contractors to install 60-kW Blink DC fast chargers. This cost would typically include permit costs, engineering drawings, contractor's

installation and administration labor, subcontracted construction labor or equipment (e.g., concrete, asphalt, trenching, and boring), and materials other than the DC fast charger itself.

To evaluate the cost drivers for DC fast charger installations during the EV Project, the AFI Pillar performed new analysis to examine some of the features of the installed hardware and site conditions. The following were found to be significant DC fast charger installation cost drivers observed during the EV Project that are not specific to the 60-kW Blink DC fast charger. Their impact on installation costs would be applicable for any installation of a DC fast charger unit rated at 20-kW or more:

- Electrical service upgrade
- Ground surface conditions
- Materials.

Data from the EV Project indicates that DC fast charger installations often require new electrical service to the host’s site. The cost of these installations is significantly higher than those that do not require new service. The magnitude of this cost increase depends on existing electrical services at the host site and costs from the electric utility to install a new, metered electrical service. Electrical service extension costs also vary depending on the electric utility’s policies for aboveground or underground service. Overhead service is typically less expensive and quicker than trenching for an underground service extension. The cost of underground service extension varies depending on the distance (i.e., the length of the underground passage) from the transformer. Therefore, to determine the economical suitability of the location for DC fast charger installation, each site needs to be vetted for available power and proximity to existing power service. To quantify association between total installation cost and the above-mentioned cost drivers, several attributes of the DC fast charger sites from the EV Project were collected via invoices and interviews with the contractors.

An ordinary least-squared regression was estimated to examine the statistical association between total cost and the identified cost drivers. The coefficient estimates and the 95% confidence intervals are shown in Table 2-10. The mean DC fast charger installation cost at a site with preexisting electricity service (i.e., not requiring a service upgrade) is estimated to be \$18,290. This installation cost is significantly affected by the electricity service upgrade, which adds an additional cost of between \$1,400 and \$7,800. The cost of service upgrade depends on whether the service is overhead or underground. If the electricity service is underground, the cost of service upgrade is affected by the type of ground service and the distance of the needed underground power feed. If the ground surface is gravel rather than concrete or asphalt, installation cost is reduced by an estimated \$200–9,100, and the cost of trenching or boring for DC fast charger installation, if required, is estimated at between \$39 and \$175 per foot.

Table 2-10. DC fast charger installation cost attribute data collected.

Variable Name	Description
Service Upgrade	Binary variable where 1 indicates that new service was required and 0 indicates new service was not required
Underground Service	Binary variable where 1 indicates that new service was required and 0 indicates new service was not required
Surface material	Binary variable where 1 indicates that ground surface is gravel and 0 indicates either asphalt or concrete
Distance	Distance of underground power feed in feet

Because the exact installation location of DC fast chargers at each of the 12 sites recommended by EVI-Pro is unknown and a slight change in the installation position may significantly affect the installation cost, the potential range of installation costs was computed based on the regression model given in Table 2-11. This range was calculated to be \$16,500 to \$45,150 per site, not including the cost of real estate or capital equipment (i.e., the DC fast chargers themselves). Even though no electrical service upgrade would be needed

at any of the 12 charging station locations recommended by EVI-Pro, the maximum potential installation cost was calculated assuming that \$7,750 upgrades would be needed.

Table 2-11. Regression model coefficient estimates for the cost to install a DCFC station.

	Coefficient	Standard. Error	P-value	2.5%	97.5%
Intercept	18,290.26	863.02	<0.01	16,574.63	20,005.88
Service Upgrade	4,559.02	1,611.92	<0.01	1,354.61	7,763.41
Underground × Distance	106.69	34.15	<0.01	38.79	174.59
Underground × Gravel	-4,687.10	2,241.56	<0.05	-9,143.19	-231.02
R-squared: 0.204, Adjusted R-squared: 0.176					

Low-cost installations require sufficient electrical power at the site to accommodate the DC fast chargers and a simple installation with either short underground conduit runs or surface-mounted conduit. According to AEP Ohio, all 12 locations selected for DCFC stations in the EVI-Pro simulation have adequate existing electrical service to serve a 60 kW DC fast charger. Because a service upgrade would not be necessary, the relative difference in installation costs among the proposed DC fast charger installation sites would primarily result from the costs of trenching and boring to extend any underground service lines. Figure 2-26 shows satellite imagery of the location suggested by EVI-Pro for charging station Location 10. Overhead power lines, which are shown in the image as blue lines, extend around the parking lot of a large retail store, making it convenient for installing DC fast chargers at some parking spaces without a need for extensive underground work. This avoids the high cost of installing long underground conduits and restoring paved surfaces.



Figure 2-26. Image of candidate location for DC fast charger 10. Satellite imagery credit: © 2017 Google, Map Data ©2017 Tele Atlas.

Total Cost for Charging Infrastructure

In addition to operating and installation costs, the total cost to own and operate a DCFC station also includes capital equipment and real estate costs. Capital cost of a single DCFC unit with one plug was assumed to be

\$40,000, not including installation. The incremental capital cost for each additional DCFC plug per site also was assumed to be \$40,000. Real estate cost was not included in this analysis due to the immaturity of the market and lack of data. (Anecdotal data suggests that real estate costs for DCFC stations have ranged from free to more than the monthly operating cost of the station.)

Capital costs for each site were added to the range of expected installation costs for each site to provide the potential range of total upfront cost. The cost per month to finance upfront capital equipment and installation expenses over 10 years at an 8% discount rate was calculated and combined with monthly operating expenses to determine the total monthly cost of charging infrastructure. These costs ranged from \$1,100 to \$1,400 per month for the least expensive station (Location 12, with a single plug and two short charges per day) and from \$6,100 to \$6,400 for the most expensive station (Location 7, with seven plugs and 48 charges per day).

To put total cost in terms that are relatable to revenue, the total cost of charging infrastructure at each location was divided by the number of charging sessions. Figure 2-27 shows this cost. The horizontal blue bar represents the mean total cost per session for each charging station. The error bars represent the range of total cost (which is synonymous with the range of expected installation costs) per session for each station. On a per-session basis, the total cost for the least-expensive charging station (Location 7) ranged from \$4.20 to \$4.50 per session, while the most expensive station (Location 4, with two plugs and two sessions per day) ranged from \$36.90 to \$42.60 per session.

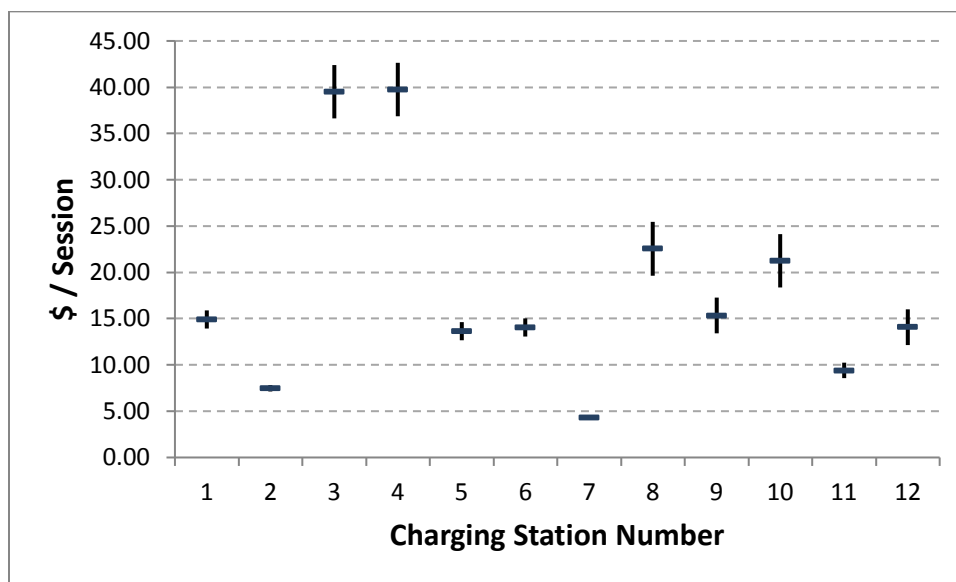


Figure 2-27. Total cost of charging infrastructure per site, calculated on a per-session basis. Error bars represent the expected range of installation cost, which varies depending on the specific location chosen for the charging site.

Because some of the recommended locations have low utilization, the uncertainty in the installation cost can affect their total cost per session considerably. However, as the number of sessions increases, the effect of installation cost variation is minimized, and operating costs dominate the total cost. Therefore, when siting DCFC stations, priority should be placed on choosing a location with potential for high utilization, rather than choosing a location with minimal installation cost.

Case Study 2: Home Charging Matters—Feasibility Analysis of Fleet Electrification in Columbus, Ohio, and Austin, Texas

Key Findings

1. Simulation based on real-world TNC and taxi data in Columbus, Ohio, and Austin, Texas, confirmed that overnight home or depot charging is necessary to allow most full-time ride-hailing drivers to adopt BEV250s and maintain driving behavior similar to past ICEVs, even when they have access to widespread 50-kW DCFC stations.

2. If public DCFC is limited to 50 kW, drivers without home charging access will not only need to frequent those charging stations, but they will also likely experience a reduction in their daily driving activity, relative to how they have historically driven ICEVs, because of the time they must spend charging.

Introduction

Simulations were performed using EVI-Pro and the data from CYC and RideAustin to identify the amount of charging necessary during dwell events to support vehicles modeled as BEV250s. Vehicle constraints (battery size, charge power), travel constraints (dwell frequency, dwell time), and infrastructure constraints (charging availability) are all considered when evaluating charging solutions. Note that the combination of factors that influence charging outcomes may result in no successful charging solution for a portion of the simulated vehicle-days; these unserved vehicles typically drive for large portions of the day, resulting in high mileage and limited charging opportunities. Use of present-day driving data implicitly assumes that future drivers will attempt to use the BEV250s in a manner consistent with current taxi operation. It is assumed that drivers of the unserved vehicles would be required to alter their travel behavior and displace some driving with charging.

Simulations were performed for two infrastructure scenarios—with and without access to overnight charging, Scenarios 1 and 2, respectively. Simulations assumed that the CYC and RideAustin trips, originally taken by gasoline-fueled vehicles, were instead taken by BEVs with prescribed vehicle ranges and levels of maximum charge power. Results indicated that the feasibility of fleet electrification is strongly correlated to charging infrastructure access. Successful charging solutions were identified for 96% of vehicle-days for Scenario 1, but only 40% of vehicle-days for Scenario 2. Results for the served vehicles indicate that overnight charging access significantly reduces DCFC activity, from 1.6 events per vehicle-day to 0.2 events per vehicle-day. Both the reduced number of mid-day charging sessions and minimal reliance on the public infrastructure support the importance of overnight charging.

Scenarios with Varying Infrastructure Access

Successful electrification of a fleet of vehicles can be accomplished through several strategies. Charging requirements necessary to support the CYC and RideAustin fleets were evaluated for the following two specific infrastructure scenarios with differing levels of charging availability:

1. Public charging, residential charging, and depot charging
2. Public charging only.

For each scenario, BEV250 vehicles with a maximum charge power of 50-kW are modeled as the fleet vehicle. Results for each scenario are discussed in the subsequent section; primary outputs include charge events, unserved vehicle counts, and analysis of fleet-wide load profiles.

The first scenario assumes generous access to EV charging. Fleet vehicles have access to charge at publicly accessible stations, at the fleet depot, and at home. Overnight charger access is prescribed at drivers' residences and the CYC depot while the locations of public chargers are generated from the spatial and temporal analysis of demand within EVI-Pro, consistent with methods introduced in Section 3.2.1.

The second scenario assumes no residential/depot charging access, leaving only public charging as the sole opportunity for vehicle fueling. Results of this scenario will inform the amount of public charging access needed and whether overnight charging is necessary to support fleet operation.

Infrastructure Sensitivity Results

The 35,000 vehicle-days within the 13-month CYC data and 33,000 vehicle-days from RideAustin (full-time drivers only) were input into EVI-Pro along with infrastructure assumptions for Scenario 1 and Scenario 2. Key results from the two simulations for the CYC fleet can be found in Table 2-12. Most notable is the vast difference in served vehicle-days. Access to overnight charging and publicly available DC fast chargers adequately services 96% of CYC vehicle-days, a number that drops to only 40% when overnight charging is no longer available. Additionally, DCFC participation rises from 0.2 events per vehicle-day when overnight charging is available to 1.6 DCFC events per vehicle-day when fast charging is the only option for replenishing battery energy. RideAustin simulation results showed similar trends with public fast charging demand increasing by over an order of magnitude in the absence of residential charging.

Table 2-12. Selected EVI-Pro Results for Scenario 1 and 2 for analysis of 35,000 CYC vehicle-days simulated as being driven by BEV250s.

	Percent of Vehicle-Days with > 0 DCFC Events	Vehicle-Days with DCFC Events	Served Vehicle-Days [% of Total]	DCFC Events Per Vehicle-day
Infrastructure Scenario 1	9%	5,655	33,604 [96%]	0.2
Infrastructure Scenario 2	100%	22,312	14,001 [40%]	1.6

It is important to note that EVI-Pro modeling provides public charging infrastructure sized to meet demand. Simulated public fast charging stations are designed to minimize queuing (i.e., vehicles waiting in line to charge). Thus, any vehicle-days that are not satisfied during EVI-Pro simulations should not be attributed to a lack of public charging infrastructure, but instead on a lack of sufficient time to charge (vehicles from real-world data did not dwell at locations for sufficient durations), given the charging-power limit specified in the simulation.

EVI-Pro also outputs spatial information associated with charging events. The unique DCFC events from Table 2-12 for both scenarios are shown spatially throughout the Columbus region in Figure 2-28. Note that the number of charge event clusters does not rise proportionately to the number of unique events; a single cluster may be composed of multiple charge events (signified by color and transparency).

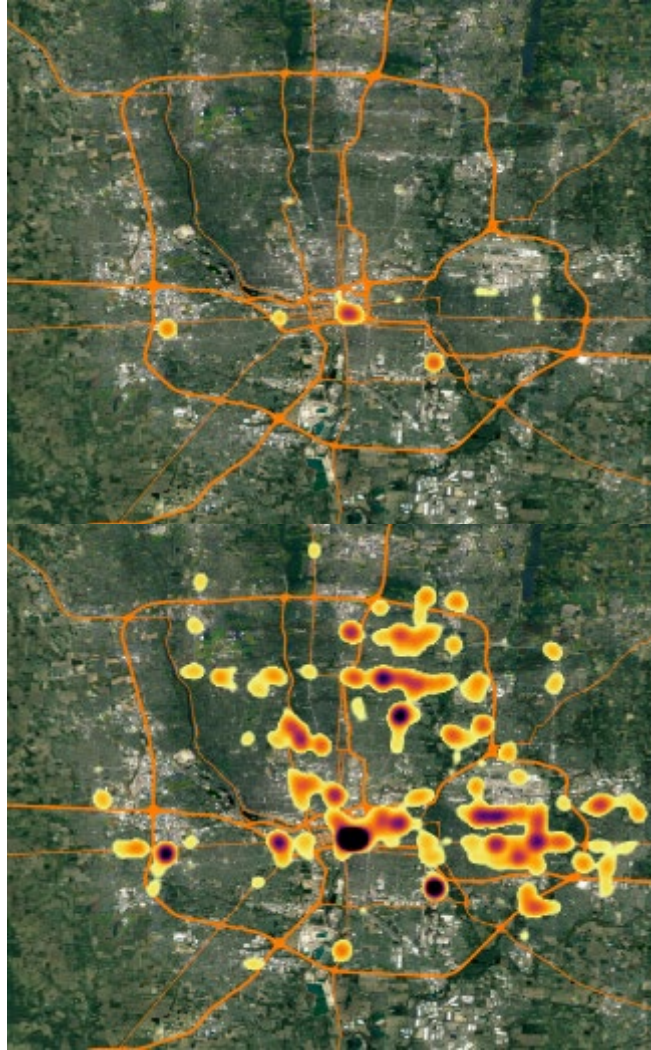


Figure 2-28. Heatmaps of simulated charging demand in Columbus, Ohio from electric taxi fleet for infrastructure Scenarios 1 (at left) and 2 (at right).

Case Study 3: Cost/Benefit Tradeoffs—Charging Infrastructure Planning for Human-Driven and Automated Electric Ride-Hailing Vehicles in the San Francisco Bay Area, California

Key Findings

A simulation case study of charging infrastructure to support AEV and human-driven ride-hailing in the San Francisco, Bay Area examined how varying vehicle range, fleet size, charge power, and number and locations of charging stations affects the ability of ride-hailing fleets to cost-effectively serve demand for passengers. The following key insights emerged from the simulation:

- Compared to a reference case of 50-kW chargers, 100-mile range BEVs, and sparse charging infrastructure, investments to increase charger power, vehicle range, and infrastructure density are all roughly equally cost-effective means of increasing the amount of travel demand served by an electric ride-hailing fleet, with charging-power increases offering slightly more benefit. Investment in additional charging locations lose cost effectiveness beyond a critical density of charging infrastructure, and this critical density decreases as charging power and vehicle range increase.
- In a hybrid ride-hailing fleet with both AEVs and human drivers, charging infrastructure can make a substantial difference in the ability of the total fleet to serve customer demand, especially for low-range EVs. With a fleet of 100-mile EVs, investing approximately \$0.01/passenger-mile (a 14% increase from

the base cost of \$0.06/passenger-mile) to add approximately 4,200 50-kW DCFC plugs to a sparse charging network can increase the number of passenger-miles served by 90%. Alternatively, if the sparse network were originally planned to be 100 kW, instead of 50 kW, the incremental cost of higher power (for the same number of charging stations and plugs) would be \$0.005/passenger-mile (a 7% increase) and provide an increase of 108% in total passenger-miles served.

- The amount of available charging infrastructure and charging-power capacity influence the ability of an AEV fleet to serve passengers. With sparse, 50-kW charging infrastructure, queuing time at charging stations become dramatically long, even with 300-mile range EVs. An electric ride-hailing fleet of inexpensive, low-range EVs (BEV100s) with access to widespread, 50-kW charging infrastructure (1 plug per 7 vehicles) can serve 150 passenger miles per vehicle in a day. Growing the charging network to 1 plug per 3 vehicles reduces queuing time and allows the fleet to serve 180 passenger miles per vehicle per day. However, adding more charging infrastructure beyond this point cannot cost-effectively increase passenger miles served by the fleet because charging time, not queuing time, becomes the bottleneck. EV range or charging power must be increased to alleviate this constraint. The same size fleet of BEV200s with access to widespread, 100-kW charging infrastructure (1 plug per 7 vehicles) can cost-effectively serve 230 passenger miles per vehicle per day. Upgrading to BEV300s captures 250 passenger miles per vehicle per day. Adding more plugs does not increase passenger miles served.
- The cost to the fleet per passenger mile served is the same for each of these cases. Therefore, fleet management should define a target for passenger miles they wish to serve and then choose the least expensive charging infrastructure/vehicle configuration that meets that target.

Introduction

For future human-driven and AEV ride-hailing fleets, DCFC would be needed to support on-shift charging of the vehicles. There is a complex set of tradeoffs to consider regarding the provision of charging infrastructure for these vehicles, especially in relation to:

- Geographic layout and design (charge plugs per location) and relative density of the charging network
- Power level of the DCFC network (i.e., 50-kW, 150-kW, etc.)
- Vehicle battery size and EV range
- Relative size of the ride-hailing fleet in a given region.

There also are questions to consider about the degree to which these DCFC networks will be dedicated to the operation of human-driven and AEV fleets, or potentially shared with personal-use vehicles. Hence, the AFI Pillar examined questions around balancing the number of stations, charge power capacity of vehicles and charging infrastructure, and EV range with the ownership cost of vehicles and charging infrastructure. Multiple metrics quantified the utility of the ride-hailing fleets as each of these parameters varied, including PMT, energy consumed, and vehicle downtime.

As described in the Research Approach section, in this effort, the concepts for charging infrastructure planning and design were combined with large-scale transportation system network modeling using BEAM, an agent-based simulation model of the San Francisco Bay Area. The simulation framework and matrix of analysis scenarios are described below, followed by example results and interpretation of the simulation scenarios.

Framework of Charging Infrastructure Planning Based on BEAM

The BEAM modeling framework was extended to simulate detailed charging operations for both ride-hailing and personal-use EVs. Ride-hailing charging behavior was modeled separately for human-driven versus AEVs. This analysis was based on the SMART Workflow Common Scenario B5, in which the ride-hailing fleet is a mixture of human-driven vehicles and AEVs and traveler preferences are weighted toward shared modes, including pooled ride hailing. The AFI Pillar developed 24 variations around scenario B5, changing the range of the EVs, the power capacity of the chargers, and the quantity and distribution of DC fast chargers. The DCFC infrastructure was separated into two distinct networks: a public network that is shared among personal-use EV drivers and human-driven ride-hailing vehicles and a depot network that is used exclusively by AEVs in the ride-hailing fleet.

Table 2-13 lists the parameters varied across the 24 BEAM model runs, along with other key assumptions used in this analysis. While it is expected that future real-world ride-hailing fleets will feature a mix of EVs with different driving ranges, modeling distributed ranges is reserved for future work due to the complex interactions between the charging network and driving range. Similarly, within each scenario, the power level of each plug in the DCFC networks is uniform (either all 50-kW or all 100-kW plugs). These scenarios thus allow for direct comparisons related to EV range and DCFC power level, recognizing that this may not be realistic in terms of expected future configurations.

Table 2-13. Three parameters (vehicle range, charger power capacity, and charging network size) varied across the 24 simulated scenarios with other key assumptions used in this analysis.

Topic	Assumptions	Value	Notes
Vehicle Properties	Vehicle range	100/200/300 miles	All BEVs were given the same range
	Market share of EVs in ride-hailing fleet	24%	Consistent with SMART Workflow Scenario B5-(BAU Technology)
Ride-Hailing Fleet Size	Total # Vehicles	137,800	See Figure 2-30 for additional information
Personal-Use Fleet Size	# EVs	145,950	
Charging-Power Capacity	Power capacity of fast chargers	50/100 kW	All charger plug power levels assumed the same within a scenario
Public Fast Charging Network Size (Number of stations / number of plugs)	Sparse	157 / 509	Public network is used by human-driven ride-hailing and personal-use EV drivers
	Rich 10%	551 / 2,311	
	Rich 20%	551 / 4,363	
	Rich 100%	551 / 21,815	
Depot Fast Charging Network Size (Number of stations / number of plugs)	Sparse	16 / 192	Depot network is used only by ride-hailing AEVs
	Rich 10%	167 / 2,174	
	Rich 20%	167 / 4,384	
	Rich 100%	167 / 21,740	

Two different styles of DCFC networks were developed to put reasonable bounds on the investment that might be required to support a fleet of ride-hailing vehicles. The sparse network was designed using a data-driven approach based on existing public charging infrastructure in the San Francisco Bay Area, as described earlier in the Research Approach section. The sparse scenario is intended to be an incremental addition of charging infrastructure, adding 50% more DC fast chargers than are available today for human-driven ride-hailing vehicles and adding an arbitrarily small number of DC fast chargers at hypothetical AEV depots. The rich charging network was designed using two tools for charging infrastructure siting; the EVI-Pro tool was used to design the public charging infrastructure and the Fast Charging Station Plan (FCSPlan) was used to design the depot charging infrastructure.⁸⁸ Because the rich scenario resulted in substantially more chargers than the sparse, two intermediate infrastructure scenarios were developed that interpolate between sparse and rich. The rich-10%, and rich-20% scenarios are the result of adding 10 and 20%, respectively, of the difference in the number of plugs between the rich and sparse scenarios. The spatial distribution of rich-10% and rich-20% were equivalent to rich scenario. In other words, the intermediate scenarios have the same number of charging sites,

just a proportional number of DCFC plugs at each site. Figure 2-29 visualizes the spatial distribution of all of these networks.

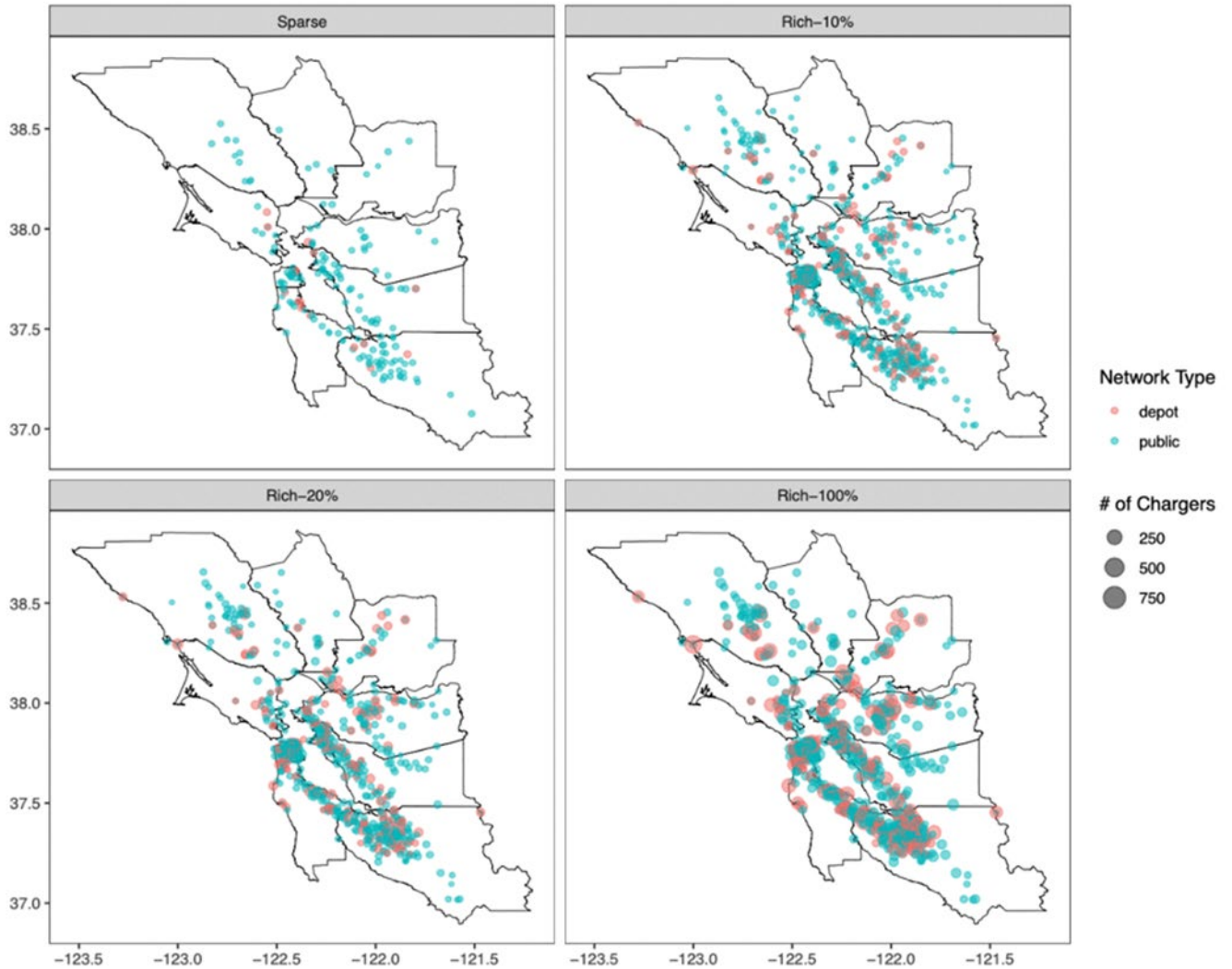


Figure 2-29. Spatial distribution of DC fast chargers in San Francisco Bay Area by network type. Depot chargers are exclusively available to AEV ride-hailing vehicles while public chargers are shared between human-operated ride-hailing and personal-use EV drivers.

In Figure 2-30, the numbers of vehicles are shown (top left) relevant to operations of the ride-hailing fleet. Personal-use EVs are included in this figure because these vehicles compete with human-driven ride-hailing

vehicles for charging; their presence therefore impacts ride-hailing fleet operations. Also shown is the number of DCFC stations (top right) and DCFC plugs (bottom) simulated across the four scenarios.

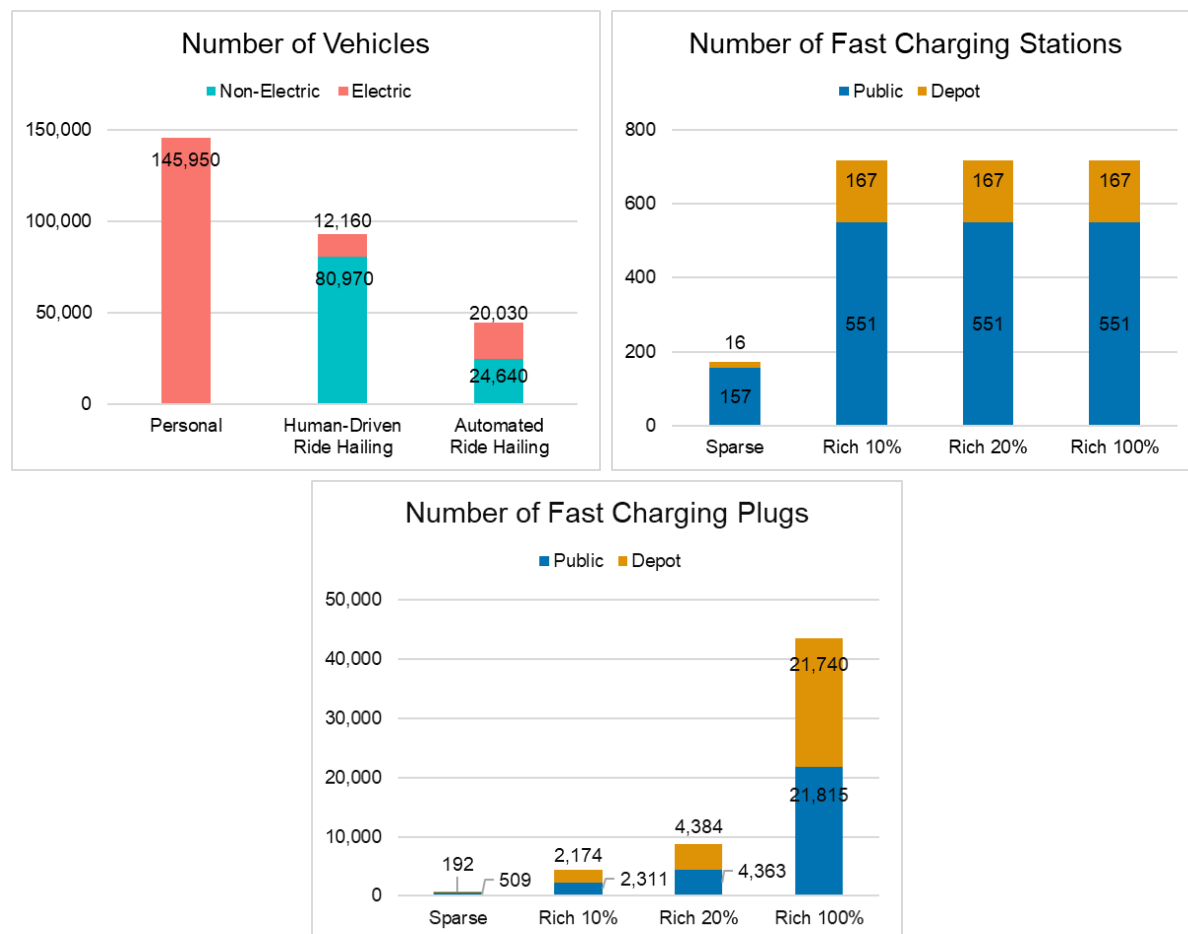


Figure 2-30. Number of vehicles (top left) in all simulation scenarios and number of fast charging stations (top right) and plugs (bottom) in each infrastructure scenario

Figure 2-31 presents the number of individual EV-charging sessions that occurred in simulation for each charging infrastructure scenario and for each combination of range and charger power capacity. The y axis is the number of charging sessions in the network, including both depot and public chargers. The size of the symbol represents the relative amount of energy delivered, or the intensity of charger utilization; the type of symbol represents the type of vehicle (personal-use or ride-hailing EV, and human-driven or AEV); and the color of the symbol relates to the charge power capacity. The figure shows that 100-mile AEVs must make much heavier use of the depot charge network, as expected, and that there is much less difference between the 200-mile EV and 300-mile EV cases. This is because 200-mile EVs are capable of completing much of their daily travel with charge in their battery at the start the day, making the charging demand only modestly higher than the 300-mile range scenarios. Across all combinations of range and charging power, it is clear that the sparse infrastructure scenario does not enable all charging that would otherwise happen by the AEV fleet. Instead, AEVs that are low on charge spend time queuing at heavily-utilized charging depots when they would otherwise be transporting passengers, providing a significant barrier to vehicle utilization. There is a dramatic jump in the number of charging sessions between sparse and rich-10%, as queues at charging depots are shorter and vehicles spend more time and energy transporting passengers. From rich-10% to rich-100% there is additional use of the infrastructure, but this growth diminishes with increases in vehicle range.

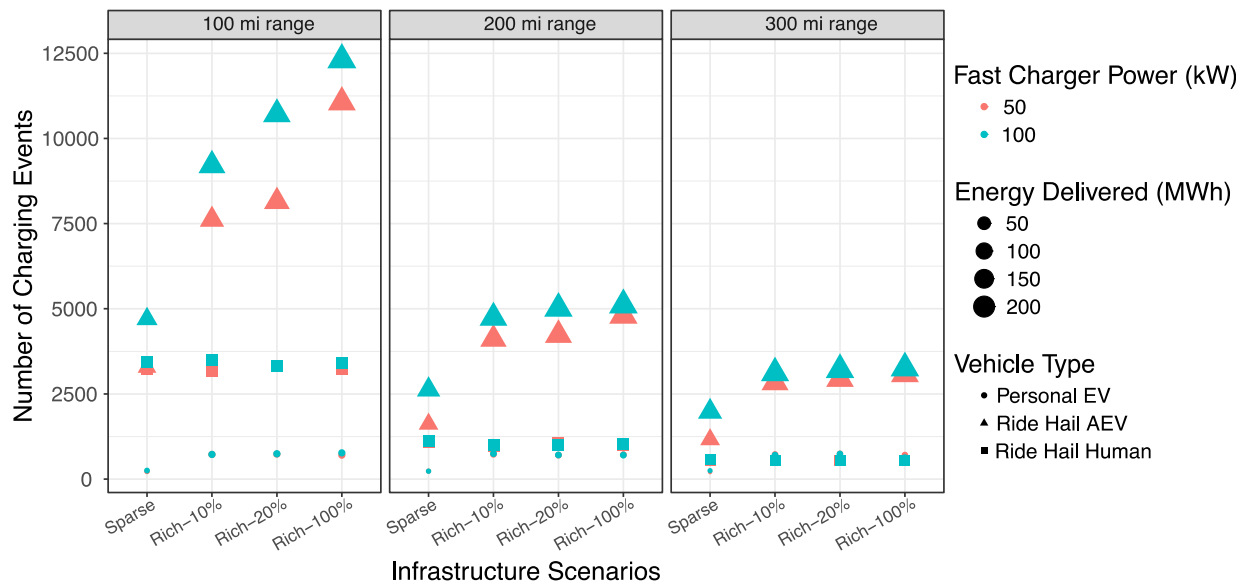


Figure 2-31. Number of charging sessions by infrastructure scenario (x-axis), vehicle range scenario (panel), and charger power (data point color)

Figure 2-32 presents the passenger-miles served by EVs in the ride-hailing fleet for each combination of infrastructure, EV range, and charging power. The 100-kW power level combined with 300-mile range EVs yields the highest levels of PMT across all infrastructure scenarios. However, when vehicle range is 300 miles and charger power is 100 kW, the benefits of infrastructure on PMT are saturated after the rich-10% scenario. Similarly, at 50 kW and 300 miles of range, the benefit is saturated after the rich-20% scenario. Across other scenarios, there is a monotonically increasing relationship between more charging infrastructure and the passenger miles than can be delivered by the fleet.

Infrastructure provides the greatest relative benefit to fleets with the lowest range, where PMT served by vehicles with a 100-mile range roughly doubles between the sparse and the rich-10% scenarios. Also, there are significant nonlinearities apparent in the results, where the benefits of providing additional infrastructure generally decrease, and very markedly for the higher EV-range vehicles and higher charging-power network cases.

Passenger Miles Served by BEVs in Ride Hail Fleet

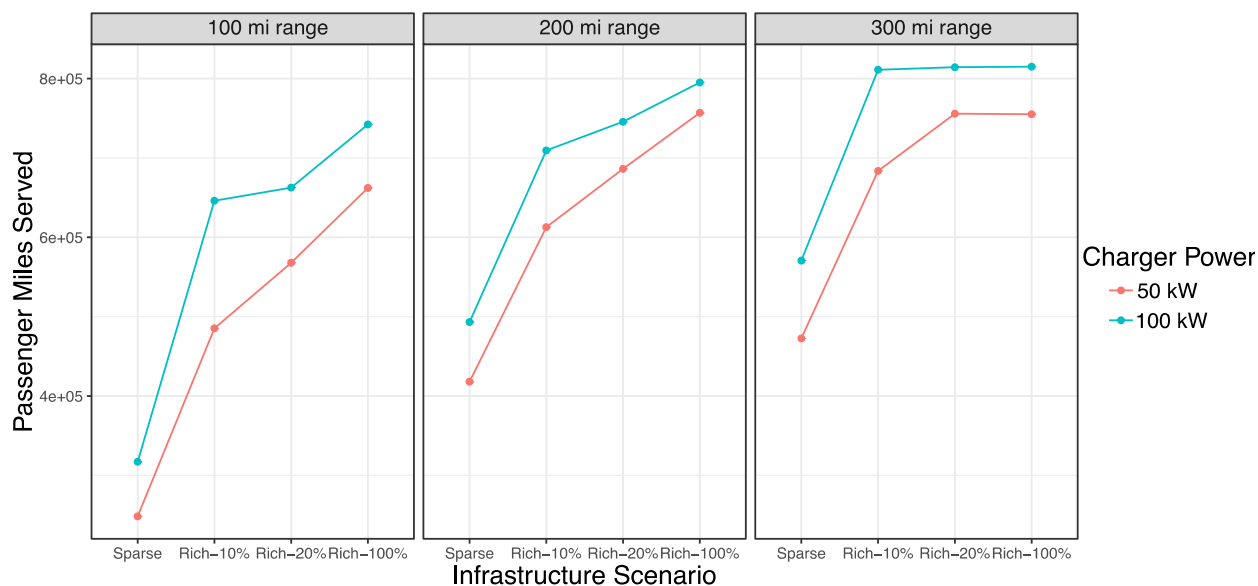


Figure 2-32. Passenger miles served by ride-hailing EVs by infrastructure scenario (x-axis), EV range scenario (panel), and charger power scenario (trend color).

The overall operational states of the vehicles in the ride-hailing fleet are shown in Figure 2-33 and Figure 2-34 for the sparse and rich scenarios, respectively, with 100-mile range EVs and 50-kW chargers. A few features are particularly noteworthy in these plots. First, the time spent and miles driven by vehicles with passengers (blue region in the plots) are much greater for ride-hailing AEVs in the rich infrastructure scenario than in the sparse. In the sparse infrastructure scenario, a large amount of queuing occurs for the AEVs (purple in the plots), especially in the middle of the day, representing pent-up demand for charging to provide more mobility services.

Second, the ride-hailing EV fleet with human drivers is much less impacted by the difference between the sparse and rich infrastructure cases. Because humans drive during a shift in the simulation (3.5 hours on average), the distance driven each day allows them to limit charging sessions to 1–2 per day. There is enough capacity in the sparse infrastructure scenario to supply this amount of demand without adversely impacting the ability of human drivers to continue serving customer demand. As was shown in Figure 2-31, the number of charging sessions for human ride-hailing drivers does not increase significantly from sparse to any rich scenario, though the use of fast chargers by personal-use EV drivers does increase with more infrastructure availability.

Finally, the improved utilization of the AEV fleet to serve passengers in the rich infrastructure scenario comes at some expense of driving intensity of the non-EV human-driven ride-hailing fleet, although this is hardly perceptible in the figures because the scenarios include mostly (about 75%) conventional vehicles that are only somewhat perturbed by this effect.

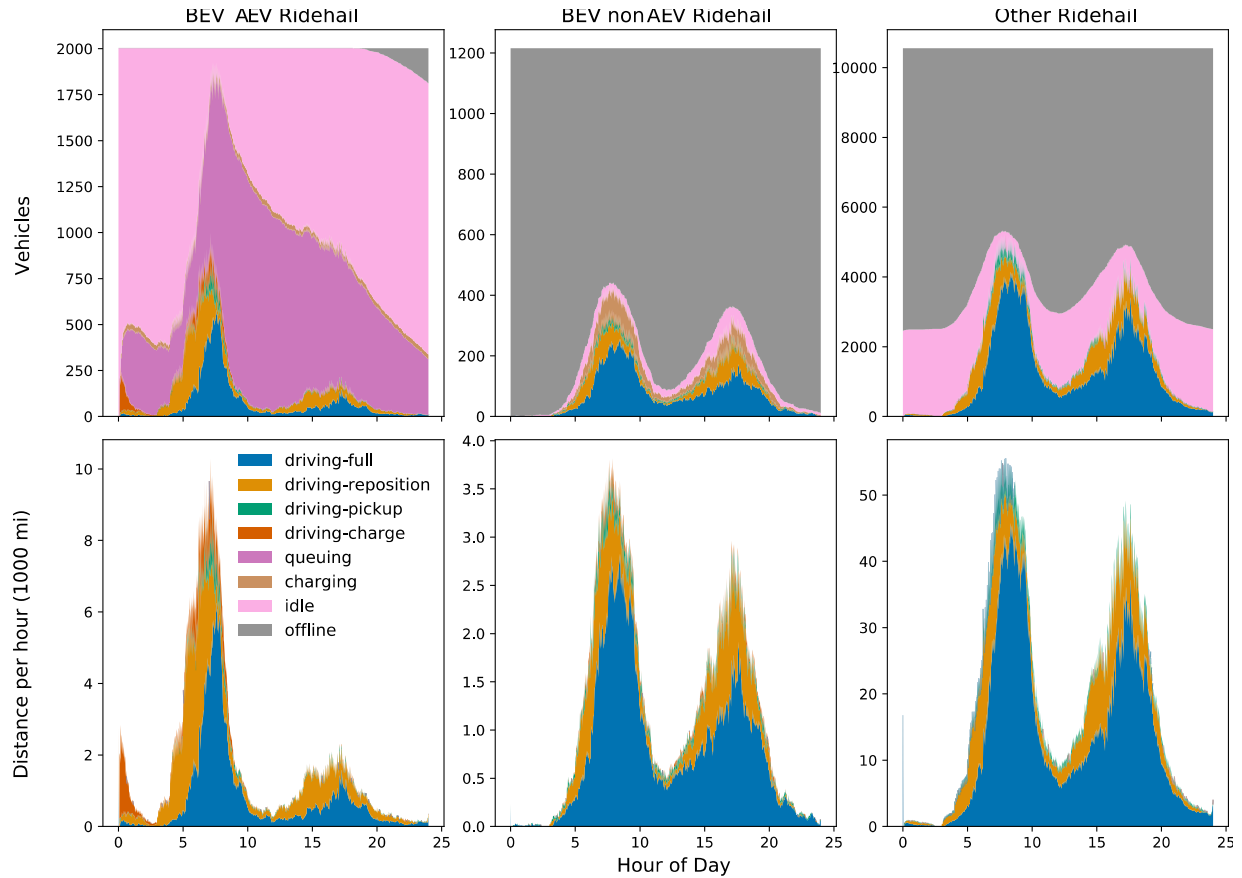


Figure 2-33. Distribution of the ride-hailing fleet into operating states over the 24-hour simulation period for scenario with 100-mile range EVs and sparse, 50-kW charging infrastructure. Horizontal panels separate vehicle types and vertical panels separate time spent by each vehicle (top) and distance traveled by all vehicles (bottom). (Note different scales.)

From the standpoint of ride-hailing fleet operations, the short length of human-driver shifts and typically high initial energy in batteries at the beginning of each shift enables the human fleet to operate with modest day-time charging infrastructure requirements. Investing in public infrastructure beyond the sparse scenario does not enable human drivers to serve additional passenger miles. The experience of individual drivers, however, could potentially be highly impacted were they required to queue at a charging site, drive long distances to find available chargers, or pay large costs associated with using fast chargers during the day or charging vehicles between shifts. Careful attention should be paid to the tail of the distribution of negative experiences borne by drivers. On the other hand, charging infrastructure can be optimized for an AEV ride-hailing fleet using only aggregate metrics because individual AEVs can be dispatched (or not) for the benefit of the fleet.

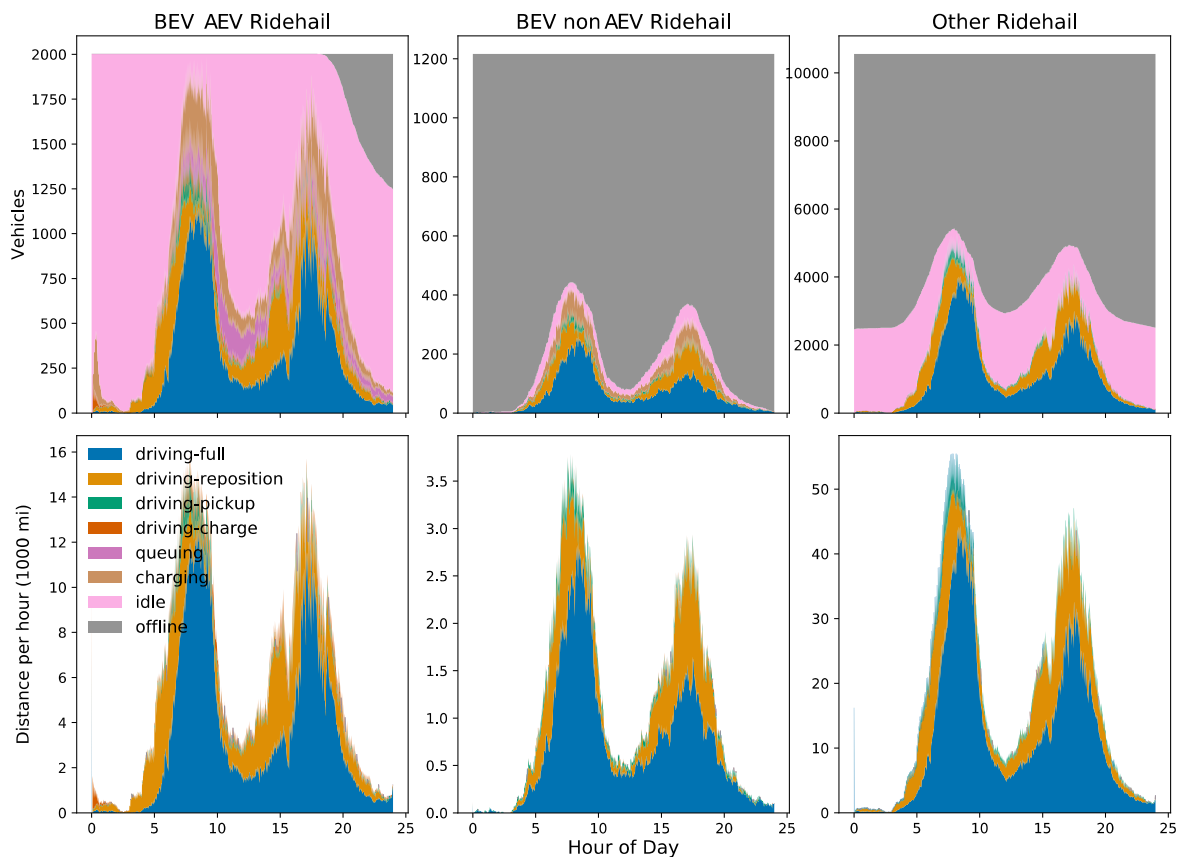


Figure 2-34. Distribution of the ride-hailing fleet into operating states over the 24-hour simulation period for scenario with 100-mile range EVs and rich, 50-kW charging infrastructure. Horizontal panels separate vehicle types and vertical panels separate time spent by each vehicle (top) and distance traveled by all vehicles (bottom). (Note different scales.)

Finally, Figure 2-35 summarizes the cost results of each scenario. Included in the cost is the vehicle capital cost for both the AEV and non-AEV (i.e., human-driven) ride-hailing fleets, the infrastructure cost for all fast charging (both the depot and public networks) and the electrical energy required to charge all vehicles in the ride-hailing fleets. All costs were normalized by the number of passenger-miles served by the EVs in the fleet.

Key details of the cost estimates include capital costs for human-driven EVs (e.g., \$34.5K for 100-mile and \$43.5K for 300-mile range), AEVs (e.g., \$41.4K for 100-mile and \$52.2K for 300-mile range), and installed costs for commercial-grade DC fast chargers by power capacity (e.g., \$46K for 50-kW and \$94K for 100-kW chargers). Also included were composite time-of-use rates for electricity of \$0.20/kWh and an additional commercial electricity demand charge of \$13.75/kW-month. EVs were assumed to consume 300 Wh/mile on average, and charging efficiency was estimated at 92%.

In the sparse scenarios, the majority of costs is in the vehicles, but in the three rich scenarios, increases in total VMT lead to more energy required per passenger-mile served (due to extra miles driven both to charge and associated with deadheading and repositioning). In the rich-100% scenario, DCFC infrastructure becomes a major component (roughly 1/3) of the total cost.

Overall, the cost results argue that investment in charging infrastructure to go past the sparse level could be warranted given the dramatic increases in level of service they enable with modest increases in cost. There are diminishing returns to passenger-miles served by going from rich-10% to rich-100% (see Figure 2-35), and the per-mile cost increase is a roughly linear trend. At what point an entity might stop investing in infrastructure would depend on the priorities and competing opportunities to enhance fleet performance, as well as the specific combination of vehicle range and charger power that is desired.

Cost per Passenger-Mile of Ride Hail Fleet and Public + Depot Charging Infrastructure

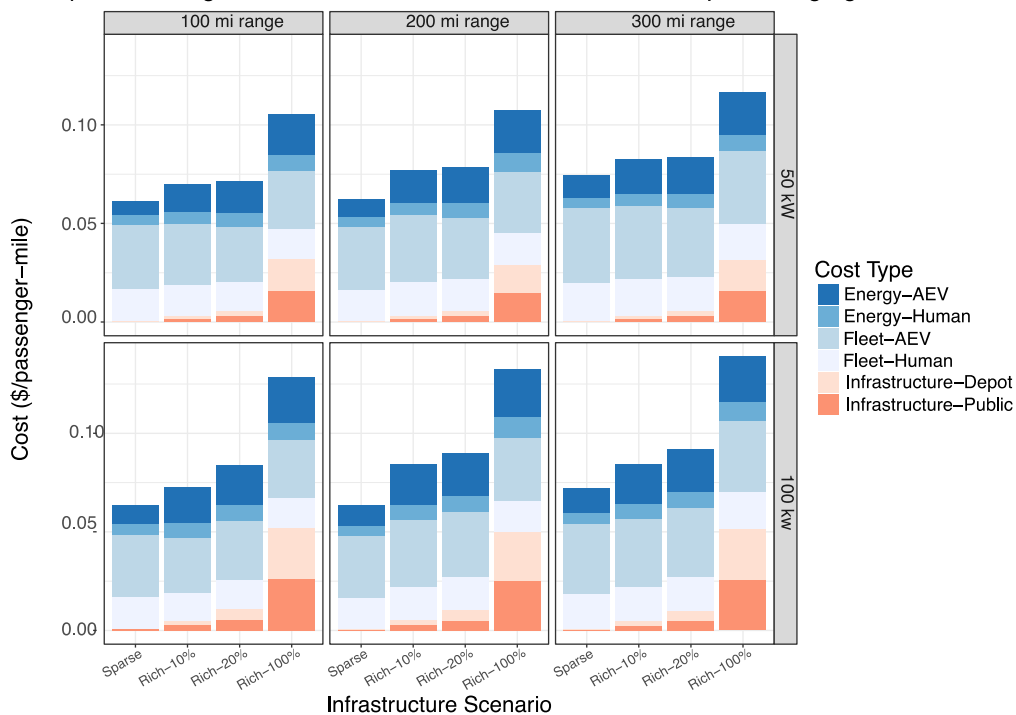


Figure 2-35. Cost per passenger-mile traveled for ride-hailing EVs (both human-driven and AEVs) for both DCFC networks (public and depot) and for cost of electricity necessary to fuel the fleet. The PMT are only those that occur in EVs. The range scenarios vary with the columns of the panels, the charge power capacity scenarios vary with the rows, and the infrastructure scenarios vary across the x-axis. For an electric ride-hailing fleet of a given size, time spent driving to chargers, queuing at chargers, and plugged in to chargers is all time that cannot be spent serving passengers. This unproductive time leads to more unmatched passengers who must complete their trips with other modes and longer waits for passengers that are matched, decreasing the appeal of ride-hailing and also reducing the amount of travel demand served by the ride-hailing fleet. This charging-related downtime can be shortened either by investments in a denser charging network, in faster chargers, or in longer-range vehicles. Indeed, when compared to a reference case of 50-kW chargers and 100-mile range vehicles, buying additional capacity (in terms of passenger-miles served) through any of these types of investments comes at a roughly equal cost per additional PMT. This is seen in the left half of the plot in Figure 2-36, where the points showing different combinations of network density, charger power, and EV range collapse onto approximately the same linear cost-PMT curve. The average slope of this group of lines represents the marginal cost of serving an additional passenger-mile. For the group of lines excluding the reference case (red line), the average slope between the sparse (circle) and rich-20% (square) data points is slightly lower than the average slope of the same section of the reference case line. This is because the lowest cost per PMT comes in the reference case, as seen in Figure 2-35. If the ride-hailing fleet operator desires to serve more passenger miles than the reference case enables, this can be achieved with roughly equal cost effectiveness through investments in either DCFC network density, charger power, or EV range. (Note that real estate cost is not included in cost calculations.)

A deeper dive into the results found that increasing charging power offers slightly more benefit than increasing charging network size, relative to the sparse 50-kW charging network. With a fleet of 100-mile EVs, investing approximately \$0.01/passenger-mile (a 14% increase from the base cost of \$0.06/passenger-mile) to add approximately 4,200 50-kW DCFC plugs to the sparse network can increase the number of passenger-miles served by 90%. Alternatively, if the sparse network were originally planned to be 100 kW instead of 50 kW, the incremental cost of higher power (for the same number of charging stations and plugs) would be \$0.005/passenger-mile (a 7% increase) and lead to an increase of 108% in total passenger-miles served.

Eventually, increasing DCFC network density loses cost effectiveness as a means of increasing the utility of a ride-hailing fleet. While most of the scenarios in Figure 2-36 fall on the same curve of constant marginal cost,

all rich-100% charging infrastructure scenarios (i.e., all combinations of EV range and charging power with rich-100% charging infrastructure) deviate from the relationship, showing instead far higher marginal costs per additional passenger-mile served. This suggests that, at some threshold density of charging infrastructure lower than rich-100%, investment in additional charging plugs becomes less cost effective than equivalent investments in either charging power or vehicle range. This critical charging infrastructure density, beyond which investment in new charging plugs stops being cost competitive, depends on charging power and vehicle range. In all three scenarios with 100-kW chargers and 100, 200, or 300-mile EV range, the rich-20% scenario also deviates from the linear curve in Figure 2-36, suggesting a substitution effect whereby investments in increased charger power limit the gains possible through investing in additional charging infrastructure density (i.e., increasing the number of plugs).

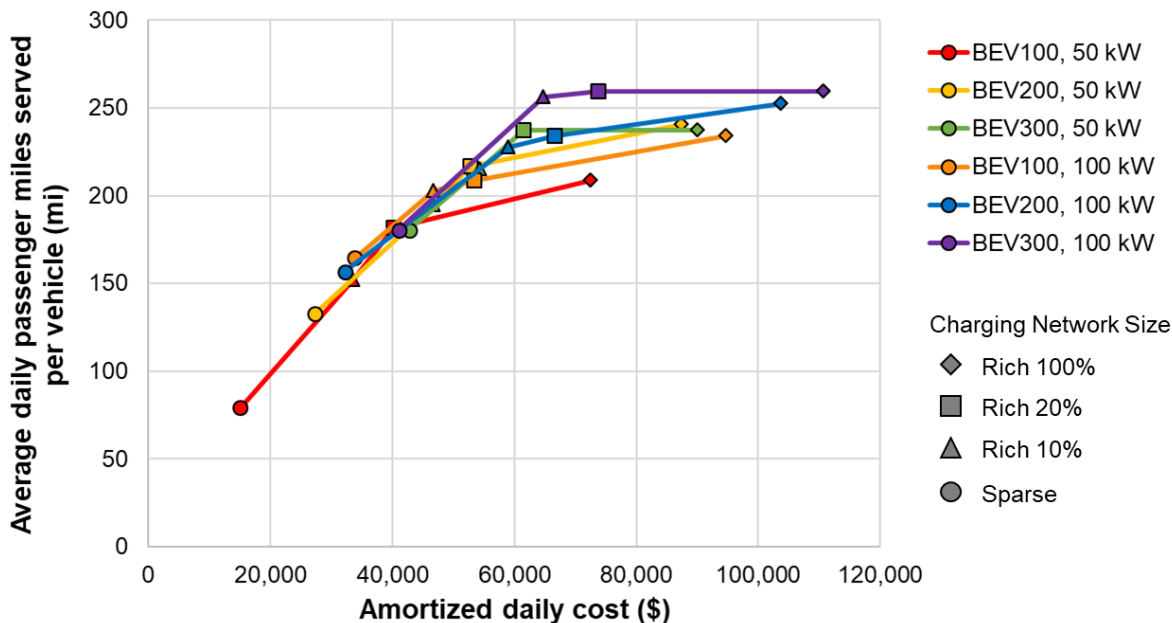


Figure 2-36. Average passenger-miles served per vehicle as a function of total amortized daily cost of operating a ride-hailing fleet (both human-driven and AEVs), showing the cost effectiveness of serving additional passenger travel demand through investments in increased vehicle battery capacity, charging power, and number of charging plugs, while holding the total number of ride-hailing vehicles constant.

In a market with many competing ICE-powered ride-hailing vehicles, such as the one simulated, an electric ride-hailing fleet of inexpensive, low-range EVs (BEV100s) with access to widespread, 50-kW charging infrastructure (1 plug per 7 vehicles) can serve 150 passenger miles per vehicle in a day. This is indicated by the red triangle in Figure 2-37 that represents the scenario with rich-10% charging network size. Growing the charging network to 1 plug per 3 vehicles (red square representing the rich-20% scenario) reduces queuing time and allows the fleet to serve 180 passenger miles per vehicle per day. However, adding more charging infrastructure beyond this point cannot cost-effectively increase passenger miles served by the fleet because charging time, not queuing time, becomes the bottleneck. EV range or charging power must be increased to alleviate this constraint.

The same size fleet of BEV200s with access to widespread, 100-kW charging infrastructure (1 plug per 7 vehicles) can cost-effectively serve 230 passenger miles per vehicle per day. Upgrading to BEV300s captures 250 passenger miles per vehicle per day. Adding more plugs does not increase passenger miles served.

The cost to the fleet per passenger mile served is the same for each of these cases. Therefore, fleet management should define a target for passenger miles they wish to serve and then choose the least expensive charging infrastructure/vehicle configuration that meets that target.

2.2.2 Charging Network Design to Support Electric Vehicles in Free-Floating Car-Sharing Fleets

Key Findings

- A case study of BEV100s operating in a free-floating car-sharing service in Seattle, Washington, showed that, when fleet managers reposition vehicles to and charge at 50-kW DC fast chargers within the Seattle city boundaries, charging time is the dominant factor in the total downtime of a charging trip.
- Optimizing the number and location of charging stations within the city can reduce the time and miles required for fleet managers to reposition vehicles to charging stations by up to 49%; however, adding many charging stations reduces the total downtime required for charging by just a small fraction (2–4%).
- If the goal of a car-sharing service provider whose vehicles operate in a small geographic area is to minimize vehicle downtime due to charging to avoid lost revenue, then the provider should prioritize an increase in charging power above 50 kW over the addition of charging stations.

Introduction

As mentioned earlier, the AFI Pillar also considered the human-driven, free-floating car-sharing market segment. Free-floating car-sharing services allow customers to rent vehicles by the minute and/or mile, for one-way trips or series of trips. Customers use a smart phone app to locate and reserve vehicles, which are parked anywhere within a designated geographic area, such as a city boundary. Customers travel to vehicles, unlock them using the app, drive the vehicles themselves, and leave the vehicles in any legal parking space within the service’s designated home area at the end of their rental period.⁸⁹ Major car-sharing service providers such as Autolib, car2go, and ReachNow have included EVs in their fleets.

The AFI Pillar characterized EV operation in free-floating car-sharing fleets to understand their charging needs. Whereas the focus with ride hailing was on individual drivers, analysis of this segment focused on fleet operators. Although car-sharing drivers (i.e., customers) have unique interests and may use vehicles differently, vehicle charging is centrally managed by fleet operators. (Car-sharing companies have mentioned plans to incentivize drivers to charge vehicles in the future, but the AFI Pillar did not consider this case.⁹⁰) Therefore, charging infrastructure must be designed to serve the needs of the fleet, not the individual users.

One challenge to charging infrastructure design for free-floating car-sharing fleets is identifying the best location for charging stations to minimize time and distance driven for charging by the fleet. Because the cars are free-floating, the location from which they must be retrieved for charging is highly variable. Operators need to decide on one optimum charger assignment for the EV based on charging-station status, the condition of the EV, and traffic in the area. An optimization model investigating infrastructure planning, design, and operation of an emerging free-floating car-sharing transportation system operating with EV is important because a car-sharing service provider loses potential revenue during the time when EVs are out of service for charging. At those times, they are not available to customers.

Research Approach

The AFI Pillar collaborated with ReachNow, a car-sharing service provider owned by BMW Group that provided United States operations in Seattle, Washington, and Portland, Oregon, between 2016 and 2019. ReachNow provided the AFI Pillar with a private data set describing driving and charging of 100 BMW i3s (considered BEV100s) in its fleet from May 2016 to February 2017. Following analysis of this data set and discussion with ReachNow about fleet operation, the AFI Pillar input this data set into a charging infrastructure modeling tool. The tool was used to optimize the location of charging stations and simulate car-sharing fleet operation as the number of charging stations increased.

The AFI Pillar developed the charging-management and infrastructure-planning (CMIP) model⁹¹ to explore various charging infrastructure network designs that would serve a free-floating car-sharing fleet and to determine the charging downtime experienced by the fleet under each design. Development of the CMIP model had two major steps: (1) describing modeling assumptions and (2) developing an integer program (IP) that jointly optimizes decisions about locations to install DC fast chargers and EV-to-charger assignments. The components of the CMIP model are visualized in Figure 2-37. A detailed description of the model and assumptions have been published in the article “Optimal charging management and infrastructure planning for free-floating shared EVs”⁹² and Appendix B of this report.

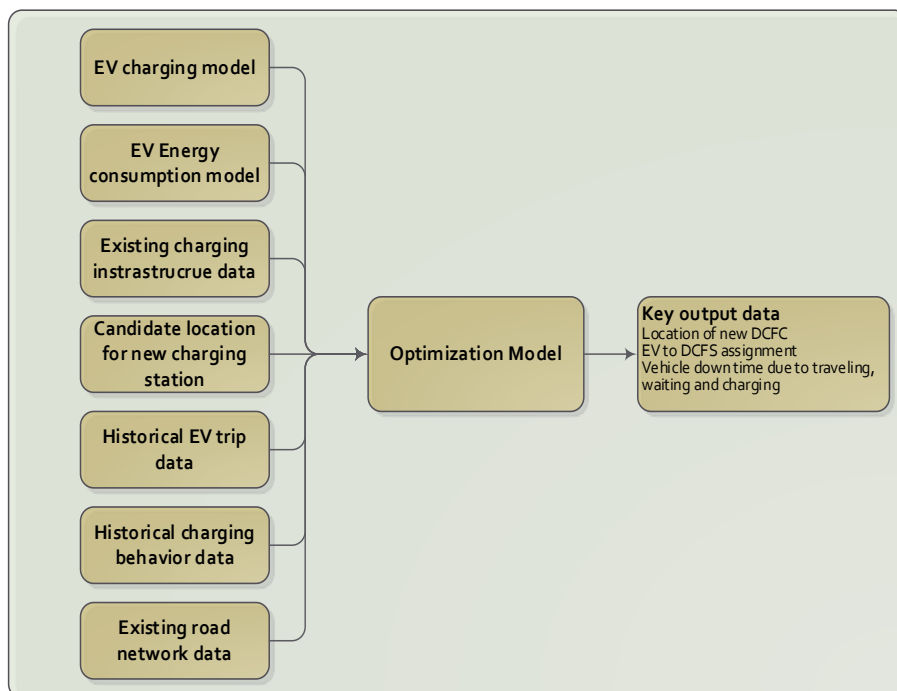


Figure 2-37. Computational framework of the CMIP model.

The CMIP model integrates an EV charging model, EV energy consumption model, and heterogeneous, real-world vehicle use data with an integer programming optimization model to identify optimal locations for new charging stations and calculate vehicle downtime for charging. The trip-level data provided by ReachNow were processed to determine the trips dedicated to charging, the origin of the charging trips, and the interval between two consecutive charging trips across the fleet. Real-world energy consumption data of the 2014 BMW i3 were utilized to construct a data-driven model for energy-cost estimation of each charging trip. This data set was collected by the U.S. DOE Advanced Vehicle Testing Activity.⁹³

This study captured vehicle downtime associated with charging trips. The components of downtime in this study are (1) waiting at the origin of the charging trip or at the destination (i.e., the charging station) due to occupancy by other vehicles, (2) travel time from trip origin to the charging station, and (3) the total time spent charging the vehicle. Vehicle downtime could also be caused by other factors, such as maintenance and cleaning, but these were not considered in this study. Travel time considered in this study was limited to the travel time from the origin of the charging trip—i.e., the location where the last user of the vehicle parked it—to the charging station. The travel time did not include any time fleet operators spent repositioning the vehicle from the charging station to another location—i.e., the origin of the next user’s trip. According to ReachNow, that time was usually minimal.

The charging time of an EV depends on several factors, including the charging rate, initial battery SOC, and desired final SOC. A data set from the testing of a 50-kW DC fast charger charging a 2014 BMW i3 was used to obtain the charging time model.⁹⁴ Test data included the charge duration, energy transferred, and SOC. Estimations of vehicle travel time for a given pair of origin and destination points were calculated based on OpenStreetMap by using the open-source routing machine (OSRM) engine.^{95, 96} Candidate locations for new charging stations were determined from the 866 commercial census blocks in the Seattle area.

The minimum SOC threshold below which a charging trip is triggered was set to 18%, chosen because modeling indicated that it was possible for vehicles with 18% SOC to reach one of the six existing charging stations from anywhere within the city. Fleet operators would reposition any EVs with SOC below this threshold to charging stations for charging. After completing this travel to a charging station, an EV is charged to 90% SOC from the SOC level at which the vehicle arrived at the station. The CMIP model constrains EV-to-charger assignments so that SOC upon arrival at the charging station is greater than 0.01%. As different

trips have different distances, the SOC level after travel is also different and may not reach the 0.01% SOC level. After charging, all vehicles have 90% SOC in all scenarios.

The CMIP model also included probabilistic modeling of DC fast charger occupancy (i.e., whether or not it is in use by another vehicle) and the length of time it is occupied by another vehicle. These two conditions are affected by various factors, such as the location of the DCFC station, the time of day and day of the week, and whether the charging station has public or restricted access. Historical charging behavior data were used to estimate the utilization probability of a DC fast charger. A model was created to generate an expected waiting time due to the occupancy of another vehicle at the DC fast chargers. This model took into account utilization probability and average waiting time from historical data, specific to a given time and day (e.g., morning or night by weekday or weekend).

Case Study: The Case for Faster Charging—Free-Floating Electric Car Sharing in Seattle, Washington

A case study explored the relationship between fleet vehicle downtime and the number of charging stations by modeling the fleet operations of a major car-sharing service provider. The CMIP model was applied to the case study using input data to understand: (1) the reduction of EV fleet downtime if an additional fast-charging station is added to the current infrastructure and (2) to what extent total vehicle downtime would be sensitive to additional charging infrastructure. Five scenarios were generated for analysis, as shown in Table 2-14. Scenario 1 did not include any new charging stations. Scenarios 2–5 increased the number of DCFC locations beyond the six existing DC fast chargers used by ReachNow in Seattle.

Table 2-14. Number of charging stations in each modeling scenario.

Scenario ID	Total Number of Charging Stations	Number of Existing Charging Stations	Number of New Charging Stations	Number of Charging Trips
1	6	6	0	1256
2	11	6	5	1256
3	16	6	10	1256
4	21	6	15	1256
5	26	6	20	1256

Impact on Downtime

Table 2-15 summarizes the average travel time to a charger per charging trip, average charging time, average time spent waiting to use the charger, and average total downtime under the various scenarios. These averages were calculated based on 1,256 modeled charging trips, with charging trip origins specified in the historical data set from ReachNow. Results show that downtime caused by traveling can be reduced significantly by adding new charging stations. The case study calculated average total downtime per charging trip to be 49 minutes to 51 minutes, depending on scenarios. Comparison of Scenario 1 to Scenario 5 shows that by adding 20 new DCFC stations to the existing infrastructure, the travel time per trip could be reduced from 4.0 minutes to 2.0 minutes. This 49% reduction in travel time is attributed to the reduction of travel distance as additional charging stations were optimally located by the CMIP model. Note that this travel time did not take variations in travel time due to traffic congestion into account, which can be significant in the Seattle area. Table 2-15 also indicates that the charging time for EVs varies from 72 to 75% of the total downtime, indicating that charging time is the dominant factor in the total downtime for charging the fleet.

Table 2-15. The number of charging stations and fleet downtime for traveling, charging and waiting in minutes.

Scenario	Number of	Average Per-Trip	Average Per-Trip	Average Per-Trip	Average total down time
----------	-----------	------------------	------------------	------------------	-------------------------

	Charging Station	Travel Time (min)	Charging Time (min)	Waiting Time ^a (min)	per charging trip (min)
1	6	4.0	36.8	10.4	51.3
2	11	3.0	36.6	10.4	50.1
3	16	2.5	36.6	10.4	49.4
4	21	2.2	36.5	10.4	49.1
5	26	2.04	36.5	10.4	49.0

a Includes waiting time either at origin of charging trips or at the destination (i.e., the charging station)

Comparison between Scenario 1 and Scenario 5 also shows that adding 20 new DC fast chargers to the existing infrastructure could reduce the charging time per trip from 36.8 to 36.5 minutes. This small reduction in travel time is due to the slightly higher average SOC at the start of a charging event due to a shorter travel distance to reach the charging location.

Figure 2-38 shows the impact of adding new charging stations on waiting time. This waiting time includes waiting at the origin of the charging trips [§] or at a charging station. Results show that adding new charging stations does not significantly reduce waiting time because there was minimal queuing by ReachNow vehicles during the 9-month data collection period. Adding five to 20 new charging stations reduces total downtime by 2 to 4%, while reducing travel time by 26 to 49%.

In addition, Figure 2-38 shows the incremental reduction of total travel time and charging time as the CMIP model strategically located additional DC fast chargers around the city. Adding the first new charging stations reduced traveling time drastically, but there were decreasing returns on time improvements as additional stations were added.

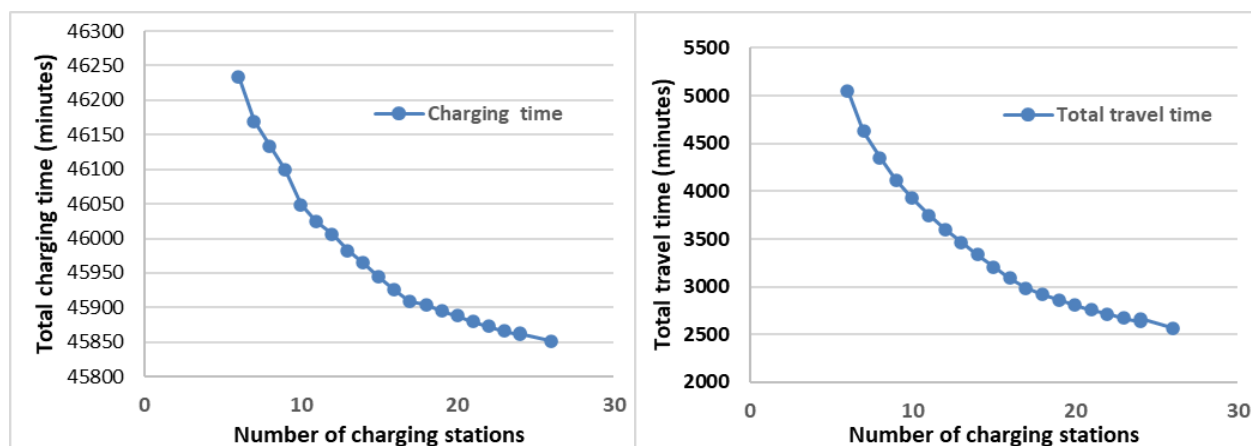


Figure 2-38. The impact of adding a new charging station on total travel and charging times. Travel time includes the time a vehicle spends during traveling from trip origin to a DCFC. Charging time is the total time to charge the vehicle based on the charging rate model, initial battery SOC, and desired final SOC.

Optimal Locations of New Charging Stations

The CMIP model identified the locations for new charging stations that would most effectively complement the six existing charging stations. Figure 2-39 shows the optimal locations of 10 new charging stations

[§] An EV can wait at its last used location. This avoids long waiting times at a given DCFC, allowing operators to choose the next available DCFC elsewhere.

(Scenario 3), indicated by blue stars. These 10 new locations were selected from 100 candidate locations, evenly dispersed across the region in commercially zoned census blocks.

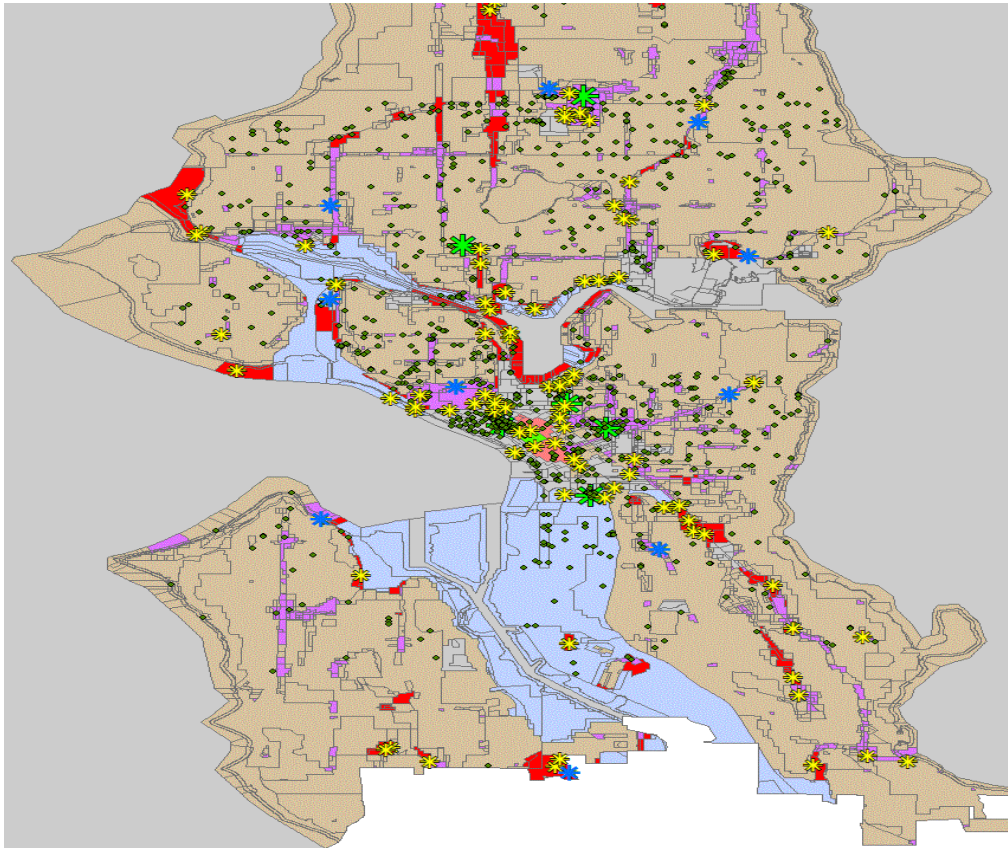


Figure 2-39. The optimal locations of an additional ten new charging stations (blue stars) based on historical trip information. The new locations are dispersed across the region.

Impact of an Increased Number of Charging Trips on Average Downtime Time and Number of New Charging Stations

A sensitivity analysis measured the impact of an increased number of charging trips on average downtime per charging trip. To do this, the number of charging trips were increased by 50 and 100% from the base-case of 1,256 charging trips. These trips were generated randomly at any of the historical origins of charging trips and at any period. Figure 2-40 shows the impact of the increased number of trips on the average downtime per charging trip with varying numbers of DC fast chargers. Results shows that a 50% increase in charging trips increases the average downtime for charging trips from 51.3 minutes to 52.0 minutes when only six DC fast chargers exist in the home area (see Scenario 1). This increase is attributed to a wait at a DC fast charger when assigned to a charger because of increased trips and limited charging stations. Similarly, given that there are only six DC fast chargers in the home area, a 100% increase in the charging trips increases the average downtime for charging trips from 51.3 minutes to 53.4 minutes.

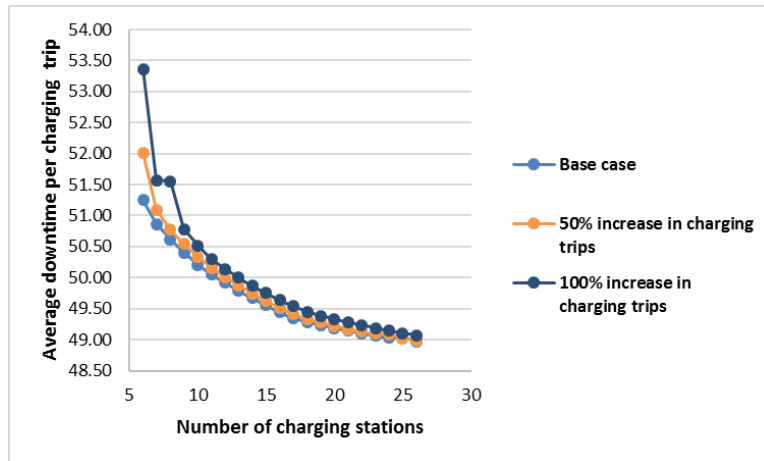


Figure 2-40. The impact of an increased number of trips on average downtime per charging trip from the base-case scenario. The y axis shows the total downtime due to a charging trip. The components of downtime are: (a) waiting at the origin of the charging trip or at the destination (i.e., the charging station) due to occupancy by other vehicles at the DC fast chargers, (b) travel time from the trip origin to the charging station, and (c) the time spent charging the vehicle.

The impact of the increased number of trips on average downtime per charging trip is negligible when there are more DC fast chargers in the home area. Given 20 new DC fast chargers in the home area, a 100% increase in the charging trips increases the average downtime for charging trips from 48.97 minutes to 49.07 minutes. Having adequate DC fast chargers in the home area prevents any waiting at a charging station or at the origin location of a trip.

Figure 2-40 was used to analyze the impact of increased number of trips on the number of new charging stations. Results show that a 50% increase in the charging trips increases the average downtime for charging trips from 51.3 to 52.0 minutes in Scenario 1. To keep the average downtime of Scenario 1 to 51.3 minutes per trip with 50% increased trips, at least one additional DC fast charger would be required in the home area. Similarly, to keep the same average downtime with 100% increased trips, a second additional DC fast charger would be needed in the home area. As the number of new DC fast chargers increases in the home area, the impact of the increased number of trips on the number of new charging stations becomes minimal.

Impact of Increasing Charging Power Compared to Increasing Number of Charging Stations

The simulation results discussed thus far show that increasing the number of charging stations and placing them in optimal locations within the home area yields only modest reductions in downtime due to charging. As a comparison, the AFI Pillar also calculated downtime due to charging if the charging power were approximately doubled, such that charging time was cut in half. Results show that by reducing the charging time at the original six DCFCs by half, the average downtime for charging decreases from 51 to 33 minutes, a 36% reduction. Figure 2-41 compares the average downtime per charging trip as the number of charging stations increases, for both 50-kW and 100-kW charging. These results make it clear that increasing charging power has considerably more effect on downtime than adding charging stations.

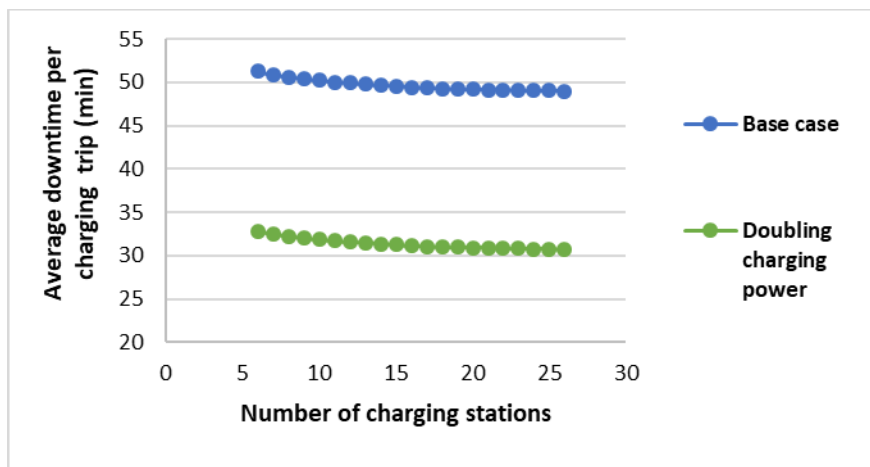


Figure 2-41. Average downtime per charging trip as the number of 50-kW charging stations increases (base case) and as the number of 100-kW charging stations increases (case where charging power is doubled).

Conclusion

This case study showed that charging time is the dominant factor in the total downtime of a charging trip in car-sharing EV fleets. Current case study results indicated charging times for EVs in a car-sharing fleet vary from 72 to 75% of the total downtime of a charging trip. The study also indicated that adding five to 20 new charging stations could reduce total downtime and travel time for car-sharing EV fleets by 2 to 4% and 26 to 49%, respectively. This indicates that although adding new charging stations to the existing service region reduces vehicle downtime from travel time of each charging trip significantly, it does not reduce total downtime for charging significantly. This implies that if a car-sharing company wants to reduce the average time per charging trip, adding additional DC fast chargers would not help much. If the goal of a car-sharing service provider is to minimize vehicle downtime due to charging to avoid lost revenue, then the provider should focus on increasing charging power to reduce charging time. This is expected to be possible in the future as manufacturers bring high-power DCFC units to market and automakers produce EVs capable of accepting higher charge power. In the meantime, the provider can minimize lost revenue due to downtime by studying user demand and minimizing downtime due to charging during periods of peak customer demand through careful scheduling.

The travel time considered in this study is limited to the travel time from the last used location before a charging trip to the charging station. The travel time did not consider travel time from the charging station to the origin of the next trip, which could also be an important part of the downtime. Another limitation of this study is the exclusion of fleet-operator assignment during optimization modeling. This study assumed that after a customer finishes with a vehicle with an SOC below the minimum threshold, a fleet operator would be available to drive the vehicle to a DC fast charger for charging. If a fleet operator is not available to reposition the vehicle to a charging station, it could also increase the downtime of an EV fleet. This study did not consider any heterogeneity of EVs in a fleet. Variability in battery type and maximum driving range of the vehicles in the fleet could affect downtime as well. Incorporating EV relocation fleet-operator assignment, and heterogeneous EVs in the fleet within the CMIP model are logical areas for follow-on work.

2.2.3 Charging Network Design to Support Electric Trucks for Freight Delivery

Key Findings

- In a case study of a private, regional-haul, hub-and-spoke motor carrier based in Dallas, Texas, truck fleet operation was modeled with high-power fast chargers at the central distribution center and at the loading docks of all destinations.
- Real-world data describing the operation of this fleet indicated that drivers often chain trips together, such that their overall distance traveled before returning home often exceeded 500 miles. Modeling found that even when employing trucks with 500 miles of EV range and 350-kW chargers during loading, unloading,

and other typical dwell locations, trucks did not have sufficient range to complete 6% of their trips. This suggests that freight-trucking fleets of this type will need to adjust their operations to accommodate electrification. Fleets may need to lengthen dwell times to allow for sufficient charging, take time to charge at public charging stations, and/or limit electric trucks to specific routes.

- These complexities add real costs to fleet operations that must be balanced with the cost of increasing EV range and charging power to realize the financial benefits of electrification. All these factors limit the utility of electric trucks relative to their conventional counterparts, which reduces resale value and puts pressure on the business case for heavy-duty truck electrification.
- Tools to integrate charging infrastructure planning and investment decisions into overall operational financial planning will be important for successful deployment of electric vehicles in freight operations.

Introduction

Charging infrastructure design choices for freight delivery are likely to be dictated by cost/benefit considerations, as is the case with other capital-intensive investment decisions. Truck fleet managers must decide whether to invest in a strategy that fits charging within existing operating patterns or change their operations to accommodate charging. Additionally, fleet owners must decide whether to install a private charging infrastructure or rely on third-party public charging. For both private and third-party charging infrastructure providers, the challenge is to identify the type, number, and location of charging stations that best serve truck fleets at minimal cost. Tools are needed to guide either stakeholder in making their decisions.

Research Approach

To address this barrier, the AFI Pillar studied tradeoffs inherent with different approaches to designing charging infrastructure for Class 7–8 electric trucks for freight transport, with the intent to recommend the attributes of a modeling tool to be developed to guide investment decisions. First, the Pillar identified trucking business needs and operating constraints that charging infrastructure must support (as described in Sections 3.1.2). Next, researchers identified potential charging infrastructure design approaches for specified freight-trucking scenarios. Finally, Pillar researchers developed a simple model to explore how the different charging infrastructure designs might meet general fleet needs and looked at how the model would be applied to a specific fleet (as described in the next section).

A critical consideration for the trucking industry is charging time because time spent charging directly impacts a fleet's bottom line and driver pay, which is usually based on miles driven, rather than time spent driving. Charging time is dictated by (1) the size of the battery to be charged, (2) the battery's SOC at the start of charging, which is a function of driving distance and energy efficiency, and (3) the power capacity of the charging infrastructure and vehicle.

On the vehicle side, truck batteries are expected to be large—in terms of storage capacity, volume, and weight—in order to provide heavy-duty trucks with up to 500 miles of range. Some estimates indicate that a 500-mile range battery could weigh approximately 11,000 pounds.⁹⁷

Several truck companies have estimated that the average energy use of electric heavy-duty trucks will be approximately 2 kWh per mile, which is the value used in this analysis.^{98, 99}

On the infrastructure side, multiple charging technologies are available for freight trucks. The primary technologies available today include conductive (plug-in) chargers with power levels up to 600 kW (with faster capacity being studied); static inductive wireless charging that provides up to 250 kW to the vehicle while parked; and catenary technology that provides a direct feed of electricity to trucks along fixed routes, either while parked or during driving.

These assumptions fed simple estimates for the time required to fully charge an electric Class 8 truck with a nearly empty battery. For comparative estimates, Table 2-16 below shows charging times when using 150 kW, 250 kW, 350 kW, and 600 kW charging systems to replenish batteries sufficient to provide 150 miles and 500 miles of driving range.

Table 2-16. Approximate charge times (in hours) for different types of chargers based on a 2 kWh/mile usage.

Charge Power:	150 kW	250 kW	350 kW	600 kW
150 Mile Range	2.0	1.2	0.85	0.5
500 Mile Range	6.6	4.0	2.85	1.6

The location of chargers is another critical consideration for fleet managers. Options include using private charging infrastructure that is installed on company-owned properties or using publicly accessible, third-party-owned charging infrastructure.

Installations on private facilities could be placed at distribution centers, centralized depots, or privately owned loading docks. Private charging infrastructure may be used to take advantage of times and locations where trucks may already be stopped for longer periods of time to provide charging opportunities. Installation and operation costs would be balanced against lower charging rates and increased efficiency for the operations to determine the business case for private infrastructure. Some businesses may even offer to charge non-fleet vehicles at locations like loading docks for a fee to improve the business case for installing and maintaining an infrastructure.

In the case of the trucking industry, public charging would likely be at truck stops, usually along interstate corridors. These public charging stations for trucks will need to provide high-power charging stations, relatively long charging times, and space for larger vehicles that will have an impact on the design and placement of these facilities.

The AFI Pillar chose to model a fleet of electric Class 7/8 trucks with 300 and 500 miles of electric range that charge at 150 and 350 kW. Although researchers and manufacturers are developing high-power charging, the Pillar selected these power levels because commercial DC fast chargers at these power levels are available today. FleetDNA, a database of real-world data managed by the National Renewable Energy Laboratory (NREL), provided real-world operational data describing the driving and parking behavior of 22 conventional diesel-powered trucks in a private, regional-haul motor carrier fleet based in Dallas, Texas.¹⁰⁰ These data were used to create spatial-temporal trip segments as inputs to the model. The model implementation included two different charging station location scenarios.

Case Study: Considering Charging Infrastructure for a Regional-haul Private Motor Carrier in Dallas, Texas

Many tradeoffs must be considered for electrification of heavy-duty trucks. Decisions around the use of electric trucks and the installation of charging infrastructure are significantly impacted by different business dynamics and the unique needs of individual fleets. To examine charging infrastructure options to support truck fleet electrification in more depth, AFI Pillar researchers used real-world data from a private, regional-haul motor carrier fleet based in Dallas, Texas. This fleet ships freight and palletized goods from a regional distribution center (RDC) near Dallas to retail stores and other RDCs in several states in the American South. The fleet drives trips in a variety of scenarios, from short-haul circuits that return to the home RDC after a single stop to long-haul circuits chaining several trips, with stops at multiple locations over several days. All stops of trucks in this private fleet are at properties owned by the fleet’s parent company. This affords several options for installing chargers at destination locations and a chance to examine the impacts of different charging infrastructure solutions on the fleet’s ability to complete trips and circuits using electric trucks.

The data describing the operation of the fleet were collected from 22 trucks operating out of the home RDC near Dallas over a period of one month. The shipping routes represented in the data set are shown in Figure 2-42; some of the retail stores (green stars) and other RDCs (red squares) the trucks stock are marked on the map.

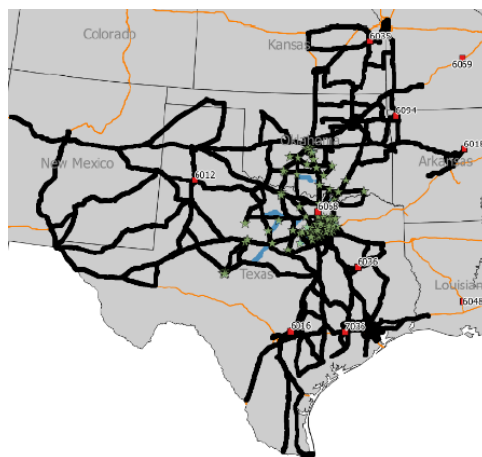


Figure 2-42. Distribution routes for 22 trucks originating from their home RDC near Dallas, Texas. Some destinations are shown as red squares (RDCs) and green stars (retail stores).

All trucks were Class 7 or 8 heavy-duty diesel tractor-trailers. Their operational data was analyzed, and each stop was identified. Trips were defined as drives between stops, and circuits were defined as the chain of trips that started and ended at the home RDC. During each circuit, data loggers recorded the driving duration between stops, the distance between them, and the time the truck dwelled at each destination. At most destinations, trucks were parked at the loading docks while goods were unloaded. Trucks were sometimes parked at other destinations overnight.

Figure 2-43 shows the circuits driven by a single truck in the fleet. Each circuit started at the home RDC north of Dallas, marked with a yellow star. Each line color represents a single, distinct circuit driven by the truck during the month. The figure shows that some circuits are longer, with multiple loops or legs in different directions, requiring multiple days of driving before returning to the home RDC. Some circuits (i.e., Circuits 1, 2, and 6) keep the truck close to the RDC and are obscured in the figure.

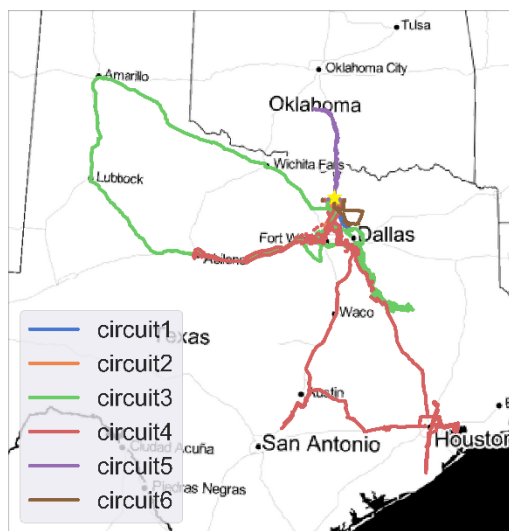


Figure 2-43. Circuits driven by a single truck over several days, each starting and ending at the home RDC (yellow star).

The data indicate a wide variety of circuit types over the month, with some circuits having only short trips to local stops, returning the same day, and others involving multi-day circuits covering hundreds of miles. This means that a single truck tractor is assigned to many different circuits during a month.

AFI researchers examined several infrastructure and vehicle configuration options to electrify this fleet. First, because all circuits start at the home RDC and some stop at other RDCs, researchers assumed a scenario under

which the fleet would install chargers at the home RDC and other RDCs to charge the trucks while they dwelling there (e.g., while loading or unloading goods). This means that trucks could charge at the home RDC at the end of every circuit. Because this fleet’s hub-and-spoke operation often included visits to other RDCs on longer routes, the first analysis also assumed that the vehicle could charge at any other RDC that the trucks visit. In a second scenario, it was assumed that chargers were installed at the loading docks of every destination so that trucks could charge while they dwell at the docks.

In this analysis, it was assumed that the trucks would dwell at destinations for the same amount of time as was recorded in the existing real-world data; they would not lengthen their stay to complete a charge. Furthermore, this analysis included the ideal assumptions that any truck needing to charge could do so immediately, without waiting in a queue, and that trucks could charge for the entire time they were parked at a location. The first and second scenarios described above were repeated to vary charging power and EV range. Charger power capacity was uniformly set at either 150 or 350 kW. EV range was uniformly set at either 300 or 500 miles.

Modeling the Effect of Charging Infrastructure Design on Driving Range of a Single Vehicle

To help examine the feasibility of electric truck operation in the fleet, an individual driving schedule for one of the trucks in the data set was chosen for a case study. For schedule chosen, the truck drove 24 distinct trips, defined as the distance driven between successive stops on a circuit. The circuits originated at the home RDC, included a set of trips between retail stores and other RDCs, and terminated back at the originating RDC. Trip distances ranged from 50 to 400 miles. Four trips exceeded 300 miles, and none of the trips exceeded 500 miles. (See Figure 2-43 above and Table 2-17 below)

Table 2-17. Summary table of truck sample.

Summary of Truck Sample	
Total distance driven (miles)	3,733
Number of trips	24
Total dwell time (hours)	142
Number of trips exceeding 300-mile range	4
Number of trips exceeding 500-mile range	0
Circuits (trip chains starting and ending at home RDC)	6
Number of stops at home and other RDCs	11

To examine how much charging energy would be needed to complete a given trip, the analysis looked at the amount of range that would remain when the truck arrived at the end of each trip. Assuming the truck started with either 300 or 500 miles of range, the truck would consume that range to reach a destination. If the remaining range available was negative at the end of a trip, that meant that the vehicle needs to charge during the trip, perhaps by using a public charging station, to complete the trip. Then, if charging was available at that destination, the amount of charge they would have received at the given charge rate and truck dwell time (given by the time stopped either for unloading or at the end of the travel day) was converted to a range and added back to the available range used for the next trip.

The first case considered a scenario in which charging was only available at RDCs. This meant that the vehicle would primarily be able to charge using the private infrastructure at the beginning and end of each circuit, and occasionally at other RDCs. (Two of the six circuits in this example included stops at other RDCs.)

Figure 2-44 shows the calculated range remaining at each stop. Stars represent charging opportunities, with yellow stars representing trips that ended at the home RDC and blue, trips that ended at other RDCs. Negative range remaining indicates that charging previous to the trip or circuit was not sufficient to cover the distance to the next charging opportunity.

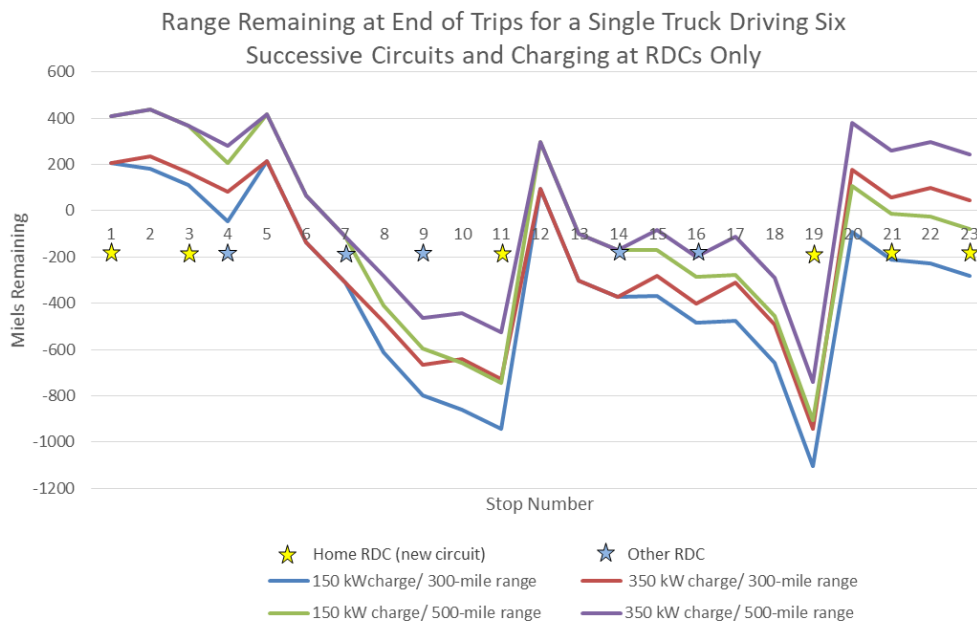


Figure 2-44. Range remaining at the end of each trip for six successive circuits. Charging was only allowed at RDCs, marked with stars.

For the shorter circuits, the 150-kW charger and either 300- or 500-mile range vehicles were sufficient. But on circuits with longer distances between RDCs or when the RDC visits were relatively short, the need for public charging increased. At Stop 11, the 300-mile range vehicle with 150-kW chargers would have required 944 miles to be replenished by public charging (equivalent to at least 12.5 hours of charge at the 150-kW rate). The 350-kW, 500-mile vehicles would have required 527 miles of charging (equivalent to 5.2 hours at the 350 rate). Similarly, at Stop 19, the 300-mile, 150-kW scenario needed 1,106 miles worth of public charging while the 500-mile, 350-kW scenario needed 741 miles worth of public charging.

The second scenario involved the company’s installing a charger at each of the docks, which would allow trucks to charge during every stop, either during loading and unloading or overnight. Again, researchers assumed that dwell time at stops would not be changed from the current data set, and chargers would be available for every truck, as needed. These additional chargers would increase the range of the truck at every stop they made, but still might not offset the range lost in reaching the delivery location. Once again, the remaining range at the end of each trip was recorded, with negative range reflecting the need for public charging during trips in order to extend range sufficient to reach destinations. Figure 2-45 shows the resulting range available at the end of each trip for each charging power and EV range combination modeled.

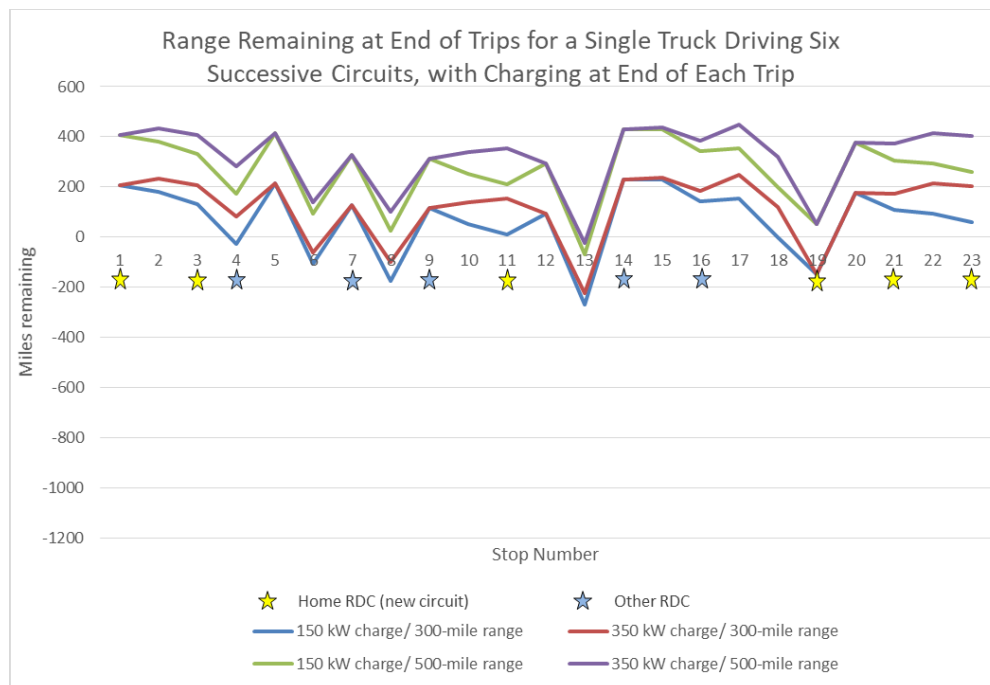


Figure 2-45. Range remaining at each stop on a journey of six successive circuits if charging is available at each stop.

In these scenarios, the bulk of trips were covered by private charging at destinations. Five trips would require public charging, with a total of 726 miles of range extension required, with the 150-kW chargers and the 300-mile range. Changing to 350 kW chargers would reduce the number of trips needing charging to four, with a total of 537 miles of range extension needed. If EV range were increased to 500 miles, then only one trip would need public charging to extend range by 68 miles using a 150 kW charger or by 25 miles with a 350-kW charger.

This single-vehicle example shows that having charging stations at each location makes truck electrification feasible for a far greater percentage of trips (even with slower 150-kW charge rate). Note, however, that having access to charging infrastructure at every stop is a highly idealized assumption, and even with these conservative assumptions, electric trucks, as modeled, could not complete all trips as they currently drive them.

Modeling the Effect of Charging Infrastructure Design on Driving Range of an Entire Fleet

After evaluating the outcomes of this single vehicle, the AFI Pillar also modeled the charging infrastructure to serve electric trucks in the entire fleet. The entire data set of 819 trips by 22 trucks was used. One hundred and thirty-five of these trips were longer than 300 miles. Thirty were more than 500 miles and would be considered true long-haul trips. In total, 84% of the trips were less than 300 miles across the whole fleet.

Researchers applied the same set of options for charging infrastructure and EV range to the entire fleet. Table 2-18 lists the number of trips during which sufficient range allows trucks to complete trips without the need for public charging. Charging exclusively at RDCs was sufficient for only 23% and 33% of trips by 300-mile trucks, for 150-kW and 350-kW charging, respectively. For 500-mile vehicles, charging at RDCs provided sufficient range to complete 37% and 49% of the trips, for 150-kW and 350-kW charging, respectively. Thus, RDC-only charging means that a maximum of half of the trips could be completed. Adding charging at other stops (e.g., delivery locations) allowed charging infrastructure to support a minimum of 70% and a maximum of 94% of the trips recorded.

Table 2-18. Number and percentage of all trips driven by the fleet that ended with range remaining without public charging during the trip.

Vehicle Range (mi)	Charging Power (kW)	Charging Location	Number of Trips Completed with Range Remaining	Percent of Trips Completed with Range Remaining
300	150	RDC only	190	23%
300	350	RDC only	271	33%
500	150	RDC only	305	37%
500	350	RDC only	398	49%
300	150	At all stops	577	70%
300	350	At all stops	650	79%
500	150	At all stops	732	89%
500	350	At all stops	772	94%

Figure 2-46 and Figure 2-47 show breakdowns of the trips into different categories based on the miles of range remaining at the end of the trip. These trips are based on the second scenario, where charging was allowed at the end of each trip. Trips in bins below 0 miles would require public charging during a trip to reach the trip’s destination. Negative bins represent the range extension that would be needed from public charging en route. This evaluation shows that when charging infrastructure is available at all stops, a majority of trips could be completed with significant range remaining at the end of the trip. However, a small number of trips would need significantly more range than is available. The difference between the 150- and 350-kW chargers is not as significant in vehicles with 500-mile range.

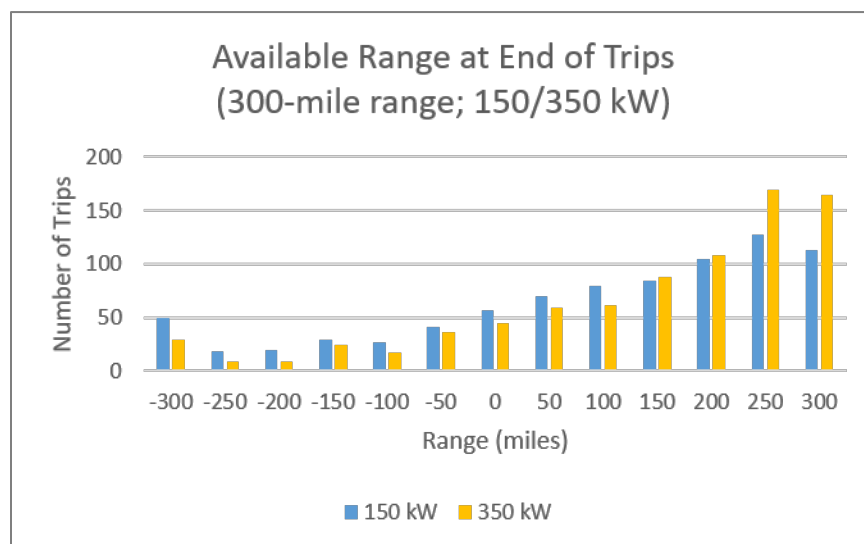


Figure 2-46. Distribution of range remaining at the end of trips for 300-mile range trucks charging at 150 or 350 kW at the end of every trip.

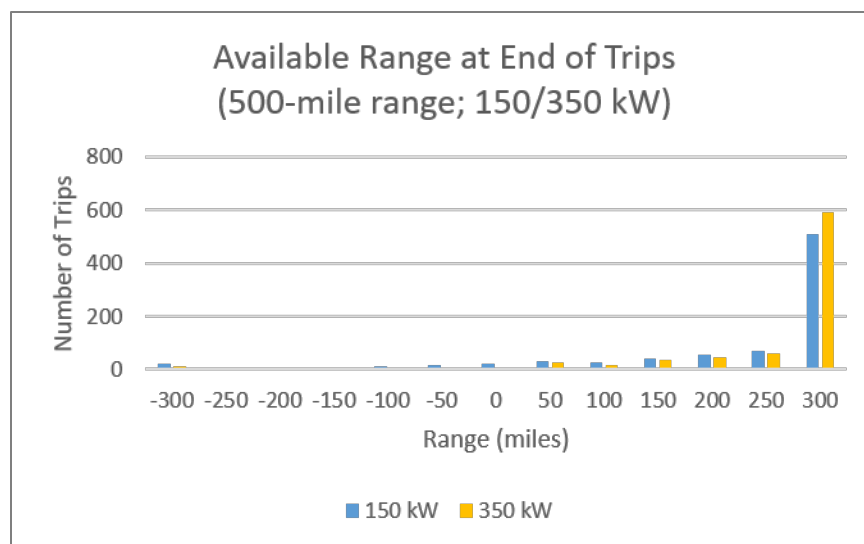


Figure 2-47. Distribution of range remaining at the end of trips for 500-mile range trucks charging at 150 or 350 kW at the end of every trip.

Conclusion

This analysis showed that strategically placing chargers at locations where trucks already spend time parked could satisfy a large majority of the charging needs for a regional-haul fleet and would significantly reduce the dependence on public chargers. However, with the modeled charging infrastructure and EV range, some trucks would still not be able to complete their circuits, and the fleet operator would be forced to alter operations. Furthermore, these scenarios use idealized assumptions, such as allowing a charger at every location and assuming that there is never any queuing or curtailment of available charging power.

Fleets would wish to consider costs of the installations and rates of electrical charges as well as the types and number of chargers needed. They would also benefit from the ability to analyze their operational network depending on their business characteristics to determine which portions of their fleet would be easiest and most cost-effective to electrify. They would then need tools to help them optimize their routing and operations to take advantage of these choices and minimize overall cost.

The results of this analysis indicate the need for further sets of tools and tradeoff analyses to help fleet operators deal with the complex issues of choosing both EVs for their operations and the means to implement infrastructure support for their freight vehicles.

2.3 Exploring New Paradigms Created by Automated-Vehicle Charging

Advances in technologies that automate vehicles and charging have the potential to change the way EV charging infrastructure is designed and used. The AFI Pillar explored two potential new paradigms for EV charging and how they might impact ride-hailing, transit, and trucking. These paradigms either eliminate the need for the vehicle user to charge the vehicle or eliminate the need for discrete charging events entirely.

The first new paradigm is automated-vehicle charging. Simply stated, self-driving cars can drive themselves to charging stations after passengers leave the vehicles. This precludes the need for widely distributed charging stations at every destination, eliminates time spent waiting at DC fast chargers that today’s EV drivers experience, and eliminates range anxiety by relieving drivers of charging decisions. To realize this paradigm shift, vehicles must have the intelligence and awareness to decide when and where to charge optimally, and they must have access to compatible, automated-charging equipment. Different approaches may be taken for privately owned, personal-use vehicles and commercial fleet vehicles, with central management possible for fleets.

The second new paradigm is DWPT. A DWPT system is embedded in roadways to allow EVs to charge while driving. Provided sufficient coverage across a road network, DWPT may preclude the need for distributed

destination charging and fast charging stations, eliminate downtime, and also enable reductions in battery size and cost. However, this concept faces considerable technological and financial challenges. DWPT systems require highly complex hardware and controls that are presently in the nascent stages of development. Roadway electrification may be exceedingly expensive to install and maintain.

2.3.1 Charging Decision Making for Automated Ride-Hailing Fleets

Key findings

An optimization-based approach to managing fleets of automated electric ride-hailing vehicles while they are idle between fares, including both repositioning and charging station selection, can help satisfy considerably more passenger ride requests and reduce zero-occupancy vehicle miles, as compared to a simple approach where vehicles follow set rules to independently decide where to reposition and charge. A simulation case study of automated electric taxis in New York City found that, for a fleet of 1,750 ride-hailing AEVs, optimization-based, centralized fleet management would result in 14% more ride requests satisfied and 43% fewer zero-occupancy miles traveled than if AEVs make independent decisions based on simple rules.

Repositioning idle vehicles properly can effectively increase the number of passenger ride requests satisfied, but it increases fleet operation costs because overall zero-occupancy vehicle miles (i.e., deadheading) increases. Optimization-based fleet management can balance these two competing priorities at the fleet level.

Applying an optimization-based fleet management strategy can reduce the necessary AEV fleet size by 7% while satisfying the same level of customer demand for ride hailing relative to a fleet of AEVs that make independent repositioning and charging decisions based on simple rules.

Introduction

Private industry is investing heavily in AEV development for use in ride-hailing fleets. Corporate announcements, media interviews, market analysts' reports, and academic articles have provided insights into possible future automated vehicle technologies and how automated vehicles may be used in commercial ride-hailing services.^{101, 102, 103, 104, 105} The AFI Pillar used this information to consider factors that may influence driving and charging behavior of AEVs for ride hailing.

It is expected that AEVs in commercial ride-hailing fleets will be centrally managed. Because human drivers motivated by individual interests are removed from the decision process, AEV ride-hailing fleet managers can dispatch individual vehicles according to the overall needs of the fleet. Therefore, driving and charging behavior of AEVs in this market segment is deterministic; fleet managers can develop means to systematically direct vehicle operation, including picking up passengers, repositioning in anticipation of future demand for rides, or removing vehicles from service for cleaning, maintenance, or charging. Sophisticated dispatching algorithms can be used to incorporate charging decisions into the overall vehicle dispatching strategy for ride-hailing AEVs.

Developing a Method to Govern Automated Electric Vehicle Charging Behavior

The definition of charging behavior depends on the point of view taken. From the perspective of an individual AEV, charging behavior is when, where, and for how long the vehicle is charged and what kind of charging-power profile the vehicle uses. From the fleet's perspective, charging behavior is the spatial-temporal distribution of charging across the entire fleet. From the perspective of charging infrastructure, charging behavior is the charging-power demand over time at each charging station.

A thorough discussion on charging behavior for an AEV ride-hailing fleet should be based on the following three parts: (1) available charging infrastructure, (2) passenger travel demand, and (3) a structured framework for charging decision making.

Available Charging Infrastructure

Charging behavior of AEVs in a ride-hailing fleet is influenced by the design of the charging infrastructure network available to the fleet. The location of charging stations compatible with AEVs, number of vehicles that can be charged simultaneously at each station, and cost to charge are some of the factors that influence charging decisions.

Competition with vehicles that do not belong to the AEV fleet for the use of available charging stations is another important factor. AEV fleet operators may choose to install their own charging infrastructure and restrict competitors’ access, enter into agreements with third-party charging network providers to gain preferential access to charging stations owned by others, or use public third-party charging stations in competition with others. For its research, the AFI Pillar assumed there is no competition for charging.

Ride-hailing Customer Travel Demand

AEV fleet dispatching is centered on satisfying ride-hailing customer (i.e., passenger) travel demand. Passenger travel demand can be described as the spatial-temporal distribution of customer pickups and drop-offs. A visualization of the spatial and temporal distributions of customer pickups from today’s human-driven ride-hailing services in San Francisco, California, is shown in Figure 2-48.

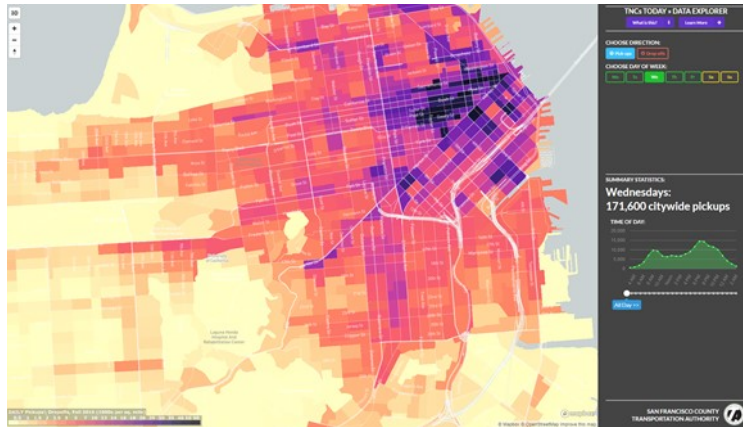


Figure 2-48. Uber and Lyft customer pickup location distribution in San Francisco on a weekday. Source: tncstoday.sfcta.org.

The fleet operator must dictate charging behavior that ensures that its AEVs are capable of satisfying ride-hailing customer demand, in terms of two criteria. First, AEVs must have enough charge for the range needed to transport passengers to their requested destinations. Second, charging must be timed so that there are enough vehicles in service across a region to maintain a desired level of service quality at any given time. One measure of quality of service is customer wait time, which is the time customers must wait for vehicles to pick them up after they request rides. A higher-level metric that can be used to measure ride-hailing fleet utility or effectiveness is the percent of ride requests that can be satisfied within customers’ threshold for maximum wait time.

Decision-making Framework for Dispatching and Charging Management

The design of a ride-hailing AEV fleet management system will govern the charging behavior of autonomous ride-hailing fleets. The architecture of such a system can be distributed or centralized, the latter being depicted in Figure 2-49. The system contains complex algorithms for demand forecasting, vehicle and charging infrastructure monitoring, dispatching, and other fleet management functions.

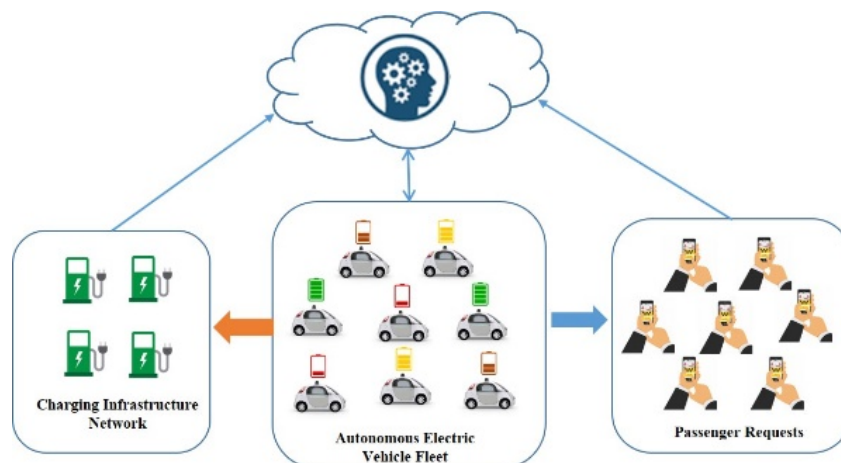


Figure 2-49. A diagram of centralized framework for AEV fleet dispatching and charging management.

To focus the scope of its research on AEV charging decision making, the AFI Pillar developed a decision-making framework that performs a subset of functions that would be performed by a fleet management system—namely, dispatching of idle vehicles for charging and repositioning in anticipation of future ride requests. The details of this approach are described in this section.

The introduction of autonomous driving technology to EVs would remove the challenge of collocating charging infrastructure with driver destinations and present a driver-free method for EVs to reach nearby charging stations. This would significantly change the charging behavior of EVs. EV drivers would no longer need to be present at charging stations for charging actions. AEVs could drive themselves to charging stations after passengers leave the vehicles, eliminating the need for widely distributed charging stations at every destination and eliminating the time today’s EV drivers spend waiting at fast chargers. However, in order to implement automated charging decision making, a charging infrastructure network with compatible and automated charging equipment must be constructed. Wireless charging may be one of the potential solutions for this issue. Another important aspect is that onboard automated driving systems must have the intelligence to decide when and where to charge optimally, which is the focus of this research. Due to various uses of private and commercial vehicles, different intelligent approaches to charging decision making must cooperate with specific driving needs and behaviors. In this work, the AFI Pillar chose to focus on charging intelligence for a commercial AEV fleet providing ride-hailing service.

Research Approach

The overall goal for ride-hailing AEV fleet management is to improve the efficiency and productivity of the fleet. The desired management strategies for operating efficiency will impact the behavior of AEVs and then influence charging infrastructure design. Operational efficiency can be defined broadly as the ratio between an output gained from a business operation and an input to run that business operation. Both output gains and input costs can be calculated using monetary measurements. When improving operational efficiency, the output-to-input ratio increases. With the transition to AEVs, a commercial AEV fleet would gain more flexibility both to manage its vehicles in a systematic way and to improve operational efficiency. The approach to managing an AEV fleet needs to incorporate charging decision making with other operations (e.g., repositioning or maintenance).

This research focused on the dispatching algorithms for an AEV fleet. It aimed to reduce input costs and increase the output revenue; for example, revenue can be increased by satisfying more passenger requests, e.g., through reducing passenger waiting time for pick-up and improving the travel experience or by reducing the deadheading time and the energy cost for capturing ride requests and traveling to and from charging stations. Zero-occupancy vehicle cost, in this research is defined as the travel time spent, distance traveled, and energy consumed when AEVs are operated without passengers (i.e., during the period between when they drop off a passenger to when they pick up the next passenger). It could include the cost of repositioning to capture the next ride request, the cost of traveling to charge, or the cost to travel to pick up passengers after a new ride

request was made and accepted. Balancing zero-occupancy vehicle cost to AEV ride-hailing fleets with the effectiveness of the fleet in satisfying ride requests is one of the main focuses of this research.

To study future commercial AEV fleet-management approaches, this research started with a centralized dispatching framework, as shown in Figure 2-50. The overall process included two main function modules: vehicle allocation to passenger requests and idle-vehicle management. The function module “Vehicle Allocation for Passenger Requests” in Figure 2-50 refers to allocation strategies that are used to match idle, available vehicles to new ride requests. A heuristic method, assigning the closest idle vehicle to a customer requesting a ride, was implemented to study the influence on deadheading cost (miles or time) of different idle-vehicle management strategies. This work put its main effort on idle-vehicle management. Figure 2-51 provides a decision-making process the AFI Pillar developed for idle-vehicle management. The decision-making process includes both repositioning and charging-station selection for idle vehicles. These actions could be conducted by using either heuristic approaches or advanced, systematic optimization approaches.

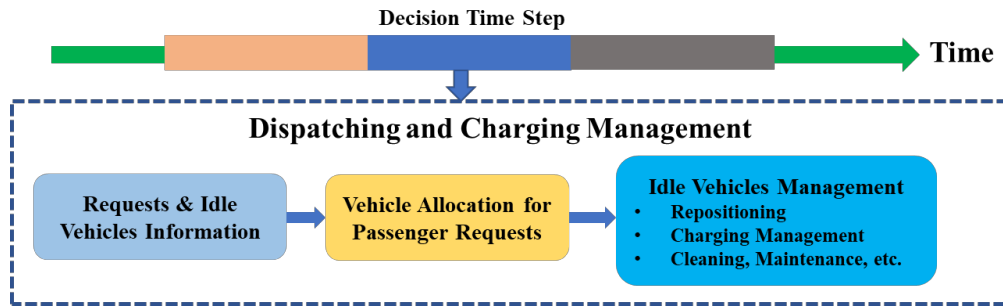


Figure 2-50. A promising procedure for fleet dispatching and charging management.

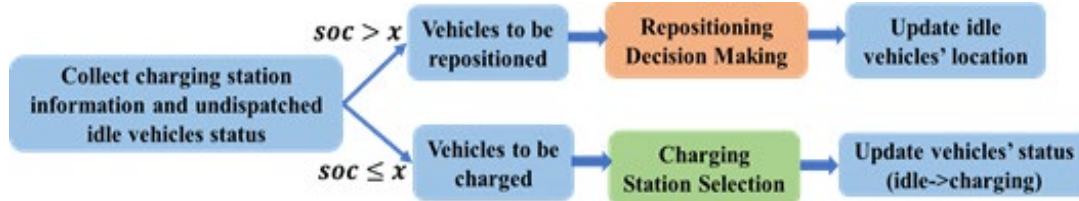


Figure 2-51. A potential procedure for idle-vehicle management.

Heuristic Approaches

A heuristic approach usually proposes strategies for repositioning and charging decision making according to some set rules for each AEV. For example, for repositioning, a rule can be established that assigns idle vehicles to reposition themselves to areas where there has been, currently is, or may soon be, high demand for ride-hailing. This research used a rule that directs AEVs to areas where there are current, unsatisfied ride requests. For charging decision making, vehicles can simply select the charging stations that are closest; this is, in fact, the method used in this research. A framework for heuristics, illustrated in Figure 2-52, was implemented for idle-vehicle management to study the zero-occupancy cost behavior under a heuristic method.

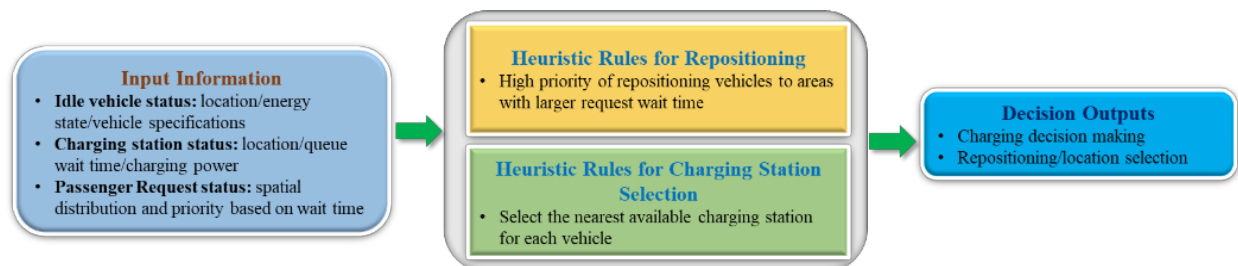


Figure 2-52. Information flow of heuristic approach.

Systematic Optimization Approaches

Systematic optimization approaches for idle-vehicle management were proposed to seek overall benefits of the whole AEV fleet. This approach utilized system-wide information to build advanced optimization models for generating repositioning and charging decision strategies, as shown in Figure 2-53. These strategies manage zero-occupancy vehicle miles traveled for the entire ride-hailing AEV fleet according to specific operational requirements. AEV repositioning and charging decision making has been modeled as an integer programming problem. The decision-making process could be modeled as either a one- or multi-step dynamic programming problem, the latter of which can use forecasted system state information. In general, a multi-step dynamic programming approach can provide more robust long-term strategies for fleet management. To demonstrate the preliminary potential of optimization-based fleet management quickly, a simpler one-step dynamic programming model produced the results in the next section. This approach assumed that fleet vehicle state information and ride-hailing request information in future time steps were unknown at the current decision-making time step.

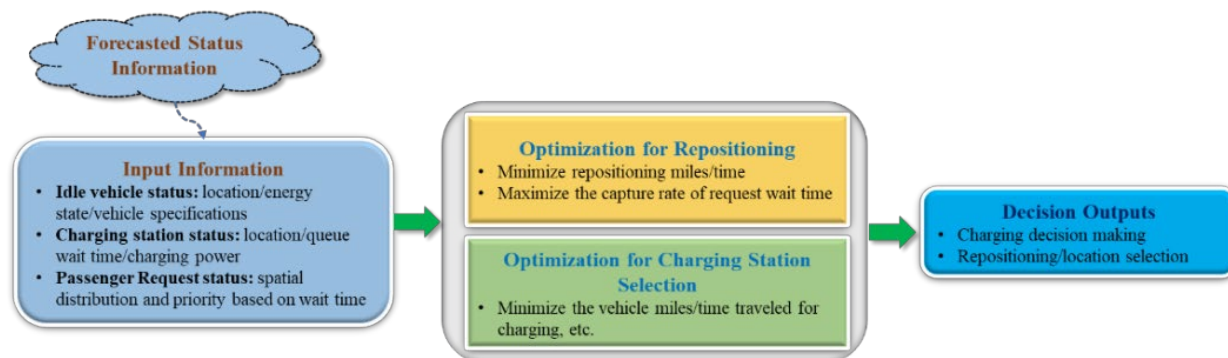


Figure 2-53. Information flow of optimization-based approach.

To conduct research to study potential benefits under different repositioning and charging decision-making strategies, input data describing ride-hailing requests and charging infrastructure availability were required to feed into simulations. Therefore, two real-world data sets were employed to conduct a simulation case study which is presented in the next section.

Real-world New York City taxi data were used to model patterns of passenger requests from ride-hailing services. The Monte Carlo simulation method was used to generate request samples, including pickup and drop-off time and location. The purpose of Monte Carlo simulation was to generate data sets of different sizes. The generated data sets would keep similar patterns of passenger requests, but their size could be smaller or larger than the size of original data set, depending on specific simulation requirements. This was useful to run simulation scenarios of different sizes. Figure 2-54 illustrates probability density functions from both the original historical data set and a sampled data set with 100,000 ride requests. This figure shows that the sampled data set had a smaller size than the original data set, but it had a very similar pattern of requests to the original. The sampled data set was used for the case study described in the next section.

Public charging station data in New York City—including location, power level, and number of charging stations and plugs—from the AFDC was used to configure the charging-station network in the simulation. Figure 2-55 illustrates the spatial distribution of the 415 charging stations and 958 plugs of the AC Level 2 and DCFC stations in New York City today. This data set was used to generate realistic locations of charging stations in New York City for use in the case study.

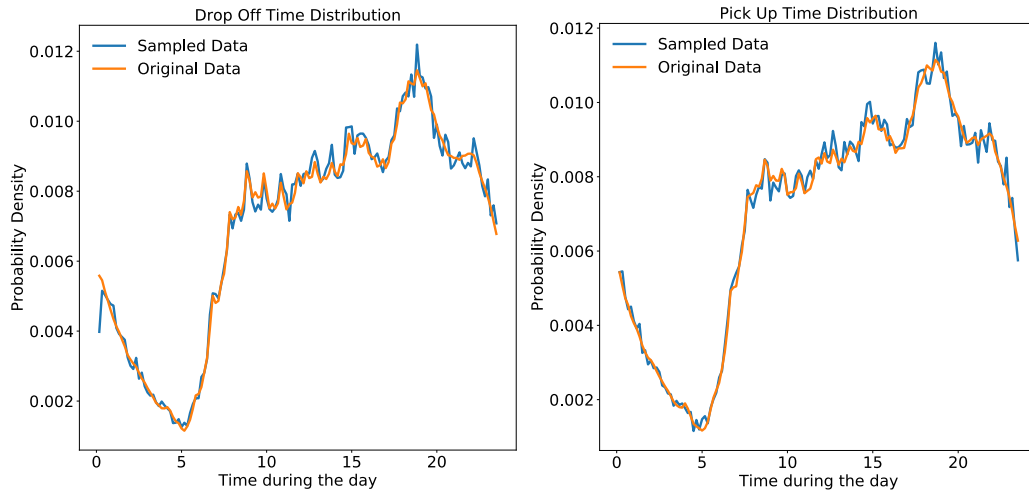


Figure 2-54. Probability density of time distribution across a day for both pickup and drop-off actions.

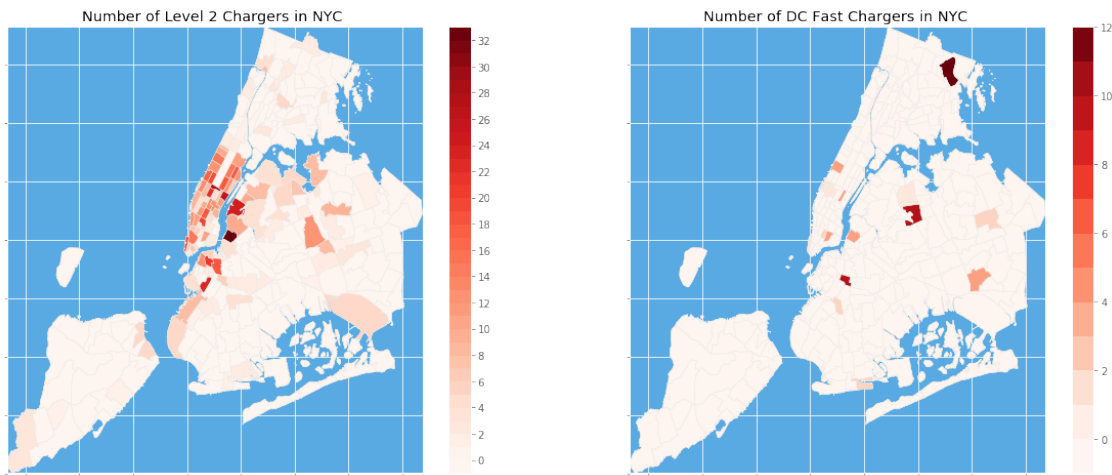


Figure 2-55. Spatial distribution of public charging stations (AC Level 2 and DCFC stations) in New York City.

Case Study: Comparing Fleet Management Strategies for an Automated Ride-hailing Fleet in New York City, New York

Introduction

Commercial AEV fleets of different size were simulated, using either the heuristic approach or the systematic, optimization-based approach for repositioning and charging decisions introduced previously. The purpose of these dispatching strategies was to improve the operational efficiency of an AEV fleet. To understand the operational performance for a ride-hailing AEV fleet, several different metrics were investigated (zero-occupancy vehicle miles traveled, the overall ratio of successfully serving customers’ riding requests, the utilization rate of charging infrastructure, etc.).

Zero-occupancy vehicle miles traveled can be divided into the miles traveled for vehicle allocation, vehicle reposition, and vehicle charging trips. Vehicle allocation represents AEVs traveling from locations where they receive and accept specific ride-hailing requests to locations where they pick up passengers. Vehicle repositioning occurs when idle AEVs move to some other locations to capture future ride-hailing requests. Vehicle charging trips entail AEVs being dispatched to charging stations. These three components can be combined into the measure of overall zero-occupancy vehicle miles traveled. Based on this information, five different subcriteria were used to demonstrate the performance of idle-vehicle management: (1) overall average zero-occupancy cost per vehicle per day, (2) average allocation cost per vehicle per day, (3) average

charging cost per vehicle per day, (4) average repositioning cost per vehicle per day, and (5) average increased zero-occupancy vehicle miles by miles traveled per allocation mile reduction. Criterion 5 aimed to quantify the relationship between zero-occupancy miles driven and vehicle allocation miles, or the distance driven to pick up a passenger. A lower value of this criterion means the proposed method was more powerful in improving operational efficiency.

In the following simulation, three categories of dispatching methods were illustrated: (1) dispatching without repositioning and with heuristic charging decision making, (2) dispatching with heuristic repositioning and heuristic charging decision making, (3) dispatching with systematic optimization for both repositioning and charging decision making. Besides different dispatching and charging decision-making strategies, different scenarios were generated to perform simulations and case studies in New York City. In the simulation settings, three main factors were used to define a unique scenario/simulation:

- Number of ride-hailing requests during a day: A fixed number of requests (i.e., 100,000) within each day was used in all simulations.
- AEV fleet configuration: 15 different AEV fleet sizes were selected for simulations, ranging from 500 to 4,000 vehicles. The battery capacity of each AEV in the fleet was randomly selected in the simulations to be 24, 42, 60, 80, or 100 kWh.
- Charging station network power level: Two different cases were considered in the simulations. One case used the charging power level from today's charging network in New York City, with both 6.7-kW AC Level 2 chargers and 50-kW DC fast chargers. As shown in Figure 2-54, 415 charging stations with 958 plugs are currently distributed spatially in NYC. The other case uses 50 kW for all chargers to simulate a pure DCFC station network. Queuing was not considered in the simulations. When charging stations were in use, AEVs would select other available chargers.

There were 60 cases in total for simulation. Each simulation case had a unique combination of dispatching strategy, AEV fleet size, and charging station network power level. Each case simulated three consecutive days for ride-hailing services. In all cases, the number of requests within each day was 100,000, which is much smaller than the actual number of daily requests in NYC (around 300,000 requests per day). The maximum fleet size in simulation was 4,000 AEVs. For comparison, there are currently about 13,500 taxis in NYC.¹⁰⁶ These assumptions for lower ride-hailing demand and smaller fleet sizes were used to reduce the simulation time for each scenario and results were then scaled appropriately. This allowed for more multi-day simulations that diminished the effect of initial conditions and achieved operational equilibriums. Also, only AEVs were considered in this research. Compared to human-driven ride-hailing vehicles, commercial ride-hailing AEVs could be operated for longer times using well-designed management approaches. These would enable a smaller fleet size to meet given ride-hailing requests, compared to traditional human-driven taxis. By varying fleet size, the dynamics of fleet operation were understood, allowing researchers to identify the most beneficial AEV fleet size to meet given ride-hailing demand.

Simulation Results

Figure 2-56 illustrates zero-occupancy vehicle miles traveled by AEVs in fleets of different sizes when using today's charging infrastructure network. This figure shows that the optimization-based approach dramatically reduced zero-occupancy vehicle miles traveled—e.g., 43% for a fleet of 1,750 vehicles. This figure also shows that, in general, the zero-occupancy vehicle miles decreased when the AEV fleet size increased because more ride requests could be served directly without waiting for repositioned vehicles.

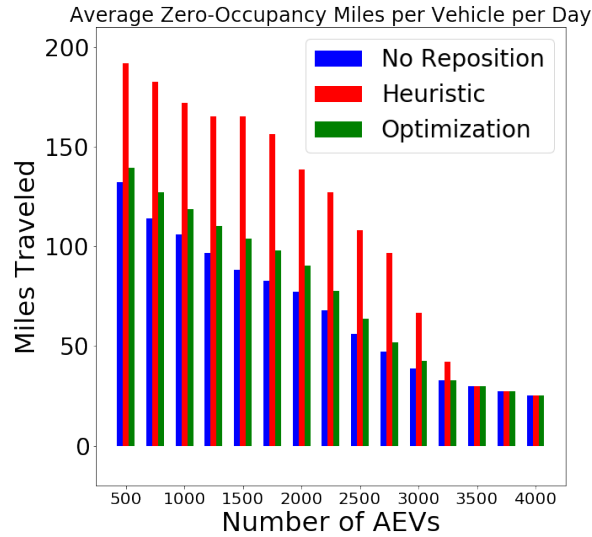


Figure 2-56. The overall average zero-occupancy miles traveled per vehicle per day for different fleet sizes. The series labeled “No Reposition” represents the case where AEVs do not reposition between customers and use heuristic charging decision making. The “Heuristic” series represents the case where AEVs make repositioning and charging decisions using heuristics. The “Optimization” series represents AEVs dispatched using systematic optimization for both repositioning and charging decision making.

Figure 2-57 provides the breakdown of zero-occupancy miles traveled by component. These results demonstrate the performance of repositioning and charging decision-making strategies under different AEV fleet sizes. According to overall average zero-occupancy cost per vehicle per day in Figure 2-56, both heuristic and optimization-based approaches increased zero-occupancy miles travelled. This was because both approaches tried to reposition vehicles in order to move AEVs close to ride requests as shown in Figure 2-57(a).

Looking at the average allocation miles per vehicle per day in Figure 2-57(b), both the heuristic and optimization approaches reduced the allocation miles traveled because they repositioned vehicles near to the requests. However, this benefit was obtained by increasing the zero-occupancy miles traveled, both the repositioning miles traveled shown in Figure 2-57(a) and the charging trip miles traveled illustrated in Figure 2-57(c) and, also, Figure 2-58, which uses a different y-axis scale.

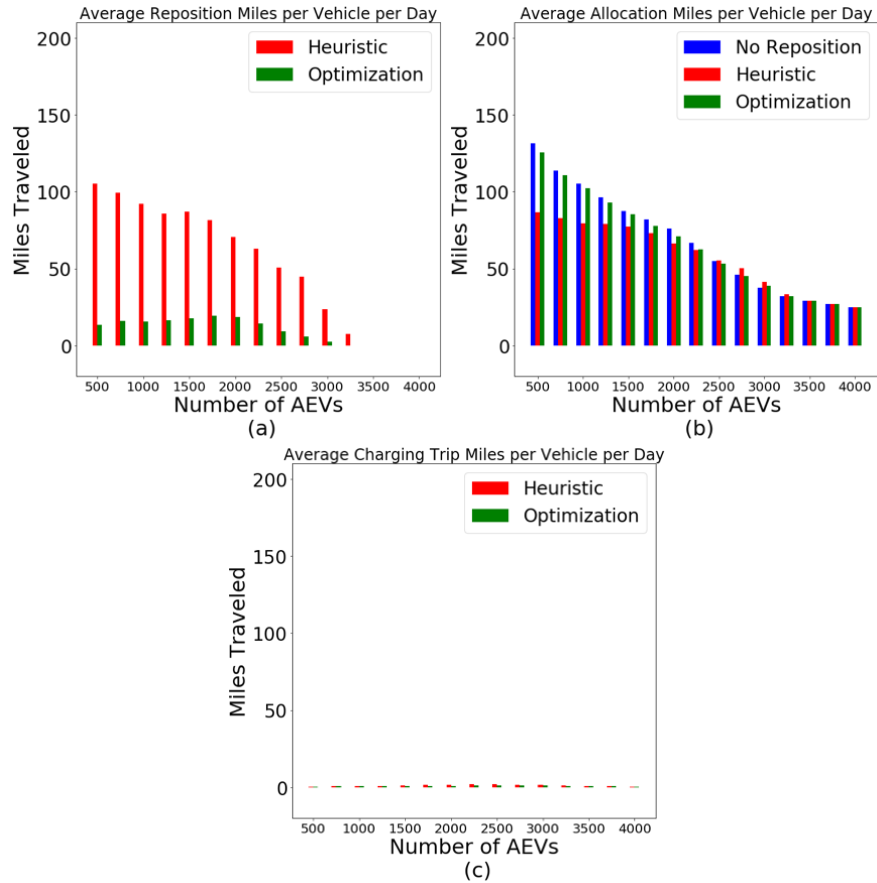


Figure 2-57. Detailed zero-occupancy vehicle miles traveled, including: (a) average reposition miles traveled per vehicle per day, (b) average allocation miles traveled per vehicle per day, (c) average charging trip miles traveled per vehicle per day.

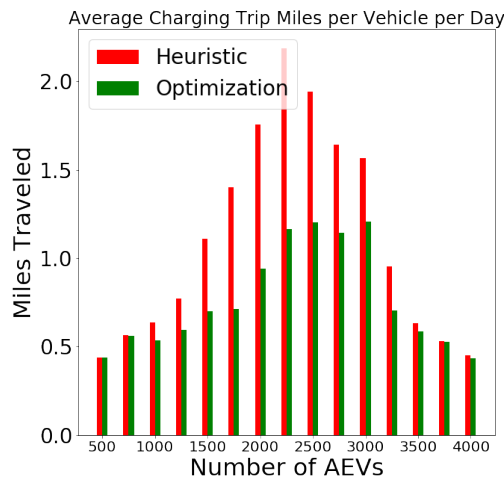


Figure 2-58. Average charging trip miles per vehicle per day, which is an enlarged version from Figure 2-57(c).

Results also show that the increase in miles from the optimization approach was much smaller than from the heuristic approach. The optimization approach thus has more capability to balance zero-occupancy cost and service benefits. This is illustrated in the average increase zero-occupancy cost per allocation mile reduction in Figure 2-59, which shows that a ride-hailing AEV system gained higher operational efficiency when using a well-designed optimization approach. This is because the optimization approach could be designed to involve

multiple cost factors and global system conditions to find a better dispatching and charging strategy that would benefit the entire fleet.

Results in Figure 2-59 show that the optimization approach could be more beneficial when the AEV fleet size was between 1,500 to 2,500 vehicles. An AEV fleet management system needs to balance demand from ride-hailing requests and supply from the AEV fleet. If the AEV fleet size is too small, AEVs are in use in most of time, so there were limited opportunities to optimize repositioning and charging scheduling. If the fleet size is relatively large, all ride-hailing requests would be satisfied immediately, and there would be no need to optimize repositioning and charging scheduling. Therefore, given a fixed demand from ride-hailing requests, the benefits of optimization increase at first then decrease as the fleet size increases. Peak patterns are thus observed at a fleet size between 1,500 and 2,500 vehicles, as shown in Figure 2-58 and Figure 2-59.

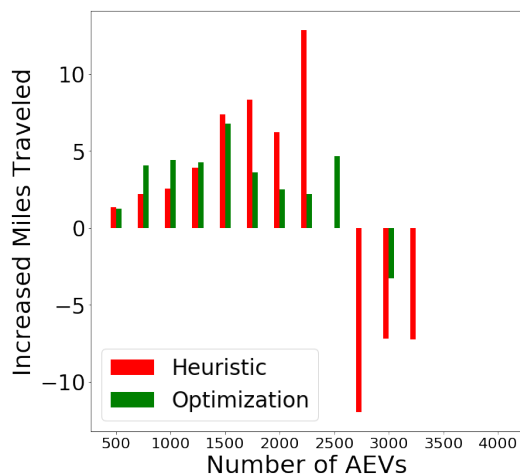


Figure 2-59. Average increased zero occupancy vehicle miles per vehicle allocation mile reduction.

Figure 2-60 shows the simulation results for a DCFC network with 50-kW for all chargers, instead of today’s mix of 6.7-kW and 50-kW chargers. Compared to the results in Figure 2-57, most types of zero-occupancy miles traveled in the case with only DCFC were larger except for the charging trip miles. Charging trip distance decreased because the AEV fleet could get more energy in a shorter time when DC fast chargers were used, so the number of charging trips decreased. This also allowed AEVs more time in service.

The larger DCFC network allowed AEVs in the fleet to achieve higher operational utilization and capture more ride-hailing requests, as shown in Figure 2-61. This increased the overall average zero-occupancy miles traveled (e.g., allocation miles traveled and reposition miles traveled) when there were not enough AEVs to meet all ride requests. However, when the AEV fleet was big enough to serve all requests, the final overall zero occupancy cost was close to the case using a realistic charging infrastructure network as illustrated in Figure 2-56 and Figure 2-60(a) because of the same travel demand from ride requests for both cases. Therefore, a DCFC network improved the operational efficiency by reducing the time spent at charging stations and increasing the operation time for serving ride requests. This generally means that a smaller AEV fleet size could achieve the same service level by using higher-power charging stations.

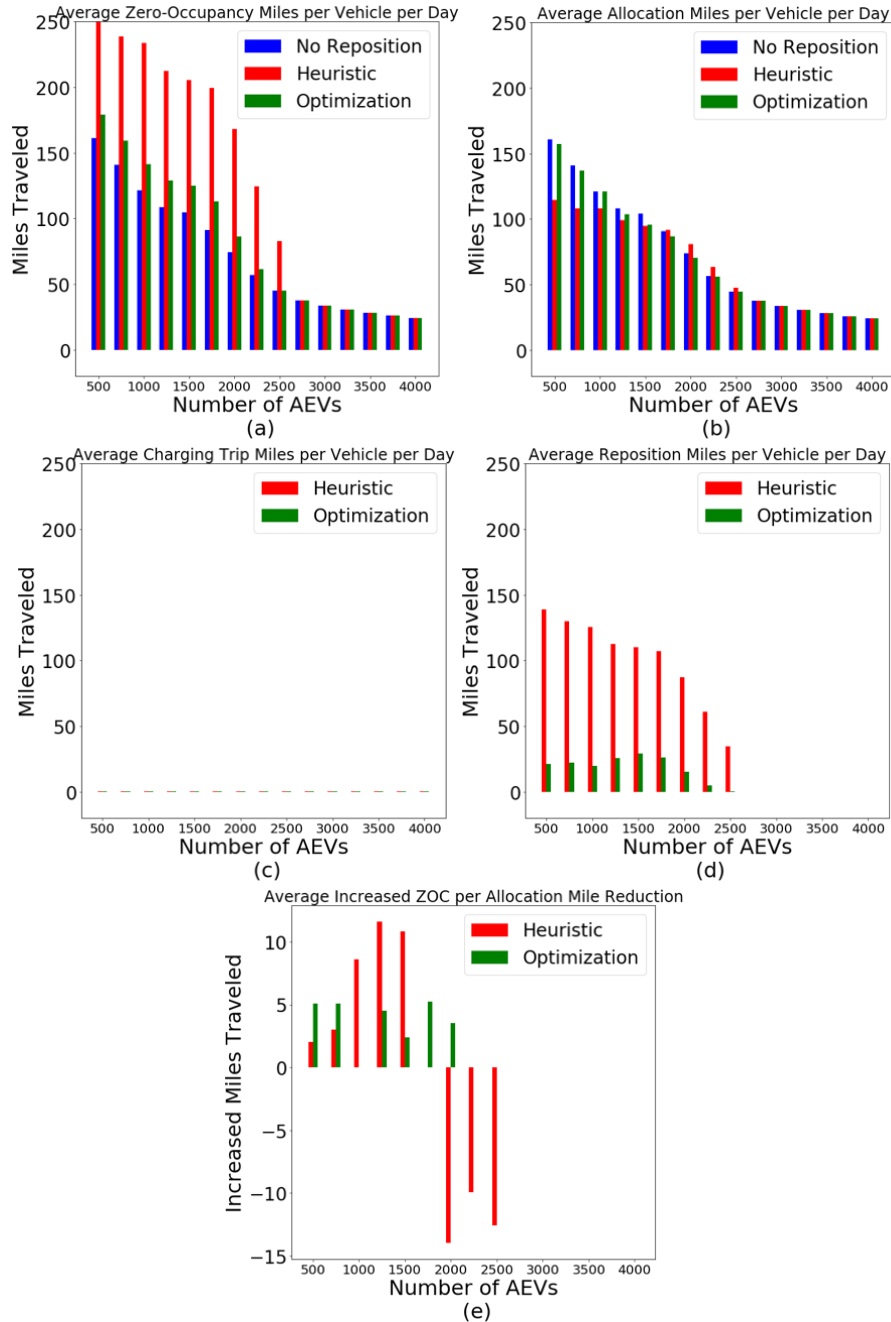


Figure 2-60. Zero-occupancy vehicle miles traveled for simulation case where all charging stations have 50-kW DCFC

Figure 2-61 illustrates the success ratio for serving ride requests under different fleet sizes and different fleet management strategies, including results for both the mixed and 100% DCFC network scenarios. A shortage of AEVs during peak hours meant that not all ride requests were satisfied during that time. A large AEV fleet could successfully serve all ride requests. For a same-sized AEV fleet, a fleet management system with an optimization-based dispatching strategy was more successful than that with a simple heuristic approach. This improvement was 14% when the fleet size was 1,750 vehicles. For a given AEV fleet size, the 100% DCFC network served about 10% more ride requests than the mixed-power charging network due to a reduction in AEV charging downtime. This means that a higher-power charging network is capable of improving the ride-hailing service level and increasing revenue.

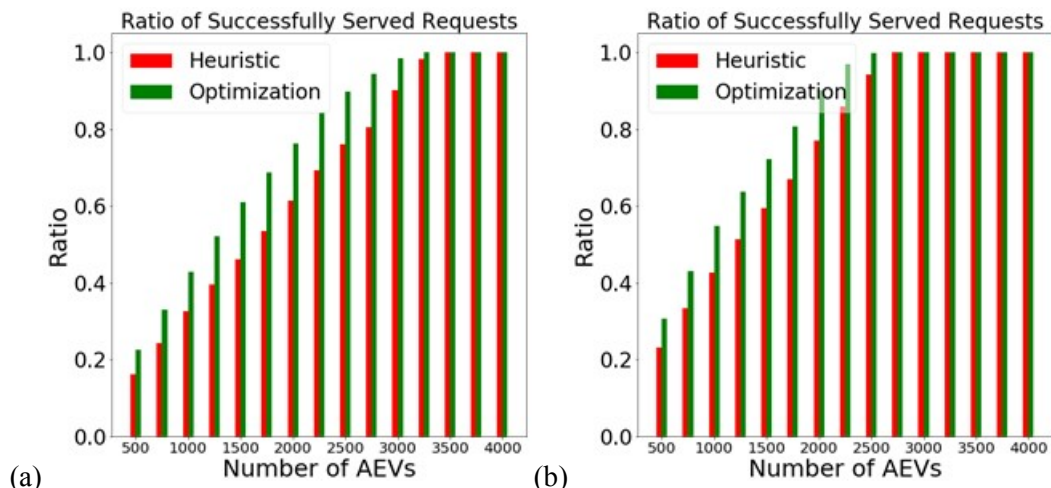


Figure 2-61. Ratio of ride requests successfully served under different fleet sizes and different fleet management strategies: (a) mixed AC Level 2 and DCFC stations; (b) all 50-kW DCFC stations.

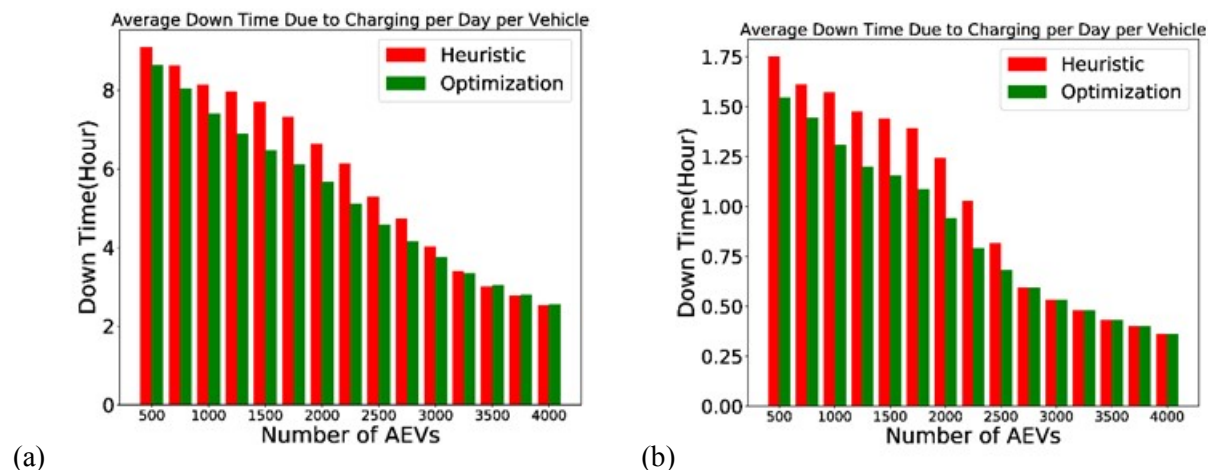


Figure 2-62. Average charging downtime per vehicle per day: (a) mixed AC Level 2 and DCFC stations; (b) all 50-kW DCFC stations.

Figure 2-62 illustrates average charging downtime per vehicle per day under different fleet sizes and dispatching strategies for both charging infrastructure settings. The charging downtime included the travel time to the charging station and charging time spent at the station. Figure 2-62 demonstrates that the average charging downtime monotonically decreases as the AEV fleet size increases. The decrease rate was relatively smaller when the fleet size is small. When the fleet size was relatively large, the overall charging downtime becomes steady due to the constant demand for ride-hailing requests used in these simulations. This causes a faster decrease in the average downtime per vehicle as fleet size increases.

Charging downtime could be reduced considerably by increasing the power level of the charging station network, in this case from multiple hours per vehicle to less than one hour. This means increases in charging power could create a big improvement in fleet operation by reducing the amount of time AEVs spend at charging stations. Among the two charging infrastructure scenarios in the simulation, the optimization-based approach has better performance in the 50-kW power level scenario than the heuristic approach. This implies that a high power level for charging can create more opportunities to optimize fleet operation regarding to charging decision making.

Figure 2-63 provides the overall average utilization rate along the simulation time for the entire charging station network with realistic charging power (today’s mix of Level 2 and DCFC stations) when using the heuristic and optimization approaches. The overall average utilization rate is the average of all utilization values of each charging station in this charging infrastructure network. The total simulation time was three days (72 hours). Each curve with a unique color represents the utilization pattern across a simulation for a specific AEV fleet size, from 500 to 4,000 vehicles. These results show that the utilization rate of charging stations at the beginning of the simulations were lower than other time periods because all AEVs were assumed to start with fully charged batteries. Peak utilization rates occurred around 8:00 pm each day because the peak hour for travel requests took place right before this time period every day, so more vehicles needed to charge. The charging station utilization rate was smaller when the AEV fleet size was small; a fleet of 500 AEVs had the lowest charging station utilization, especially during the second and third day. The charging station utilization rate reached a maximum when the AEV fleet size was around 2,500, which was when the fleet size matched the travel demand from ride requests. In this case, more AEVs could be fully utilized and needed more energy to be charged, increasing charging station utilization rates relative to operations with smaller AEV fleets. But when the fleet size increased beyond 2,500, charging station utilization decreased because the AEV fleet was not fully utilized; therefore, the fleet did not need to charge as frequently during the day.

Comparing results between the heuristic and optimization approaches, the latter can optimize dispatching strategies to reduce the overall zero occupancy cost. This offered benefits through increases in operational efficiency, reductions in cost of operations, and decreases in overall charging station utilization. Furthermore, the optimization approach could help reduce the time period for peak use of charging stations by distributing charging actions to low-utilization periods. This is beneficial for smoothing the charging load from an electrified ride-hailing fleet. Current results did not show obvious improvements from optimization-based approaches. Future research on predictive charging capabilities will be necessary for this beneficial charging optimization to be realized.

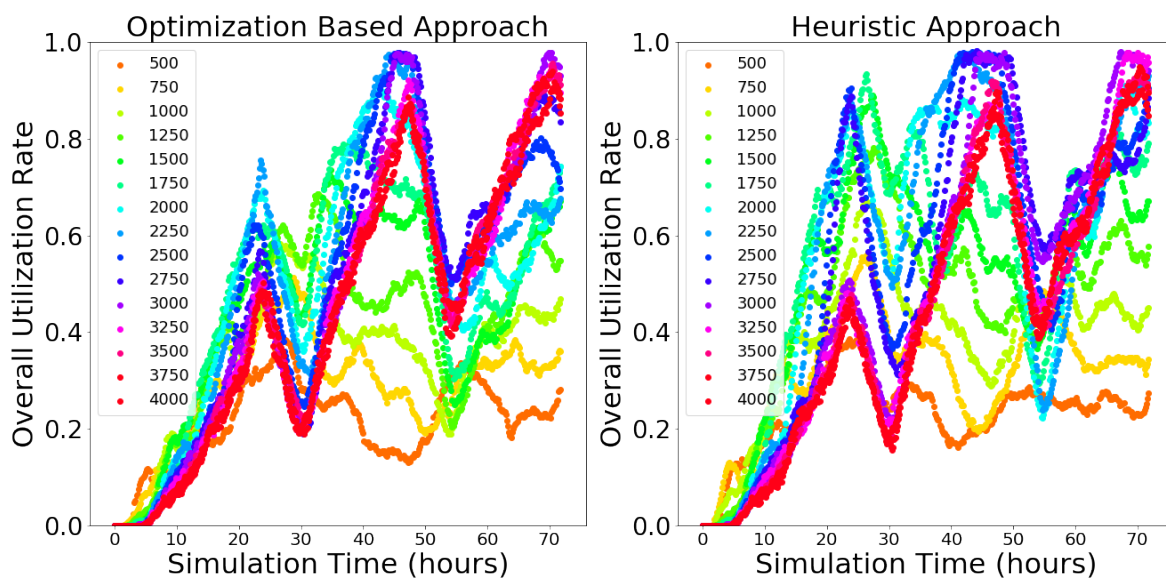


Figure 2-63. Overall average utilization rate for the entire charging station network with mixed AC Level 2 and DCFC when using optimization (left) and heuristic (right) approaches for fleet management.

Figure 2-64 demonstrates the overall average utilization rate for the entire charging station network with all simulated 50-kW chargers when employing the heuristic (right) or optimization (left) approach. Compared to the results in Figure 2-63 with today’s charging power, when increasing the power level, the average charging station utilization rate decreased because vehicles spent less time to recharge. Therefore, charging stations are more likely to be unoccupied relative to the lower-power chargers case. Thus, a DCFC network is more available to support the ride-hailing AEV fleet.

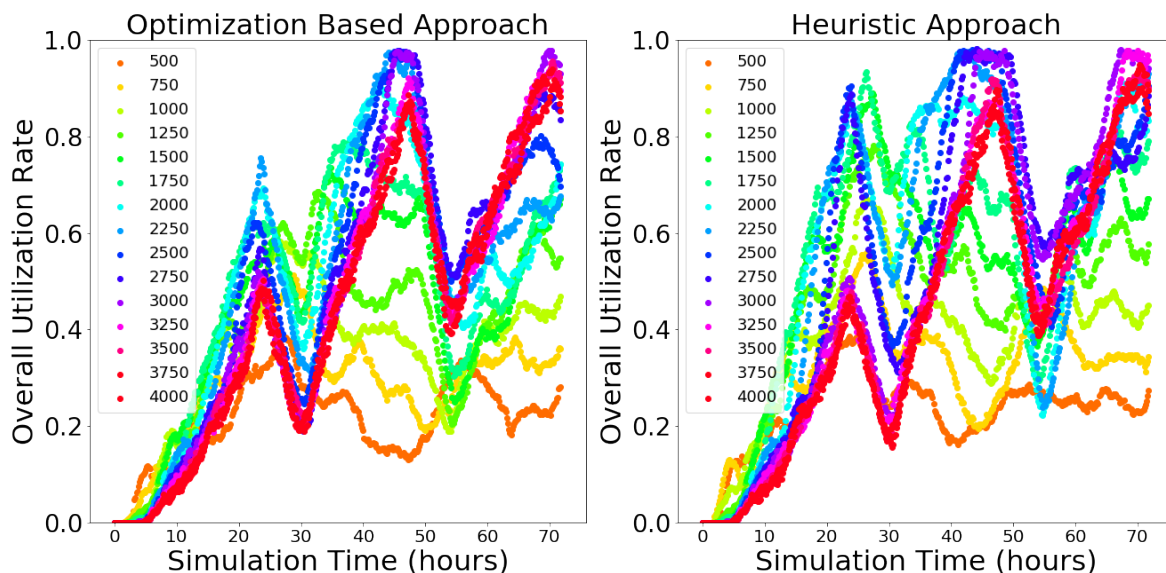


Figure 2-64. Overall average utilization rate for the entire charging station network with all 50kW chargers when using optimization (left) and heuristic (right) approaches for fleet management.

Conclusion

This research illustrated the following strategies for improving idle vehicles management and operational efficiency for supporting an electrified ride-hailing fleet with a charging infrastructure network:

- An optimization-based approach to managing fleets of automated electric ride-hailing vehicles while they are idle between fares, including both repositioning and charging station selection, can help satisfy considerably more passenger ride requests and reduce zero-occupancy vehicle miles traveled, as compared to a simple approach where vehicles follow set rules to independently decide where to reposition and charge.
- A simulation case study of automated electric taxis in New York City found that optimization was most effective for a fleet size of between 1,500 and 2,000 vehicles. For a fleet of 1,750 ride-hailing AEVs, optimization-based, centralized fleet management would result in 14% more ride requests satisfied and 43% fewer zero-occupancy miles traveled than if AEVs make independent decisions based on simple rules.
- Given fixed fleet size and ride-hailing request demand, repositioning idle vehicles properly can reduce the vehicle allocation miles traveled, but may simultaneously increase the overall zero-occupancy vehicle miles traveled. This generally means that, in order to reduce customer wait times for ride-hailing services (represented by reducing the vehicle allocation distance and time costs), more overall zero-occupancy miles traveled from the ride-hailing fleet are usually needed.
- Using a well-designed idle-vehicle management strategy can improve an AEV fleet’s operational efficiency by systematically repositioning AEVs close to upcoming ride-hailing requests and reducing the cost of charging trips.
- Compared to a heuristic approach, the advantages from one-step systematic optimization approach are dependent on specific system assumptions (i.e., AEV fleet size and the amount of ride-hailing demand). The one-step optimization-based approach would gain more benefits when more flexibilities exist at each decision time step—for example, when idle vehicles and ride-hailing requests are more broadly distributed spatially. Optimization-based approaches might not be able to achieve a better performance than heuristic approaches when fleet size is very small or very large for a given ride-hailing demand. However, multi-stage optimization-based approaches that forecast system states in future time steps would be able to provide additional benefits by involving another optimization dimension (e.g., the dimension of time).

2.3.2 Dynamic Wireless Charging for Automated Electric Transit

Key Findings

- Implementing in-route wireless charging technology for SAEVs shows promising potential for realizing a fully automated mobility system (vehicle and charger) for a transit application.
- Simulation of three fixed-route automated electric shuttle bus networks showed that installing 100-kW DWPT systems with 5-meter track length at bus stops has the potential to meet all the energy needs of low-speed (up to 15 mph) and high-speed (up to 50 mph) automated electric shuttle buses.
- In-route wireless charging has the potential to allow the driverless shuttle buses to operate with near-zero downtime, which greatly reduces operating cost compared to equivalent human-driven shuttle buses without DWPT.
- Implementing such a system also has the potential to reduce the size and cost of vehicle batteries by more than 50%.
- Preliminary cost analysis suggests that a DWPT system can be cost competitive with high-power conductive charging in automated electric transit applications.

Introduction

Wireless charging is a safe, convenient, flexible, and efficient method to charge AEVs (sometimes also referred to as CAVs) without needing to physically plug in to charge the EVs.¹⁰⁷ In fact, wireless charging is a key enabling technology for the future of AEVs, but no specific research has been reported so far on wireless charging system integration, including DWPT, with these vehicles.

DWPT is a charging method where the EVs can be charged while the vehicles are in motion. With dynamic wireless charging, the following benefits can be achieved:

- EV range can be so increased as to make unlimited all-electric range possible
- EV battery pack size can be reduced, resulting in overall weight and cost reduction while improving fuel economy
- DWPT can replace many distributed charging stations at destinations.

Furthermore, according to one study,¹⁰⁸ the market share of plug-in EVs could increase up to 65% among total light-duty vehicle sales if 1% of roadways were electrified with 60-kW dynamic wireless charging systems. Thus, dynamic wireless charging systems can be a means of increasing the adoption rate of EVs.

DWPT offers the following benefits specific to AEVs:

- Automating the charging process allows AEVs to self-charge while driving
- Providing range extension would offset the increased electrical load of onboard computing resources.

DWPT technology is based on the electromagnetic coupling between a roadway electrified with coils or long wire loops under the road surface and a receiver/coupler mounted underneath the EV. Although simple in concept, DWPT systems are highly complex and are still in the research stage. Many design parameters must be carefully optimized to achieve a functional, cost-effective design. These parameters include power rating, the length of electrified roadway sections (referred to as track length) and the distance between tracks, and design of the electromagnetic coils within each track and resonant tuning configurations. The selection of these and other parameters influence electric and electromagnetic field emissions, charging efficiency, power transfer continuity, and system cost. The AFI Pillar explored DWPT designs for EVs and AEVs to determine the technoeconomic feasibility of DWPT for future mobility.

System Description

In a DWPT system, the system components include electrical infrastructure (i.e., the grid), grid-side power electronics (including the front-end rectifier and the high-frequency power inverter), electromagnetic couplers and resonant tuning components, and vehicle-side power electronics (including the rectifier and filter stage), as

shown in Figure 2-65. In this section, vehicle energy consumption, finite element analysis (FEA)-based modeling for power transfer characteristics, grid impact and requirements analysis, and the DWPT system optimization are presented.

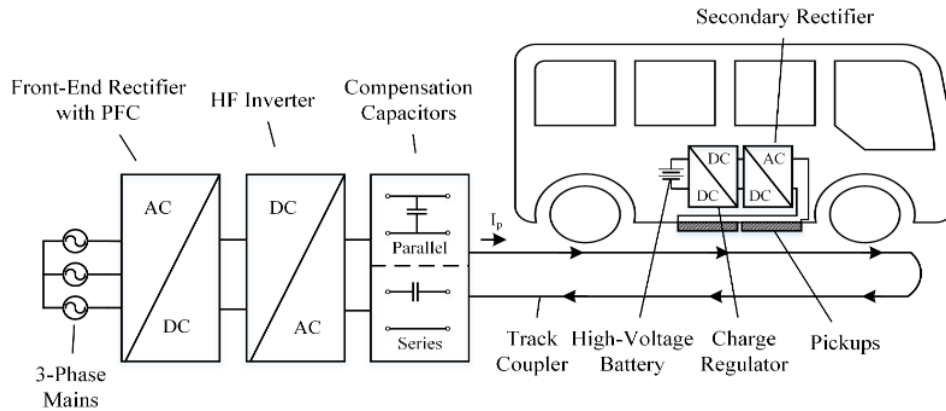


Figure 2-65. Block diagram of a typical track-based DWPT system.

Research Approach

Modeling of Vehicle Energy Consumption

The power ratings and sizing of DWPT systems depend on vehicle energy consumption levels because DWPT systems must be sized and designed to accomplish either charge sustaining operation or considerable range extension. Energy consumption of vehicles should be evaluated on known duty cycles and constant-speed operations. For vehicle energy consumption levels, models and databases created by other national laboratories were used. Point A-to-B constant-speed modeling for light-, medium-, and heavy-duty vehicle classes were analyzed with and without auxiliary power. Constant-speed energy consumption models can be especially useful where the automated driving infrastructure can potentially eliminate the stops. Using vehicle-average-power consumption levels and the route distance, the DWPT system can be sized to both the power level of the electrified roadway track and its section length under the assumption of a rectangular and continuous power transfer profile to the vehicle. To begin the development of the DWPT system design, the Pillar used the average power consumption of AEVs at constant speed, as found in [109], with the rolling coefficient $\mu_r = 0.0065$, equivalent powertrain efficiency $\eta_{eq} = 85\%$, and air density $\rho = 1.225 \text{ kg/m}^3$. More details on the vehicle energy consumption model are covered in Appendix C.

Modeling of Dynamic Wireless Power Transfer Systems

Inductive power transfer is used to transmit power from DWPT transmitters to receivers mounted on the underside of the AEVs. Due to the airgap between the transmitters and receivers, the inductive links are loosely coupled, and the coupling coefficient, $k_i = \frac{M_i}{\sqrt{L_0 L_i}}$, is significantly less than 1; the couplers in the inductive link are designated by number i where $i = 0$ designates the roadside DWPT transmitter and $i = 1, 2, \dots$ are receivers. Multiple AEVs can be powered from the same DWPT transmitter. The equivalent receiver loads R_{Li} can be varied to regulate power flow between the roadside DWPT transmitter and vehicle receivers¹¹⁰. This can be accomplished by onboard DC/DC converters. Conduction losses are calculated for the DWPT transmitter and receivers from the parasitic resistances $R_i = (2l_i + 2W_i)\rho$ where ρ is the equivalent DC resistance of the Litz cable per length. (Litz cable is a special multistrand wire used for carrying AC at high frequencies.) For the DWPT transmitter and receivers, 4/0 Litz wire cable is assumed with $\rho = 0.056 \frac{\Omega}{1000} ft$.¹¹¹ Skin-effect losses and bundling effects are neglected because the cable is made from braided 38-American wire gauge (AWG) wire. With an operating frequency of 85 kHz, the strand diameter of 38-AWG wire will be less than one-half of skin depth, virtually eliminating that component of AC resistance.¹¹² The input voltage and current as well as the input and output power expressions of the DWPT system model are provided in Appendix C.

Finite Element Analysis-based Modeling of Mutual Inductance and Power Transfer Characteristics

To analyze and validate the power transfer characteristics of long-track-based DWPT deployments, an FEA model of a DWPT road section was completed. This FEA model validates the assumptions in the power transfer profile and continuity along the track. While the approach using smaller coils has very high-peak efficiency because of the limited coil length, there are power pulsations as each vehicle passes from one coil to another. Moreover, the energy delivered to the vehicle is limited in this approach because energy delivery is a function of the time integration of the power transfer curve. With a long-track approach, the power starts from zero and gradually increases to the peak value as the vehicle aligns with the transmit track; next, power transfer stays constant along the track, and it gradually falls as the vehicle clears the track. Because the track is longer, the power transfer stays almost constant along the track. The FEA model validates these power transfer characteristics while identifying DWPT track parameters, track-to-vehicle power transfer efficiency as a function of the track length, and mutual inductance variation with respect to vehicle position. The DWPT track-to-vehicle mutual inductance has also been modeled and is an indication of power transfer profile to the vehicle. The block diagram of the system is shown in Figure 2-65. More details on power transfer efficiency with respect to track length and ferrite thickness, with the parameters of the FEA model, are provided in Appendix C. In addition to the trapezoidal-shaped mutual inductance and power transfer characteristics shown by the FEA model, the other important key takeaway is that track-to-vehicle efficiency can be 95% for tracks shorter than 100 m with a ferrite thickness of 1/16 in. Longer tracks require thicker ferrites to maintain similar levels of efficiency.

Grid Impact and Requirements Analysis for DWPT Systems

The AFI Pillar also evaluated the impact of DWPT systems on the power grid to assess grid infrastructure requirements to power DWPT systems. Additionally, electromagnetic transient (EMT) studies were performed to quantify the impact of DWPT systems on the grid. These studies aid in understanding grid infrastructure requirements to reduce voltage variations in the grid. Reduced voltage variations improve the stability of grids and avoid inadvertent protection triggers. For the models, DWPT system requirements were quantified based on a charge-sustaining mode of operation for vehicles. Grid impact and grid infrastructure requirement analyses are detailed in [113]. According to those findings, a DWPT system with conventional grid-interface converters would produce considerable voltage fluctuations on the grid side from power pulsations. Smart inverters with Volt/VAR supply capability or integration with energy storage systems and/or renewable energy can be a viable solution to improve the grid stability and resiliency.

Design Optimization Approach for a Single Vehicle in an Electrified Lane on a Highway

Sizing and designing a full-scale DWPT system for highway applications is a vast problem area that has not been fully addressed in the literature. It is thought that the first deployment of DWPT technology will occur in primary roadways, which corresponds to interstates and other freeways and expressways. This is because 10% of total roadways carry 60% of all travel. Because more vehicle-miles are traveled on primary roadways, the first deployments will more likely occur there. As with high-occupancy vehicle lanes, there will initially be a single lane electrified with DWPT technology. If transmitter lengths are designed correctly, for a given average speed and following distance, it can be assumed that only one vehicle can be coupled with one transmitter at a time. Under congested traffic, where more vehicles exist on transmitter couplers, the total power from the transmitter would be regulated to the maximum power (i.e., vehicles would share the total available power), which would change the findings. Alternatively, a DWPT systems could be designed for worst-case scenarios in which a maximum number of vehicles on a transmitter is considered; however, this option would require significant overdesign, which is not an optimal solution.

Once power transfer characteristics are determined, optimal sizing of a DWPT system can be analyzed for highway applications. System parameters must be carefully selected to reduce overall cost per mile of DWPT. Among these parameters, system length is important due to its impact on system coupling coefficient, overall efficiency, and cost of construction and installation. The impact of this effect will increase if the quality factor (the ratio of system reactance over the resistance ($Q = X/R$)) of the system is low. Because high-efficiency operation is paramount for DWPT to be practical from both a capital and operational cost standpoint, and the quality factors of systems may be limited, transmitter sizes will be constrained by the dimensions of smaller vehicles. In this case, there would be advantages to using multiple parallel receivers for longer vehicles, such

as Class 8 tractor-trailers. This will both decrease the initial capital cost and ensure the maximum utilization of the DWPT system, driving down the cost of using the system for all. If these costs are low enough, DWPT could revolutionize future transportation by eliminating range-anxiety and enabling long-distance, charge-sustaining trips in AEVs. This would increase the mobility of both freight and passengers and, ultimately, help remove the barrier of long-distance travel from transportation electrification.

The analysis included an interoperable DWPT system that can be used to charge all classes of AEVs including LDVs and heavy-duty vehicles (HDV). For example, a DWPT system may be designed to have transmitter lengths shorter than the length of an HDV to maximize efficiency for an LDV. Multiple receivers on an HDV would then be used to scale the power transfer for these vehicles. A block diagram of such a system with 100-kW transmitters is illustrated in Figure 2-66. With 42% roadway coverage,^h the system could enable charge-sustaining operation for both LDVs and HDVs at 70 mph.

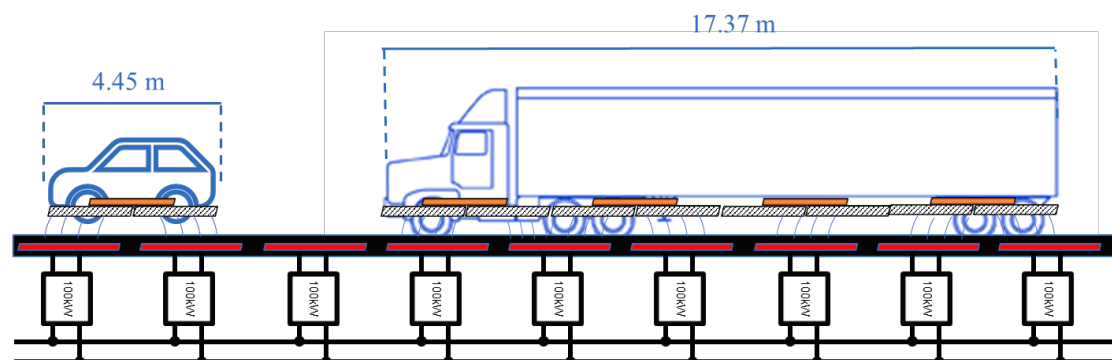


Figure 2-66. An example of a DWPT system using paralleled short sectional 100-kW primary couplers and arrays of pickup couplers. As displayed, the light-duty vehicle is receiving 200-kW and the HDV is receiving 600-kW.

For the system depicted in Figure 2-66, a multi-objective optimization system based on the models is developed. The multi-objective optimization developed is detailed in Appendix C.

Design Optimization Approach for Multiple Vehicles in Electrified Highway Lanes

The AFI Pillar also analyzed DWPT system designs considering multiple vehicles on electrified highway lanes. In this research, the Pillar developed a DWPT system design optimization for a future highway where AEVs travel in coordinated groups, with each AEV in the group powered by the same DWPT section.

As the distribution of smaller LDVs and larger HDVs in each group is varied, the DWPT system power level, transmitter length and the equivalent receiver loads should be adjusted to minimize infrastructure requirements and energy losses of the system. The outputs from this analysis were used to determine the optimal groupings of vehicles for a given DWPT system. The analysis suggested that AEV coordination could aid in the deployment of DWPT and reduce the overall infrastructure and energy losses of DWPT systems. A system showing the operation of groups of AEVs over a DWPT-enabled roadway is shown in Figure 2-67.

^h Assuming that the DWPT system is installed in a single lane only.

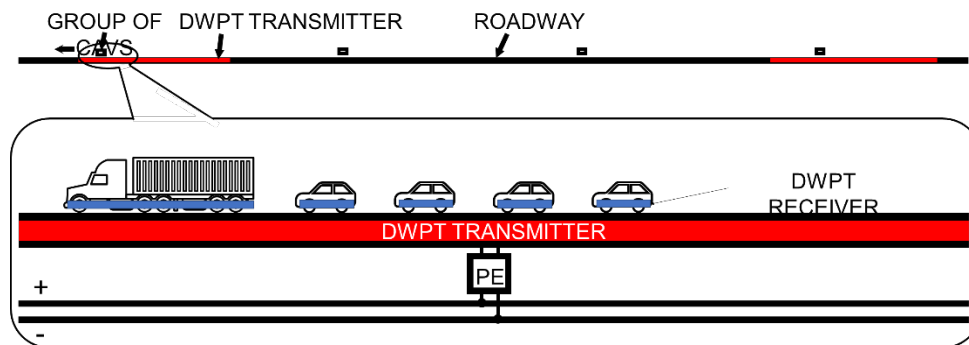


Figure 2-67. Illustration of groups of AEVs over a DWPT enabled roadway

In this case, the group shown is composed of one HDV and four LDVs. It was assumed that groups are spaced on the roadway such that only one group is over a DWPT section at a time. The power electronics (PE) block shown is composed of one or more inverters.

The modeling methodology here involves using vehicle energy consumption information, inductive power transfer model, and optimization formulation. This methodology is detailed in Appendix C.

Design Optimization Approach for Automated Electric Shuttle Buses on Fixed Transit Route

Currently, the major focus for automating transit vehicles is with automated electric shuttles capable of transporting eight to 12 passengers. In this report, these vehicles are considered SAEVs. Although this application is today a small niche case, these vehicles have the potential to significantly decrease operational cost, increase safety, and expand more flexible route designs for transit agencies. This could prompt these vehicles to become more mainstream as transit agencies look for ways to increase efficiencies and the levels of service they provide to riders.

Utilizing wireless power transfer (WPT) technology to charge SAEVs fits well for realizing a fully automated mobility system (integrating the vehicle and charger). Furthermore, wireless chargers can be installed at designated stops or on the road and safely operated due to the elimination of the plug-in cables.^{114, 115} However, investment in wireless charging infrastructure (WCI) presents a critical barrier for commercializing and adopting this technology. This barrier can be overcome by proper system planning and optimization to balance the cost increase due to WCI and the cost reduction from decreased battery size and extended driving range. The AFI Pillar conducted a system planning optimization analysis for in-route, WCI-serving, fixed-route, on-demand and circulator SAEVs. A system design optimization tool, WPTSim, was developed for this study.

The WPTSim tool, described in Figure 2-68, incorporates a vehicle energy estimation and powertrain model, considering drag power, acceleration power, ascent power, and auxiliary-load power. It also integrates a wireless charger power model, considering dimensions, structure, locations, efficiency, and misalignment in both travel and lane directions. As shown in Figure 2-69, WPTSim consists of two layers: energy analysis and optimization. The former receives driving data (speed, route, road grade), either simulated or collected in the real world, and predicts the battery power, energy, and SOC profiles for specific system design parameters. The optimization layer provides an automatic search capability to change input parameters, run the energy estimation layer, evaluate predefined objectives and constraints, and update the input parameters. This process continues until the optimal combination of the system key design parameters is determined.¹¹⁶ This platform was utilized for planning and optimization of wirelessly charged SAEVs operating in a fixed route.

AFI Pillar researchers used WPTSim to conduct the following three simulation case studies:

- Two fixed-route, high-speed, on-demand SAEVs operating on a hypothetical diamond-shaped mobility network
- Four fixed-route, high-speed, on-demand SAEVs operating on a planned route in Greenville, South Carolina

- Two NAVYA “Arma” low-speed SAEVs operating on a circulator route at the University of Michigan in Ann Arbor.

In all cases, the goal was to find the optimum combination of four key system-design parameters: (1) number and placement of each wireless charger ($x_1 = N_{WPT}$), (2) charging-power level ($x_2 = P_C$), (3) number of track segments per position ($x_3 = N_S$), and (4) battery capacity ($x_4 = Q_b$) that achieves minimum vehicle and charger cost and charge-sustaining operation.

For the third case study, real-world drive cycle and energy consumption data were collected from two NAVYA Arma SAEVs operating at the University of Michigan at Ann Arbor. The data provided information about vehicle energy consumption (kWh/mile), speed, and location for three different operating days (July 16, 17, and 19, 2018). The measured energy consumption data were used to tune parameters in the SAEV powertrain model and validate its performance. In addition, the drive cycle data were integrated into WPTSim and used for planning and optimization of in-route WCI serving the SAEVs.

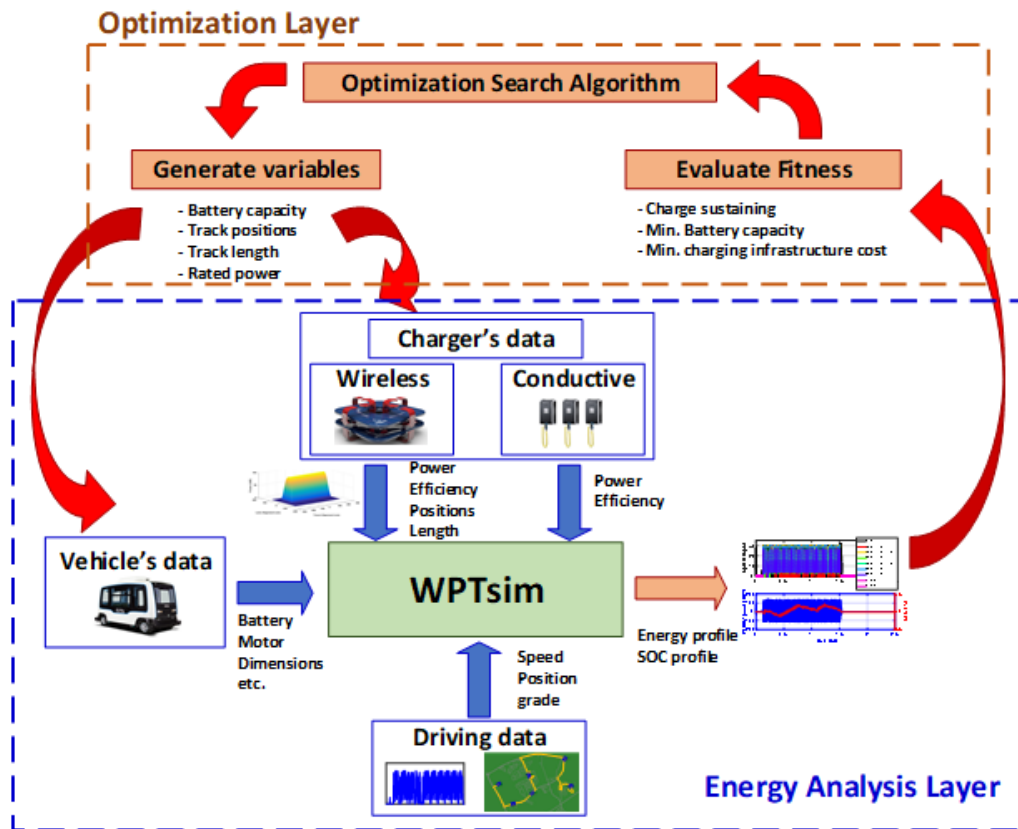


Figure 2-68. WPTSim, a system planning and optimization platform.

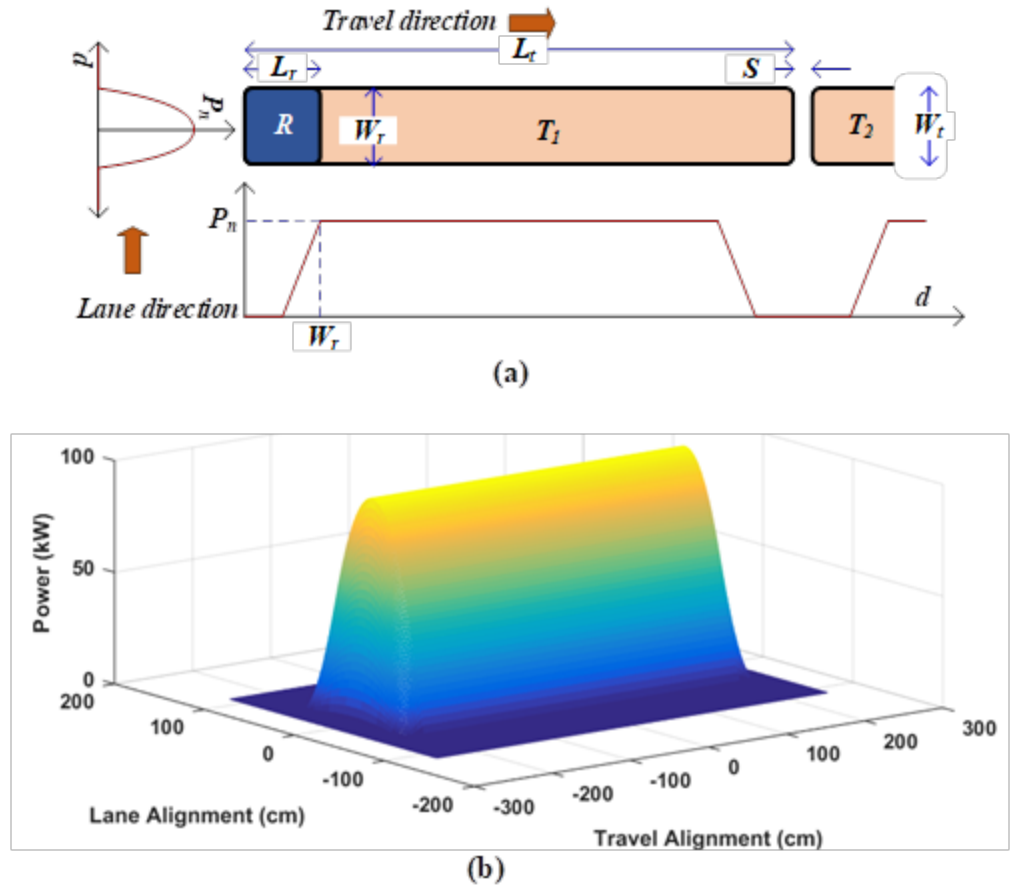


Figure 2-69. Wireless charger power model including (a) power profiles in travel and lane direction and (b) a look-up table integrated with WPTsim for a 100-kW system.

A nonlinear mixed-integer single-objective planning optimization problem for a wirelessly supported SAEV system was formulated and solved. The main goal was to define the best combination of the key system-design parameters that allows the SAEVs to achieve charge-sustaining operation at minimum vehicle component and charging infrastructure component cost. Both the problem formulation and optimization model are found in Appendix C.

Case Study 1: Modeling a Single Vehicle in an Electrified Highway Lane

Key Findings

A 250-kW DWPT system installed in 8 to 10% of primary roadways in the U.S. is sufficient to support charge-sustaining operation of an LDV traveling at 65 mph.

Discussion of Results

It is important to limit the coverage of DWPT systems due to the large expense of roadway construction. Moreover, practical tradeoffs exist between the power rating and coverage of the system. With low coverage, the onboard energy storage and electronics of EVs must facilitate high charge rates. However, power ratings in this case may still be lower than what would be required for high-power static charging because the DWPT system can transfer energy over a longer period of time than can static charging systems by charging while the EV is on the move. An upper limit to the area-related power density can also be achieved by wireless charging systems. Figure 2-70 shows that, for transmitters with a power rating of 200 to 250 kW, 8 to 12% of the roadways should be electrified for an LDV (represented by blue data points in plot) to be able to maintain charge-sustaining operation at 65 mph. This seems to be a reasonable solution that could be practically achievable, in terms of cost.

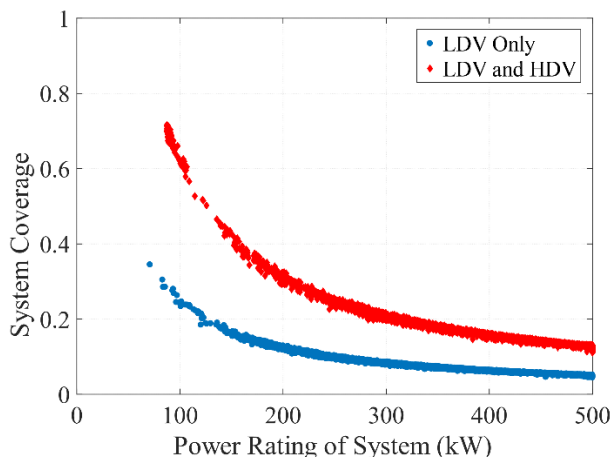


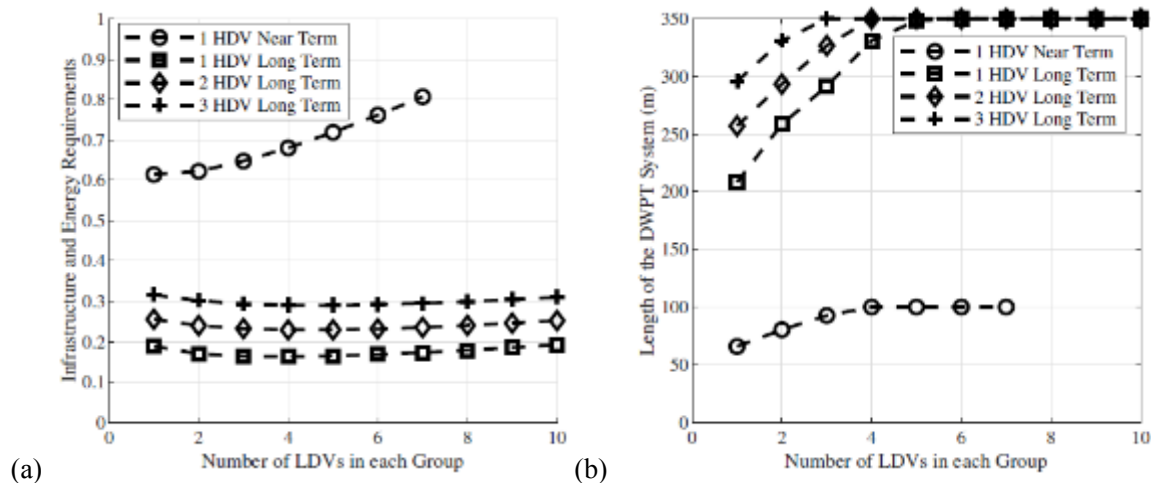
Figure 2-70. Pareto solutions from the optimization model for two different cases (LDV only [blue] and LDV and HDV [red]).

Case Study 2: Modeling Multiple Vehicles in Electrified Highway Lanes

Discussion of results

In Figure 2-71 (a–c), the optimization outputs for 55 mph are given. In Figure 2-71(a), the sum of the energy and infrastructure requirements for each group of vehicles is plotted as a function of numbers of LDVs and HDVs. The vertical axes, labeled as infrastructure and energy requirements, represents the fraction of roadway coverage of the DWPT system (where 0 mean no roadway electrification; 1 means 100% of roads have a single lane with continuous DWPT coverage). Alongside this, the DWPT transmitter length, and the system coverage are displayed in Figure 2-71(b) and (c), respectively. Likewise, results for 70-mph are shown in Figure 2-71(d–f). In the near-term case for these two speeds, the system can only support up to one HDV and seven LDVs at a time in the 55-mph case and one HDV and three LDVs simultaneously in the 70-mph case due to the limitation of the 200-kW inverter power rating. Past these points, the coverage in Figure 2-71 (c) and (f) both exceed 100%. In both cases, the output from optimization are at the upper bounds of the power rating: 200 kW for the near-term and 2 MW for the long-term cases. Note that near-term systems represent currently achievable designs based on past work in this field while long-term systems show what is possible with higher power ratings and charging limits; refer to Appendix C for more information.

Several observations can be made from these outputs. In Figure 2-71(a) and (d), the number of LDVs and HDVs on the DWPT transmitter affects the overall infrastructure and energy requirements of the DWPT system.



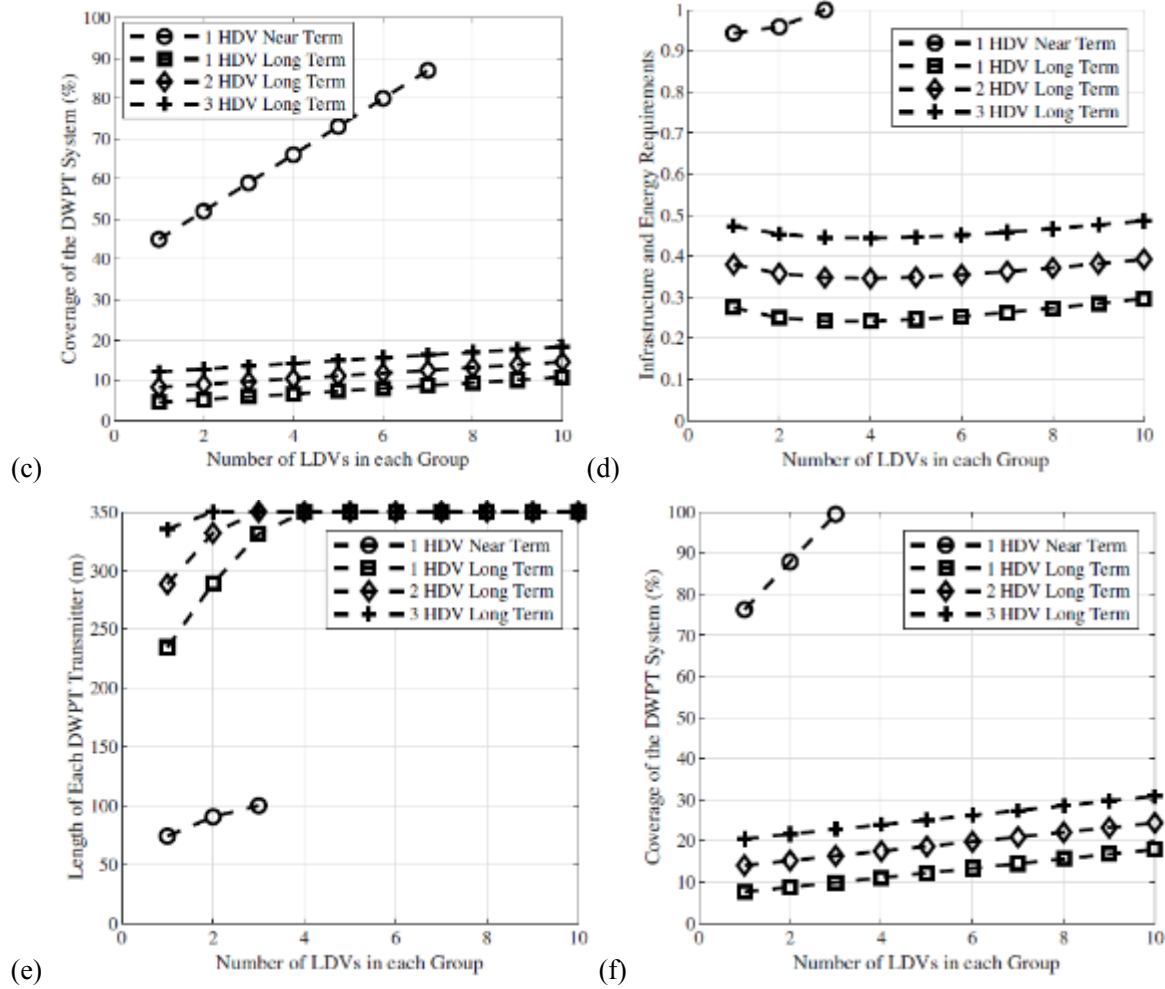


Figure 2-71. Optimization output for the short-term and long-term cases at 55 and 70 mph. In (a), the infrastructure and energy requirements for 55-mph are given. In (b) and (c), the length of each DWPT transmitter and coverage are shown, respectively, for the 55-mph case. In (d-f), the plots are repeated at 70 mph. At both 55 and 70 mph, the outputs for the power rating of the DWPT system are 200 kW for the near-term case and 2 MW for long-term cases.

For the bounds and weights used in this work, the optimal group for the long-term cases in Figure 2-71(a) and (d) is one HDV and four LDVs at both 55 and 70 mph in terms of overall energy and infrastructure requirements. This suggests that grouping LDVs and HDVs together can help minimize infrastructure and energy loss requirements of the system by decreasing energy losses over the operating lifetime of a DWPT system. The limitation of system power level and DWPT transmitter length also affects the output of the optimization. In the optimal group for the long-term scenario of one HDV and four LDVs in Figure 2-71(c) and (f), the vehicles would only cover 35 m of the approximately 350 m transmitter. Optimization of infrastructure and energy requirements for the long-term case also occurs where the system length begins to be limited.

Case Study 3: Fixed-route, High-speed, On-demand, Automated Electric Shuttle Bus in a Hypothetical Diamond Road Network

Key Findings

For high-speed (40–50 mph) SAEVs, implementing in-route wireless chargers at designated stops with maximum power level has the potential to provide a charge-sustaining operation with 52% reduction in the onboard battery and presents the most cost-effective solution.

Introduction

In this study, a hypothetical diamond-shape automated mobility network was simulated in the Simulation of Urban Mobility (SUMO) microscopic traffic tool.¹¹⁷ It has 13 nodes and 48 links and includes all expected automated electric mobility elements, such as SAEVs, fixed-route on-demand service, and SAEV stops, as indicated in Figure 2-72. Four on-demand SAEVs are running on fixed routes in the middle loop (shown with yellow dashed line) in the network. The simulated drive cycle data from SUMO and the parameters of the EasyMile EZ10 SAEV are integrated with WPTSim and used for system planning and optimization analysis.¹¹⁸

Discussion of results

A multi-objective optimization problem was formulated and solved for the system key design parameters of the wirelessly charged SAEV.¹¹⁹ The optimization objectives are to achieve charge-sustaining operation and minimize overall system cost. The optimal system design solution is presented in Table 2-19, which incorporates the first four positions for the wireless chargers that match the designated SAEV stops, the maximum power level (100 kW), and the minimum track length (one segment/position), which lead to minimum charging infrastructure cost. The battery capacity was minimized to 9 kWh instead of 19 kWh, as initially installed by EasyMile. The system performance under the optimum solution is evaluated, as indicated in Table 2-20, and Figure 2-73, in which the charge-sustaining operation is evident, with a 0.04% variation of SOC from the beginning to the end of the drive cycle.

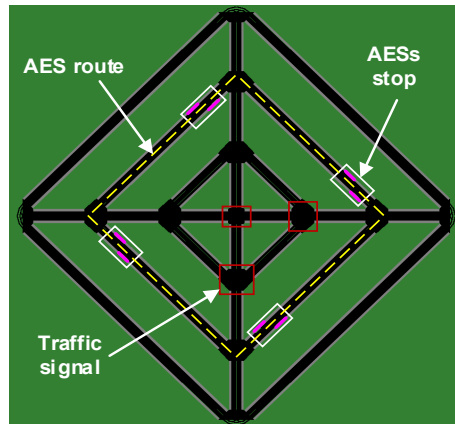


Figure 2-72. The hypothetical diamond-shape automated mobility network in SUMO tool.

Table 2-19. Optimal design solution.

Parameter	Optimal value
NWPT	[1, 2, 3, 4]
PC	100-kW
Qb	9 kWh
NS	1

Table 2-20. Performance parameters.

Parameter	Value
SOCmax	79.14%
SOCmin	59.37%

SOCinitial	70%
SOCfinal	70.04%
SOCfinal – SOCinitial	0.04%

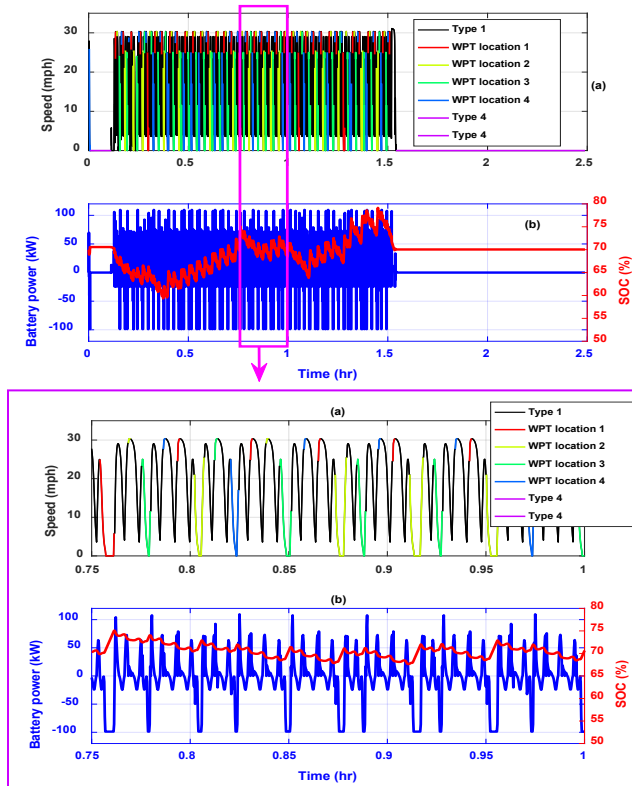


Figure 2-73. Optimal driving performance of SAEV.

Case Study 4: Fixed-Route, High-Speed, On-Demand, Automated Electric Shuttle Bus in Greenville, South Carolina

Key Findings

For high-speed (40–50 mph) SAEVs, implementing wireless charging at a few designated stops with proper design allows the vehicles to realize charge-sustaining operation (unlimited range and zero recharge downtime) with a 36% reduction in the onboard battery capacity, at minimum cost.

Introduction

In 2017, the Federal Highway Administration awarded a \$4M grant to the county of Greenville, South Carolina, to demonstrate the use of automated taxis to provide a local mobility solution in three distinct locations in the county, shown in Figure 2-74.¹²⁰ The network was imported into the SUMO tool, visualized in Figure 2-75, and three travel modes were modeled: (1) regular car, (2) walk, and (3) on-demand fixed route SAEV.¹²¹ The Greenville SAEV pilot project has two phases. Phase 0 deploys two SAEVs and two stops, while Phase 1 accommodates four SAEVs and six stops. The designated stops are the locations at which the SAEVs will pick up and drop off passengers. In this work, the WCI is investigated for serving the SAEVs in Phase 1. The drive cycle data from SUMO simulation has been integrated with WPTSim, considering the group rapid transit (GRT) autonomous electric shuttle parameters.¹²²

Discussion of Results

The current driving performance of the SAEVs without wireless charging capability is analyzed considering GRT parameters and drive cycle data from SUMO, as presented in Figure 2-75. All SAEVs show a current driving range of less than 3 hours. The key design parameters ($x_1 - x_4$) are analyzed and optimized using WPTSim for charge-sustaining operation at minimum total cost.¹²³ The optimal solution incorporates six WPT positions that match the designated stops in Figure 2-76. These results are logical because SAEVs spend more time at these positions due to transient stops and low speeds, which allow the WPT system to transfer more energy. Furthermore, the algorithm chose the maximum charging-power level of 100-kW at each position. The battery capacity was optimized to 23 kWh, a 36% reduction compared to the currently installed 36 kWh battery. The driving performance of all SAEVs, considering the optimal solution is presented in Figure 2-77. All SAEVs show charge-sustaining operation, with almost infinite driving range and no violation of any of the predefined constraints.



Figure 2-74. Test network at Greenville, South Carolina.

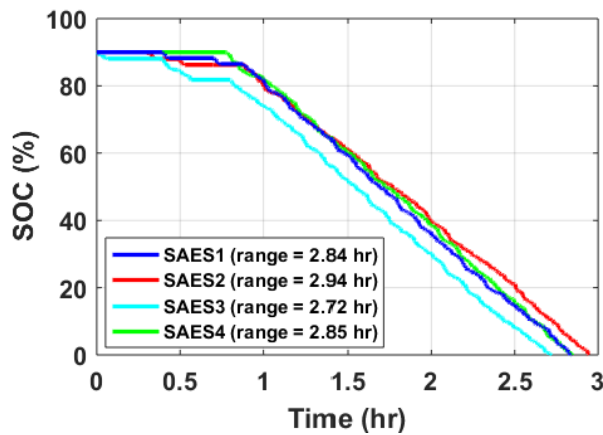


Figure 2-75. Current driving performance.



Figure 2-76. Greenville SUMO simulation network and fixed-route configuration.

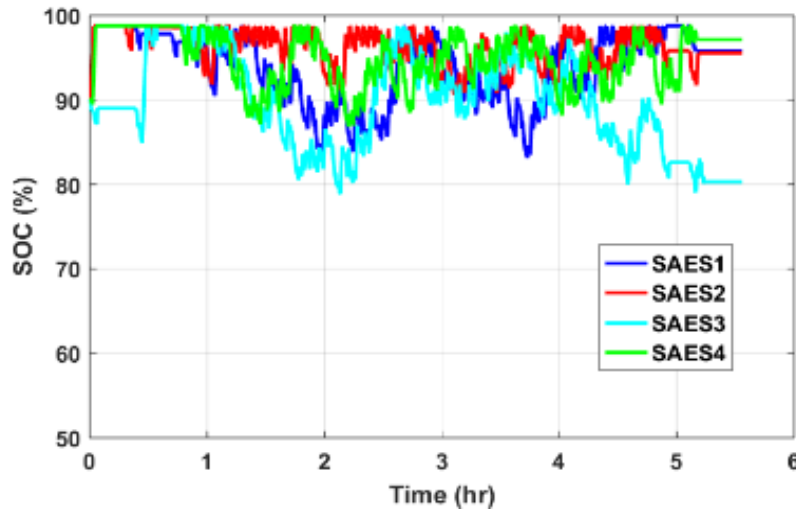


Figure 2-77. Optimal driving performance.

Case Study 5: Fixed-Route, Low-Speed, Automated Electric Shuttle at University of Michigan in Ann Arbor, Michigan

Key Findings

- For low-speed (i.e., 10–15 mph) SAEV operations (at university campuses, airport, research facility), considering present-day cost and vehicle capabilities, charge-sustaining operation is realized by implementing 50-kW quasi-dynamic wireless chargers at the two stops with one segment (5-meter) per position, and a 29 kWh onboard battery.
- The minimum-cost solution involves only one 100-kW quasi-dynamic wireless charger at one stop with one segment per position and a 28 kWh onboard battery. This allows the vehicles to realize charge-sustaining operation.
- Considering future-day cost and vehicle capabilities, charge-sustaining operation was realized using either one 40 kW charger at one stop with a 29-kWh battery or one 50-kW charger at one stop with a 14-kWh battery.

- In addition, the results showed that quasi-dynamic wireless solutions are cost competitive with the DCFC technology.

Introduction

Real-world GPS and energy consumption data were collected from two NAVYA Arma SAEV operating at the University of Michigan. These shuttles operate as a circulator in a fixed route, shown in Figure 2-78. The route has two regular designated stops: North and South, where they pick up and drop off passengers. Both shuttles park overnight at a garage area where L2 conductive chargers are installed for overnight charging. These vehicles run at very low speed (10 mph maximum). A powertrain and energy estimation model for these shuttles has been developed. The model parameters are tuned to correlate with the measured energy consumption (kWh/mile) data. The accessory power demand for the onboard sensing and computing systems (auxiliary loads) is analyzed for both vehicles, as indicated in Figure 2-79 and Figure 2-80, and Table 2-21.

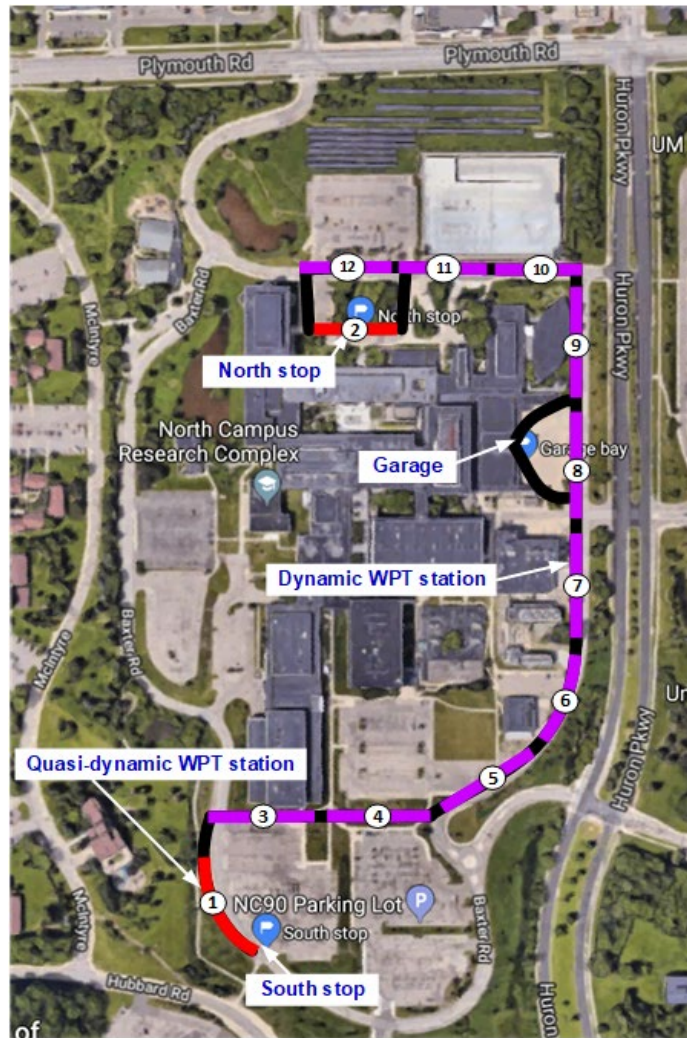


Figure 2-78. NAVYA Arma SAEV route at University of Michigan, Ann Arbor, Michigan.

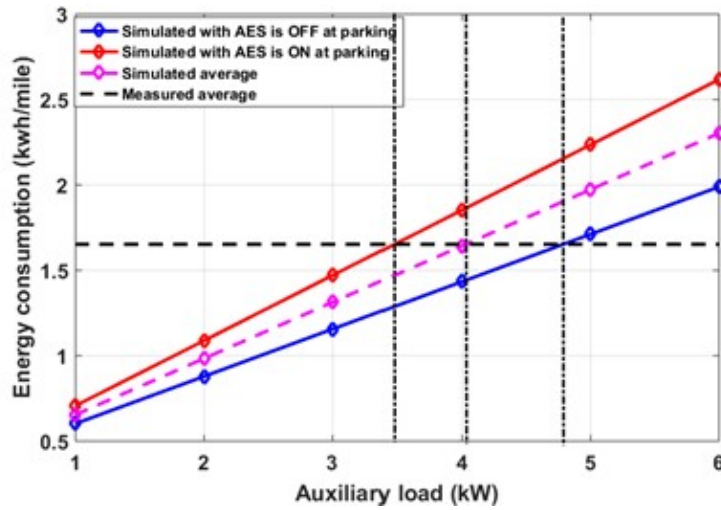


Figure 2-79. DC kWh/mile versus aux. load for ARMA 1.

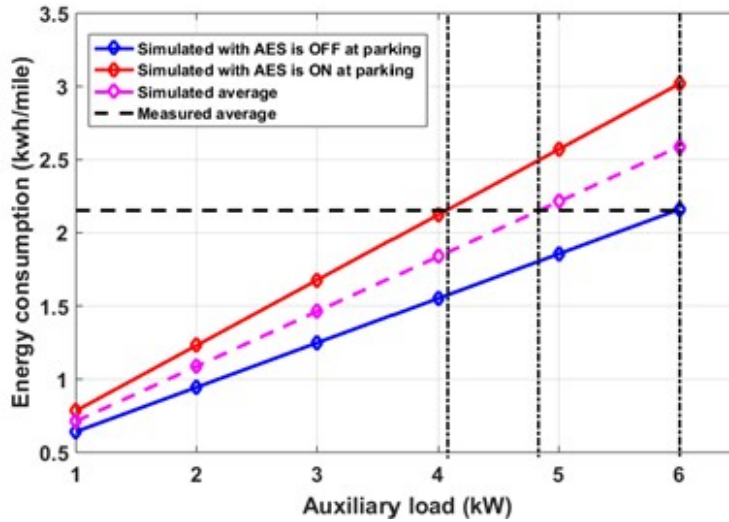


Figure 2-80. DC kWh/mile versus aux. load for ARMA2.

Table 2-21. Auxiliary load results for Arma1 and 2 considering different charger efficiency and vehicle status. Min was estimated assuming the vehicle was ON at parking. Max was estimated assuming the vehicle was OFF at parking.

Charger efficiency	AES Arma1			AES Arma2		
	Min	Max	Ave.	Min	Max	Ave.
85%	3.236	4.458	3.75	3.797	5.582	4.52
90%	3.476	4.788	4	4.065	5.975	4.838
95%	3.716	5.119	4.307	4.333	6.33	5.157

Discussion of results

The results show that present-day auxiliary loads range from 3.2–6.3 kW. Arma1 averages 4 kW, and Arma2 averages 4.84 kW. Considering the average auxiliary load values, the current operation of the two SAEVs is analyzed in Figure 2-81. The results show that a full charge cycle allows the vehicle to run for about 5–7 hours continuously. The collected real-world drive cycle data, vehicle model, and wireless charger model are integrated with the WPTSim tool for investigating and optimizing wireless charging infrastructure for realizing charge-sustaining operation.

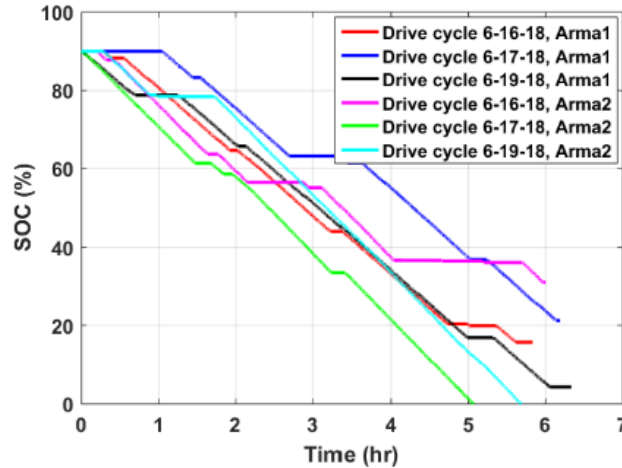


Figure 2-81. Current driving performance of Arma 1 and Arma 2.

Planning optimization analysis for the different charging technologies considered two operating scenarios: present- and future-day. For both scenarios, low-speed driving data were considered because of the needs of the university campus, both now and in the future. The main differences between the two analyses are the vehicle model, represented by the auxiliary load estimation, the system unit- and installation-cost assumptions, and the expected driving range. These differences are indicated in Table 2-22. Considering both operating scenarios (present and future), four different charging technologies are explored:

1. Small onboard battery with in-route quasi-dynamic charger at designated stops.
2. Small on-board battery with in-route dynamic and quasi-dynamic charger.
3. Large onboard battery with DCFC.
4. Large onboard battery with L2 charger.

Table 2-22. Parameters for present and future-day.

Coefficient	Future-day	Present-day
Driving range for overnight	12 h	6 h
Auxiliary loads (kW)	1.4 and 1.7	4 and 4.38
Road retrofitting cost coefficient (M\$/mile/lane)	1	1.2
Road PE, capacitors, and materials cost coefficient (M\$/mile/kW/lane)	0.0273	0.033
Grid connectivity cost coefficient (M\$/mile/kW/lane)	0.015	0.018
Primary side installation cost coefficient (M\$/position)	0.005	0.005
Vehicle assembly cost coefficient (\$/kW)	29	66.67
Battery cost coefficient (\$/kWh) @ 1C and 80% ΔSOC	80	103
DCFC unit cost (\$/kW)	300	600
DCFC installation cost (\$/kW/port)	400	400
L2 unit cost (\$/kW)	125	250
L2 installation cost (\$/port)	2,500	2,500
L2 Onboard charger (\$/kW)	50	100

A planning optimization problem was solved for an SAEV supported with in-route wireless charging using a nonlinear mixed-integer solver based on a genetic algorithm (GA). Several optimization problems were analyzed for in-route wireless charging, considering different charging positions: quasi-dynamic at stops (red segments in Figure 2-78) and dynamic (purple segments in Figure 2-78).

Planning for quasi-dynamic wireless power transfer (QDWPT) charging with optimizing on-board battery (QDWPT1): In this case, wireless chargers are allocated at designated stops only. Therefore, only three options for the allocation are considered: at north stop, at south stop or at both. A fixed one segment (5-meter) of primary coil is assumed at each position. Three variables are optimized: NWPT, PC, and Qb.

Planning for QDWPT charging considering current SAEV (QDWPT2): in this case, the current installed on-battery is kept fixed (30-kWh) and only two variables are optimized: NWPT and PC.

Planning for DWPT charging: in this case, both quasi-dynamic and dynamic positions for wireless charger are considered and four variables are optimized: NWPT, NS, PC and Qb. The ranges for these variables considered at each optimization are indicated in Table 2-23.

Table 2-23. Search variables for different optimizations

Variable	QDWPT1 (3 variables)	QDWPT2 (2 variables)	DWPT (4 variables)
x1=NWPT	{1, 2, 3}	{1, 2, 3}	[1-4095 (212-1)]
x2=PC	{10, 20, ..., 100} kW	{10, 20, ..., 100} kW	{10, 20, ..., 100} kW
x3=NS	1 segment	1 segment	[1-10] segment
x4=Qb	{1, 2, ..., 100} kWh	30-kWh	{1, 2, ..., 100} kWh

DWPT and QDWPT scenarios were optimized considering both present- and future-day operation. The results show that for the present-day scenario, charge-sustaining operation was realized by implementing 50-kW quasi-dynamic wireless chargers at the designated stops (north and south) with 1 segment (5-meter) per position, and a 29-kWh on-board battery. Another optimal solution shows that only one 100-kW quasi-dynamic wireless charger at the north stop with 1 segment per position and a 28-kWh on-board battery allows the vehicles to realize charge sustaining operation. This is the minimum cost solution as indicated in Table 2-24 (QDWPT1, Sol 2). This solution is valid even if the current vehicles with 33-kWh battery are considered, as indicated in Table 2-24 (QDWPT2, Sol 1). Solving for DWPT with consideration of the purple segments in Figure 2-78 shows the same solutions as the quasi-dynamic, which makes perfect sense for

minimizing system cost. For the future-day scenario, charge-sustaining operation was realized either using one 40-kW charger at the north stop with a 29-kWh battery or one 50-kW charger at the north stop with a 14-kWh battery. This is because lower vehicle energy consumption is expected in the future-day scenario.

Table 2-24. Planning optimization results for different charging technologies, considering different operating scenarios (present- and future-day).

	Present-day scenario (6 h range, current cost and vehicle consumption)						Future-day scenario (12 h range, expected future cost and vehicle consumption)					
Technology	QDWPT1		QDWPT2	DWPT	DCFC (15 min.)	Level 2 (8 h)	QDWPT1		DWPT	DCFC (15 min.)	Level 2 (8 h)	
Solution	Sol. 1	Sol. 2	Sol. 1	Sol. 1	-	-	Sol. 1	Sol. 2	Sol. 1	-	-	
# of chargers	2	1	1	1	1	2	1	1	1	1	2	
Charger position	south and north stop	north stop	north stop	north stop	garage	garage	north stop	north stop	north stop	garage	garage	
Power level (P_c)	50-kW	100-kW	100-kW	100-kW	132 kW	4.1 kW	40-kW	50-kW	40-kW	109 kW	3.4 kW	
# segments (N_s)	1 segment	1 segment	1 segment	1 segment	-	-	1 segment	1 segment	1 segment	-	-	
Battery size (Q_b)	29 kWh	28 kWh	33 kWh	28 kWh	36.7 kWh	36.7 kWh	29 kWh	14 kWh	29 kWh	30.2 kWh	30.2 kWh	
Charging rate (C-rate)	1.55	3.2	2.73	3.2	3.24	0.1	1.24	3.2	1.24	3.24	0.1	
Energy consumption	1.6471	1.6467	1.649	1.6467	1.911	1.91	0.7918	0.785	0.7918	0.7865	0.7865	
Vehicle comp. cost	\$13.1k	\$21k	\$22k	\$21k	\$13.3k	\$9.1k	\$7.2k	\$5.9k	\$7.2k	\$9.2k	\$5.5k	
Road comp. cost	\$33.3k	\$24.6k	\$24.6k	\$24.6k	\$132.1k	\$7.1k	\$13.3k	\$17.7k	\$13.3k	\$76.1k	\$5.8k	
Total comp. cost	\$46.4k	\$45.6k	\$46.6k	\$45.6k	\$145.4k	\$16.1k	\$20.5k	\$20.6k	\$20.5k	\$85.3k	\$11.4k	

One optimum solution for each scenario was inserted into WPTSim to explore the performance of SAEVs with QDWPT, as indicated in Figure 2-82. The figures show the charge-sustaining operation with zero downtime in both present-day (6 h operation) and future-day (12 h operation).

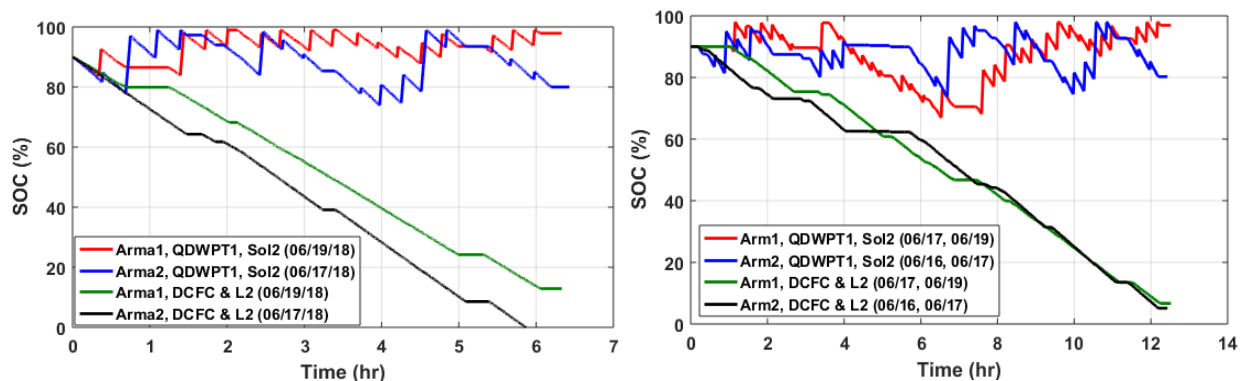


Figure 2-82. SAEV's performance, considering different charging technology designs for present- (left) and future-day (right) operations.

The outcomes from wireless charging optimization are compared with stationary DCFC and L2 technologies, as indicated in Table 2-25. QDWPT solutions are cost effective compared with DCFC (15-min charging time). Even though L2 chargers with 8-hour charging time show the least cost, these chargers are not appropriate for automated vehicles as they are not automatic, present a high risk of service interruption, and provide limited (i.e., 6–12 hour) range. In addition, this solution involves a large onboard battery for a given driving range, which leads to large vehicle weight and high energy consumption and operation cost. A performance comparison among the three technologies is summarized in Table 2-25.

Table 2-25. Performance comparison among QDWPT, DCFC, and L2 charging technology.

Performance index	QDWPT	DCFC	L2
Range	Infinite	Limited (6-12 h)	Limited (6-12 h)
Recharge time	Zero	15 min.	8 h
Vehicle comp. cost	High	Medium	Low
Road comp. cost	Medium	Very high	Low
Total comp. cost	Medium	High	Low
Service interruption risk	Low	Medium	High
Land requirement	Low	High	
Energy consumption	Low	High	
Automatic	Yes	No	
User discomfort	Low	High (plug-in)	
Hazards	EMF	Mechanical connection, arcing, exposed conductor, etc.	
Visual pollution	Low	High	

Conclusion

The feasibility study of in-route wireless charging technology for fixed-route shared automated mobility shows the effectiveness of the developed system design and optimization tool (WPTSim) for optimizing the system key design parameters. The main conclusion of this study can be summarized as follows:

- Implementing in-route wireless charging technology for SAEV shows good alignment for realizing a fully automated mobility (vehicle and charger) system.
- Installing quasi-dynamic (opportunistic) wireless chargers at designated SAEV stops with high power capability (~50 or 100 kW), and minimum track length enables the vehicle to realize charge-sustaining operation (infinite driving range and zero downtime) and makes the system cost competitive compared to DCFC technology.
- In-route wireless charging shows a 36–57% reduction in the onboard battery capacity.

2.4 National Impact of Charging Infrastructure for Electric Ride-hailing Vehicles

2.4.1 Key Findings

- National energy consumption would be reduced by up to 38% in 2030 from 2017 levels. Twenty-five percent of the reduction is from increased electrification due to non-infrastructure factors, 2–3% is due to increased infrastructure support, and 10–11% is due to ride-hailing and fast fleet turnover.
- Gasoline consumption would be reduced by up to 51% in 2030, relative to 2017, of which 33% is from increased electrification due to non-infrastructure factors, 4–6% is due to increased infrastructure support, and 12–14% is due to fast fleet turnover.
- A top-down model identified the charging infrastructure coverage needed as a function of the number of ride-hailing battery EVs and ride-hailing demand. Validated by available regional simulation results from other AFI tasks, this approach enables robust estimation of charging coverage needed to support electrified ride-hailing vehicles with different EV ranges and charging levels.
- Sensitivity analysis shows that improved charging infrastructure, faster fleet turnover rate due to ride-hailing, and high BEV market penetration can significantly reduce national energy consumption of LDVs. However, deadheading may compromise the benefits of ride-hailing vehicles when transitioning from a low ride-hailing-demand market to a high ride-hailing-demand market.
- Because of deadheading trips, petroleum consumption reductions will begin when BEV market penetration (i.e., sales) is higher than 40% and ride-hailing demand is higher than 35% in urban areas in 2030 with optimized charging infrastructure support. Electricity consumption, in consequence, has an opposite trend.

2.4.2 Introduction

The tradeoff studies described previously in this report have shown that electrification of shared mobility has the potential to produce benefits for vehicle owners and fleet operators that justify the cost of charging infrastructure. It is also important to assess the benefits of electrification more broadly. The AFI Pillar used sophisticated modeling tools to estimate the influence of charging infrastructure designed to serve light-duty electric shared mobility on overall LDV electrification. The AFI Pillar then modeled the energy consumption and emissions of the nationwide LDV fleet for various future scenarios to determine the societal benefit of electrification and the charging infrastructure necessary to enable it.

2.4.3 Research Approach

Introduction of Model Framework

It is critical to understand the national energy impact of electrified ride-hailing vehicles with different levels of charging infrastructure support. Charging infrastructure plays an essential role in supporting ride-hailing BEVs, stimulating BEV penetration in the personal-use vehicle fleet. It influences overall fleet fuel efficiency and national energy consumption of LDVs. However, ride-hailing, as an emerging and disruptive mobility type, also affects personal vehicle adoption, induces more travel, reduces vehicle lifetime due to much higher annual mileage, all of which eventually result in changes in energy consumption.

However, the methodology of aggregating impact of electrified ride-hailing vehicles from the regional to the national level is not established in the literature. Regional simulations give the number of chargers by location and charger type for a given ride-hailing BEV fleet size. First, a bottom-up methodology was developed to extrapolate regional simulation results to the national level by quantifying the impacts of ride-hailing and

charging infrastructure on personal BEV adoption, overall vehicle-miles traveled, and vehicle survival. To overcome the limitations in availability of regional simulation results, a top-down approach was developed to mathematically identify charging coverage needed for different ride-hailing BEV fleet sizes. Sensitivity analysis was conducted to examine a range of key inputs and assumptions such as ride-hailing demand and fleet turnover rates, etc.

Energy consumption and emissions of the national LDV fleet are functions of the amount of VMT, vehicle efficiency miles-per-gallon-gasoline equivalent (MPGGE), vehicle market shares (sales), and vehicle survival rates by segment and powertrain technologies. This study separates LDVs into three segments: urban ride-hailing, urban personal vehicles, and non-urban personal vehicles. Vehicle market share and survival rates together determine fleet composition. The following sections explain the assumptions and methodologies used in estimating fleet VMT and fleet composition in more detail.

National Fleet Vehicle Miles Traveled from 2017 to 2030

National fleet VMTs of personal vehicles and ride-hailing vehicles' service VMTs (excluding deadheading) are assumed to follow Energy Information Administration (EIA) Annual Energy Outlook (AEO) projections.¹²⁴ This study focuses on urban areas because ride-hailing vehicles are mainly located and operate in urban areas in the short to middle term.¹²⁵ According to the United States Census, urban is defined as any area with a population of more than 50,000.¹²⁶ Using National Household Travel Survey (NHTS) results¹²⁷, highway statistics¹²⁸, and census data,¹²⁹ urban areas were estimated to cover 72% of the total population and 65% of total LDV stock.

Ride-hailing VMT consists of (1) VMT with passengers, (2) VMT without passengers (deadheading or empty miles), and (3) VMT while out of service.

1. VMT with passengers is defined by ride-hailing demand, which is the percentage of total VMT in urban areas that needs to be served by ride-hailing vehicles.
2. Ride-hailing would affect total VMT due to induced travel (not considered in this study) and deadheading (considered in the sensitivity analysis). When ride-hailing demand and the number of ride-hailing vehicles are low, at the 2017 level (e.g., national average, 0.29% of total vehicle-miles traveled), deadheading miles account for 49% of total travel distance for ride-hailing vehicles, according to RideAustin.¹³⁰ In the modeling of national energy and emissions as a function of ride-hailing demand, deadheading miles were assumed to drop significantly when ride-hailing demand and the number of ride-hailing vehicles are both high (e.g., 100% of total PMT). Literature on this issue is still very limited. The relationship between ride-hailing demand and deadheading miles, which is affected by driver behavior, urban layout, and traffic conditions, is not well established in the literature. Therefore, for the purpose of showcasing the spectrum of the potential national energy impact from ride hailing, when ride-hailing demand grows from 0.29 to 100%, it was assumed that deadheading miles as a percentage of total travel drop linearly from 49 to 5%.
3. VMT while out of service refers to personal-use miles that were not considered in this study because only full-time ride-hailing drivers were modeled.

Composition of the Fleet

Fleet composition depends on vehicle market (sales) penetration by powertrain technologies and vehicle survival rates. The ride-hailing and personal-use vehicle fleets were estimated separately from 2017 to 2030 because they have different survival rates and market composition. BEV share, or the percentage of ride-hailing BEVs in the ride-hailing fleet, is an input. It is estimated based on given ride-hailing demand and average VMT per ride-hailing vehicle. With the estimated number of ride-hailing BEVs, regional simulation provides future charging coverage, optimized to support their travel. The model quantifies charging opportunities for any given charging coverage and projects the resulting market penetration of personal EVs due to increased charging opportunities and other factors. Market penetration of vehicle powertrain technologies other than BEV and PHEV was assumed to follow the EIA AEO projection.¹³¹

Vehicle survival rate is the percentage of vehicles remaining on the road by vehicle age. Fast vehicle turnover or a shorter survival rate would lead to more and newer vehicles on the road and result in a higher fleet average fuel efficiency. For example, a full-time ride-hailing vehicle travels 29,000 miles per year on average, which is

twice as many as an average personal vehicle.^{132, 133} The average personal vehicle life is about 14 years.^{134, 135} Assuming the ride-hailing vehicle has similar lifetime VMT as a personal vehicle (about 200,000 miles), a full-time ride-hailing vehicle is assumed to have an average life of 7 years. Figure 2-83 shows the corresponding survival functions and vehicle-miles traveled for personal and ride-hailing vehicles. Personal vehicle survival function is from the EIA NEMS model.¹³⁶ The survival function of ride-hailing vehicles was estimated using the assumptions of lifetime VMT, annual VMT, and average vehicle age mentioned above. These estimates are factored into the VISION model¹³⁷ to estimate fleet composition.

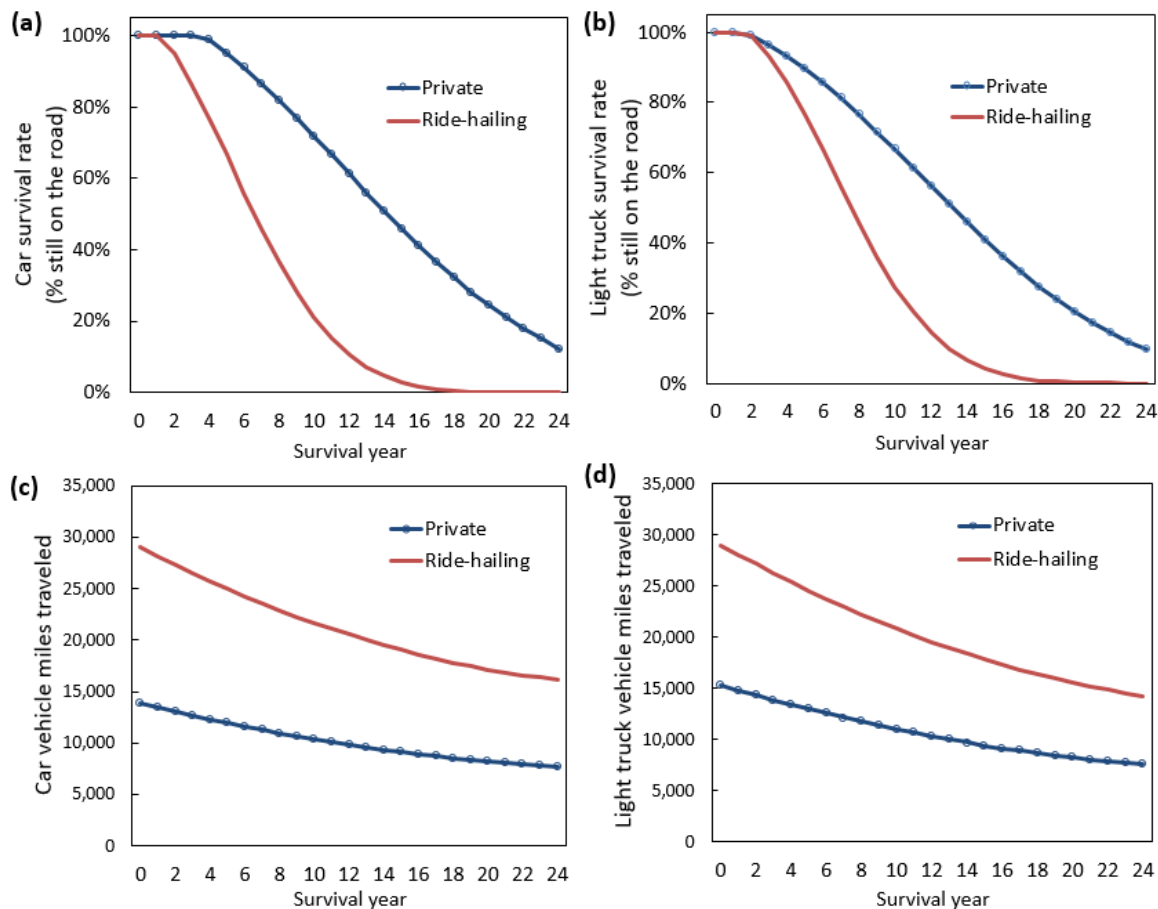


Figure 2-83. Survival functions and vehicle-miles traveled for car and light trucks: (a) car survival rate, (b) light truck survival rate, (c) car vehicle-miles traveled, and (d) light truck vehicle-miles traveled.

National Energy Consumption and Emissions

This section explains the methodology of estimating the nation’s energy consumption and emission using Argonne’s VISION model in detail. The VISION model¹³⁸ is a scenario tool that estimates the energy and emission impacts of advanced fuel and vehicle technologies in the transportation sector by fuel type, vehicle powertrain type, and vehicle class.

Methodology

Recent studies have investigated regional impacts of ride-hailing vehicles and identified contributing factors such as VMT and deadheading miles.^{139, 140, 141} Approaches were needed to aggregate regional simulation and modeling results, which were limited to certain regions, to the national level, as has been done for other emerging technologies. For example, a previous study developed a framework to account for vehicle-level energy impacts, projected adoption levels, and changes in VMT simulated from the Chicagoland Area to estimate national fuel consumption of connected and automated vehicles.¹⁴² As mentioned earlier, two approaches, bottom-up and top-down, were employed here. Both approaches rely on the relationship between

charging coverage and charging opportunities to project induced personal EV market penetration. Bottom-up approaches were mainly used for case studies of Austin and Columbus, and the top-down approach was used for evaluating a broad spectrum of ride-hailing demand and EV penetration in ride-hailing fleets in the sensitivity analysis. The following subsection explains the approaches in detail.

Data sources

The study used travel survey data and GPS travel data for seven cities to understand the charging opportunities for ride-hailing and personal vehicles for a given charging coverage. These data are from the Transportation Secure Data Center¹⁴³, RideAustin¹⁴⁴, and New York City taxi data¹⁴⁵ websites. NHTS data¹⁴⁶ were also used to develop distributions of the number of trips in a given urban area by population density group. The AFI Pillar used RideAustin data to estimate the average daily and annual mileage of ride-hailing vehicles. Other databases, such as Census data¹⁴⁷ and highway statistics,¹⁴⁸ were queried to understand the proportion of trips and vehicles in urban areas. Finally, the AFI Pillar used projections of the total LDV sales and total VMT made in the EIA AEO reference case.¹⁴⁹

Charging opportunity

A methodology initially developed by Oak Ridge National Laboratory (ORNL) was adopted to generalize the relationship between charging coverage (from regional simulations) and charging opportunities.¹⁵⁰ The purpose is to quantify the increase in charging opportunity for personal BEVs when the charging infrastructure coverage is optimized to support ride-hailing vehicles. For a given city or region, the study area was divided into 0.25×0.25 -mile grid cells. Charging coverage, also known as charging availability, is defined as the percentage of land area or grid cells that are covered by at least one charger. In other words, charging coverage represents the density or number of chargers and their spatial distribution in a given region. Charging opportunity is defined as the percentage of trips that end in the cells that have at least one charger, when ranking the cells by their popularity as trip destinations, from the most popular to the least popular. In other words, charging opportunity is the probability that a vehicle could be charged within a certain distance (.25 miles, in this case) of the trip destination. Building upon ORNL's earlier research findings from three cities, two generalized charging opportunity curves were further developed as a function of charger coverage for both ride-hailing and personal vehicle travel, using household travel survey data and GPS travel data from seven major cities, shown in Figure 2-84. These cities include Austin, Texas; Atlanta, Georgia; Columbus, Ohio; Chicago, Illinois; Los Angeles, California; Seattle, Washington; and New York City, New York. For a given charging coverage, personal travel data (i.e., Seattle, Atlanta, Los Angeles, Chicago, and Columbus) gives much lower charging opportunity than ride-hailing/taxi travel data, because ride-hailing trips are more likely to end at a central business district. The personal vehicle charging opportunity curves from different cities are close to each other. Because the changes are quantified in the charging opportunity to estimate personal EV adoption, and to be conservative, the curve derived using Chicago household travel data was chosen to quantify future charging opportunity of personal vehicle travel for any given charging coverage.

Bottom-up approach

With a given number of BEVs and travel demand, the EVI-Pro model¹⁵¹ estimated the number of chargers and charging level (e.g., Level 2, DCFC, 150 kW) by location for a given year in the chosen study area. In EVI-Pro, future charging stations are optimized to serve ride-hailing charging demand based on their travel patterns and pre-assumed electric range. Using Austin as a case study, EVI-Pro simulated the charging infrastructure requirements in 2030, which was converted to charging coverage in 2030. By dividing the 2030 coverage by 2017 coverage (i.e., the starting condition), the growth rate in charging coverage needed for Austin was estimated to support the given electrified ride-hailing fleet size and associated charging demand in 2030. The growth rate needed in charging coverage for each state was estimated, considering urban areas only, to support the same level of electrified ride-hailing fleet size and charging demand. The growth rates were weighted by state, considering their current ride-hailing demand and charging coverage in urban areas.

Following the charging opportunity curves developed earlier, charging opportunities were quantified for personal vehicle by state with the estimated charging coverage in 2030. Then, ORNL's MA3T model was used to project the personal EV market penetration by state from 2017 to 2030 with the estimated charging

opportunity and simulated average charging level.¹⁵² Other factors affecting EV market penetration are considered in the MA3T model. Details about EVI-Pro and the MA3T model can be found in Appendix D.

Finally, ANL’s VISION model uses the projected market penetration, estimated fleet VMT, and fleet composition to quantify the reduction in petroleum use and increase in electricity use due to electrified ride-hailing vehicles.¹⁵³ Figure 2-84 summarizes the overall bottom-up approach.

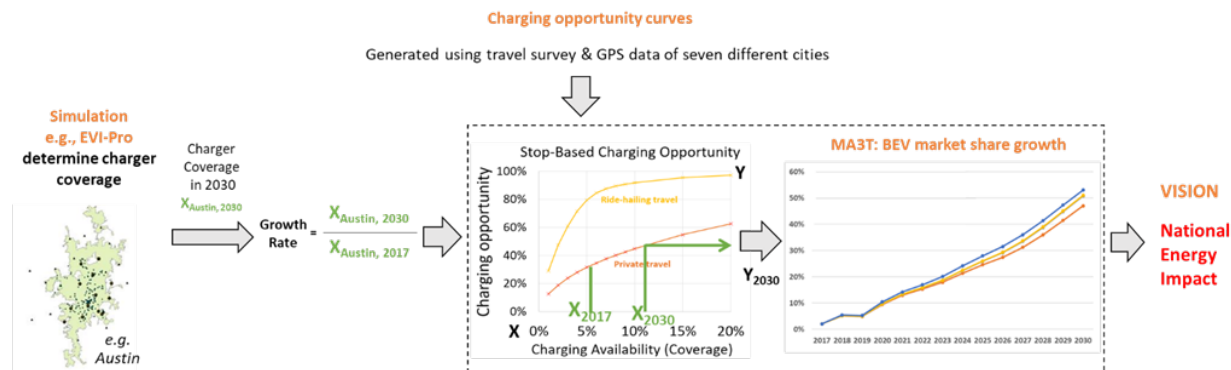


Figure 2-84. Analytical framework of national energy impacts of ride-hailing and personal EVs.

Top-down Approach

The methodology for bottom-up simulation approach is highly region-specific and dependent on the unique travel patterns of a given region. It is also subject to availability of trip data with origin and destination information. Therefore, a top-down approach, based on probability of charging, was also developed to mathematically identify the number of chargers needed with a given ride-hailing BEV fleet size and charging demand using data such as NHTS. In this approach, the number of daily stops in urban areas was first determined and categorized by population density groups. Then, the charging probability was determined at each population density group based on distribution of battery SOC and average trip distance. A M/M/c model¹⁵⁴ was used (where the first M = the arrival process as Poisson, the second M = service times as an exponent, and c = the number of servers), a multi-server queuing model where arrivals form a single queue and are governed by a Poisson process. Service times are exponentially distributed to estimate the required number of chargers for each 0.25 × 0.25 mile grid cell. Finally, the charging coverage was quantified as a function of percentage of total passenger vehicle trips served by ride-hailing BEVs and critical battery SOC. Critical battery SOC means that a vehicle needs to be recharged at this level; this can vary by driver, vehicle model, charger level, and mobility type.

After estimating the charging coverage, the charging opportunity curve was used to estimate charging opportunities and then project the personal BEV market penetration. Finally, national energy use and carbon emissions were quantified as a function of ride-hailing demand and the share of BEVs in ride-hailing fleets.

Assumptions and Definitions. In this study, all BEVs were assumed to have a rated electric range of 250 miles. The charging powers considered are 50 kW or 150 kW, depending on the scenario. One hundred percent of drivers were assumed to have access to home charging. This study does not consider induced travel due to improved convenience. The number of ride-hailing vehicles for a given region was estimated by dividing the total ride-hailing miles by the average annual mileage of a full-time ride-hailing vehicle.

Bottom-up Approach (Deterministic Approach): Determining the Number of Chargers Needed Based on Regional Travel Patterns

A bottom-up approach determines the charging infrastructure requirements for a given region based on travel demand and a given number of BEVs. Using Austin as an example, Figure 2-85 shows the number of chargers needed with different numbers of ride-hailing BEVs.

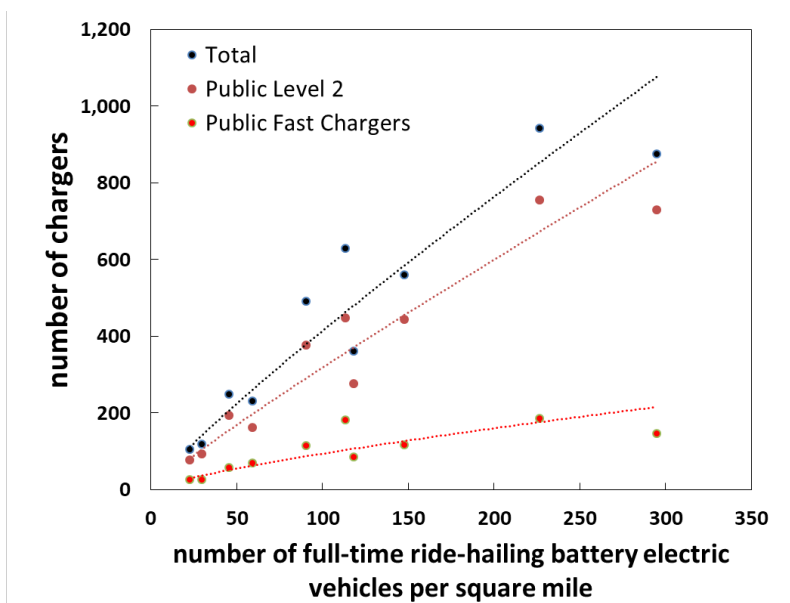


Figure 2-85. Number of chargers with respect to number of full-time ride-hailing battery EVs per square mile, based on simulation of RideAustin data in EVI-Pro.

Top-down Approach (Probabilistic Approach): Estimating the Number of Chargers Needed in Different Regions Using National Travel Survey Data

The top-down approach mathematically identifies the required number of chargers and charger coverage with a given ride-hailing BEV fleet size by quantifying charging probabilities using national travel survey data.

This approach first determined the number of daily stops in urban areas. Again, urban areas were divided into different segments based on the population density. The same density groups were used as defined in NHTS 2019. Using Chicago as an example, Figure 2-86 shows the number of grid cells N_i (0.25×0.25 mile per cell) and the percentage of total vehicle trips ending in each population density segment i using NHTS.

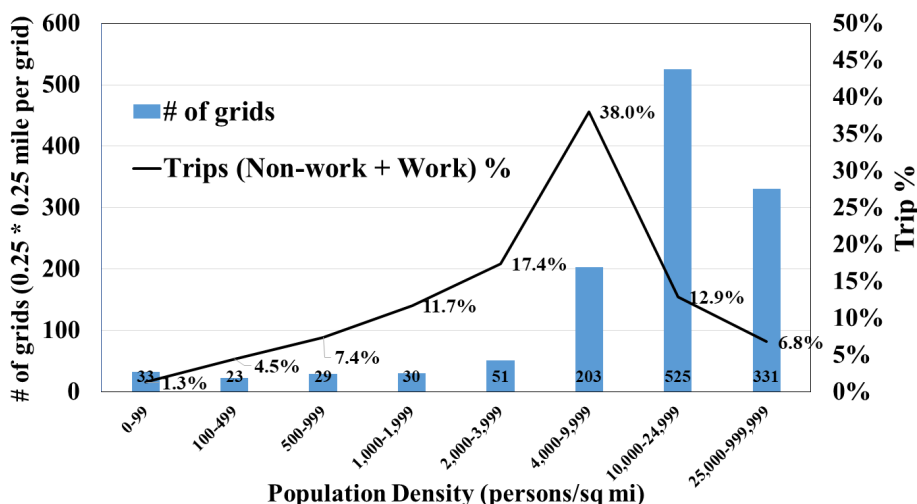


Figure 2-86. Number of grid cells and percentages of total trips ending in Chicago population-density groups.

Then the number of trip stops F_i^{Stop} were estimated for each population density segment i assuming different percentages of trips served by ride-hailing BEVs, shown in Table 2-26.

Table 2-26. Daily trip stops by ride-hailing BEV penetration levels.

Population Density (persons/sq mi)	Ride-hailing BEV penetration levels (% of trips served by ride-hailing BEVs)						
	1%	5%	10%	25%	50%	75%	100%
0-99	9.8	48.8	97.6	244.1	488.2	732.3	976.3
100-499	48.5	242.5	484.9	1212.3	2424.5	3636.8	4849.0
500-999	63.2	316.2	632.4	1581.0	3162.1	4743.1	6324.2
1,000-1,999	96.7	483.3	966.6	2416.4	4832.9	7249.3	9665.7
2,000-3,999	84.6	422.8	845.6	2113.9	4227.8	6341.8	8455.7
4,000-9,999	46.4	232.0	463.9	1159.8	2319.7	3479.5	4639.3
10,000-24,999	6.1	30.4	60.9	152.2	304.5	456.7	609.0
25,000-999,999	5.1	25.5	50.9	127.3	254.6	381.9	509.2

Finally, the required number of chargers was estimated at each segment and resulting charging coverage based on the charging probability at a trip destination. Figure 2-87 shows the charging coverage at different critical SOC r^L as a function of percentage of trips served by ride-hailing BEVs. The critical SOC of 30% was chosen for this analysis because it relatively matches the results from the bottom-up approach.

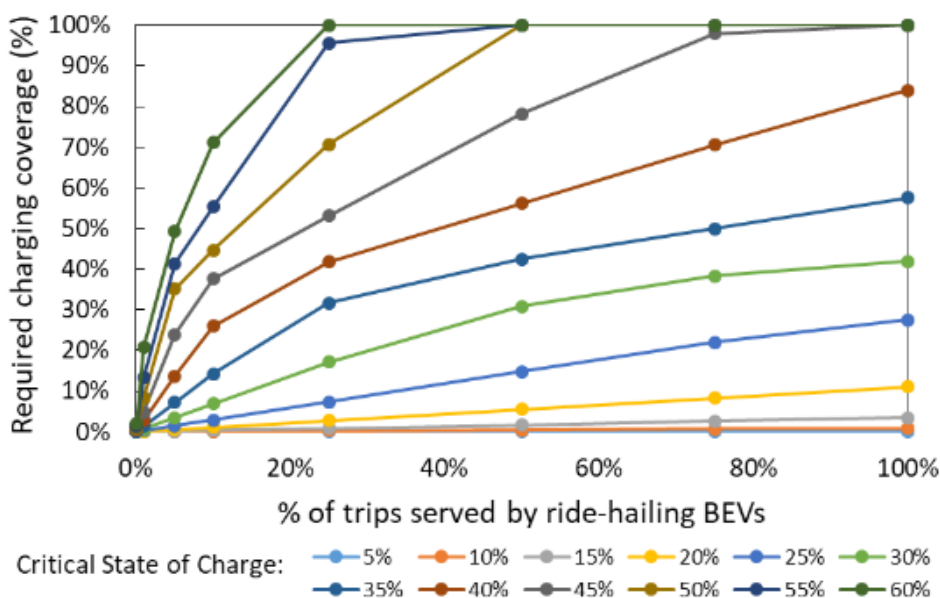


Figure 2-87. Probabilistic approach to estimate required charging coverage, based on percentage of trips served by ride-hailing BEVs.

2.4.4 Quantifying Energy Consumption of National Light-duty Passenger Vehicle Fleet

Two cases—low ride-hailing demand and high ride-hailing demand—were developed to show the upper- and lower-bound effects of ride-hailing and charging infrastructure on national energy consumption. Table 2-27 summarizes the assumptions, simulated charging coverage, and resulting personal BEV market penetration of these two cases. Details about each scenario are discussed in following sections.

Table 2-27. Definition of low ride-hailing demand case and high ride-hailing demand case.

	Scenario names	Result year	Ride-hailing demand	% BEV of ride-hailing vehicle sales	% BEV of personal vehicle sales	Average lifetime of ride-hailing vehicles (years)	Average lifetime of personal vehicles (years)	Average lifetime of both ride-hailing and personal vehicles (years)	Infrastructure coverage	Average charge power (kW)
Low ride-hailing demand case (based on Austin)	-RH/ -Infrastructure	2030	0.29%	32.4%	32.4%	7	14	14	11.07%	7.9
	Base RH/ Base EV + Infrastructure	2030	0.29%	47%	47%	7	14	14	11.15%	9.7
	Low RH/ Base EV + Infrastructure	2030	1.4%	51%	51%	7	14	14	11.46%	16.2
	Base RH/ 100% EV + Infrastructure	2030	0.29%	100%	51%	7	14	14	11.50%	17.1
	Low RH/ 100% EV + Infrastructure	2030	1.4%	100%	53%	7	14	14	13.09%	43.6
High ride-hailing demand case (based on Columbus)	2017	2017	0.29%	1%	1%	7	14	14	5.3%	11.4
	- Ride-hailing - Infrastructure	2030	0.29%	32.4%	32.4%	7	14	14	5.3%	11.4
	+ Ride-hailing - Infrastructure	2030	100%	32.4%	32.4%	7	14	7 (faster turnover)	5.3%	11.4
	- Ride-hailing + Infrastructure	2030	0.29%	50%	50%	7	14	14	15.2%	150
	+ Ride-hailing + Infrastructure	2030	100%	50%	50%	7	14	7 (faster turnover)	15.2%	150

Note: RH = ride-hailing.

Low Ride-hailing Demand Case

Figure 2-88 shows the results of the low ride-hailing demand case using regional simulation outputs from Austin. Four scenarios were developed to evaluate the impact of vehicle electrification and ride-hailing, respectively: (1) base RH/base EV, (2) low RH/base EV, (3) base RH/100% EV, and (4) low RH/100% EV, where “base EV” means the BEV percentage in the full-time ride-hailing fleet is the same as for personal vehicles in 2030; “100% EV” means 100% BEV in the full-time ride-hailing fleet in 2030; “base ride-hailing” means holding the national average ride-hailing demand constant (ride-hailing miles are 0.29% of total LDV miles in urban areas, according to NHTS); and “low ride-hailing” means that, in 2030, all urban areas will reach the ride-hailing demand of 1.4%, or what urban areas in New York State have in 2017. Even though the ride-hailing demand in New York State is much higher than all other states (urban areas only), it is still a low share of total LDV miles. Therefore, the four scenarios are similar to the scenario where ride-hailing demand is 0.29% and charging infrastructure is kept at the 2017 level until 2030 (defined as -RH/-Infrastructure in Table 2-27). The “low RH/100% EV + Infrastructure” scenario reaches the lowest energy consumption among the four scenarios. The petroleum consumption is 9.28 quad in 2030, which is 1.09 quad less than in the RH/Infrastructure scenario in 2030 and is 6.16 quad less than the 2017 level.

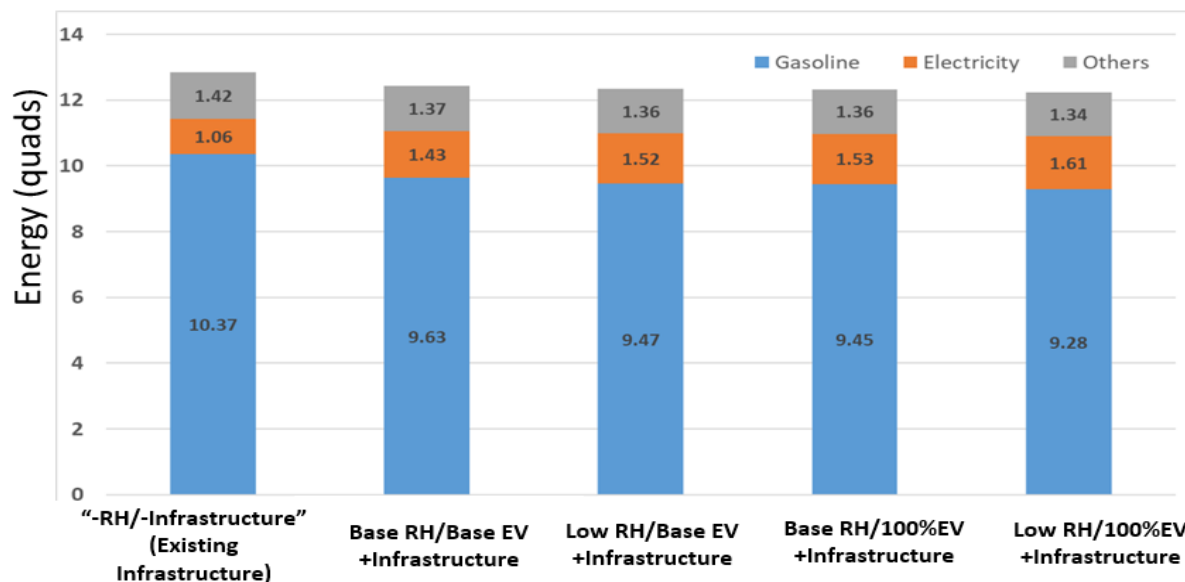


Figure 2-88. National energy impact of electrified ride-hailing light-duty vehicles in 2030 (based on Austin simulation results). RH = ride-hailing, EV = electric vehicles, +Infrastructure = charging infrastructure growth in response to number of ride-hailing EVs.

High Ride-hailing Demand Case

Figure 2-89 shows energy consumption in quads of the high ride-hailing demand (100%) case, using regional simulation results from Columbus, Ohio. In this case, it was assumed all LDVs are ride-hailing vehicles. Four different scenarios were developed to quantify and separate the impact of increased infrastructure support and the impact of faster fleet turn-over rate due to ride-hailing, respectively, as well as other key contributing factors. “-“ means holding 2017 levels unchanged while “+” means improved conditions or increased demand. Analysis of a separate case assuming no change in ride-hailing demand and charging availability until 2030 found that the electrified ride-hailing vehicles could still potentially reduce petroleum consumption of LDVs by 2.79 quads. In this case, petroleum reduction is due to increased PEV adoption and faster vehicle turnover rate. However, the increased PEV adoption is less and is attributed to non-infrastructure related factors such as price drop, technology advancement, etc. The use of public charging infrastructure to support electrified ride-hailing vehicles would reduce petroleum consumption of all LDVs by 7.86 quads in 2030, compared to 2017. A further 18% petroleum reduction (2.79 quads) is due to the impact of both improved charging infrastructure availability and increased ride-hailing: (1) improved charging availability and charging power significantly induce PEV adoption and increases eVMT, which contributes about 0.60–0.92 quads of petroleum reduction and (2) increased ride-hailing demand enables faster vehicle turnover rate, bringing newer and more efficient vehicles on the road, so the fleet average fuel efficiency is improved, which contributes about 1.87–2.19 quads of petroleum reduction.

Overall, national energy consumption is reduced by up to 38% in 2030 relative to 2017, of which 25% is from increased electrification due to non-infrastructure factors, 2–3% is due to increased infrastructure support, and 10–11% is due to fast fleet turnover. Gasoline consumption is reduced by up to 51% in 2030 relative to 2017, of which 33% is from increased electrification due to non-infrastructure factors, 4–6% is due to increased infrastructure support, and 12–14% is due to fast fleet turnover.

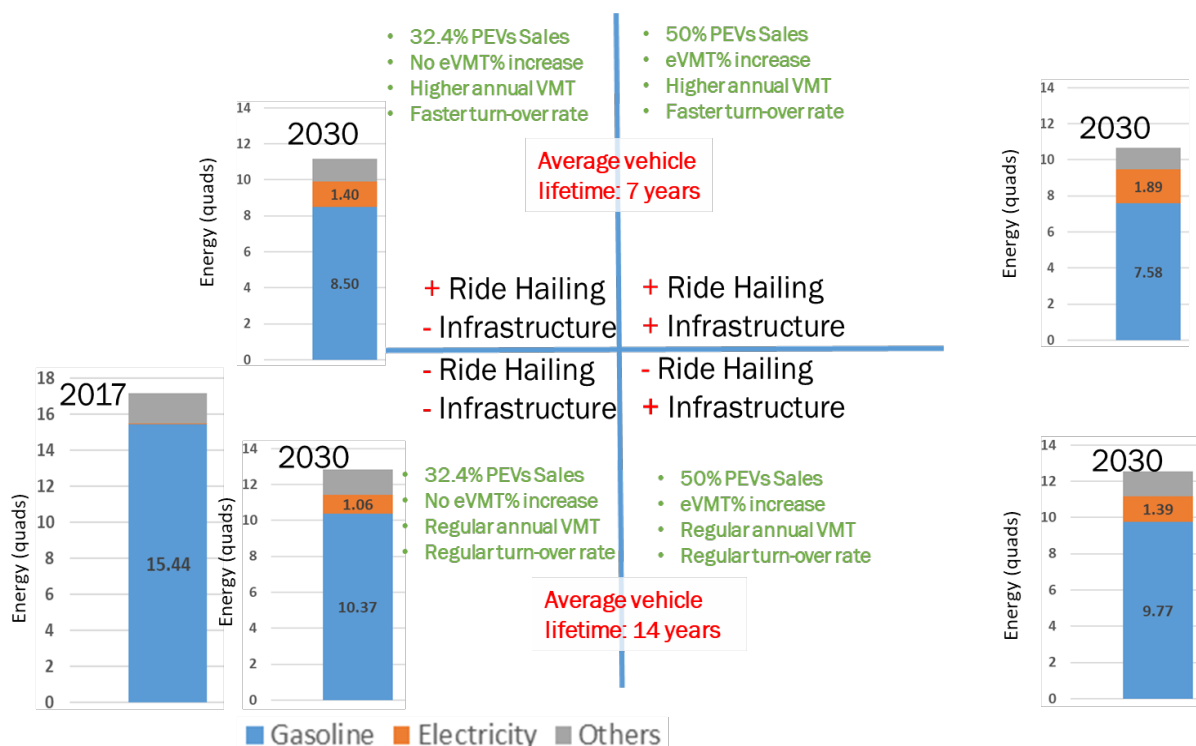


Figure 2-89. National energy impact of electrified ride-hailing light-duty vehicles in 2030, based on Columbus simulation results.

For the low and high cases, the impact of deadheading was neglected because of the following assumptions: (1) at low levels of ride-hailing demand (e.g., 1.4% or less), even though deadheading can be as high as 40–50% of vehicle-miles traveled, the overall impact on total LDV energy consumption is small because the percentage of ride-hailing vehicle is small in the fleet and (2) when ride-hailing demand is high (e.g., all urban travel is fulfilled by ride-hailing), the fleet operation efficiency is assumed to be so high that deadheading is kept to a low level (e.g., 5% or less). However, deadheading was considered in the sensitivity analysis. A lack of data necessitated an assumption in the sensitivity analysis that deadheading decreases linearly from 49 to 5% as ride hailing demand increases from 0.29 to 100%.

Sensitivity Analysis

Sensitivity analysis was conducted by varying the ride-hailing demand and the share of BEVs in the ride-hailing fleet. This quantified the range of resulting energy consumption and green-house gas (GHG) emission levels.

Figure 2-90 shows the percentage of energy reduction in 2030 compared to the baseline “-RH/-Infrastructure” in 2030, as a function of ride-hailing demand and BEV market penetration. Baseline “-RH/-Infrastructure” means ride-hailing demand equals to 0.29%, market share of BEV sales in 2030 is 32.4%, and infrastructure coverage remains fixed from 2017 to 2030. Red represents an increase in energy while green indicates a reduction. Ride-hailing vehicle life was assumed to be seven years.

The impact of charging infrastructure. The figure on the right is the scenario under which charging infrastructure grows in response to the growing number of ride-hailing EVs, and the left figure has charging infrastructure fixed at 2017 levels (in order to be comparable with the high ride-hailing demand case, charging infrastructure coverage is fixed at 5.3% as it is in Columbus). By comparing both sides, the effect of charging infrastructure alone was shown, and the resulting reduction in national energy consumption was about 2%.

The impact of ride-hailing and BEV penetration. High annual VMT of ride-hailing leads to faster turnover rate of vehicles, resulting in newer and more fuel-efficient vehicles in the fleet, as shown in both subfigures in Figure 2-90. In a scenario in which ride-hailing demand is high (e.g., 100% of passenger-vehicle miles

(a) Gasoline:

Ride-hailing demand	Ride-hailing battery electric vehicle stock % 2030:															
	12%	16%	19%	22%	26%	29%	32%	35%	38%	42%	45%	47%	Ride-hailing battery electric vehicle sales % 2030:			
	18%	25%	30%	35%	40%	45%	50%	55%	60%	65%	70%	74%				
0.29%	10.24	10.24	10.24	10.24	10.24	10.24	10.23	10.23	10.23	10.23	10.23	10.23	10.23	10.23		
5%	10.47	10.43	10.41	10.39	10.37	10.34	10.32	10.30	10.27	10.25	10.23	10.21	10.21	10.21		
10%	10.66	10.60	10.55	10.51	10.46	10.42	10.38	10.33	10.29	10.24	10.20	10.16	10.16	10.16		
15%	10.81	10.72	10.66	10.60	10.53	10.47	10.40	10.34	10.27	10.21	10.15	10.09	10.09	10.09		
20%	10.93	10.82	10.74	10.65	10.57	10.49	10.40	10.32	10.23	10.14	10.04	9.97	9.97	9.97		
25%	11.02	10.88	10.78	10.68	10.58	10.48	10.37	10.26	10.14	10.03	9.92	9.84	9.84	9.84		
30%	11.07	10.92	10.80	10.69	10.56	10.43	10.30	10.18	10.05	9.92	9.80	9.70	9.70	9.70		
35%	11.10	10.93	10.80	10.66	10.51	10.37	10.22	10.08	9.94	9.80	9.66	9.55	9.55	9.55		
40%	11.11	10.92	10.77	10.61	10.45	10.29	10.13	9.98	9.82	9.67	9.52	9.40	9.40	9.40		
45%	11.10	10.89	10.71	10.54	10.37	10.20	10.03	9.86	9.70	9.53	9.37	9.24	9.24	9.24		
50%	11.07	10.83	10.64	10.46	10.28	10.10	9.92	9.74	9.56	9.39	9.21	9.07	9.07	9.07		
55%	11.02	10.76	10.56	10.37	10.18	9.99	9.80	9.61	9.42	9.23	9.05	8.90	8.90	8.90		
60%	10.95	10.67	10.47	10.27	10.06	9.86	9.67	9.47	9.27	9.07	8.88	8.72	8.72	8.72		
65%	10.87	10.58	10.36	10.15	9.94	9.73	9.53	9.32	9.11	8.91	8.70	8.54	8.54	8.54		
70%	10.78	10.47	10.25	10.03	9.81	9.59	9.38	9.16	8.95	8.73	8.52	8.35	8.35	8.35		
75%	10.67	10.35	10.13	9.90	9.67	9.45	9.22	9.00	8.77	8.55	8.33	8.15	8.15	8.15		
80%	10.55	10.23	9.99	9.76	9.52	9.29	9.06	8.83	8.60	8.36	8.13	7.95	7.95	7.95		
85%	10.42	10.09	9.85	9.61	9.37	9.13	8.89	8.65	8.41	8.17	7.93	7.74	7.74	7.74		
90%	10.29	9.95	9.70	9.45	9.21	8.96	8.71	8.47	8.22	7.97	7.73	7.53	7.53	7.53		
95%	10.15	9.80	9.55	9.29	9.04	8.78	8.53	8.28	8.02	7.77	7.52	7.32	7.32	7.32		
100%	9.99	9.64	9.38	9.12	8.86	8.60	8.34	8.08	7.82	7.56	7.30	7.10	7.10	7.10		

(b) Electricity:

Ride-hailing demand	Ride-hailing battery electric vehicle stock % 2030:															
	12%	16%	19%	22%	26%	29%	32%	35%	38%	42%	45%	47%	Ride-hailing battery electric vehicle sales % 2030:			
	18%	25%	30%	35%	40%	45%	50%	55%	60%	65%	70%	74%				
0.29%	0.86	0.86	0.86	0.86	0.86	0.86	0.86	0.86	0.86	0.86	0.86	0.86	0.86	0.87		
5%	0.87	0.88	0.90	0.91	0.92	0.93	0.94	0.95	0.97	0.98	0.99	1.00	1.00	1.00		
10%	0.88	0.91	0.93	0.95	0.97	1.00	1.02	1.04	1.06	1.09	1.11	1.13	1.13	1.13		
15%	0.88	0.92	0.96	0.99	1.02	1.05	1.08	1.12	1.15	1.18	1.21	1.24	1.24	1.24		
20%	0.88	0.94	0.98	1.02	1.06	1.10	1.14	1.19	1.23	1.28	1.33	1.36	1.36	1.36		
25%	0.88	0.95	1.00	1.05	1.10	1.15	1.20	1.26	1.32	1.37	1.43	1.47	1.47	1.47		
30%	0.87	0.95	1.01	1.07	1.13	1.20	1.26	1.32	1.39	1.45	1.52	1.57	1.57	1.57		
35%	0.87	0.95	1.02	1.09	1.16	1.24	1.31	1.38	1.45	1.52	1.59	1.65	1.65	1.65		
40%	0.86	0.96	1.03	1.11	1.19	1.27	1.35	1.43	1.51	1.58	1.66	1.72	1.72	1.72		
45%	0.85	0.95	1.04	1.13	1.21	1.30	1.38	1.47	1.55	1.63	1.72	1.78	1.78	1.78		
50%	0.83	0.95	1.05	1.14	1.23	1.32	1.41	1.50	1.59	1.68	1.77	1.84	1.84	1.84		
55%	0.82	0.95	1.05	1.15	1.24	1.34	1.44	1.53	1.62	1.72	1.81	1.89	1.89	1.89		
60%	0.80	0.95	1.05	1.15	1.25	1.35	1.45	1.55	1.65	1.75	1.85	1.93	1.93	1.93		
65%	0.79	0.94	1.04	1.15	1.26	1.36	1.47	1.57	1.68	1.78	1.88	1.98	1.98	1.98		
70%	0.77	0.93	1.04	1.15	1.26	1.37	1.48	1.59	1.69	1.80	1.91	2.00	2.00	2.00		
75%	0.75	0.91	1.03	1.14	1.26	1.37	1.48	1.60	1.71	1.82	1.93	2.02	2.02	2.02		
80%	0.74	0.90	1.02	1.14	1.25	1.37	1.49	1.60	1.72	1.84	1.95	2.05	2.05	2.05		
85%	0.71	0.88	1.00	1.12	1.25	1.37	1.49	1.61	1.73	1.85	1.97	2.08	2.08	2.08		
90%	0.69	0.86	0.99	1.11	1.24	1.36	1.49	1.61	1.73	1.86	1.98	2.08	2.08	2.08		
95%	0.67	0.84	0.97	1.10	1.23	1.35	1.48	1.61	1.74	1.86	1.99	2.09	2.09	2.09		
100%	0.64	0.82	0.95	1.08	1.21	1.34	1.47	1.60	1.74	1.87	2.00	2.10	2.10	2.10		

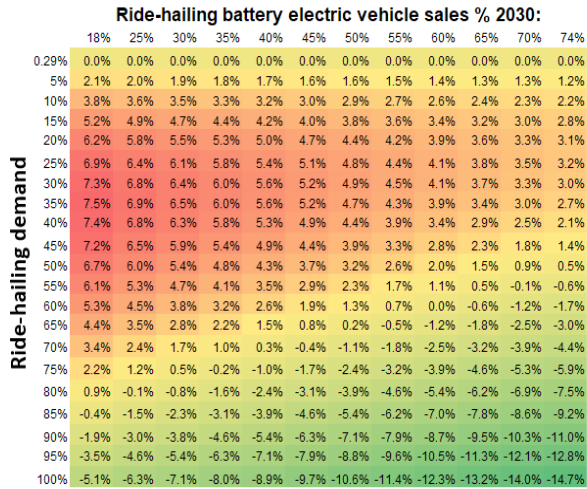
Figure 2-91. Energy consumption (quads) in 2030 for the case with charging infrastructure growth: (a) gasoline consumption, and (b) electricity consumption.

Figure 2-92 shows the percentage of carbon emissions reduction compared to the baseline -RH/-Infrastructure in 2030, as a function of ride-hailing demand and BEV market penetration. Baseline -RH/-Infrastructure means ride-hailing demand equals 0.29%, BEV market share in 2030 equals to 32.4%, with infrastructure coverage fixed from 2017 to 2030. Results indicate that the percentage reduction in carbon emissions would be similar to the percentage reduction in energy.

Figure 2-93 shows carbon emissions at different scenarios for the electricity grid mix. The scenario +RH/+Infrastructure with Renewable Electricity has the lowest carbon emissions (282.66 MMTcE). In the chart “-RH” means ride-hailing demand is 0.29%, “+RH” means ride-hailing demand is 100%, “-Infrastructure” means holding charging infrastructure coverage at the 2017 level, “+Infrastructure” means infrastructure coverage grows. The grid mix scenarios are defined as below, according to the VISION 2017 model, as shown in Table 2-28.

Carbon:

Charging infrastructure fixed at existing conditions



Carbon:

With charging infrastructure growth

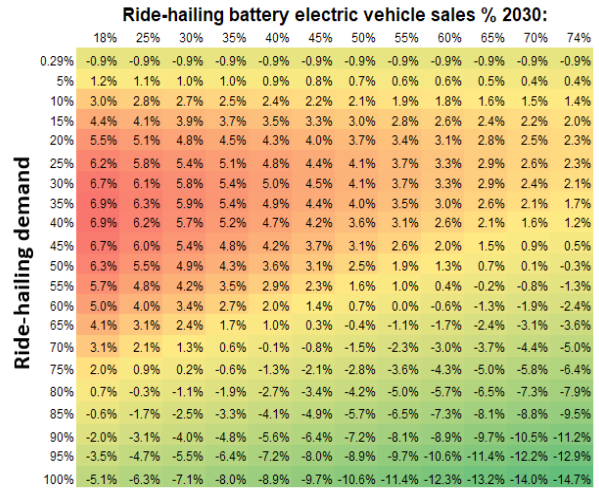


Figure 2-92. National carbon emissions reduction, shown as percentages, original unit is million metric tons of carbon equivalent (MMTC) as a function of ride-hailing demand, BEV market penetration, and charging infrastructure. Green means a reduction, yellow means relatively no change, and red means an increase. Carbon emissions include emissions from upstream and vehicle use.

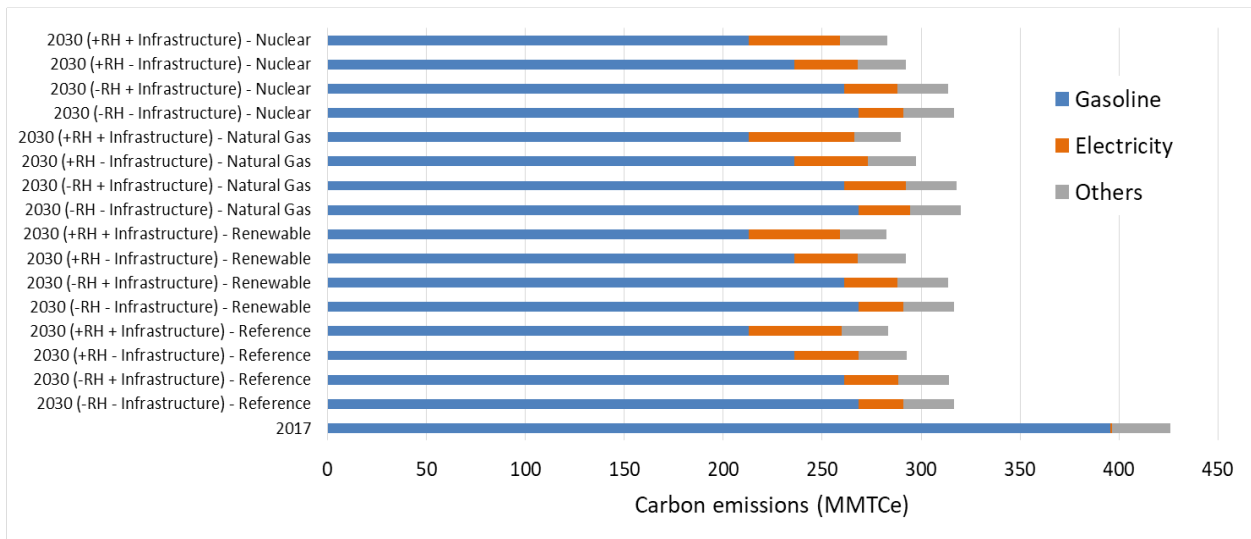


Figure 2-93. National carbon emissions at different electricity grid mixes.

Table 2-28. Grid mix assumed for each scenario.

	Coal	Petroleum	Natural Gas	Nuclear	Renewables
Reference	23.1%	0.2%	33.7%	17.3%	25.7%
Renewable	26.7%	0.2%	24.6%	17.1%	31.4%
Natural Gas	27.1%	0.2%	36.9%	17.4%	18.4%
Nuclear	26.7%	0.2%	24.6%	30.4%	18.1%

3. Conclusion

The AFI Pillar in the U.S. Department of Energy’s SMART Mobility Laboratory Consortium used sophisticated modeling and simulation tools to investigate tradeoffs in different charging infrastructure network designs for human-driven and fully automated ride-hailing EVs, electric car-sharing fleets, automated electric shuttles in transit operation, and freight delivery truck fleets. The AFI Pillar also researched the impact of two potentially game-changing charging technologies, intelligent fleet dispatching management and DWPT, on automated electrified fleet efficiency and productivity. Finally, the Pillar assessed the potential of charging infrastructure installed to support ride-hailing EVs to influence mobility and energy consumption trends on a national scale.

The AFI Pillar conducted its research to answer five questions. This section summarizes the results of the AFI Pillar’s research and answers, at least in part, each of these questions, for the benefit of planners of charging infrastructure serving diverse transportation modes. These findings also provide insights for mobility service providers and fleet managers looking to adopt EVs for ride-hailing, car-sharing, transit, and freight delivery services. Areas of future work are also recommended.

A recurring theme in the AFI Pillar’s research is that tradeoffs abound. There is no “right” amount of charging infrastructure because charging needs vary dramatically across and within increasingly diverse segments of the EV market. Circumstances, interests, and behaviors of individual EV drivers vary dramatically, rendering a single, ideal charging infrastructure design impossible. For operators of human-driven and automated EV fleets, decisions related to charging are closely coupled with many other investment and operations decisions, including the number and type of vehicles they place in their fleet and how vehicles are dispatched. The conclusions of the AFI Pillar research presented here will summarize many of the tradeoffs that must be managed and the cost/benefit relationships that emerge in different approaches to charging infrastructure network design for future electric mobility.

3.1 Summary of Findings and Their Implications

3.1.1 What are the characteristics of potential future transportation market segments employing human-driven and automated EVs that charging infrastructure will need to serve?

After considering six LDV market segments for electrification, the AFI Pillar chose to focus on two segments: human-driven and automated ride-hailing. Ride-hailing drivers are independent, self-interested, and have widely varying circumstances and motivations, such as varying shift frequency and length, typical daily driving distance, ability to charge overnight, and reasons for driving. Given such heterogeneity, no single ideal charging network meets the charging needs of or is valued by everyone. Therefore, it behooves charging network providers and mobility companies (i.e., TNCs and taxi companies) to cater to specific groups within the segment, such as drivers without home charging access, or to partner with others to address barriers to specific groups, such as reducing vehicle and charging costs through incentive programs.

Commercially owned AEVs in ride-hailing fleets can be centrally managed, with individual vehicle operation governed by the fleet manager for the good of the fleet. These vehicles need dedicated charging networks because they will either require specialized equipment for unmanned charging or manned charging stations at central depots.

Electrification of Class 7–8 heavy-duty trucks has tremendous potential for national energy consumption reduction, but the variety and complexity of operations in the freight-trucking industry make electrification challenging. Trucks are used differently across segments, across fleets, within fleets, and even from day to day. Class 7–8 trucks in for-hire/TL and for-hire/LTL motor carrier segments often do not consistently drive the same routes or stop at the same locations, making charging infrastructure siting difficult. Private carriers transport their own company’s cargo and operate exclusively among their own terminals, so installing charging infrastructure at proprietary facilities may be practical. Private, short- and regional-haul motor carriers that follow a hub-and-spoke operating model may be the most amenable for electrification; however, a case study showed that electrifying even this use case is challenging.

Electric truck operations also must be conducted within the confines of regulation, including the maximum allowable time drivers can continuously operate their trucks. The relatively long time that charging requires, even with high-power chargers, may be highly problematic for trucking companies that strive to maximize miles driven within regulated shift lengths. The fact that most drivers are paid by the mile compounds this problem.

3.1.2 What are the cost/benefit tradeoffs inherent with different approaches to designing charging infrastructure to serve light-duty human-driven and automated electric passenger vehicles?

The AFI Pillar conducted multiple case studies to investigate how charging infrastructure design influences economics for the charging network provider, the ability of electric mobility providers (ride-hailing EV drivers, car-sharing fleets, and AEV fleets) to serve customers, and the ability of motor carriers to efficiently deliver freight. Because many factors important to these relationships will always be case specific for different cities, fleets, and drivers, it is difficult to draw generalizable principles from this research. Nevertheless, some trends are evident in the Pillar's findings.

Design charging networks around demand. Charging providers are benefitted by strategically siting charging stations in locations where ride-hailing drivers need to use them, even if those locations require expensive installations. Therefore, it behooves charging infrastructure planners to partner with TNCs, automakers, or other organizations that have access to data describing ride-hailing vehicle driving behavior.

Look beyond simply adding more charging stations. Planners should be aware that there is a limit to the gains afforded to an electric vehicle fleet by increasing the number of available charging stations and plugs. This is true even if the network becomes widespread and charging stations are optimally sited. Simulation of a ride-hailing fleet in the San Francisco Bay Area demonstrated that when employing low-range EVs (i.e., BEV100s) and 50-kW DCFC stations, adding more charging infrastructure cannot cost-effectively increase the capacity of the fleet to serve more than 180 passenger miles per vehicle per day. This is because charging time itself becomes the dominant impediment to vehicle time in service for dense charging networks of 50-kW chargers. The benefit of increasing charging power beyond 50 kW was evident for all use cases studied, even in scenarios with longer EV range: human-driven ride hailing, automated ride hailing, car sharing, and trucking. Faster charging not only reduces charging time for vehicles, but also decreases queuing time by increasing throughput at charging stations, which positively affects the entire network of charging stations and EVs. A similar effect is achieved by adopting EVs with longer electric driving range to reduce charging frequency. Case studies suggest that longer EV range should be combined with increased access to charging infrastructure and/or higher-power charging to provide EVs with comparable utility to their ICEV counterparts.

Recognize there is still value in slow charging. Case studies suggest that exploiting times when vehicles are naturally parked for long periods of time is an alternative to faster charging. This is already conventional wisdom for personal-use EV drivers, and it is clear from the case study comparing TNC and taxi drivers with and without access to overnight charging. However, it is less obvious when commercial fleets that respond to time-varying customer demand can afford to charge vehicles slowly. Electric car-sharing, ride-hailing, and truck fleet managers that understand when downtime has minimal impact on their ability to serve customers can exploit this knowledge to charge slowly during those times using less expensive, low-power charging infrastructure.

3.1.3 What is needed to understand tradeoffs inherent with different approaches to designing charging infrastructure for Class 7/8 electric trucks for freight transport?

Even in a seemingly simple case for electrification—a private, regional-haul, hub-and-spoke motor carrier fleet—modeling found that electric Class 7–8 freight trucks may require substantially higher charging power than 350 kW and/or changes to fleet operations. This validates research sponsored by the U.S. DOE Vehicle Technologies Office to develop technology necessary to produce charging infrastructure with over 1 MW of charging power capacity. Undoubtedly, however, such high-power charging will come at a cost. Alternatively, fleet operators could lengthen dwell times to allow for sufficient charging at lower power, take time to charge at public charging stations, and/or limit electric trucks to specific routes. These complexities add real costs to fleet operations that must be balanced with the cost of increasing EV range and charging power to realize

financial benefits of electrification. All these factors limit the utility of electric trucks relative to their conventional counterparts, which reduces resale value and puts pressure on the business case for heavy truck electrification.

New analytical tools are needed to help motor carriers holistically manage these complex decisions. The cost of high EV range for trucks, high charging power, and/or widespread charging infrastructure must be weighed against the cost of operational changes, such as routing and dispatching changes. Motor carriers also must decide whether to invest in their own charging infrastructure, partner with other fleets, and/or rely on third-party providers in order to electrify their trucking operations. Such tools must be able to integrate charging infrastructure and electric truck performance and cost modeling with fleet operations cost models.

3.1.4 What is the potential for automated vehicle charging to create new charging paradigms that improve the automated, electric ride-hailing and transit?

In short, applying new technology for charging AEVs has significant potential to improve ride-hailing and automated transit operations.

AFI Pillar research showed that intelligent fleet management using optimization routines to manage repositioning and charging of the fleet as a whole can increase productivity and revenue potential of a fleet by increasing the number of ride requests satisfied. At the same time, this approach to fleet management can decrease wasted driving, energy consumption, and cost. It can also enable fleet downsizing and help AEVs make the most effective use of available charging infrastructure.

DWPT technology could remove the need to dispatch EVs for charging altogether by allowing vehicles to charge while driving. A natural first application for this technology is automated electric transit. A simulation of two automated electric shuttle bus networks showed that a DWPT system located at bus stops located about every mile along a fixed route could allow electric 8–12-passenger shuttle buses to operate continuously. This means that driverless shuttle buses could operate with near-zero downtime, which would greatly reduce operating cost compared with equivalent human-driven shuttle buses without DWPT. Implementing such a system also has the potential to reduce the size and cost of vehicle batteries by more than 50%. Preliminary cost analysis suggests that a DWPT system can be cost competitive with high-power conductive charging in automated electric transit applications. Although currently a niche case, adoption of automated electric shuttles could grow as transit agencies look to improve efficiency, safety, and flexibility of their operations.

Beyond transit, analysis of DWPT to support highway driving found that a DWPT system capable of providing up to 250 kW of charging power, installed in 8-10% of the primary roadways in the United States, is sufficient to enable continuous, charge-sustaining operation for light-duty vehicles averaging 65 mph. As in the transit application, DWPT technology allows EVs to have smaller batteries and use narrower SOC windows, which would reduce costs and increase battery life. Use of DWPT in the highway system at large introduces numerous challenges, but these findings suggest that further research is worth pursuing.

3.1.5 What is the benefit to the nation of charging infrastructure deployed to serve ride-hailing EVs?

The AFI Pillar quantified national energy impacts of ride-hailing EVs as a function of different levels of charging infrastructure support and ride-hailing demand. Consumer adoption modeling determined that increasing charging infrastructure availability for ride-hailing EVs induces EV adoption among personal-use vehicle owners. Also, increased ride-hailing demand creates faster vehicle turnover. Increased VMT by ride-hailing vehicles due to deadheading offsets some of the benefit from reduced energy consumption through both electrification and increased ride-hailing. With increased charging availability and very high demand for ride hailing, the average fuel consumption of the U.S. light-duty passenger vehicle fleet would decrease by 12–14% by 2030 due to fleet fuel efficiency improvement.

3.2 Recommendations for Future Work

With the private and public sector investing significant funding into charging infrastructure, considerable additional research is needed to plan and optimize economically viable, grid-integrated charging infrastructure to serve personal-use, ride-hailing, transit, and freight vehicles in and between diverse metropolitan areas. The

SMART Mobility Modeling Workflow could be leveraged to holistically simulate numerous EV modes operating in the same area to understand the interplay between modes and common charging infrastructure.

Additional research is needed to apply advanced optimization and artificial intelligence to allow EVs to interact with charging infrastructure and other transportation infrastructure autonomously in ways that make increasingly intelligent dispatching decisions to improve operational efficiency and increase mobility. Dynamic algorithms should be developed that adapt to varying grid, traffic, and other conditions. To this end, prediction capabilities for transportation system activities will be important to enable sophisticated fleet management strategies. Multi-stage optimization approaches should be investigated (as opposed to the single-stage process followed to date by the AFI Pillar). A multi-stage approach has stronger potential to yield system-level benefits because it can consider both spatial and temporal dynamics from ride-hailing requests and AEV activities. This research should also study how to enable high-mileage EV driving and charging to maximize vehicle and battery life. Researchers developing these approaches should partner with private industry to validate them in real-world experiments.

As a foundation for this work, EV TNC data collection efforts similar to those launched by the AFI Pillar should continue and expand to a larger pool of EVs operating within TNC fleets. This would benefit researchers attempting to model future networks of automated and human-driver ride-hailing vehicles.

Researchers should explore additional use cases for wireless charging technology, including full-size public transit buses, quasi-dynamic charging at intersections and traffic signals, and freight-trucking applications. Simulation at the city scale is warranted to explore how DWPT systems can be integrated into the transportation network for passenger vehicles and heavy-duty trucks. Collecting more real-world data from currently operating automated shuttles would inform more accurate powertrain and energy estimation models. Future work could also conduct battery performance and life-cycle assessment analysis in the system cost function and investigate the impact of limitations in battery technology on the wireless technology feasibility analysis.

Research could also focus on developing tools that fleet managers and planners can use to manage the complex decisions inherent to charging infrastructure planning. These tools would benefit from including factors not included in the research described in this report, including the price of real estate needed for charging stations and more detailed factors describing the cost of increasing charging power in both charging infrastructure and vehicles.

For national energy impact analysis of ride-hailing vehicles, future work could explore the relationship between deadheading trips and ride-hailing demand and quantify the impacts of ride-hailing on induced VMT and personal vehicle ownership.

4. References

- [1] “Electric Vehicle Sales: Facts & Figures.” Documents - All Documents. Edison Electric Institute, October 2019. Accessed November 14, 2019. Retrieved from https://www.eei.org/issuesandpolicy/electrictransportation/Documents/FINAL_EV_Sales_Update_Oct2019.pdf.
- [2] “Annual Energy Outlook 2019 with projections to 2050.” Energy Information Administration, January 24, 2019. Retrieved from eia.gov/outlooks/aeo/pdf/aeo2019.pdf.
- [3] Brian Solomon. “Uber Just Completed Its Two Billionth Ride.” *Forbes Magazine*, July 18, 2016. Retrieved from <https://www.forbes.com/sites/briansolomon/2016/07/18/uber-just-completed-its-two-billionth-ride/#4ca687125224>.
- [4] “Company Information: Uber Newsroom US.” Uber Newsroom. Accessed December 5, 2019. Retrieved from <https://www.uber.com/newsroom/company-info/>.
- [5] “Our Journey.” Waymo. Accessed December 5, 2019. Retrieved from <https://waymo.com/journey>.
- [6] Jamie Hall. “CA EV Infrastructure Projections,” Maven. May 23, 2018 Staff Workshop: California Plug-In Electric Vehicle Infrastructure Projections: 2017-2025. Retrieved from <https://efiling.energy.ca.gov/GetDocument.aspx?tn=224123>.
- [7] “Total Energy Monthly Data.” U.S. Energy Information Administration (EIA). DOE/EIA-0035(2019/2). January 2019.
- [8] “Evaluation of U.S. Commercial Motor Carrier Industry Challenges and Opportunities.” U.S. Department of Transportation Federal Highway Administration. February 1, 2017.
- [9] Patrick Morrissey, Peter Weldon, and Margaret O’Mahony. “Future standard and fast charging infrastructure planning: An analysis of electric vehicle charging behaviour.” *Energy Policy* 89 (2016): 257-270.
- [10] “Electric Vehicle Charging Station Locations.” DOE, AFDC. 2019. Retrieved from afdc.energy.gov/fuels/electricity_locations.html#/analyze?fuel=ELEC&country=US&access=private.
- [11] Sreten Davidov and Miloš Pantoš. “Planning of electric vehicle infrastructure based on charging reliability and quality of service.” *Energy* 118 (2017): 1156-1167.
- [12] Salvatore Micari, et al. “Electric vehicle charging infrastructure planning in a road network.” *Renewable and Sustainable Energy Reviews* 80 (2017): 98-108.
- [13] Eric Wood, Clement Rames, Matteo Muratori, Sesha Raghavan, and Stanley Young. “Charging Electric Vehicles in Smart Cities: An EVI-Pro Analysis of Columbus, Ohio.” NREL/TP-5400-70367. National Renewable Energy Lab. (NREL), Golden, CO (United States), 2018.
- [14] Fang He, Yafeng Yin, and Jing Zhou. “Deploying public charging stations for electric vehicles on urban road networks.” *Transportation Research Part C: Emerging Technologies* 60 (2015): 227-240.
- [15] Solomon, “Uber Just Completed”
- [16] “Company Information: Uber Newsroom”
- [17] S. Shaheen and A. Cohen. “[Faster toward the future of mobility](#),” *Deloitte Review*, issue 20, Jan 23, 2017. Innovative mobility carsharing outlook. University of Berkeley, California.
- [18] “Our Journey”

-
- [19] Phil LeBeau. "Waymo starts commercial ride-share service." December 5, 2018. Retrieved from cnbc.com/2018/12/05/waymo-starts-commercial-ride-share-service.html.
- [20] "Electric, Shared and Autonomous Vehicles Will Revolutionise Transport in the World's Cities over the next 15 Years." BloombergNEF, December 14, 2016. Retrieved from <https://about.bnef.com/blog/electric-shared-autonomous-vehicles-will-revolutionise-transport-worlds-cities-next-15-years/>.
- [21] Laura Bliss. "Self-Driving Cars Will Be For Sharing." CityLab, January 6, 2017. Retrieved from <https://www.citylab.com/life/2017/01/the-future-of-autonomous-vehicles-is-shared/512417/>.
- [22] "Electric, Shared and Autonomous Vehicles Will Revolutionise"
- [23] Marissa Moultak, Nic Lutsey, and Dale Hall. "Transitioning to zero-emission heavy-duty freight vehicles." *Int. Counc. Clean Transp.* September 2017.
- [24] John O'Dell. "UPS Launching World's First Fuel Cell Electric Class 6 Delivery Truck." May 02, 2017. Retrieved from trucks.com/2017/05/02/ups-fuel-cell-electric-delivery-truck/.
- [25] Kevin Walkowicz. "Medium and Heavy-Duty Vehicle Field Evaluations." *Project ID: VSS001*. National Renewable Energy Laboratory, Golden CO (United States), 2013. Retrieved from energy.gov/sites/prod/files/2014/03/f13/vss001_walkowicz_2013_o.pdf.
- [26] "2018 Feasibility Assessment for Drayage Trucks." Tetra Tech and Gladstein, Neandross & Associates. March 2019. Retrieved from <https://kentico.portoflosangeles.org/getmedia/969f3b4a-c5cc-45d4-bfec-bb3071b2350b/2018-Feasibility-Assessment-for-Drayage-Trucks>.
- [27] "Truck makers rev up for rollout of electric big rigs." Accessed September 24, 2019. Retrieved from cnbc.com/2018/10/22/truck-makers-rev-up-for-rollout-of-electric-big-rigs.html.
- [28] Jerry Hirsch. "Volvo Trucks Unveils Electric Truck, Readies Commercialization." September 2019, Accessed January 16, 2020. Retrieved from <https://www.trucks.com/2019/09/13/volvo-unveils-vnr-electric-truck/>.
- [29] "Electric Bus Fleet Conversion." Antelope Valley Transit Authority. January 2018, Accessed September 24, 2019. Retrieved from avta.com/electric-bus-fleet-conversion.php.
- [30] Dug Begley, "Metro to introduce electric bus in move to cut pollution." Houston Chronicle, Nov 29, 2016. Accessed September 24, 2019. Retrieved from houstonchronicle.com/news/transportation/article/Metro-to-introduce-electric-bus-in-move-to-cut-10643461.php.
- [31] Alison Berg. "Park City Switches to All-Electric Bus System." Deseret News. Deseret News, June 23, 2017. Retrieved from <https://www.deseret.com/2017/6/23/20614722/park-city-switches-to-all-electric-bus-system#one-six-electric-buses-in-park-citys-new-fleet-is-pictured-on-friday-june-23-2017-the-electric-express-utahs-first-all-electric-bus-fleet-will-run-every-10-minutes-from-kimball-junction-to-park-city-transit-seven-days-a-week>.
- [32] Sean O'Kane. "UPS has been quietly delivering cargo using self-driving trucks." The Verge, August 15, 2019. Accessed September 24, 2019. Retrieved from theverge.com/2019/8/15/20805994/ups-self-driving-trucks-autonomous-delivery-tusimple.
- [33] Alex Davies. "Self-Driving Trucks are Now Delivering Refrigerators." Wired, November 13, 2017, Accessed September 24, 2019. Retrieved from wired.com/story/embark-self-driving-truck-deliveries/.
-

-
- [34] “Tesla, Inc.” Tesla Semi. Accessed September 24, 2019. Retrieved from tesla.com/semi.
- [35] Skip Descant. “Autonomous Shuttles Make Debut at California State University.” February 21, 2019. Retrieved from govtech.com/fs/automation/Autonomous-Shuttles-Make-Debut-at-California-State-University.html.
- [36] Robert James. “Automated Vehicle Deployments Gaining in Popularity.” July 12, 2018. Retrieved from metro-magazine.com/mobility/article/730326/automated-vehicle-deployments-gaining-in-popularity.
- [37] Jon Murray. “Self-driving shuttle offers Denver a glimpse of its future — but will riders jump on board?” January 31, 2019 – updated February 4, 2019. Retrieved from denverpost.com/2019/01/31/denver-airport-self-driving-shuttle-easymile/.
- [38] Cory Nealon. “Self-driving shuttle Olli makes public debut.” August 10, 2018. Retrieved from [//www.buffalo.edu/ubnow/stories/2018/08/olli-debut.html](http://www.buffalo.edu/ubnow/stories/2018/08/olli-debut.html).
- [39] “About EV Charging.” Electrify America. Accessed December 5, 2019. Retrieved from <https://www.electrifyamerica.com/about-ev-charging>.
- [40] “With No Place To Charge, D.C.’s Electric Cab Drivers Ask For Help,” American University Radio, March 2017. Retrieved from wamu.org/story/17/08/14/no-place-charge-d-c-s-electric-cab-drivers-ask-help.
- [41] “Electric Vehicle Pilot: Final Report,” September 13, 2016, Retrieved from www1.nyc.gov/assets/tlc/downloads/pdf/ev_pilot_final_report.pdf.
- [42] D. Garrick. “Car2Go switching electric cars to gas,” San Diego Union-Tribune, Mar 16, 2016.
- [43] “EVgo and Maven Gig Announce Nation’s First Dedicated Fast Charging Network for On-Demand Drivers.” April 2018. Retrieved from evgo.com/about/news/evgo-maven-gig-announcements-first-dedicated-fast-charging-network-demand-drivers.
- [44] “Electrify America.” *National ZEV Investment Plan: Cycle 2*. 2019. Retrieved from epa.gov/sites/production/files/2019-02/documents/cycle2-nationalzevinvestmentplan.pdf.
- [45] John Smart. “Plugged In: How Americans Charge Their Electric Vehicles,” INL Technical Report INL/EXT-15-35584, September 2015. Retrieved from [/avt.inl.gov/pdf/arra/SummaryReport.pdf](http://avt.inl.gov/pdf/arra/SummaryReport.pdf).
- [46] John Smart. “Plugged In: How Americans Charge”
- [47] Jim Francfort. “Characterize the Demand and Energy Characteristics of Direct Current Fast Chargers.” No. INL/EXT-15-36318-Rev000. Idaho National Lab. (INL), Idaho Falls, ID (United States), 2015.
- [48] Michael Nicholas and Dale Hall. “Lessons learned on early electric vehicle fast-charging deployments.” *The International Council on Clean Transportation*. 2018. Retrieved from theicct.org/sites/default/files/publications/ZEV_fast_charging_white_paper_final.pdf.
- [49] Matthew Goetz et al. “Electric Vehicle Charging Considerations for Shared, Automated Fleets.” *UC Davis Institute of Transportation Studies*. 2017.
- [50] Johannes Asamer et al. “Optimizing charging station locations for urban taxi providers.” *Transportation Research Part A: Policy and Practice* 85. 2016: 233-246.
-

-
- [51] Jie Yang, Jing Dong, and Liang Hu. "A data-driven optimization-based approach for siting and sizing of electric taxi charging stations." *Transportation Research Part C: Emerging Technologies* 77. 2017: 462-477. Retrieved from doi.org/10.1016/j.trc.2017.02.014.
- [52] Joshka Bischoff and Michal Maciejewski. "Agent-based simulation of electric taxicab fleets." *Transportation Research Procedia* 4. 2014: 191-198.
- [53] Reinhard Sellmair and Thomas Hamacher. "Optimization of charging infrastructure for electric taxis." *Transportation Research Record* 2416.1. 2014: 82-91.
- [54] Tong Donna Chen. "Management of a shared, autonomous, electric vehicle fleet: vehicle choice, charging infrastructure & pricing strategies." Diss. 2015.
- [55] Wenwen Zhang et al. "The performance and benefits of a shared autonomous vehicles based dynamic ridesharing system: An agent-based simulation approach." *Transportation Research Board 94th Annual Meeting*. No. 15-2919. 2015.
- [56] Tong Donna Chen, Kara M. Kockelman, and Josiah P. Hanna. "Operations of a shared, autonomous, electric vehicle fleet: Implications of vehicle & charging infrastructure decisions." *Transportation Research Part A: Policy and Practice* 94. 2016: 243-254.
- [57] *Yutaka Motoaki. "Location-Allocation of Electric Vehicle Fast Chargers—Research and Practice." *World Electric Vehicle Journal* 10, no. 1. June 2019: 12. doi.org/10.3390/wevj10010012.
- [58] "Ride Austin's Datasets." data.world, November 2, 2017. Retrieved from <https://data.world/ride-austin>.
- [59] Jae Hyun Lee, Debapriya Chakraborty, Scott Hardman, Gil Tal, "Identifying Heterogeneous Electric Vehicle Charging Behavior," presented at EVS 31 & EVTeC 2018, Kobe, Japan, October 1 - 3, 2018.
- [60] "Electric Vehicle Pilot: Final Report"
- [61] R. Li and G. Fitzgerald. "Ride-Hailing Drivers Are Ideal Candidates for Electric Vehicles." Rocky Mountain Institute. March 29, 2018. Retrieved from rmi.org/ride-hailing-drivers-ideal-candidates-electric-vehicles/.
- [62] Brad Templeton. "Why Isn't Your Uber An Electric Car?" Nov 25, 2019. Accessed December 17, 2019. Retrieved from <https://www.forbes.com/sites/bradtempleton/2019/11/25/why-isnt-your-uber-an-electric-car/#3e7945954270>.
- [63] "Maven Gig Overview." Maven. Accessed December 14, 2019. Retrieved from <https://mavengig.maven.com/us/en/>.
- [64] Hall, "CA EV Infrastructure Projections"
- [65] "Maven Gig Overview"
- [66] "2017 CFS Preliminary Data, Bureau of Transportation Statistics." U.S. Department of Transportation. 2018. Accessed March 2019. Retrieved from bts.gov/surveys/commodity-flow-survey/2017-cfs-preliminary-data.
- [67] EIA, "Monthly Energy Review"
- [68] "Evaluation of U.S. Commercial Motor Carrier Industry Challenges and Opportunities." U.S. Department of Transportation Federal Highway Administration. February 1, 2017.
-

-
- [69] “Federal Motor Carrier Safety Administration.” U.S. DOT. 2019. Accessed March 2019. Retrieved from ask.fmcsa.dot.gov/.
- [70] “Federal Motor Carrier Safety Administration”
- [71] “Electrical and Electronics Technical Team Roadmap.” U.S. DRIVE (Driving Research and Innovation for Vehicle efficiency and Energy sustainability). October 2017.
- [72] “Electrical and Electronics Technical Team Roadmap”
- [73] “Motor Carrier Census Information, Federal Motor Carrier Safety Administration.” FMCSA, U.S. Department of Transportation. 2018. Accessed March 2019. Retrieved from ai.fmcsa.dot.gov/SMS/Tools/Downloads.aspx.
- [74] “Bureau of Labor Statistics 2019.” United States Department of Labor. Retrieved from <https://www.bls.gov/>.
- [75] W. Guang Chen, Karl Sieber, Jennifer E. Lincoln, Jan Birdsey, Edward M. Hitchcock, Akinori Nakata, Cynthia F. Robinson., James W. Collins, Marie H. Sweeney. “NIOSH national survey of long-haul truck drivers: Injury and safety, Accident Analysis & Prevention.” Volume 85, 2015, Pages 66-72.
- [76] “Summary of Hours of Service Regulations, Motor Carrier Census Information.” Federal Motor Carrier Safety Administration, U.S. Department of Transportation. 2018b. Retrieved from fmcsa.dot.gov/regulations/hours-service/summary-hours-service-regulations.
- [77] “Bridge Formula Weights.” U.S. Department of Transportation Federal Highway Administration. June 20, 2018. Retrieved from ops.fhwa.dot.gov/Freight/publications/brdg_frm_wghts/index.htm.
- [78] Motoaki, “Location-Allocation of Electric Vehicle Fast Chargers”
- [79] A. Schroeder and T. Traber. “The Economics of Fast Charging Infrastructure for Electric Vehicles,” *Energy Policy*, 43:136-144. 2012. Retrieved from doi.org/10.1016/j.enpol.2011.12.041.
- [80] C. Madina, I. Zamora, E. Zabala. “Methodology for Assessing Electric Vehicle Charging Infrastructure Business Models.” *Energy Policy*. 89:284-293. 2016. Retrieved from doi.org/10.1016/j.enpol.2015.12.007.
- [81] Alejandro Henao. “Impacts of Ridesourcing – Lyft and Uber – on Transportation including VMT, Mode Replacement, Parking, and Travel Behavior.” 2017. Accessed August 2017. Retrieved from media.wix.com/ugd/c7a0b1_68028ed55eff47a1bb18d41b5fba5af4.pdf.
- [82] A. Jenn and R. Clewlow. “New Mobility Services and Vehicle Electrification (No. 17-05269).” *Transportation Research Board 96th Annual Meeting Compendium of Papers*. 2017. Accessed August 2017. Retrieved from trid.trb.org/view.aspx?id=1439073.
- [83] Susan Shaheen, Nelson Chan, Apaar Bansal, Adam Cohen. “Shared Mobility: A Sustainability & Technologies Workshop: Definitions, Industry Developments, and Early Understanding.” November 2015. Accessed August 2017. Retrieved from innovativemobility.org/wp-content/uploads/2015/11/SharedMobility_WhitePaper_FINAL.pdf
- [84] Z. Wadud, D. MacKenzie, and P. Leiby. “Help or Hindrance? The Travel, Energy and Carbon Impacts of Highly Automated Vehicles.” 2016. *Transportation Research Part A: Policy and Practice*, 86:1–18.
- [85] Chen, “Operations of a Shared, Autonomous,” 243-254
- [86] Motoaki, “Location-Allocation of Electric Vehicle Fast Chargers”
-

- [87] Schroeder, “The Economics of Fast Charging Infrastructure”
- [88] H. Zhang, C. Sheppard, T Lipman, S Moura. “Joint Fleet Sizing and Charging System Planning for Autonomous Electric Vehicles.” 2018. Under peer review. Retrieved from arxiv.org/abs/1811.00234.
- [89] “ReachNow.” *ReachNow*. 2017. Cited 2017. Retrieved from reachnow.com/en/seattle-wa/?gclid=CifZoem5jtQCFQKewAodLRQLhA.
- [90] Andrew Krok, “VW enters the car-sharing game with all-electric WeShare launch in Berlin,” June 27, 2019. Accessed September 21, 2019. Retrieved from cnet.com/roadshow/news/vw-weshare-car-sharing-electric-vehicles-germany/.
- [91] *Mohammed Roni, Zonggen Yi, and John Smart. “Optimal charging management and infrastructure planning for free-floating shared electric vehicles.” 2019. *Transportation Research Part D: Transport and Environment*, 76: 155-175.
- [92] Roni. “Optimal charging management and infrastructure planning for free-floating shared electric vehicles.”
- [93] “BMW i3 2014 Testing.” INL. Accessed June 1, 2018. Retrieved from avt.inl.gov/content/pubs-az.
- [94] “Advanced vehicle testing activity.” INL. Accessed June 1, 2018. Retrieved from avt.inl.gov/vehicle-button/2014-bmw-i3.
- [95] “OpenStreetMap.” 2018. Accessed June 1, 2018. Retrieved from openstreetmap.org/#map=5/38.007/-95.844.
- [96] “Modern C++ routing engine for shortest paths in road networks.” OSRM. 2018. Accessed June 1, 2018. Retrieved from [/project-osrm.org](https://project-osrm.org).
- [97] Aaron Turpen. “Tesla Semi Truck's Battery Pack and Overall Weight Explored.” TESLARATI. February 26, 2018. Retrieved from teslarati.com/how-much-tesla-semi-truck-battery-pack-weigh/.
- [98] Kevin Walkowicz, Jason Lustbader, Ken Kelly, and Alicia Birky, “Data and Data Analytics Workshop for Medium and Heavy-Duty Commercial Trucks.” Green Truck Summit. Indianapolis Convention Center, 06-Mar-2019.
- [99] “Tesla, Inc.”
- [100] “Fleet DNA: Commercial Fleet Vehicle Operating Data.” National Renewable Energy Laboratory (NREL). Accessed September 1, 2019. Retrieved from nrel.gov/transportation/fleettest-fleet-dna.html.
- [101] Brad Templeton. “Tesla Promises Incredible Numbers For ‘Tesla Network’ Robotaxi Service.” Apr 23, 2019. Retrieved from <https://www.forbes.com/sites/bradtempleton/2019/04/23/tesla-promises-incredible-numbers-for-tesla-network-robotaxi-service/#4efd8db51a0b>.
- [102] William Smith. “Robotaxis: the future of transport.” Nov 11, 2019. Retrieved from <https://www.gigabitmagazine.com/ai/robotaxis-future-transport>.
- [103] Mollie D’Agostino. “The Future Car Is Driverless, Shared and Electric.” March 13, 2017. Retrieved from <https://www.ucdavis.edu/news/future-car-driverless-shared-and-electric/>.
- [104] “The rise of electric, shared and autonomous fleets.” KPMG, February 2019. Retrieved from <https://assets.kpmg/content/dam/kpmg/uk/pdf/2019/02/the-rise-of-electric-shared-and-autonomous-fleets.PDF>.
-

-
- [105] Jeffrey B. Greenblatt, Samveg Saxena. "Autonomous taxis could greatly reduce greenhouse-gas emissions of US light-duty vehicles." *Nature Climate Change* 5, no. 9, 2015: 860.
- [106] "Taxicabs of New York City." Accessed September 1, 2019. Retrieved from en.wikipedia.org/wiki/Taxicabs_of_New_York_City.
- [107] O.C. Onar, S. L. Campbell, M. Chinthavali, L. E. Seiber, and C. P. White, "A high-power wireless charging system and integration for a Toyota RAV4 electric vehicle." in *Proc., IEEE Transportation Electrification Conference and Expo (ITEC)*, June 2016, Dearborn, MI.
- [108] Z. Li, J. Li, and J. Dong, "Dynamic wireless power transfer: Potential impact on plug-in electric vehicle adoption," *Society of Automotive Engineers Technical Paper*, 2014-01-1965.
- [109] A. Foote, O. C. Onar, S. Debnath, M. Chinthavali, B. Ozpineci, and D. E. Smith. "Optimal Sizing of a Dynamic Wireless Power Transfer System for Highway Applications." in *Proc., 2018 IEEE Transportation Electrification Conference and Expo (ITEC)*: 1-6. June 2018, Long Beach, CA.
- [110] L. Tan, J. Guo, X. Huang, H. Liu, C. Yan, and W. Wang, "Power control strategies of on-road charging for electric vehicles." *Energies*, vol. 9, no. 7: 531, 2016.
- [111] "Product Selection Guide." New England Wire Technologies. Retrieved from newenglandwire.com/product-selection-capabilities-guide-catalog/.
- [112] J. Muhlethaler. "Modeling and multi-objective optimization of inductive power components," Thesis, ETH / Power Electronic Systems Laboratory. 2012.
- [113] S. Debnath, A. Foote, O. C. Onar, and M. Chinthavali, "Grid impact studies from dynamic wireless charging in smart automated highways." in *Proc., IEEE Transportation Electrification Conference and Expo*: 950-955. June 2018. Long Beach, CA.
- [114] Ahmed Mohamed and O. Mohammed. "Physics-Based Co-Simulation Platform With Analytical and Experimental Verification for Bidirectional IPT System in EV Applications." *IEEE Transactions on Vehicular Technology* 67, no. 1. January 2018: 275–84, doi:10.1109/TVT.2017.2763422.
- [115] Ahmed Mohamed, C. Lashway, and O. Mohammed, "Modeling and Feasibility Analysis of Quasi-Dynamic WPT System for EV Applications." *IEEE Transactions on Transportation Electrification* 3, no. 2. June 2017: 343–53, doi:10.1109/TTE.2017.2682111.
- [116] * Ahmed Mohamed, A. Meintz, and L. Zhu, "System Design and Optimization of In-Route Wireless Charging Infrastructure for Shared Automated Electric Vehicles." *IEEE Access* 7. 2019. 79968–79, doi:10.1109/ACCESS.2019.2920232.
- [117] D. Krajzewicz, J. Erdmann, M. Behrisch, and L. Bieker, "Recent Development and Applications of SUMO – Simulation of Urban Mobility." *International Journal on Advances in Systems and*.
- [118] "Home." EasyMile. Accessed September 25, 2018. Retrieved from easymile.com/.
- [119] Mohamed "System Design and Optimization"
- [120] "FHWA Awards \$4 Million Grant to South Carolina's Greenville County for Automated Taxi Shuttles." Federal Highway Administration. FHWA 17G-17. October 4, 2017. Accessed March 7, 2019. Retrieved from fhwa.dot.gov/pressroom/fhwa1717g.cfm.
- [121] * Zhu Lei, Garikapati Venu, Chen Yuche, Hou Yi, Aziz H. M. Abdul, and Young Stanley, "Quantifying the Mobility and Energy Benefits of Automated Mobility Districts Using Microscopic Traffic Simulation." *International Conference on Transportation and Development 2018*.
- [122] Rolo, "GRT vehicle: automated minibus," 2getthere, 10-Jan-2018.
-

-
- [123] * A. Mohamed, L. Zhu, A. Meintz, and E. Wood, “Optimum Planning for Inductively Charged On-demand Automated Electric Shuttles at Greenville, South Carolina.” Presented at the 2019 IEEE IAS Annual Meeting, 2019.
- [124] “Annual Energy Outlook.” U.S. Energy Information Administration (EIA). 2017. Retrieved from eia.gov/outlooks/aeo.
- [125] * Tom Wenzel, Clement Rames, Eleftheria Kontou, and Alejandro Henao. “Travel and Energy Implications of Ridesourcing Service in Austin, Texas.” *Transportation Research Part D: Transport and Environment* 70. 2019: 18-34.
- [126] “U.S. Census Database.” United States Census Bureau. 2019. Retrieved from census.gov.
- [127] “2017 National Household Travel Survey.” United States Department of Transportation. 2018. Retrieved from nhts.ornl.gov/assets/2017UsersGuide.pdf.
- [128] “Highway Statistics.” United States Department of Transportation. 2017. Retrieved from fhwa.dot.gov/policyinformation/statistics.cfm.
- [129] “U.S. Census Database”
- [130] * Matthew Moniot, Clement Rames, and Erin Burrell. “Feasibility Analysis of Taxi Fleet Electrification using 4.9 Million Miles of Real-World Driving Data”. No. 2019-01-0392. *SAE Technical Paper*. 2019.
- [131] “Annual Energy Outlook”
- [132] “2017 National Household Travel Survey”
- [133] Yan Zhou. “VISION Model.” Argonne National Laboratory. 2018. Retrieved from anl.gov/es/vision-model.
- [134] Zhou, “VISION Model”
- [135] “The National Energy Modeling System”
- [136] “The National Energy Modeling System”
- [137] Zhou, “VISION Model”
- [138] Zhou, “VISION Model”
- [139] Wenzel, “Travel and Energy Implications” 18-34
- [140] Moniot, “Feasibility Analysis of Taxi Fleet”
- [141] Alejandro Henao and Wesley Marshall. “The Impact of Ride-Hailing on Vehicle Miles Traveled.” *Transportation*. 2018: 1-22.
- [142] * Thomas Stephens, Josh Auld, Yuche Chen, Jeffrey Gonder, Eleftheria Kontou, Zhenhong Lin, Fei Xie, Abolfazl Kouros Mohammadian, Ramin Shabanpour, and David Gohlke. “Assessing Energy Impacts of Connected and Automated Vehicles at the US National Level—Preliminary Bounds and Proposed Methods.” *In Road Vehicle Automation 5*: 105-115. Springer, Cham, 2019.
- [143] “Transportation Secure Data Center (TSDC).” National Renewable Energy Laboratory. 2019 Retrieved from nrel.gov/transportation/secure-transportation-data/.
- [144] “Ride Austin Ride-Hailing Vehicles.” RideAustin. 2017. Retrieved from rideaustin.com.
-

- [145] “New York City Taxi Trip Record Data.” New York City (NYC). 2019. Retrieved from www1.nyc.gov/site/tlc/about/tlc-trip-record-data.page.
- [146] “2017 National Household Travel Survey”
- [147] “U.S. Census Database”
- [148] “Highway Statistics”
- [149] “Annual Energy Outlook”
- [150] * Eleftheria Kontou, Changzheng Liu, Fei Xie, Xing Wu, and Zhenhong Lin. “Understanding the Linkage Between Electric Vehicle Charging Network Coverage and Charging Opportunity Using GPS Travel Data.” *Transportation Research Part C: Emerging Technologies* 98. 2019: 1-13.
- [151] Eric Wood. “EVI-Pro.” National Renewable Energy Laboratory. 2018. Retrieved from nrel.gov/news/program/2018/nrels-evi-pro-lite-tool-paves-the-way-for-future-electric-vehicle-infrastructure-planning.html.
- [152] Zhenhong Lin and Fei Xie. “MA3T Model.” Oak Ridge National Laboratory. 2019. Retrieved from ornl.gov/content/ma3t-model.
- [153] Zhou, “VISION Model”
- [154] Fei Xie, Changzheng Liu, Shengyin Li, Zhenhong Lin, and Yongxi Huang. “Long-Term Strategic Planning of Inter-City Fast Charging Infrastructure for Battery Electric Vehicles.” *Transportation Research Part E: Logistics and Transportation Review* 109. 2018: 261–76. Retrieved from <https://doi.org/10.1016/j.tre.2017.11.014>.

Appendix A: Total Cost of Ownership of Ride-Hailing Vehicles

Major Assumption List

- Vehicle costs
 - ICEV: \$20,000
 - BEV 100: \$27,500 (estimate)
 - BEV 150: \$30,000 (approximate cost of a 2018 Nissan Leaf)
 - BEV 250: \$35,000 [i]
 - BEV 400: \$40,000 (estimate)
- Value of time for ride-hailing driver during a shift
 - \$15/hour (reported values from TNC drivers of money earned per hour)
- Charging costs
 - Home L2: \$0.13/kWh (national average residential electricity rate)
 - Away L2: \$0.20/kWh (survey of EVSE provider websites)
 - DCFC 50kW: \$0.30/kWh (survey of EVSE provider websites)
 - DCFC 150kW: \$0.40/kWh (based on to-be-published analysis in another project)
 - DCFC 400kW: \$0.50/kWh (based on to-be-published analysis in another project)
- Gasoline cost
 - \$3.00/gal
- Vehicle Ownership period
 - 5 years (150,000-mile lifetime at an average of ~30,000 mi/year from RideAustin analysis)
- Depreciation and maintenance [i]
 - Depreciation: 1st Year at 23%, subsequent years 15%
 - Maintenance: BEVs at \$0.025/mile, ICEVs \$0.041/mile, HEVs \$0.037/mile
- Insurance and licensing/registration are AFLEET tool values for personally owned vehicles
 - 5-year licensing/registration fees: \$671.43
- 5-year insurance cost: \$5,209.11

Table A- 1. Vehicle characteristics.

Vehicle Type	Purchase Price	Fuel Economy/ Energy Use	Charge Power Capability
ICEV	20,000	33 mpg	--
HEV	23,000	46.1 mpg	--
BEV100	27,500	285 Wh/mi	50-kW
BEV150	30,000	285 Wh/mi	50-kW
BEV250	35,000	285 Wh/mi	150-kW
BEV400	40,000	285 Wh/mi	400-kW

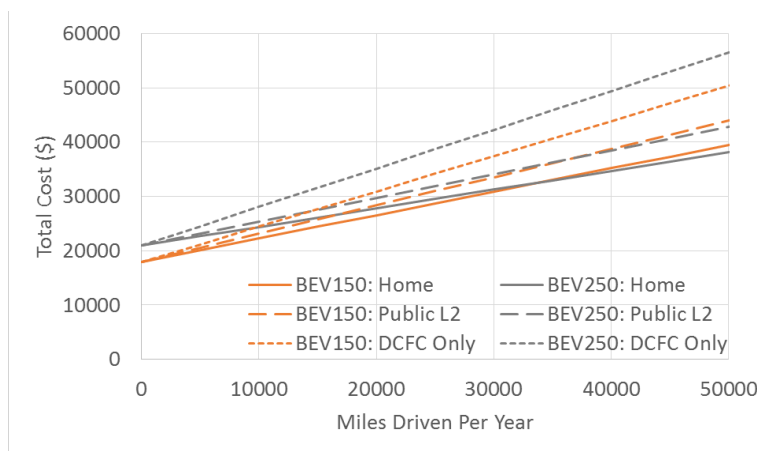


Figure A- 1. Cost variation among BEV150 and BEV250 depending upon charging availability. ‘Home’ means the driver can charge at home, ‘Public L2’ means the driver does not have home charging, but can substitute with Level 2 charging, and ‘DCFC Only’ means the driver must rely only on DCFC.

Drivers Without Access to Home Charging

If drivers cannot charge at home, they will instead have to replace all their home charging with charging at public Level 2 EVSE or DC fast chargers. In these cases, a ride-hailing driver’s per-mile costs can increase significantly. These results suggest that in a baseline case, a BEV may only be the lowest-cost vehicle for drivers with home charging who have very high yearly VMT. However, the results of this analysis are sensitive to the assumptions made and will not necessarily be the same in all driver use cases.

BEV-Specific Electricity Rates

Austin is an interesting case study for this analysis because RideAustin data are used for simulations, and Austin Energy offers special electricity rates to its residential customers who drive BEVs. Typical Austin Energy residential rates are tiered based on monthly energy use, and a full-time ride-hailing driver with a BEV can expect to pay 10.7–24.7 cents/kWh, depending upon their electricity use outside of charging their vehicle. In addition to normal residential rates, Austin Energy offers a special rate to BEV drivers, which includes unlimited off-peak charging for a flat cost of \$30 per month. Assuming that ride-hailing drivers could complete all of their charging off-peak, the costs for a driver with home charging and the special charging rate are shown in Figure A- 2.

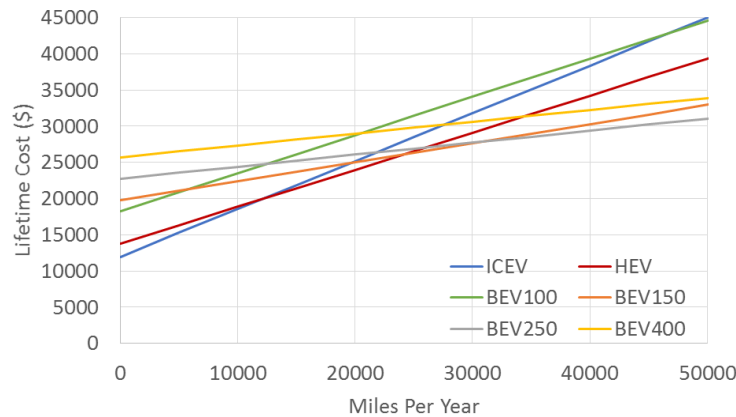


Figure A- 2. Cost comparison when BEV drivers have Austin Energy BEV-specific home electricity rate

With the special electricity rate, BEVs can have a much lower cost than ICEVs or HEVs at high yearly VMT. At 25,000 miles or above, BEVs become the lowest-cost vehicle. Notice that BEV100 is still one of the highest total cost vehicles because it needs to do a large amount of fast charging, which both is expensive and takes time during a driver’s shift.

Company-Owned Driver-Leased Vehicles

It is becoming more common for companies to provide short-term leases of vehicles for use in ride-hailing, and several different companies have BEVs available for lease. The largest of these programs is through a company called Maven, which provides short-term leases of Chevrolet Bolts at a rate of \$229 per week. The rate includes all necessary costs, and currently includes free charging at any EVgo charging station. The comparison between this weekly rate, plus the cost of time spent charging during shifts, and the weekly cost of a full-time driver’s ownership is shown in Figure A- 3. For this comparison, insurance and registration costs are included for the full-time drivers.

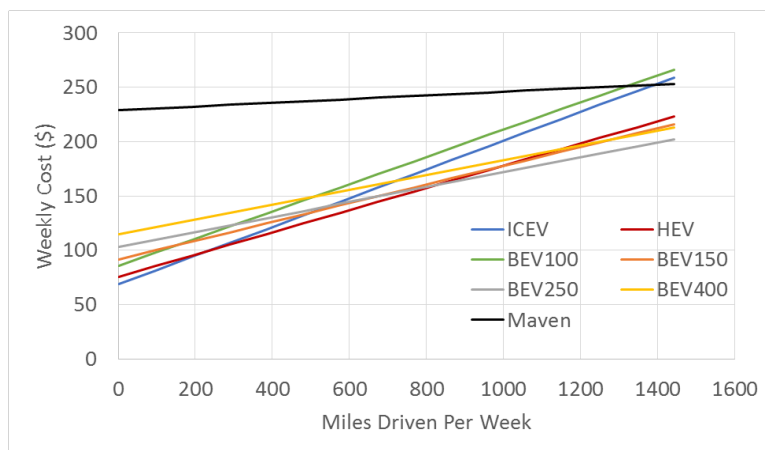


Figure A- 3. Comparison of weekly costs for full-time driver with weekly lease rate offered by Maven for use of a Chevrolet Bolt

The costs of leasing a ride-hailing BEV tend to be higher than the average weekly cost to use one’s own vehicle, but the low-risk prospect of a short-term lease could be very beneficial to someone who is not a full-time driver. It could also bring ride-hailing to a new segment of potential drivers because owning ones vehicle does is not a necessity under this model. It could also represent a different use case, with different driving patterns than a typical ride-hailing vehicle and cover drivers with different motivations.

Appendix B: Charging Network Design to Support Electric Vehicles in Free-floating Car-sharing Fleets

Modeling Scenario Characteristics

Vehicles: All EVs have the same characteristics. The battery type and maximum driving range are the same for each vehicle. EVs are 100% electric.

Charging stations: A finite number of charging stations, charging points, and EVs are available in the service region. All charging stations have the same characteristics. It is assumed that each charging station employs 50-kW DCFCs to recharge their EVs. Each DCFC station can simultaneously serve multiple EVs, according to the number of charging ports at the station.

System operations: A customer initiates service by finding a vehicle at a location in the service region. Service terminates at any legal parking space in the home zone. It is assumed that a customer uses a mobile app to locate the nearest EV for rent. A customer can only see the vehicles in the app that are available for rent. As EVs have a limited range, they need to be recharged before being available for use. For the purposes of this study, it was assumed that an EV was locked by the service provider as the SOC dropped below a certain level, referred to in this report as the “minimum SOC threshold.” It was also assumed that after a customer finishes with a vehicle with an SOC below the minimum threshold, a fleet operator will be available to drive the vehicle to a DCFC for charging. The operator stays with the vehicle until it is charged and is ready for relocation.

Charging operations: In the CMIP model, EV travel for charging is referred to as a “charging trip.” A charging trip involves traveling from the last used location to a charging station, waiting for an available charge port at the DCFC station (if necessary), and charging the vehicle. Relocating the vehicle after charging is not scoped within modeling. When EVs are assigned to DCFCs, three potential scenarios can take place: (1) an EV travels to a DCFC for recharging and is charged immediately without waiting; (2) an EV travels to a DCFC and waits for the next available charging station slot; and (3) an EV waits at its parking location to be scheduled for a trip.

Period: The planning horizon in the CMIP model consists of a finite number of “periods”—that is, the time during which any EV in the fleet is locked for charging. Based on historical charging trip data, the difference between two consecutive events requiring the locking of the vehicle for recharging is calculated to determine the length of that period. The length of a period is not homogenous.

Demand: The total number of charging trips that must be completed within a time horizon is known as “demand” in this study. The unique identifier of a charging trip is defined by two attributes: (1) the time at which a vehicle is locked for charging and (2) the location where a vehicle is locked for charging. This demand can be estimated based on historical data.

Vehicle downtime: The CMIP model captures vehicle downtime associated with charging trips. The components of downtime are: (1) waiting at the origin of the charging trip or at the destination (i.e., the DCFC) due to occupancy by other vehicles, (2) travel time from trip origin to the DCFC station, and (3) the total time spent charging the vehicle. To reduce the computational burden, it is assumed that a vehicle can wait at the trip origin or at the DCFC for up to three periods before a DCFC port becomes available. Vehicle downtime could also be caused by other factors, such as maintenance. This downtime is not considered in this modeling study.

Availability of charging stations: The availability of a DCFC is defined by two factors: (1) DCFC occupancy (i.e., whether or not it is in use by another vehicle) and (2) the length of time it is occupied by another vehicle. These two conditions are affected by various factors, such as the location of the DCFC, the hour of operations given a certain weekday, and the characteristic public or private ownership of the DCFC.

Figure B- 1 illustrates the probability that three actual DCFCs will be occupied at different hours of the day on weekdays and weekends. The historical data used for constructing this figure were collected from public DCFCs in Seattle in 2014. Historical charging behavior data show different utilization patterns across charging

stations over time. The low utilization use probabilities in these data are caused by the low penetration of EVs in 2014. If more EVs are adopted in the market, the utilization probabilities will become larger, but may have similar patterns. These were modified to estimate the utilization probability in the future by approximating the highest utilization rate in 2014 to 100%. Therefore, 100% utilization rate at certain hours of the day implies that the DCFC will not be available to use during that hour, and a charging assignment will require the vehicle to wait before it is available again for use.

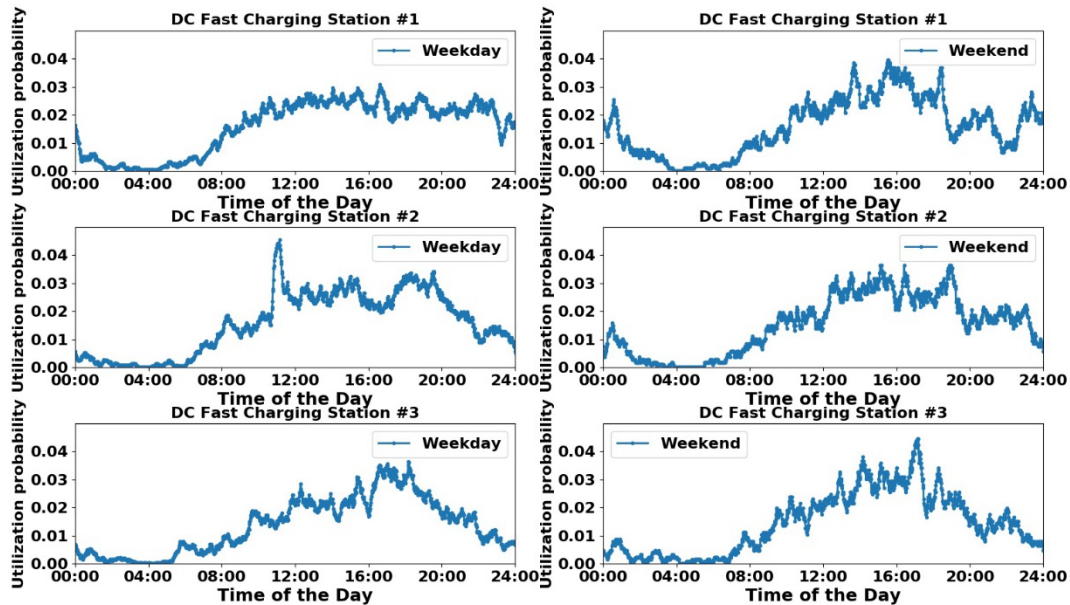


Figure B- 1. Utilization probabilities of three DC fast-charging stations in Seattle in 2014. Historical charging behavior data show different use patterns across charging stations over time. The low utilization probabilities in these data are caused by the low penetration of EVs in 2014.

Figure B- 2 demonstrates the average waiting time if EVs plan to charge at the three DCFCs from historical data. Each DCFC includes two subfigures to illustrate the average waiting time during both weekdays and weekends, respectively. It shows that waiting time varies for each DCFC at different times of the day on weekdays or weekends. Compared with other times during a given day, some perturbations for the average waiting time occur at around 4 am in each figure. The reason for this is fewer charging actions are available at 4 am. A lack of charging actions in the historical data can cause large fluctuations when average waiting time is studied. These analyses indicate that the waiting time can be zero near 4 am, which means no charging action exists in the DCFCs from the historical data. This fact generally tells us that less waiting time is needed when EVs need to be charged around 4 am. Therefore, as with occupancy, the potential waiting time for a charging action also depends on time and location.

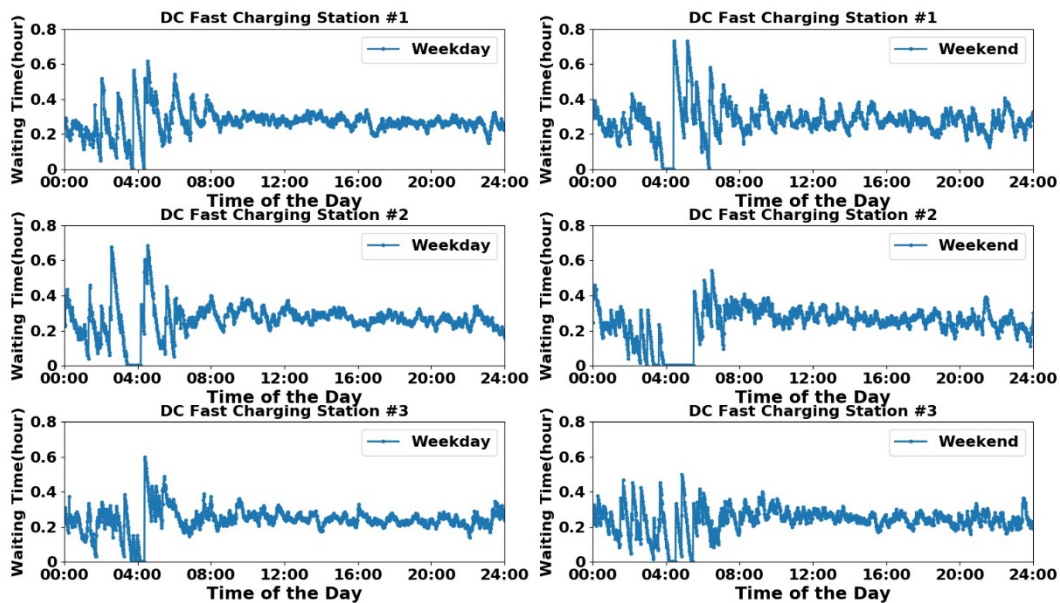


Figure B- 2. Average waiting time of three DC fast-charging stations in Seattle in 2012. Each DCFC includes two subfigures to illustrate the average waiting time during both weekdays and weekends, respectively.

A model was created to generate an expected waiting time due to the occupancy of another vehicle at the DCFC. This model takes into account use probability and average waiting time from historical data, specific to a given time and day (e.g., morning or night on a weekday or weekend).

Estimating Charging Time

The charging time of an EV depends on several factors, including the charging rate, initial battery SOC, and desired final SOC. A data set from the testing of a 50-kW DCFC charging a 2014 BMW i3 was used to obtain the charging time model. Test data included the charge duration, energy transferred, and SOC. Figure B-3 illustrates the BMW i3 ending SOC as a function of charge time from actual testing, performed during the U.S. DOE’s Advanced Vehicle Testing Activity. As a function of these tests, the experiment was started from the zero SOC level and the charging time was recorded when each SOC value was reached. This means that the charging time of the y axis in Figure B- 3 is the time cost when the SOC increases from zero to each ending SOC.

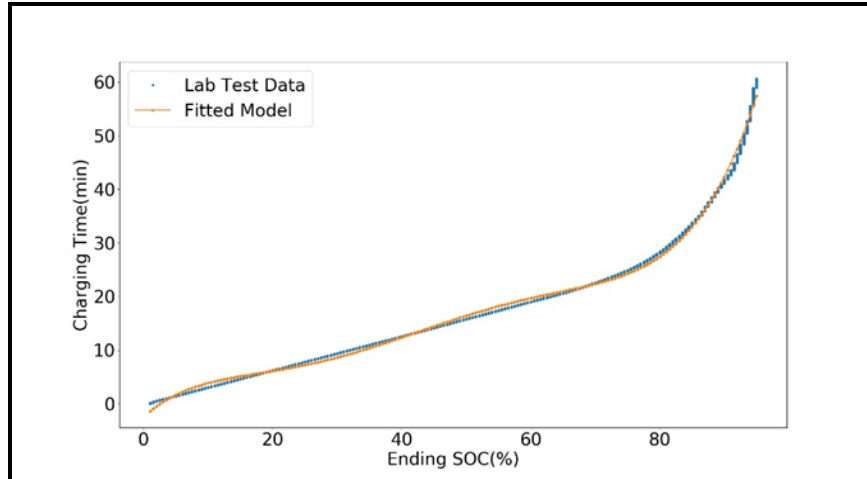


Figure B-3. Ending SOC of 2014 BMW i3 relative to charging time when charging using a 50-kW DCFC. The charging time of the y axis in this figure is calculated as the time cost when the SOC increases from zero to each ending SOC.

To create the charging-time prediction function, a 7th order polynomial is used to fit the model for the estimating charging time of a BMW i3 under a DCFC setting. In this model, the range of SOC percent is from 0 to 100. The following model is presented as Equation B-2 while the corresponding coefficients are found in Table B-1.

$$f_{ct}(SOC) = a_7SOC^7 + a_6SOC^6 + a_5SOC^5 + a_4SOC^4 + a_3SOC^3 + a_2SOC^2 + a_1SOC + a_0 \quad (B-1)$$

where $f_{ct}(SOC)$ is the function to calculate the charging time to achieve energy state SOC percent from zero. Assuming the starting SOC percent is SOC_{start} and the required SOC percent is SOC_{end} , then the necessary charging time T_c can be calculated as:

$$T_c = f_{ct}(SOC_{end}) - f_{ct}(SOC_{start}) \quad (B-2)$$

Table B-1. Coefficients of the charging time estimation model.

a_7	a_6	a_5	a_4	a_3	a_2	a_1	a_0
8.866e-11	-2.778e-8	3.473e-06	-2.191e-4	7.276e-3	-0.1207	1.160	-1.676

Due to the lack of other available data, a high-order polynomial model is used to catch charging-time behavior in the laboratory test data. If more data were to become available, a polynomial model with better generalization could be derived for more robust charging-time estimations.

SOC Depletion During Each Charging Trip

Real-world energy consumption data of the 2014 BMW i3 are used to construct a data-driven model for energy-cost estimation of each charging trip. This data set was collected by DOE’s Advanced Vehicle Testing Activity. The energy cost distribution per mile, relative to average vehicle speed, is illustrated in Figure B-4. The historical data are shown as the blue dots in Figure B-4. Large uncertainties exist in real-world EV energy consumption. In the CMIP model, an average energy-consumption model is developed to describe general energy-cost behavior. This data-driven model is derived based on the vehicle’s longitudinal dynamics.

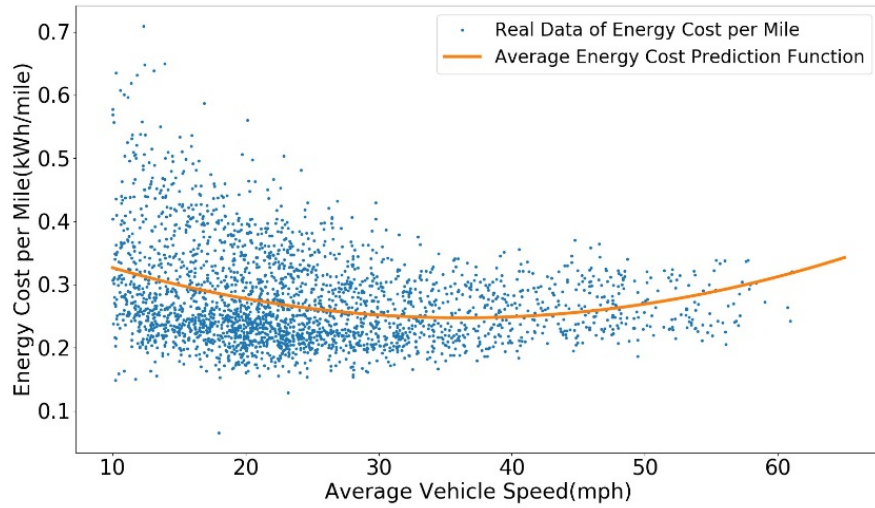


Figure B- 4. The energy-cost distribution per mile relative to vehicle speed. The energy cost per mile of the 2014 BMW i3 is relative to the average vehicle speed (blue dots) and the fitted average energy-cost prediction function (orange line).

A longitudinal dynamic model is one powerful method to estimate EV energy consumption. Longitudinal tractive force is represented by $F(v)$, and can be expressed as:

$$F(v) = \frac{1}{2} \rho C_d A v^2 + C_r M g v \cos \alpha + \tilde{M} a + M g \sin \alpha \quad (\text{B-3})$$

where v = speed of the vehicle;

C_d = the air drag coefficient;

A = projected frontal area;

ρ = air density;

M = mass of the vehicle;

C_r = the coefficient of rolling resistance;

α = angle of road surface for the slope or grade;

\tilde{M} = the equivalent mass considering the inertial mass factors, and

a = the vehicle acceleration.

The detailed analysis of this equation was derived from the EV energy consumption study.

From the longitudinal dynamic model, the energy cost per mile represented by e should have an approximate quadratic relationship with vehicle speed, as shown in Equations (B-4) and (B-5), where E_c is the energy cost during a trip segment; E_{ac} is the energy cost of accessory loads; d is the distance of trip segment; η is the powertrain efficiency; and $\gamma_0, \gamma_1, \gamma_2$ are the coefficients that can be derived by incorporating Equation (B-3) with Equation (B-4). This function can model the average energy cost per mile of an EV along a trip segment.

$$E_c = \eta(F(v)d) + E_{ac} \quad (\text{B-4})$$

$$e = \frac{E_c}{d} = \eta(\gamma_2 v^2 + \gamma_1 v + \gamma_0) + \frac{E_{ac}}{d} \quad (\text{B-5})$$

Based on the historical data shown in Figure B- 4 and the underlying quadratic model in Equation (B-5), the model parameters to obtain an average energy cost per-mile model can be derived as follows:

$$e = 0.0001153 v^2 - 0.008357 v + 0.3988 \quad (\text{B-6})$$

Vehicle speed, v , in this model has the unit of miles per hour. Although this model is approximate, it can provide an average energy-consumption estimation based on realistic vehicle speed. This is adequate for the specific purpose of this report.

Estimating Vehicle Travel Time from Origin to Destination

The CMIP model captures the estimated vehicle travel time of a charging trip from origin to destination using existing tools. Estimations of vehicle travel time for a given pair of origin and destination are conducted based on OpenStreetMap by using the OSRM engine. The OSRM routing engine provides HTTP service requests, as well as the corresponding APIs, making the routing request available on the OpenStreetMap data. The “Route Service” in an OSRM API is utilized to obtain travel-time information. Giving the longitude and latitude information for both origin and destination, a route object can be returned. This route object includes useful information, such as travel distance and duration, which can be used directly for the vehicle travel-time estimation. Furthermore, according to both travel distance and duration, an estimation of average travel speed for a given trip can be derived, which is the necessary information for the EV energy-consumption estimation.

Determining Candidate Locations for New Charging Stations

The process to determine the candidate locations for new DCFCs includes two steps. Step 1 identifies the number of commercial census blocks in Seattle. It was identified that there are 866 commercial census blocks in the Seattle area. Step 2 identifies the number of candidate locations for new charging stations from the centroid of the commercial census block. A spatial-clustering algorithm named SKATER (Spatial ‘K’luster Analysis by Tree Edge Removal) was implemented to identify the sites for new charging stations, leveraging information on the centroid of each commercial census block and the origin of each charging trip. The SKATER algorithm first constructed a connectivity graph representing the neighborhood relationships among commercial census blocks and the origin of historical charging trips. The connectivity graph was reduced to a minimum spanning tree (MST) by using Prim’s algorithm. The MST was subsequently broken into a set of contiguous clusters by implementing an MST-partition algorithm described in an efficient regionalization techniques study. The above-mentioned spatial-clustering algorithm was applied to identify the desired number of clusters. The centroid of each cluster was selected as a candidate location for a new charging station.

Taking all of these assumptions into account, the mathematical formulation of the CMIP model, which jointly optimizes decisions about the location for charging stations and the EVs charging trip to charging station assignment, is described below.

Mathematical Model

The problem of finding optimal locations for charging stations and optimal EVs to a charging station assignment is a hybrid formulation of a capacitated facility location problem and an assignment problem. This location problem comprises selecting what facilities with the proper capacity should be opened, and then assigning a demand level to all open facilities that minimizes the total cost for opening the facilities. The cost of facilities and the transportation or connection costs derive from a set of potential facilities, each having opening cost and a finite capacity to satisfy a set of delineated client demand. This “assignment problem” is a well-known problem in operational research; it has applications to research fields and study variables, such as job scheduling and vehicle routing, among others. As part of this work, the best charging locations were found, as well as the optimal assignment of EVs to charging stations while minimizing the total travel and waiting times for a total number of periods.

EV assignments to charging stations are subject to change depending on the time windows. It is possible that a DCFC is not immediately available for charging due to occupancy. This means that EVs will have to wait until the charging service is available. An EV can wait at its last used location. This avoids long waiting times at a given DCFC, allowing operators to choose the next available DCFC elsewhere. Figure B- 5 shows the assignment of EVs to the DCFCs and the wait at different time windows in a time-space network. Network nodes represent the charge state of each vehicle requiring charging. The state is defined by time (t) and location (j) of the vehicle, and changes based on different types of assignments. Each type of assignment is represented by an arc in the time-space network. It has three different arcs: (1) an origin-destination traveling arc, (2) a waiting arc at DCFCs, and (3) a waiting arc at parking locations. The goal is to optimize the assignment of each arc so that travel, charging, and wait times are minimized.

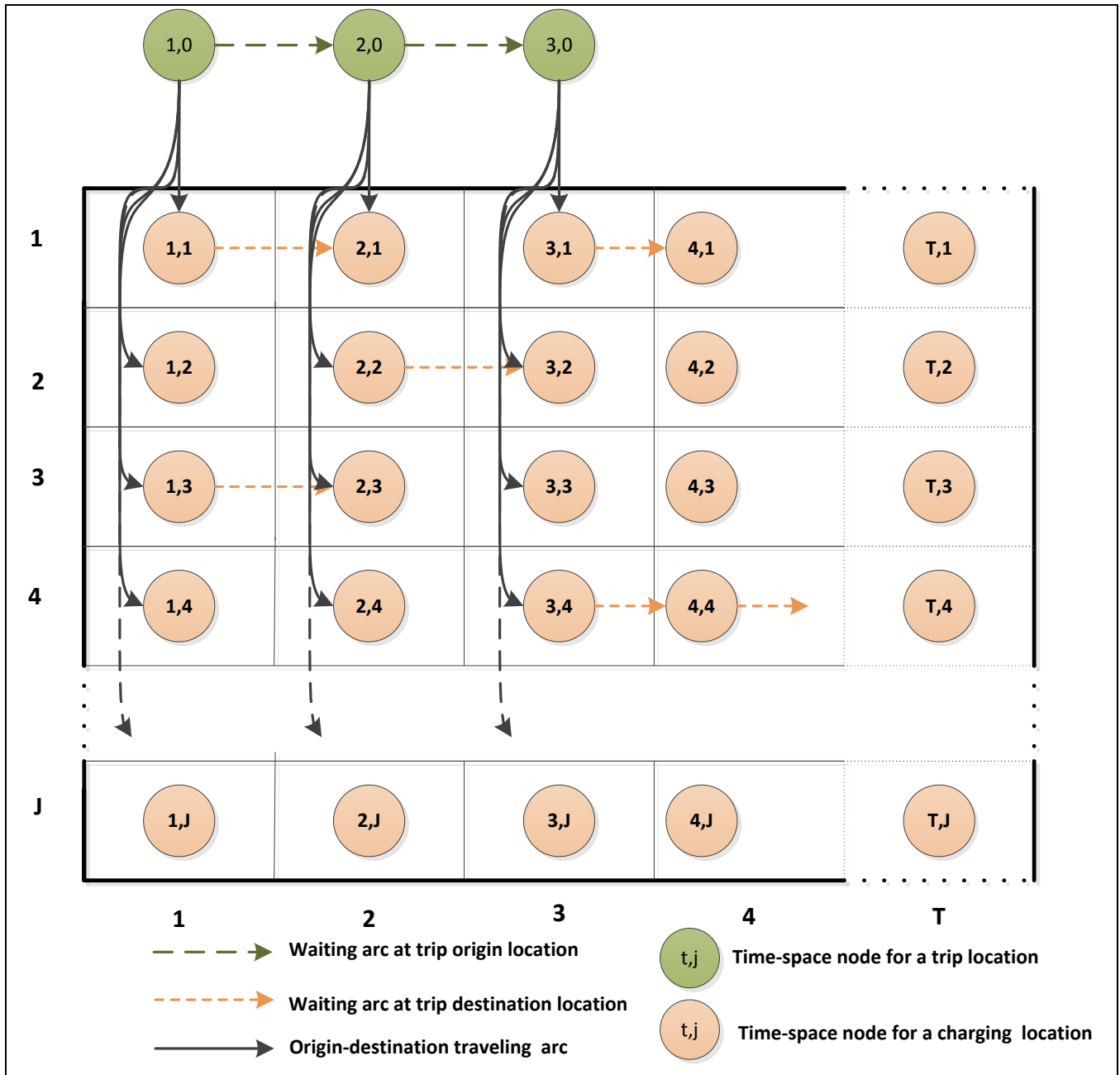


Figure B- 5. Assignment EVs to charging stations in a time-space network. Each node represents the charge state of an individual vehicle.

IP Model Formulation

An IP model is developed to determine optimum assignments. The following notations listed in Table B- 2 are used to establish this IP model.

Table B- 2. Definitions of sets and input parameters for the IP model.

Set definitions	
I	Set of trips
L	Set of trip origins
J	Set of existing charging stations
S	Set of potential locations for new charging stations
P	Set of parking spaces at a charging station
V	Set of charging ports at a charging station
K	Set of assignments
T	Set of time intervals (periods)
Parameters	
π_{ij}	Total travel time of trip origin i to j
ρ_{jt}	Expected waiting time due to occupancy of other vehicle at charging station j at time t
σ_{ij}	Total charging time from initial SOC to final SOC determined by Equation (B-1) for trip i at charging station j
w_{ijkt}	Wait time for trip i to location j for k types of assignments at time period t
τ_{ijkt}	Total assignment cost of trip i to location j for k types of assignments at time period t
n	Total number of existing charging stations
n^{\wedge}	Total number of new charging stations to be selected from the set of candidate locations of new charging stations
N_j	Number of charge ports at charging station j
P_j	Number of parking spaces at charging station j
ρ_{ijt}	SOC depleted during travel from i to j at time t
$\bar{\rho}$	Minimum SOC
ρ	SOC before charging trip (i.e., minimum SOC threshold)

Two primary decision variables are shown in the optimization variables X_{ijkt} and Z_{jpv} . Decision variable X_{ijkt} has a value of 1 when a trip i is assigned to location j with k types of assignments at time period t . Location j can either be at the origin of the trip or at the charging station. Charging stations consist of both existing charging stations and new charging stations. Set k consists of multiple subsets and defined by $k = \{k_{33}, k_{23}, k_{13}, k_{123}, k_{22}, k_{11}, k_{12}\}$, where subset k_{33} represents a trip assignment to a charging station; k_{23} represents a trip assignment that is scheduled to wait at a charging station before being assigned to a charger; k_{13} represents a trip assignment where the EV is scheduled to wait at its origin location before being charged; k_{123} represents a trip where the EV is assigned to wait both at its origin location and charging station before being charged; k_{22} represents a trip assignment where the EV must wait at the parking station of a charging station; k_{11} represents a trip assignment where the EV must wait at the origin location of a trip; and k_{12} represents the assignment to wait at the origin location of a trip first, before again being assigned to wait at a charging station. Figure B- 6 shows an example of the various types of trip assignments with one trip, three

charging stations, and four periods. The objective function essentially minimizes the times associated with each assignment k . The decision variable Z_{jpv} takes the value 1 if location j is selected as the charging station location, with p charging stations and v parking spaces taking the value of 0 otherwise (that is, it is binary).

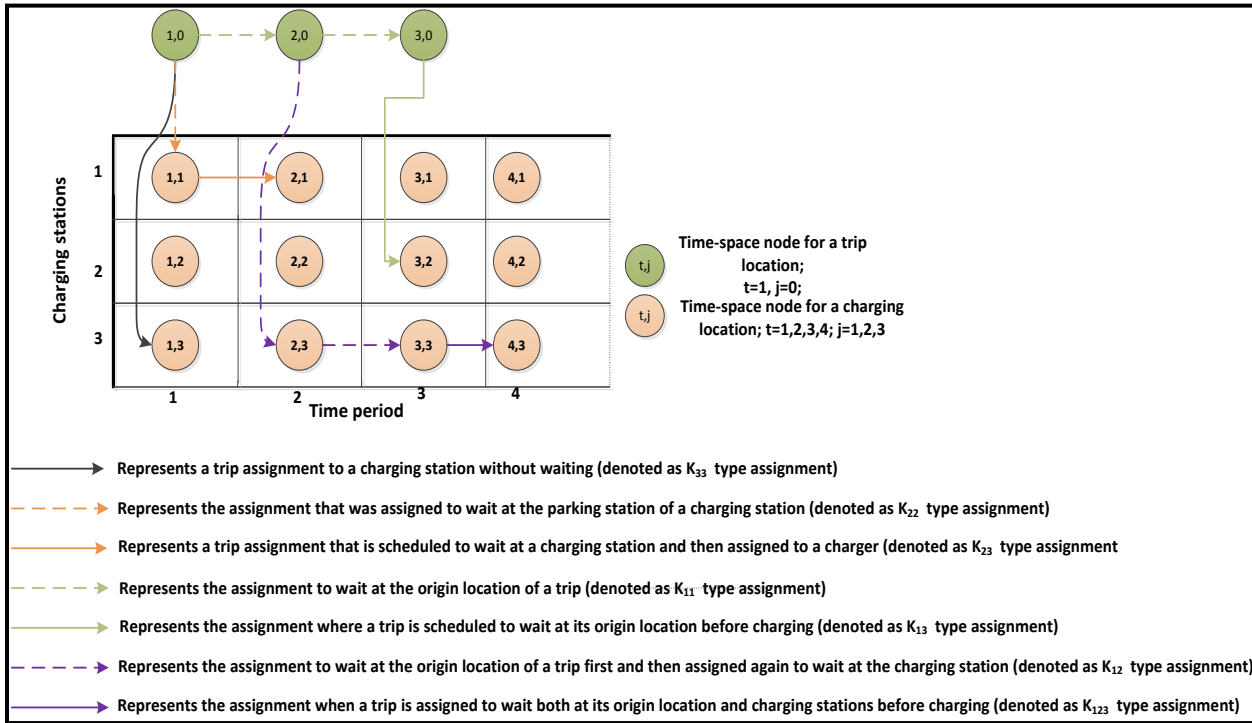


Figure B- 6. An example of the various types of trip assignments with one trip, three charging stations, and four periods. Assignment types defined by $k_{33}, k_{23}, k_{13}, k_{123}, k_{22}, k_{11}, k_{12}$ are shown as colored arrows.

Objective Function

Let $\tau_{ijk_{33}t}, \tau_{ijk_{23}t}, \tau_{ijk_{13}t}$ and $\tau_{ijk_{123}t}$ represent the cost of $k_{33}, k_{23}, k_{13},$ and k_{123} types of assignment respectively. The cost of each assignment is calculated by Equations (B-7)–(B-10). Equation (B-7) calculates total time for k_{33} types assignment where π_{ij} represents total travel time of trip i to j , ρ_{jt} shows expected waiting time due to occupancy of another vehicle at charging station j at time t and σ_j denotes total charging time from initial state of charge S_0 to final SOC S_e determined by Equation (B-1) and Equation (B-2). The terms

$$\sum_{\zeta=t_0}^{t-1} w_{ijk_{22}\zeta}, \sum_{\zeta=t_0}^{t-1} w_{ijk_{11}\zeta}, \sum_{\zeta=t_0}^{t'} w_{ijk_{11}\zeta}, \sum_{\zeta=t'+1}^{t-1} w_{ijk_{12}\zeta}$$

in Equations (B-8)–(B-10) sum the total wait time from the beginning period to the prior period of starting charging trip for $k_{22}, k_{11},$ and k_{12} types of assignment. The term t_0 in Equations (B-9)–(B-10) defines the beginning period of a trip. The term t' in Equations (B-9)–(B-10) is used to define allowable the maximum number of periods a vehicle can wait.

$$\tau_{ijk_{33}t} = \pi_{ij} + \rho_{jt} + \sigma_{ij} \quad \forall i \in I, j \in (J \cup S), t \in T \quad (\text{B-7})$$

$$\tau_{ijk_{23}t} = \pi_{ij} + \rho_{jt} + \sigma_{ij} + \sum_{\zeta=t_0}^{t-1} w_{ijk_{22}\zeta} \quad \forall i \in I, j \in (J \cup S), t \in T \quad (\text{B-8})$$

$$\tau_{ijk_{13}t} = \pi_{ij} + \rho_{jt} + \sigma_{ij} + \sum_{\zeta=t_0}^{t-1} w_{ijk_{11}\zeta} \quad \forall i \in I, j \in (J \cup S), t \in T \quad (\text{B-9})$$

$$\tau_{ijk_{123}t} = \pi_{ij} + \rho_{jt} + \sigma_{ij} + \sum_{\zeta=t_0}^{t'} w_{ijk_{11}\zeta} + \sum_{\zeta=t'+1}^{t-1} w_{ijk_{12}\zeta} \quad \forall i \in I, j \in (J \cup S), t \in T \quad (\text{B-10})$$

The objective-function equation is shown as Equation (B-11), where $k'' = \{k_{33}, k_{23}, k_{13}, k_{123}\}$, and τ_{ijkt} is calculated by Equation (B-12). The objective function simultaneously minimizes the total time of travel and the waiting for charging periods for all trips.

$$\text{minimize: Total time(TT)} = \sum_{i \in I} \sum_{j \in J} \sum_{k \in k''} \sum_{t \in T} \tau_{ijkt} X_{ijkt} \quad (\text{B-11})$$

$$\tau_{ijkt} = \tau_{ijk_{33}t} + \tau_{ijk_{23}t} + \tau_{ijk_{13}t} + \tau_{ijk_{123}t} \quad (\text{B-12})$$

Constraints

A series of constraints are used in the model to establish assignment rule. These constraints are discussed in the following subsections.

Demand constraint: demand constraint (Equation B-13) enforces that all trips must be charged by utilizing existing charging stations or new charging stations.

$$\sum_{j \in (JUS)} \sum_{k \in \{k_{13}, k_{23}, k_{123}, k_{33}\}} \sum_{t \in T} X_{ijkt} = 1 \quad \forall i \in I \quad (\text{B-13})$$

Assignment constraints: Constraint (Equation B-10) ensures that each trip must be assigned to any of the assignment types of k_{11} , k_{22} , and k_{33} as soon as the trip arrives at period t_0 . Constraint (Equation B-15) ensures that all assignment types assigned to k_{11} are forced to schedule wait times at the same location in the next period or are scheduled to travel to a charging station for waiting or charging. Constraint (Equation B-12) states that the k_{12} type assignment must be assigned to either waiting in the next period or to a charging station. Constraint (Equation B-13) states that the k_{22} type assignment must be assigned to wait for the next period or to a charging station.

$$\sum_{j \in (JULUS)} \sum_{k \in \{k_{11}, k_{22}, k_{33}\}} X_{ijkt} = 1 \quad \forall i \in I, t = t_0 \quad (\text{B-14})$$

$$X_{ijk_{11}(t-1)} = X_{ijk_{11}t} + \sum_{j \in JUS} X_{ijk_{13}t} + \sum_{j \in JUS} X_{ijk_{12}t} \quad \forall i \in I, t \in T \quad (\text{B-15})$$

$$X_{ijk_{12}(t-1)} = X_{ijk_{12}t} + X_{ijk_{13}t} \quad \forall i \in I, j \in (JUS), t \in T \quad (\text{B-16})$$

$$X_{ijk_{22}(t-1)} = X_{ijk_{22}t} + X_{ijk_{23}t} \quad \forall i \in I, j \in (JUS), t \in T \quad (\text{B-17})$$

Charging station engagement constraints: Constraint (Equation B-18) states that if a trip is assigned to a charging station and the assignment lasts more than one period, then only one charging assignment can be performed during the charging period. The parameter t_0 defines the starting period of charging and t_{ijt} defines the charging-completion period. These constraints also imply that no trip can be assigned to a charging station while it is occupied in a given period.

$$\sum_{t=t_0}^{t_{ijt}} \sum_{j \in JUV} X_{ijkt} = 1 \quad \forall i \in I, k \in \{k_{13}, k_{23}, k_{123}, k_{33}\} \quad (\text{B-18})$$

Capacity constraints: Constraints (Equation B-19) and (Equation B-20) are the capacity constraints of both existing and candidate locations of new charging stations. The number of vehicles that can be assigned to a charging station are limited by the number of parking spaces (P_{jt}) and charging points (N_{jt}).

$$\sum_{i \in I} X_{ijk_{22}t} + \sum_{i \in I} X_{ijk_{12}t} + \sum_{i \in I} X_{ijk_{23}t} \leq P_j \quad \forall j \in JUV, t \in T \quad (\text{B-19})$$

$$\sum_{i \in I} X_{ijk_{13}t} + \sum_{i \in I} X_{ijk_{123}t} + \sum_{i \in I} X_{ijk_{23}t} + \sum_{i \in I} X_{ijk_{33}t} \leq N_j \quad \forall j \in (J \cup V), t \in T \quad (\text{B-20})$$

State of charge constraints: Constraint (Equation B-21) ensures that a vehicle has a minimum SOC after a charging trip. In this constraint, ρ defines the initial SOC of the vehicle before the trip, the term $\rho_{ijt} X_{ijkt}$ defines the charge depletion (energy consumption) during traveling from the trip origin to a charging station, and $\bar{\rho}$ defines the minimum SOC before charging.

$$\rho - \rho_{ijt} X_{ijkt} \geq \bar{\rho} \quad \forall i \in I, j \in (J \cup V), k \in \{k_{13}, k_{23}, k_{123}, k_{33}\}, t \in T \quad (\text{B-21})$$

Charging-station location constraints: Constraint (Equation B-22) ensures that an EV can be assigned to a charging station only if the charging station exists. Note that charging stations consist of both existing and new charging stations. Constraint (Equation B-23) limits the total number of existing and new charging stations.

The term n in this constraint defines the total number of existing charging stations, while n' defines the total number of new charging stations to be selected from a set of potential sites on which charging stations might be developed (S). Constraint (Equation B-24) enforces the utilization of existing charging stations. These constraints ensure that existing charging stations are always selected in the optimal solution.

$$X_{ijkt} \leq Z_{jpv} \quad \forall i \in I, j \in (JUS), k \in \{k_{13}, k_{23}, k_{123}, k_{33}\}, t \in T, v \in V, p \in P \quad (\text{B-22})$$

$$\sum_{j \in JUS} Z_{jpv} \leq n + n' \quad \forall k \in K, p \in P \quad (\text{B-23})$$

$$Z_{jpv} = 1 \quad \forall j \in J, k \in \{k_{13}, k_{23}, k_{123}, k_{33}\}, t \in T, v \in V, p \in P \quad (\text{B-24})$$

Integrity constraints: Constraints (Equation B-21) and (Equation B-22) are binary constraints on the decision variables.

$$X_{ijkt} \in \{0,1\} \quad \forall i \in I, j \in (JUSUV), k \in K, t \in T \quad (\text{B-25})$$

$$Z_{jpv} \in \{0,1\} \quad \forall j \in (JUS), t \in T, v \in V, p \in P \quad (\text{B-26})$$

Solution Methodology

The CMIP was solved using IBM's CPLEX Version 12.6.2 with C++ Concert Technology. The base-case optimization model has 3,776,506 binary variables with 7,805,123 constraints and is solved by the branch-and-cut algorithm. The default settings solver in CPLEX can solve the optimization model in 213.91 seconds using only a desktop computer using an Intel Xeon CPU E5-2637, 3.50 GHz processor with a 32-GB memory limit and running a Windows operating system. Note that this time does not include the computing time to build the optimization model.

Appendix C: Dynamic Wireless Power Transfer System Modeling

Modeling of Vehicle Energy Consumption

Average power consumption at constant speeds is based on Equation (C-1) with the rolling coefficient $\mu_r=0.0065$, equivalent powertrain efficiency $\eta_{eq}=85\%$, and air density $\rho=1.225 \text{ kg/m}^3$.

$$P(v) = \frac{\mu_r M g}{\eta_{eq}} v + \frac{C_d A v^3}{2\eta_{eq}} + P_{aux} \tag{C-1}$$

The resultant power use, $P_{LDV}(v)$ and $P_{HDV}(v)$, of a LDV and a HDV at a constant speed v are given in Figure C-1. The lengths l , masses M , drag form factors $C_d A$, and auxiliary power P_{aux} of the two vehicles are shown in Table C-1. The difference between the LDV and HDV power use increases at higher speeds due to the large aerodynamic drag and vehicle mass of the HDV.

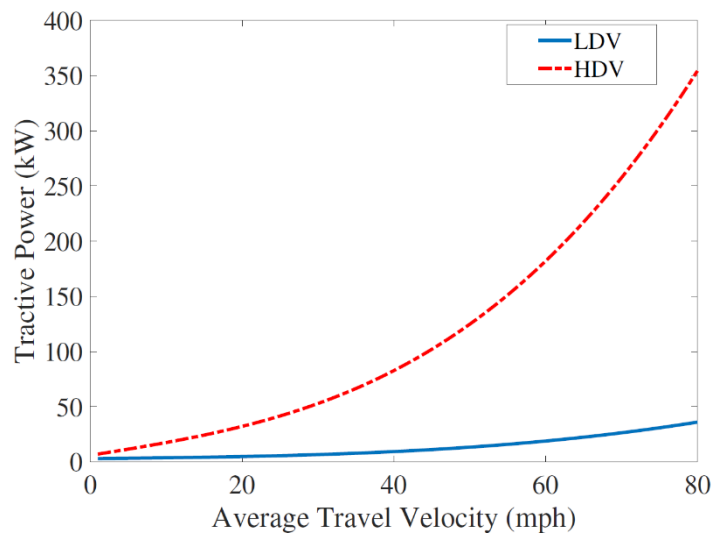


Figure C- 1. Power consumption of LDV and HDV at constant speeds.

Table C- 1. Vehicle parameters.

Light-Duty Vehicle		Heavy-Duty Vehicle	
Parameter	Value	Parameter	Value
M	1700 kg	M	33021 kg
C _d A	0.72 m ²	C _d A	7.88 m ²
l _{LDV}	4.45 m	l _{HDV}	17.37 m
P _{aux}	3 kW	P _{aux}	6 kW

Modeling of Dynamic Wireless Power Transfer Systems

Through the mutual coupling of the inductors M_i , each load resistance R_{Li} is reflected to the DWPT transmitter. Due to the following distance between the vehicles, the cross coupling between the receivers $M_{1,i}$ is assumed to be zero. At resonance, this provides the following relationship for the input voltage V_o and current I_o .

$$V_o = I_o \left(R_o + \sum_{i=1}^N \frac{(\omega M_i)^2}{R_i + R_{Li}} \right) \quad (\text{C-2})$$

From this relationship, the transmitter input power P_o and the receiver output powers P_i are written as a function of the input voltage V_o , the input current I_o , parasitic resistances R_i , and loads of the system.

$$P_o = V_o I_o = I_o^2 \left(R_o + \sum_{i=1}^N \frac{(\omega M_i)^2}{R_i + R_{Li}} \right) \quad (\text{C-3})$$

$$P_i = I_o^2 \frac{(\omega M_i)^2 R_{Li}}{(R_i + R_{Li})^2} \quad (\text{C-4})$$

The mutual inductance between the DWPT transmitter and receivers with salient features can change significantly by position. Because of this, each M_i is calculated as the RMS value of the mutual inductance between the DWPT transmitter and each receiver over the span of position by an analytical expression as in.

Finite Element Analysis-based Modeling of Mutual Inductance and Power Transfer Characteristics

For the FEA, the embedded ferrite track efficiency and characteristics are analyzed. When ferrites are embedded in the roadway, while confining the field and reducing field emissions, they slightly reduce the efficiency of the track per unit length as their magnetic core losses are higher. This effect can be remedied by increasing the thickness of the ferrites (to reduce the peak flux density) but very thick ferrites may pose undue infrastructure costs. In this case, $P_{loss} = l_t (2N_{tp} I_p \rho J + p_f)$ where p_f is the ferrite loss per unit length.

Figure C-2 shows the track-to-vehicle power transfer efficiency as a function of track length for various assumed ferrite thicknesses. With 1/16" thick embedded ferrites, the efficiency of a 100 m track is about 84%. The efficiency increases to 92 and 95% for ferrite thicknesses of 2/16 in. and 3/16 in., respectively. The dotted line depicts the loose upper bound on efficiency assuming lossless ferrites. Figure C-2 gives the parameters of the secondary coil assuming roadway embedded ferrites. With the use of ferrites, coupling factor between the track and the vehicle assembly increases which allows a smaller number of turns on the secondary to achieve the required mutual inductance. Figure C-3 shows the airgap field distribution which is much more directed than seen in ferrite-less configuration. The inductance per unit length and voltage per unit length of the track were 3.09 $\mu\text{H/m}$ and 0.380 kV/m, respectively. For a 100 m track, the total capacitor compensation voltage will need to be on the order of 38 kV, which should be noted as an important design parameter.

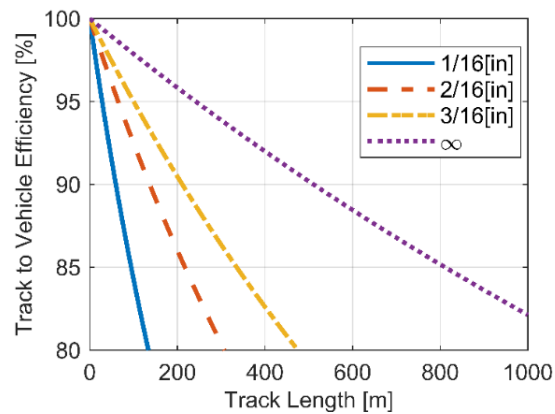


Figure C-2. Example 100 kW dynamic WPT secondary coil parameters for a roadway embedded ferrite track.

Table C- 2. Efficiency analysis of track-based DWPT system with respect to the track length.

Parameter	Value
Ls	63.3 μ H
M	4.81 μ H
Vs	5.75 kV
Dx, Dy	48"
Ip	3.09 μ H/m
Vp	0.380 kV/m

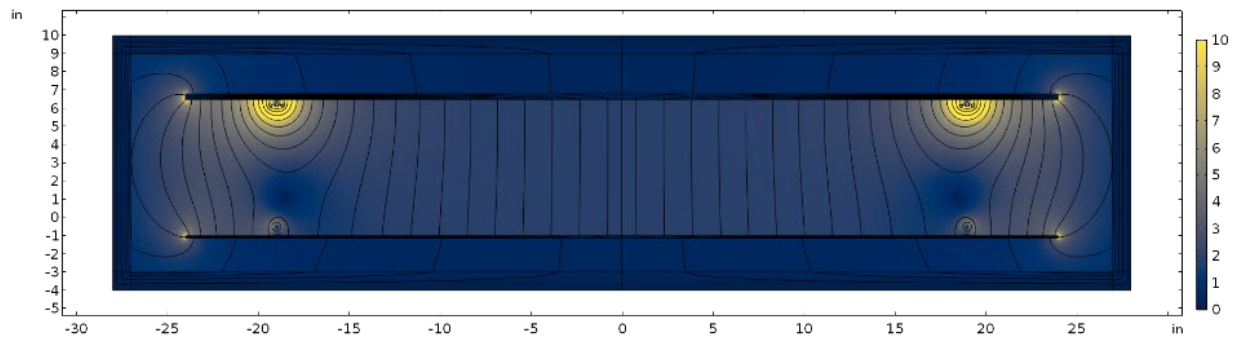


Figure C- 3. Airgap field distribution for the 100kW DWPT system deployment.

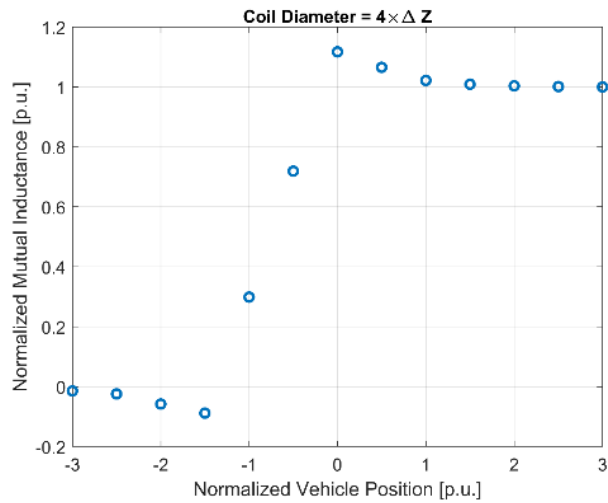


Figure C- 4. Variation of track-to-vehicle mutual inductance with respect to vehicle position.

Figure C- 4 shows a normalized plot of track-to-vehicle coil mutual inductance as the vehicle moves over the track. Far away from the track, the mutual inductance is zero. As the vehicle begins to approach the track, the mutual inductance becomes negative (indicating reversed polarity coupling). Starting from a distance of about 1.5 coil diameters, the mutual inductance begins to ramp up. The peak value of about 1.1 times the nominal value is obtained when the vehicle coil is aligned with the end-turn of the track. The mutual inductance reaches the nominal steady-state value after the coil is overlapping the track by about two diameters. This mutual-

inductance variation demonstrates that the power transfer is continuous and has a trapezoidal profile as the vehicle moves over the track.

Design Optimization Approach for Single Vehicle in Electrified Lane on Highway

The optimization model uses Equations (C-5)–(C-9):

$$\min_{\mathbf{x}} f(\mathbf{x}, \mathbf{p}) = W_1 W_2 C_{inv}(\mathbf{x}, \mathbf{p}) + (1 - W_1) W_2 \cdot C_{road}(\mathbf{x}, \mathbf{p}) + (1 - W_2) C_{coupler}(\mathbf{x}, \mathbf{p}) \quad (C-5)$$

$$\begin{aligned} \bar{P} + P_{aux} - P_{sys} \cdot \frac{\ell_{vehicle}}{\ell_T} \cdot \beta_{road} \cdot \eta_{coupler}(\ell_T) &\leq 0 \\ [0 \quad 0.5 \quad 0]^T &\leq [P_{sys} \quad \ell_T \quad \beta_{road}]^T \leq [500 - \text{kW} \quad 10 \text{ m} \quad 1]^T \\ W_i &\in (0, 1) \end{aligned} \quad (C-6)$$

$$C_{inv}(\mathbf{x}, \mathbf{p}) = \frac{P_{sys} \beta_{road}}{\ell_T} \quad (C-7)$$

$$C_{road}(\mathbf{x}, \mathbf{p}) = \beta_{road} \quad (C-8)$$

$$C_{coupler}(\mathbf{x}, \mathbf{p}) = \frac{P_{sys} \beta_{road}}{\ell_T} \cdot (2\ell_T + 2W_T) \cdot N_T \quad (C-9)$$

The upper bound chosen for the system power rating P_{sys} is based on the limits of the current state-of-art high-power wireless power transfer systems. Three objective functions are used: $C_{inv}(x,p)$ represents the cost of PE, $C_{road}(x,p)$ is the cost of road construction, and $C_{coupler}(x,p)$ approximates the cost of the coupler material. The constraints of the optimization in Equation (C-2) are charge-sustaining operation for the light and HDVs at a constant speed of 70 mph. $C_{inv}(x,p)$ is calculated by considering the number of power electronic converters needed when each inverter is connected to one transmitter. $C_{road}(x,p)$ is modeled as the road construction costs for trenching and resurfacing roadways to install the system. $C_{coupler}(x,p)$ is calculated as proportional to the amount of wire in air-core transmitters, given that the needed section of Litz wire is proportional to P_{sys} for a fixed output voltage. All these functions are scaled by appropriate economic values and then multiplied by varying weighting factors W_i to produce the objective function. This, with the inclusion of $\eta_{coupler}(\ell_T)$ in the constraints is used to generate the Pareto fronts of solutions by using a weighted sum method.

Design Optimization Approach for Multiple Vehicles in Electrified Highway Lanes

Vehicle energy consumption and inductive power transfer models were covered previously. The optimization formulation uses variables including system power level P_{sys} , DWPT transmitter length l_{sys} , system coverage β_{road} , and the value of the equivalent receiver loads, $R_{L,LDV}$ and $R_{L,HDV}$. The optimization is then performed for many possible numbers of LDVs n_{LDV} and HDVs n_{HDV} . This formulation seeks to minimize the infrastructure and energy requirements of the DWPT system on a per-mile basis as a function of the required number and power rating of inverters, road construction, the Litz wire, and energy losses over a 5-year lifetime of the system given the average annual daily traffic (AADT) and velocity. The optimization is formulated as follows:

Minimize x

$$f(x) = M_{inv}(x) + M_{road}(x) + M_{Litz}(x) + M_E(x) \quad (C-10)$$

subject to

$$\begin{aligned} P_{LDV}(\vartheta) - P_i(x) \beta_{road} &\leq 0 \\ 0.5 P_{HDV}(\vartheta) - P_i(x) \beta_{road} &\leq 0 \\ P_0(x) - P_{sys} &\leq 0 \\ n_{LDV} l_{LDV} + n_{HDV} l_{HDV} - 0.5 l_{sys} &\leq 0 \end{aligned} \quad (C-11)$$

$$M_{inv}(x) = W_{inv} \frac{P_{sys} \beta_{road}}{l_{sys}}$$

$$\begin{aligned}
 M_{road}(x) &= W_{road}\beta_{road} \\
 M_{Litz}(x) &= W_{Litz} \frac{N_t\beta_{road}}{l_{sys}} (2l_{sys} + 2w_{sys}) \\
 M_E(x) &= W_E \frac{(AADT \times 365) Y_{LT}}{n_{LDV} + n_{HDV}} \times \frac{\beta_{road}(P_0(x) - \sum P_i(x))}{\vartheta}
 \end{aligned} \tag{C-12}$$

In the optimization formulation constraints listed above, the first constraint represents the charge-sustaining mode of operation for the LDVs and the second requires the system to provide enough power to the HDV for range extension. The third constraint is the capability of the inverter to provide the necessary input power to the DWPT transmitter, and the fourth sizes the DWPT transmitter length to be twice as long as the sum of the lengths of the vehicles in the group. The objective functions M_{inv} , M_{road} , M_{Litz} , and M_E in above formulation represent the number and power rating of inverters, road construction, Litz wire usage, and energy loss requirements of the system, respectively. Different fixed weights have been included within each objective function to normalize each objective. In Table C- 3, two different scenarios are considered by two variable bounds. In the near-term scenario, the power rating of the inverter is limited to 200 kW and the length of the DWPT transmitter is constrained to 100 m.

The near-term system represents a currently achievable design, based on past work. The long-term scenario illustrates what would be possible with higher power ratings and charging limits, and longer DWPT transmitter lengths. In this long-term case, the transmitter length is limited to 350 m to limit the length to one tenth of a wavelength to prevent radiative effects. There are several practical considerations in the design of such a system, such as the bending radius of large cables and the design of high-voltage, higher-frequency inverters. In the parameters given within Table C- 3, the equivalent number of turns of the DWPT transmitter is set as $N_t = 1$ with 4/0 Litz wire cable. This represents the number of turns with the least use of Litz wire cable. Likewise, the number of turns of the LDV receivers $N_{LDV} = 4$ and the HDV receivers $N_{HDV} = 4$ are set with 4/0 cable. The number of LDVs n_{LDV} and HDVs n_{HDV} on each transmitter at a time is iterated to study the impact of AEV grouping on system design. In practice, the groupings will be determined by traffic engineers with statistics of the vehicles per lane per hour on a stretch of highway and the allowable spacing between AEVs. This depends on the future traffic behavior and coordination of AEVs. The speed of travel v is fixed at 55 mph (88 kph) and 70 mph (112 kph), which represent the speed limit of typical state highways and interstates, respectively. The AADT is set to 150,000 to represent a baseline highway scenario.

The optimization parameters and variables are summarized in Table C- 3.

Table C- 3. Optimization variables and parameters

Variable Definitions and Upper Bounds		
Variable Definitions	Near Term	Long Term
P_{sys} : DWPT section power level	200 kW	2 MW
l_{sys} : DWPT transmitter length	100 m	350 m
β_{road} : coverage ratio per mile	100%	100%
Optimization Parameters		
N : Constant travel speed of AEVs	55 mph, 70 mph	
I_o : Constant inverter current	200 A	
ω : Frequency of DWPT system	$2\pi \times 85$ kHz	
z : system magnetic airgap	162 mm	
n_{LDV} : LDV numbers in group	1:10	
n_{HDV} : HDV numbers in group	1:3	
w_{sys} : Width of DWPT couplers	1.5 m	
Y_{LT} : Lifetime of WPT system	5 years	
$AADT$: Average daily traffic	150,000 per day	
N_t : Equivalent turns in transmitter	1 turn	
N_{LDV} : turns in LDV couplers	4 turns	
N_{HDV} : turns in HDV couplers	4 turns	

Design Optimization Approach for Automated Electric Shuttle Buses on Fixed Transit Route

Decision variables: (1) number and locations of wireless chargers ($x_1=N_{WPT}$), (2) charging-power level ($x_2=P_C$), (3) number of wireless track segments at each position ($x_3=N_S$), and (4) battery capacity ($x_4=Q_b$).

Optimization constraints:

- C_1 : charge sustaining operation: $|SOC_f - SOC_i| \leq \varepsilon\%$
- C_2 : acceptable minimum SOC limit: $SOC_{min} \geq A\%$
- C_3 : acceptable maximum SOC limit: $SOC_{max} \leq B\%$
- C_4 : acceptable maximum battery C – rate: $C_{rate} \leq C_{r,lim}$
- C_5 : bound constraints: $x_k^L \leq x_k \leq x_k^U$; $k = 1, 2, 3, 4$
- C_6 : integer variable constraints: $x_k > 0, x_k \in Z^+$; $k = 1, 2, 3, 4$

where, A is the minimum acceptable SOC, B is the maximum acceptable SOC, α is the maximum allowed difference in SOC, $C_{r,lim}$ is the maximum allowable C-rate, x refers to a decision variable with x_k^U as its upper boundary, and x_k^L as its lower boundary.

Fitness (cost) function: for optimizing the design parameters of SAEV supported by DWPT system, a cost model for the components that are impacted by deploying DWPT technology was developed. The model considered unit and installation costs for both the roadway and vehicle. The roadway component cost includes the construction work, materials, PE, control, grid-connectivity, and installation costs, as formulated in Equation (C-13). The vehicle-component cost includes the onboard battery and wireless vehicle pad costs, as indicated in Equation (C-14). The total overall system cost, in Equation (C-15), is described as the summation of the two cost components.

$$F_r(x) = N_L L_s N_{WPT} N_s (c_r + c_e P_c + c_g P_c) + c_i N_{WPT} \tag{C-13}$$

$$F_v(x) = N_{EV} (c_b Q_b + c_{VA} N_{pad} P_c) \tag{C-14}$$

$$F_t(x) = F_r(x) + F_v(x) \tag{C-15}$$

where:

- x = a decision variable (N_{WPT}, P_c, N_s or Q_b)
- L_s = the WPT segment length (mile)
- N_L = the number of electrified lanes per road
- N_{WPT} = the number of WPT positions per road
- N_{EV} = the number of SAEVs to be served
- N_{pad} = the number of vehicle’s wireless pads
- c_r (\$/mile/lane) = the road retrofitting cost coefficient
- c_e (\$/mile/kW/lane) = the road PE, capacitors and material cost coefficient
- c_g (\$/mile/kW/lane) = the grid-connectivity cost coefficient
- c_i (\$/position) = the primary side installation-cost coefficient
- c_{VA} (\$/kW) = the vehicle assembly cost coefficient
- c_b (\$/kWh) = the battery-cost coefficient

The cost function coefficients are determined based on: (1) the U.S. DOE Vehicle Technologies Office 2015 target for power electronic cost of \$12/kW, (2) the current market price for materials (ferrite, Litz wires, shield) and resonance capacitors, considering cost-scaling factors for bulk purchases and gross manufacturing, and (3) data from the literature and construction companies for construction costs. For battery costs, the battery-cost coefficient (cb) is variable according to the charging rate (C-rate) capability and the operating SOC window, as was reported in the DOE Vehicle Technologies Office report, “Enabling Fast Charging: A Technology Gap Assessment.” For the same ΔSOC , the battery cost increases as the C-rate increases because higher C-rate requires thinner electrodes. For the same C-rate, the battery cost decreases as the operating ΔSOC decreases. Considering the NMC622-Graphite, 85-kWh, 900-DCV battery pack, the variation of cb with respect to C-rate and ΔSOC . In this case, the DOE target for battery cell cost, \$80/kWh, was considered for 1C and 80% ΔSOC . The battery cell cost (\$/kWh) is analyzed at different charging-power level and battery capacity at 20% ΔSOC , as presented in Figure C- 5. As can be noted, low charging power leads to low C-rate and low battery-cost coefficient. High charging power and high battery capacity show low C-rate and low cb . High charging power and small battery capacity result in high C-rate and high cb .

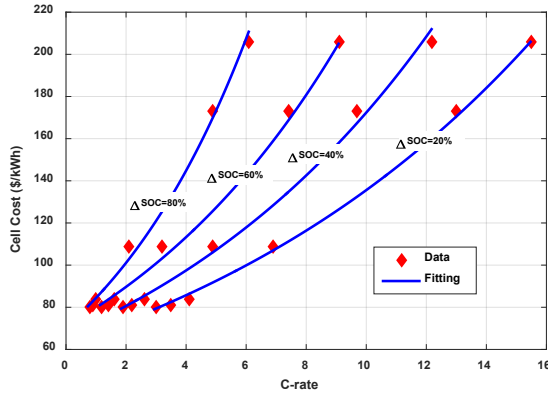


Figure C- 5. Battery cell cost (\$/kWh) at different C-rate and Δ SOC (NMC622-Graphite, 85-kWh, 900-DCV battery pack, \$80/kWh for 1C, 80% Δ SOC)

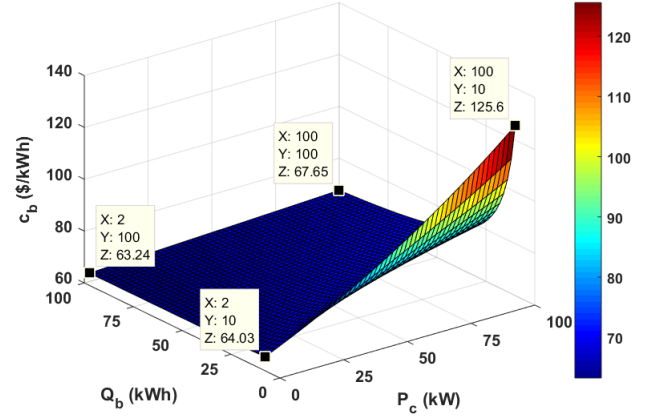


Figure C- 6. Battery cell cost coefficient at different charging power and battery capacity

In addition to the in-route wireless charging, stationary, overnight conductive charging options AC Level 2 (L2) and DCFC are investigated and compared with in-route wireless charging. In this case, the vehicle is supported with a large onboard battery to satisfy a specified driving range (e.g., 6 or 12 h) and a stationary charger is installed for overnight charging for a predefined refueling time. The cost model of DCFC and L2 charging are indicated in Equations (C-16) and (C-17).

$$DCFC \text{ cost} = N_{DCFC} \times [c_{DCFC} \times P_c + c_{DCFC_i}] + N_{EV} \times c_b \times Q_b \quad (C-16)$$

$$L_2 \text{ cost} = N_{L2} \times [c_{L2} \times P_c + c_{L2_i}] + N_{EV} \times [c_b \times Q_b + c_{OBC} \times P_c] \quad (C-17)$$

where, N_{DCFC} and N_{L2} are the number of charging ports, c_{DCFC} and c_{L2} are the unit cost coefficients (\$/kW), c_{DCFC_i} and c_{L2_i} are the installation-cost coefficient (\$/port), and c_{OBC} is the L2 onboard-charger-cost coefficient (\$/kW).

Appendix D: National Energy Impact of Charging Infrastructure for Ride-Hailing EVs

Probabilistic Approach

A probabilistic approach was developed, also known as top-down approach, to mathematically identify the number of chargers needed and charger coverage with a given ride-hailing BEV fleet size and charging demand. The top-down probabilistic approach uses Steps 1–4, below, to determine the number of chargers and charging availability based on different ride-hailing BEV fleet sizes.

1. Quantify the number of daily stops in urban areas. This approach first determines the number of daily stops in urban areas. Urban areas are classified into different segments using census data based on population-density groups defined in NHTS. Using Chicago as an example, the number of grid cells N_i (0.25×0.25 mile per cell) and the percentage of total vehicle trips ending in each population-density segment i are determined using NHTS. Based on percentage of trips ending in each population segment, the number of trip stops F_i^{Stop} were estimated for each population-density segment i with given assumptions of percentages of trips served by ride-hailing BEVs.

1. Assess charging probability at the trip destination/population group based on distribution of battery SOC and average trip distance. At the beginning of each trip, there are five possible scenarios:

Initial SOC below r^L —i.e., $r \leq r^L$:

$$P_1 = \int_0^{r^L} f(r)dr \quad (D-1)$$

Initial SOC higher than r^L , but deadheading trip makes it out of range—i.e., $r > r^L$, $rB - y \leq 0$:

$$P_2 = \int_{r^L}^{r^H} \int_{rB}^{+\infty} f(r)f(y)drdy \quad (D-2)$$

Initial SOC higher than r^L , deadheading trip does not make it out of range, but passenger trip is infeasible—i.e., $r > r^L$, $rB - y > 0$, $rB - y - x \leq 0$:

$$P_3 = \int_{r^L}^{r^H} \int_0^{rB} \int_{rB-y}^{+\infty} f(r)f(y)f(x)drdydx \quad (D-3)$$

Initial SOC higher than r^L , both deadheading and passenger trips are feasible, but the ending SOC is below r^L —i.e., $r > r^L$, $rB - y > 0$, $0 < rB - y - x < r^L B$

$$P_4 = \int_{r^L}^{r^H} \int_0^{rB} \int_{rB-y-r^L B}^{rB-y} f(r)f(y)f(x)drdydx \quad (D-4)$$

Initial SOC higher than r^L , both deadheading and passenger trips are feasible, and the ending SOC is higher than r^L —i.e., $r > r^L$, $rB - y > 0$, $rB - y - x > r^L B$

$$P_5 = \int_{r^L}^{r^H} \int_0^{rB} \int_0^{rB-y-r^L B} f(r)f(y)f(x)drdydx \quad (D-5)$$

$$P_1 + P_2 + P_3 + P_4 + P_5 = 1 \quad (D-6)$$

where,

x = ride-hailing passenger trip distance, ≥ 0

y = ride-hailing deadheading trip distance, ≥ 0

r = initial SOC at the beginning of trip, $[0, r^U]$

$f(\dots)$ = pdf distribution for each variable

r^L = lower bound of initial SOC, requires charging if below this range

r^U = upper bound of initial SOC or full SOC, default – 100%, and

B = full range in miles, default – 250 miles.

Therefore, the probability of services not taken is $P_1 + P_2 + P_3$, and the probability of recharging at end of trip is $P^{Charge} = P_4/(P_4 + P_5)$. Note P^{Charge} is dependent on the predefined critical SOC r^L . The frequency of charging sessions for each cell segment is $F_i^{Charge} = F_i^{Stop} \times P^{Charge}$.

1. Estimate the required number of chargers for each segment. M/M/c queuing model was used, where the first M = the arrival process as Poisson, the second M = the service times as exponents, and c = the number of servers), a multiserver queuing model where arrivals form a single queue and are governed by a Poisson process and service times are exponentially distributed, to estimate the required number of chargers for each 0.25×0.25 mile grid cell. Charger capacity was described in terms of level of service, namely maintaining certain probability for BEV users to find available chargers within certain time period. 18 hours' service window was assumed for each charger. To determine required number of chargers X_i for each cell in segment i :

$$X_i = \inf\{X | Pr(\text{waiting time} \leq \alpha) \geq \beta\} \quad (D-7)$$

where,

$$Pr(\text{waiting time} \leq \alpha) = 1 - \frac{\frac{(\lambda_i \mu)^X}{X!}}{\frac{(\lambda_i \mu)^X}{X!} + \left(1 - \frac{\lambda_i \mu}{X}\right) \sum_{k=0}^{X-1} \frac{(\lambda_i \mu)^k}{k!}} \times e^{-\frac{(X - \lambda_i \mu)\alpha}{\mu}} \quad (D-8)$$

X_i = Required number of chargers for each cell in segment i

λ_i = Arrival rate (hourly expected number of charging sessions received for each cell, 18 hours service time) for each cell for segment i ,

$$\lambda_i = F_i^{Charge} / 18 \quad (D-9)$$

μ = Service rate (expected service time (hours) for each charging session, 30 mins' average service time)

α = Waiting time to find available charger at each cell (hours)

β = Probability of BEV to find available charger within waiting time α

2. Finally, the charging coverage was characterized as a function of percentage of total passenger-vehicle trips served by ride-hailing BEVs, at different assumptions of critical battery SOC levels. Critical battery SOC means that vehicles need to be recharged when battery depletes to this level, which could vary by driver, vehicle model, charger level, and mobility type.

Because only positive integer number of chargers could be considered for each cell, with above equations, if there is positive charging demand (even very small), at least one charger is installed if the demand is planned to be satisfied. However, the charger capacity may not be fully utilized. This occurs when only one charger is needed for the cell segment i . Let C be the capacity of one charger that satisfies the above M/M/C level of service condition.

Then, since only one charger is needed:

$$\lambda_i \leq C \quad (D-10)$$

When $\lambda_i = C$, it means the charger is fully utilized, and the charging availability is 100%.

However, when $\lambda_i < C$, the charger is underutilized, indicating the capacity is larger than the actual charging demand needed. In this circumstance, for cost benefits, the AFI Pillar let multiple cells in the same segment share one charger. The number of cells σ_i that could share one charger is determined as follows:

$$\sigma_i = \sup\{\sigma | \sigma \lambda_i \leq C\} \quad (D-11)$$

Then:

$$\sigma_i = \frac{C}{\lambda_i} \quad (D-12)$$

By definition, $1/\sigma_i$ is the charging availability when there is one charger needed for the cell.

However, when multiple chargers are needed for one cell, it indicates that the cell receives relatively large charging demand. In this situation, the charging availability is 100% for the cell, which leads to the following conditions:

$$\sigma_i = \begin{cases} \sup\{\sigma | \sigma \lambda_i \leq C\}, & X_i = 1 \\ 1 & X_i > 1 \end{cases} \quad (D-13)$$

Finally, total charging availability and total number of chargers in the urban area are determined by:

$$\text{Total Availability} = \frac{\sum_{i \in I} N_i / \sigma_i}{\sum_{i \in I} N_i} \quad (D-14)$$

$$\text{Total Number of Chargers} = \sum_{i \in I} \frac{N_i X_i}{\sigma_i} \quad (D-15)$$

As a result, the required number of chargers were estimated at each cell segment and resulting charging coverage based on charging probability at trip destination.

Appendix E: Calculating Monthly Electricity Bill

In addition to the utility company rate plan, estimating the charging station’s monthly bill requires knowing its electricity usage. The monthly energy usage is estimated by multiplying the daily energy usage by 30. Table E-1 is the simulated charging station’s operational data, which needs to be preprocessed as input parameters to calculate the monthly electricity bill for charging stations. The input parameters are listed in Table E- 1.

Table E- 1. Input parameters needed to calculate electricity bills

Input	Symbol	Unit	Description
Monthly Energy usage	E_u	kWh	kWh used this month
Maximum demand	D_u	kW	Highest power needed this month
Maximum demand from previous year	AD_u	kW	Highest power demand last year
On-peak energy usage	ON_u	kWh	Total on-peak energy used this month
Off-peak energy usage	OFF_u	kWh	Total off-peak energy used this month
On-peak demand	OND_u	kW	Maximum on-peak demand
Off-peak demand	$OFFD_u$	kW	Maximum off-peak demand
Number of days this month	$DAYS$	days	Total number of days in this month

This study uses the Ohio Power Company’s Columbus Southern power rate zone bill calculation spreadsheet to estimate monthly electricity bills. The spreadsheet receives a month-long hourly energy usage profile (in kWh) and outputs the approximate monthly bill from that data for each applicable rate plan. For the GS2 secondary-service rate plan, the simplified equation for the monthly bill is:

$$\text{Monthly bill} = M_c + D_c D_u + R_c, \tag{E-1}$$

where M_c is monthly charge, D_c is demand charge, D_u is customer maximum demand, and R_c is total applicable riders.

If more than one utility supplies the target charging station, the equation for a monthly electricity bill must include all types of charges in the relevant rate plan of each utility. The equation is:

$$\text{Monthly bill} = \text{MAX}(MB_c DAYS, E_c E_u + D_c D_u + ON_c ON_u + OFF_c OFF_u + OND_c OND_u + OFFD_c \text{IF}(OFFD_u - OND_u > 0, OFFD_u - OND_u, 0)) \left(1 + \frac{SUR_c}{100}\right), \tag{E-2}$$

- where MB_c = minimum bill
- $DAYS$ = number of days this month
- E_c = energy charge
- E_u = energy usage
- ON_c = on-peak energy charge
- ON_u = on-peak energy usage
- OFF_c = off-peak energy charge
- OFF_u = off-peak energy usage
- OND_c = on-peak energy demand charge
- OND_u = on-peak energy demand
- $OFFD_c$ = off-peak energy demand charge
- $OFFD_u$ = off-peak energy demand
- SUR_c = surcharge.

The function $\text{MAX}(\text{val}_1, \text{val}_2)$ returns the greater of val_1 and val_2 , and the function $\text{IF}(\text{condition}, \text{val}_1, \text{val}_2)$ returns val_1 if the condition is true, and val_2 otherwise.

(This Page Intentionally Left Blank)

U.S. DEPARTMENT OF
ENERGY

Office of
**ENERGY EFFICIENCY &
RENEWABLE ENERGY**

For more information, visit:
energy.gov/eere/vehicles

DOE/EE-2062 July 2020